T cell-mediated immune regulation in Spondyloarthritis

Davide Simone

University College

SUPERVISORS

Professor Paul Bowness

Doctor Hussein al Mossawi

Professor Paul Klenerman

Thesis submitted to the University of Oxford

towards fulfilment of the degree of

DPhil in Musculoskeletal Sciences

I. Abstract

CD4+ T cells are essential components of the immune system. Dysregulated or excessive T cell responses can cause, in susceptible individuals, a group of immune-mediated conditions termed Spondyloarthritis (SpA), characterized by chronic inflammation and structural damage of various musculoskeletal structures. While well-documented genetic and immunological alterations in SpA explain the overactivation of effector T cells, the intrinsic regulatory functions exerted by a specialized T cell subset (Tregs) have been studied only marginally. Exploring the natural suppressive functions of Tregs could reveal novel regulatory pathways that can be leveraged for patient benefit.

In its first part, this thesis focuses on the phenotypic and transcriptional diversity of regulatory T cells in the peripheral blood and synovial fluid in Spondyloarthritis. Through the use of high-resolution techniques and unbiased analytical methods, I identify and characterize specialized regulatory subsets in the blood and joints of patients with SpA. One of these subsets, which presents features shared with Th17 cells and similarities with intestinal Tregs, preferentially expresses the regulatory markers IL-10 and LAG-3. LAG-3, in particular, is an emerging inhibitory receptor expressed on T cells. I show that LAG-3 is able to control blood-derived monocyte activation in vitro, reducing production of the inflammatory cytokines IL-12/23 and TNF, and downregulating costimulatory molecules necessary for T effector activation. This mechanism is predicted to restrain inflammatory responses, making LAG-3-based therapeutic

interventions promising novel strategies for immune driven diseases such as SpA.

A further emerging therapeutic strategy for SpA and other inflammatory arthritides consists in targeting inflammatory signaling pathways. The intracellular kinase MK2 is involved in the post-transcriptional regulation of cytokine expression. In the last part of the thesis I show that a novel small molecule MK2 inhibitor is effective in reducing T cell mediated inflammatory responses, including Th17, making it a promising novel therapeutic agent for SpA.

II. Declaration

I hereby declare that this submission is my own work and to the best of my knowledge contains no materials previously published or written by another person. Any contribution made to the research by others, with whom I have worked, is explicitly acknowledged in this thesis.

III. Acknowledgements

I would like to thank my main supervisor Professor Paul Bowness, a true role model. His passion for science, his warmth towards patients and colleagues and his calm leadership have been a constant inspiration. If working towards this DPhil was so enjoyable, it was largely thanks to him. To Dr Hussein al Mossawi I owe a great deal: a true force of nature, a great friend, and without a doubt a future bright leader in the field. I'm also grateful to Dr Frank Penkava, with whom we shared most of the PhD path. We embarked together on this adventure that is the single cell world, and it has been an exciting ride. Professor Paul Klenerman's brilliant inputs were also incredibly valuable.

A big thank you goes to all the present and past members of the Bowness Lab: I couldn't have hoped in a better group of colleagues and friends; to all the healthy volunteers, our patients of the SpA clinic; the entire Rheumatology team at the Nuffield Orthopaedic Centre and the researchers at the Botnar, two incredibly stimulating places to work in.

I'm also grateful to my funders, the University College and Oxfordshire Health Services Research Committee.

Finally a massive thank you goes to all my friends in Oxford, to my family for their support and encouragement, and to Lavinia for being there when it mattered.

IV. Contents

V. List of Tables

VI. List of figures

VII. List of abbreviations

ANOVA	Analysis of variance
APC	Antigen Presenting Cell
AS	Ankylosing Spondylitis
BASDAI	Bath Ankylosing Spondylitis Disease Activity Index
BSA	bovine serum albumin
C	Celsius
C. albicans	*Candida albicans*
CBA	Cytokine Bead Array
CDR3	Complementarity-determining region 3
CFSE	Carboxyfluorescein succinimidyl ester
CNS	Central Nervous System
CRP	C-Reactive Protein
DC	Dendritic Cell
DMSO	Dimethyl sulfoxide
EAE	experimental allergic encephalomyelitis
EDTA	Ethylenediaminetetraacetic acid
e.g.	exempli gratia
FACS	fluorescence activated cell sorting
FBS	fetal bovine serum
GEX	Gene Expression
GO	Gene Ontology
GWAS	Genome Wide Association Study
HC	healthy control
HLA	human leukocyte antigen
HTO	Hashtag Oligonucleotide
i.e.	id est
IL	Interleukin
ILC	innate lymphoid cells
IQR	interquartile range

JAK	Janus kinase
LAG-3	Lymphocyte-activation gene 3
LPS	Lipopolysaccharide
MACS	magnetic activated cell sorting
MAPK	Mitogen-activated protein kinase
MFI	mean fluorescence intensity
MHC	major histocompatibility complex
MK2	Mitogen-activated protein kinase-activated kinase 2
mRNA	messenger Ribonucleic acid
NKT	Natural Killer T
PB / PBMC	Peripheral Blood (Mononuclear Cell)
PBS	phosphate buffered saline
PC	principal component
PCR	Polymerase chain reaction
PMA	Phorbol 12-myristate 13-acetat
PsA	Psoriatic Arthritis
QC	Quality Control
RA	Rheumatoid Arthritis
rh	recombinant human
RPMI	Roswell Park Memorial Institute (medium)
S. typhimurium	*Salmonella typhimurium*
scRNAseq	single cell RNA sequencing
SD	standard deviation
SEB	Staphyolococcus enterotoxin B
SEM	standard error of the mean
SF / SFMC	Synovial Fluid (Mononuclear Cell)
SpA	Spondyloarthritis
Stat	signal transducer and activator of transcription proteins
TCR	T cell Receptor
Teff	T effector
TF	Transcription Factor
TG	transgenic
Th	T helper
TNF	Tumour Necrosis Factor
TNFi	Tumour Necrosis Factor inhibitor
TNFRSF	Tumour Necrosis Factor receptor superfamily

Tr1	Type 1 regulatory cells
Treg	Regulatory T cell
tSNE	t-distributed Stochastic Neighbor Embedding
UMAP	Uniform Manifold Approximation and Projection
UMI	Unique molecular identifier

1 Introduction and aims

The immune system is a network of specialised structures and processes that the organism employs to defend itself from pathogenic agents and to preserve tissue homeostasis. The first lines of defence against pathogens are specialised anatomical structures with barrier function and neutralising secreted mediators. A second, more complex, subsystem is defined by cell-mediated immunity, which relies on the activation and intercommunication between specialised cell types, further classified in two groups. Innate immune cells, highly conserved across species, provide rapid recognition of molecular patterns expressed by pathogenic organisms and their clearance. Adaptive immune cells, thanks to a clonal recognition of non self (foreign) proteins (antigens), confer life-long protection against a vast numbers of challenges, and orchestrate the response of the entire immune system.

T helper lymphocytes, characterised by the expression of the costimulatory molecule CD4 on their surface, are central in adaptive immunity. They recognise protein antigens thanks to a unique receptor expressed on their surface and shape an organised response to external challenges. When a self antigen is erroneously recognised or when the activation mechanisms are altered or dysregulated, $CD4^+$ T cells can cause pathology, among which inflammatory arthritides, including Spondyloarthritides (SpA).

The focus of this thesis will be on $CD4^+$ T cells in SpA, in particular on their regulatory functions on the immune system, either exerted by a specialised subset, or by molecular interventions that restrain their inflammatory responses. The overarching aim of this work is to explore novel mechanisms of T cell regulation for patient benefit.

1.1 $CD4^+$ T CELLS

1.1.1 Development, antigen recognition and activation

The recognition of amino acid sequences (epitopes) from peptides presented by MHC molecules on the surface of antigen-presenting cells (APCs) is the mainstay of adaptive immunity. The first encounter of CD4+ T cells with an antigen happens in the thymus, where they are generated. Here, a large array of antigens is presented by medullary or cortical thymic epithelial cells to the antigen-naïve CD4+ T cells in a process known as thymic selection. A specialised complex named the T cell receptor (TCR), expressed on the T cell surface,

recognises and binds the antigen with different levels of affinity. High avidity for self-antigens leads to T cell programmed cell death, in order to limit autoreactivity. Cells that show low affinity survive and egress the thymus as naïve T cells (positive selection). Within the T cells with intermediate affinity for the antigen, some become centrally primed regulatory T cells (Tregs) (**Figure 1.1**), whose activation and further differentiation will be discussed in 1.2

The selection process, fundamental to instruct recognition of foreign antigens and tolerance towards self proteins, essentially depends on the TCR, which is a heterodimer formed by two chains; more exactly, in the vast majority of T cells, an alpha and a beta chains (a smaller subset of T cells, with a specific role in barrier immunity, expresses a gamma-delta chain pairing). In the developing T cell, the genes encoding alpha and beta chains (named *TCRA* and *TCRB* respectively) undergo a complex rearrangement of multiple non-contiguous segments (called somatic recombination). These segments are contained in gene loci called variable (V), diversity (D), joining (J) and constant (C) in the *TCRB* gene and V, J and C in the *TCRA*. The resulting protein chain generated and expressed on the T cell surface is the product of only one sequence from the multiple copies that exist in the various VDJ segments, in a process called V(D)J recombination. The combinatorial associations of the gene segments for each chain, plus the addition or removal of random nucleotides at the site of recombination generates a vast number of variants that composes the enormous TCR repertoire needed to recognise the high number of antigens presented in the thymus, making each T cell essentially unique. The functional key site is the sequence encoded by the V(D)J junction, which forms the highly

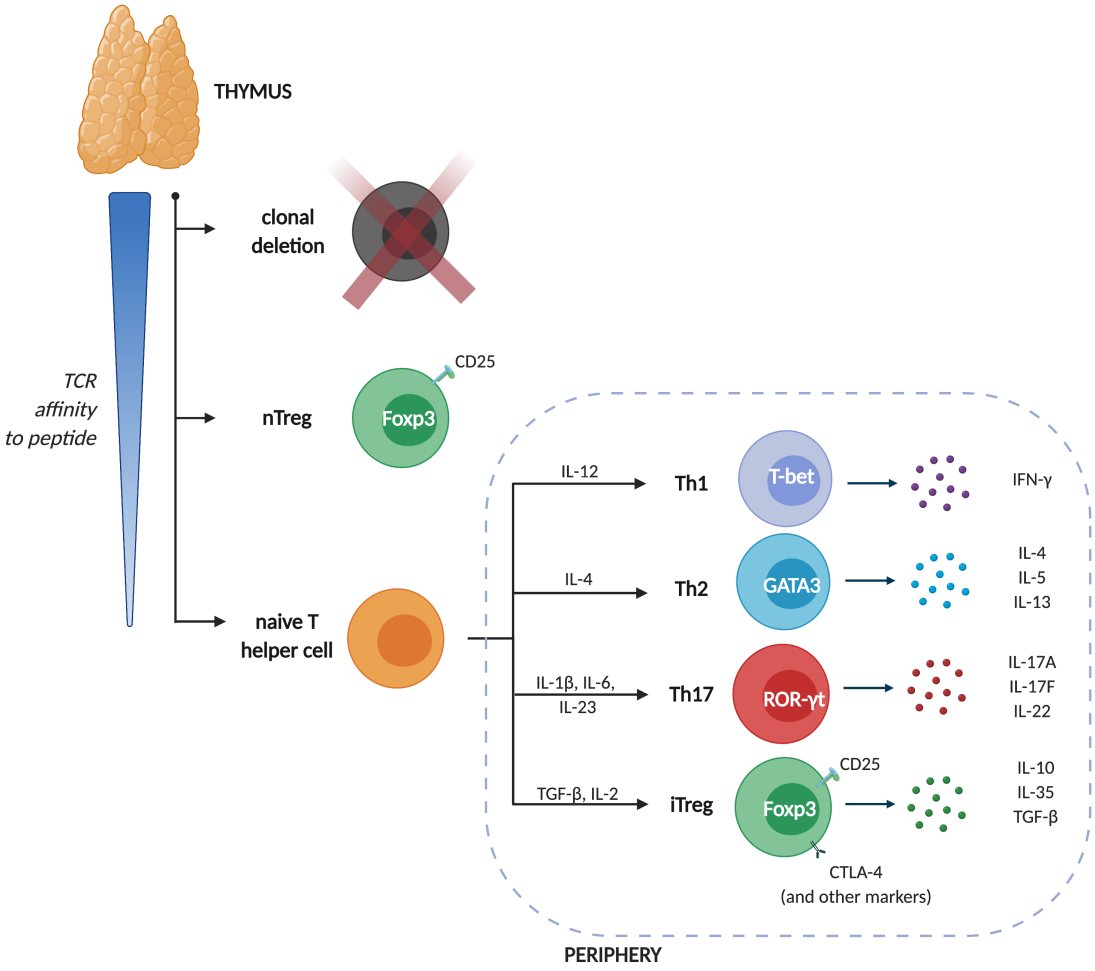

Figure 1.1. Cartoon showing CD4⁺ T cell thymic maturation and differentiation. The CD4⁺ cell fate is dependent on the T cell receptor (TCR) recognition of self-peptides presented by APCs in the thymus. T cells with high affinity for self-peptides or MHC molecules undergo programmed cell death with aim of removing self-reactive T cells. Through mechanisms not entirely understood, T cells with high or intermediate affinity for self peptides are instructed to become regulatory cells (nTregs).

variable complementarity determining regions (CDR) 3, representing the area that enters in contact with the antigen.

After the thymic education, the cells that are positively selected migrate to the periphery where they will be able to recognise the same peptides presented on MHC class II molecules by the professional APCs.

1.1.2 Differentiation and heterogeneity

Together with the recognition of the antigen and the TCR engagement signal, integrated stimuli dictate the transcriptional changes that guide the differentiation of the naïve T cell. These include: the level of the stimulation from the APC, the presence of cell-cell costimulatory signals and the cytokine milieu in the microenvironment (together with a finer regulation provided by other soluble mediators or bacterial products). Specific intracellular pathways, including Stat (signal transducer and activator of transcription) proteins, regulate this process, which eventually leads to the induction of a dominant transcription factor (**Table 1.1** and **Figure 1.1**). The master transcription factor (TF) controls the transcriptional programme of the cell, including specific cytokine production and the expression of chemokine receptors that mediate trafficking to the organs: these help each subset to exert specific functions in response to antigens and in tissue immunity. Dysregulated mechanisms of T cell commitment or maturation can be contributing to pathogenic responses, such as autoimmunity for Th1 and Th17 cells, and allergic responses for Th2 cells. Genome Wide Association Studies (GWAS) have been instrumental in unveiling the associations between many different genomic loci associated with T cell function, and autoimmune

diseases, providing new insights into pathogenesis and identification of possible drug targets (Knight, 2013). One important T helper subset, Tregs, is specialised in terminating the host immune response, regulating tissue homeostasis and preventing autoimmunity.

	Signalling pathway	Master TF/Gene	Functions	Chemokine receptors	Reference
Th1	Stat1/Stat4	T-bet/TBX21	immunity against intracellular microorganisms	CCR5, CCR4, CXCR3	(Szabo et al., 2000, 2002)
Th2	Stat6	Gata-3/*GATA3*	humoral immunity against extracellullar pathogens	CCR4	(Zheng and Flavell, 1997)
Th17	Stat3	ROR-γt/*RORC*	immunity against pathogens incl. fungi and mucosal immunity	CCR4, CCR6	(Harrington et al., 2005; Park et al., 2005)
Treg	Stat5	Foxp3/*FOXP3*	regulation of immune system activation		(Fontenot et al., 2005)

Table 1.1. Master transcription factors, functions and signature chemokine receptors of major human T helper cell subsets.

T helper subsets	Genes	Conditions associated (include)
Th1	*STAT4, IL12A, IL12B*	Systemic Lupus Eryhtematosus (SLE), RA, Primary Biliary Cholangitis (PBC), Inflammatory Bowel Diseases (IBD),
Th2	*IL6R, IL33, IL1R1, RORA, IL18R1*	Asthma, Vitiligo
Th17	*STAT3, TYK2, IL6R, IL23R, IL23A, CCR6, JAK2*	AS, Psoriasis, PsA, IBD

Treg	*CD28, IL2RA,*	Type I diabetes, RA
Misc T cell responses	*PTPN22, TNFRSF9, TNFRSF14, CD40, BACH2*	RA, Multiple Sclerosis, Autoimmune thyroid disease, IBD, Coeliac disease

Table 1.2. Genes linked with T helper subset function and their association with immune-driven diseases (data from the NHGRI-EBI GWAS Catalog, https://www.ebi.ac.uk/gwas/home)**.**

1.2 REGULATORY T CELLS (Tregs)

1.2.1 Discovery, origin and development

The first description of Tregs dates back to the 1990s when Shimon Sakaguchi first identified a circulating subset of $CD4^+$ T cells expressing high levels of CD25 (the α-subunit of the IL-2 receptor) (Sakaguchi et al., 1995). The adoptive transfer of these $CD25^+$ T cells was able to prevent the multi-organ autoimmune disease observed in thymectomized mice (Suri-Payer et al., 1998). An analogue phenotype was also identified in humans, characterised by expression of CD25 and responsiveness to IL-2 (Baecher-Allan et al., 2001; Ng et al., 2001). Subsequently, the *FOXP3* gene product was identified (Fontenot et al., 2003; Hori et al., 2003) as the master Treg transcription factor with a central role in development, survival and regulatory function. Its mutation was then associated with fatal autoimmune diseases, both in mice, in a phenotype that was already known as *scurfy* (Brunkow et al., 2001), and in humans (IPEX, or Immunodysregulation polyendocrinopathy enteropathy X-linked, syndrome)

(Wildin et al., 2001). The severity of these clinical pictures, caused by the complete lack of functional Tregs, highlights the critical, non-redundant role of these cells in the maintenance of self-tolerance.

Tregs, as is the case for the vast majority of T helper cells, have TCRs constructed with combination of alpha and beta chains (although $\gamma\delta$ T cells with regulatory properties have been described, see (Xiaoyan et al., 2011)). The TCR engagement, co-stimulation by CD28 (Tai et al., 2005) and high levels of IL-2 induce FOXP3 and CD25 expression via activation of Stat5 (Burchill et al., 2007; Lio and Hsieh, 2008). Recent studies have shown that activation of enhancers in genes associated with the Treg lineage (eg. *IKZF2* (Helios), and *IKZF4* (Eos)), is present even before the *FOXP3* mRNA induction, indicating the existence of permissive epigenetic changes in the Treg precursor (Kitagawa et al., 2017).

Tregs generated in the thymus then egress to form the so-called thymic Tregs (tTregs). These cells recognize self or tolerised antigens and are generally functionally stable. The maintenance of their regulatory role is coordinated by an epigenetic landscape of specific regions of the genome. The DNA methylation status, in particular, in regions such the Treg-specific demethylated region (TSDR) situated inside the *FOXP3* conserved non-coding sequence 2, is the key epigenetic control of the Treg specific gene expression (Polansky et al., 2008).

Tregs can also be generated peripherally. Naïve T cells that exit the thymus can be later differentiated into Foxp3+ Tregs following antigen recognition, if required complementary events take place. These cells are labelled peripheral Tregs (pTregs) or induced Tregs (iTregs). The methylation status of Treg-specific regions controls the stability of Foxp3 expression. As shown in

mouse Tregs, environmental signals (eg. soluble inflammatory mediators, the strength of the TCR signal) can induce methylation of key genetic loci, increasing cell plasticity and potentially limiting suppressive function and even loss of FOXP3 expression (Ohkura et al., 2012).

1.2.2 Classification and phenotypic heterogeneity

Despite differences in origin and epigenetic control, distinguishing thymic and peripheral Tregs with common markers is challenging (Shevach and Thornton, 2014). The TF Helios and the surface protein Nrp1 (neuropilin-1) (Weiss et al., 2012; Yadav et al., 2012), lacking on peripherally-primed Tregs, have been proposed as markers for thymic origin.

As said, FOXP3 is the master and lineage defining TF for Tregs, but although in mice is a marker exclusive of Tregs, in humans FOXP3 can be induced in conventional T cells upon activation. The Sakaguchi group proposed a classification of circulating Tregs based on the expression levels of three markers: CD45RA+FOXP3low/CD25low were defined resting or naive Tregs; CD45RA- FOXP3hi/CD25hi effector Tregs; and CD45RA- FOXP3low/CD25low non Tregs (Miyara et al., 2009). Further studies showed that CD25 and FOXP3 expression are neither exclusive nor sufficient to define Tregs, and that the Treg pool is highly heterogeneous. A number of additional Tregs markers, reflecting maturation or activation state, have been described. Similarly to T effectors (Teffs), Tregs can be subdivided into naive and memory cell compartments based on the expression of CD45RA/CD45RO, and can express other markers such as CCR7, HLA-DR, and CD27. Other important functional markers include:

cytotoxic T-lymphocyte antigen-4 (CTLA-4) (Wing et al., 2008), GITR (glucocorticoid-induced TNF receptor family related protein; *TNFRSF18*) (Shimizu et al., 2002), and the lack of expression of CD127 (the IL-7 receptor α-chain) (Liu et al., 2006). Although none can be singularly used to univocally define Tregs, they all concur to define their identity.

Finally, not all $CD4^+$ T cells with regulatory functions express FOXP3 or CD25: as in the case for the so called type 1 regulatory cell, or Tr1, that have an important role in tissue immunity (Pot et al., 2011). Tr1 are generated in the periphery from naïve T cells and are characterised by the production of IL-10 and Granzyme B and the expression of LAG-3 and CD49b (Gagliani et al., 2013). In the mouse, the Tr1 phenotype can be reproduced in vitro exposing murine naïve $CD4^+$ T cells to IL-27. The master TF controlling the transcriptional profile of these cells has not yet been identified, but the induction of *Irf1* and *Batf* is required for the differentiation into Tr1 (Karwacz et al., 2017).

1.2.3 Treg Plasticity

The T cell subsets shown in **Figure 1.1** should not be interpreted as terminal differentiation: the lineage commitment is not irreversible and the epigenetic regulation of the various TFs is permissive of coexpression. Tregs in particular have the capacity in certain circumstances to acquire, in overlap with FOXP3, the transcriptional signature associated with specific T helper subsets. The co-expression of the key TF of a certain lineage in Tregs may endow with expression of trafficking and migration markers to inflammation sites, cytokine receptors required for adaptation in a certain environment or even the ability to

regulate inflammation orchestrated by “shadowing” T helper cells, while maintaining a suppressive module (Wing and Sakaguchi, 2012).

This is evident in the Tregs expressing the Th17 signature TF ROR-γt, a subset first described in the mouse intestine. The acquisition of ROR-γt by gut Tregs would be instrumental to adapt the cell to tissue cues such as IL-6, and offer a competitive advantage against Th17, which have the same differentiation requirement (Chaudhry et al., 2009). ROR-γt also induces CCR6 expression in Tregs, a chemokine receptor that mediates migration to Th17-driven inflammation sites, such as the central nervous system (CNS) in the course of experimental autoimmune encephalomyelitis (EAE), a model of human demyelinating disease (Kim et al., 2017). A similar role for the TFs T-bet and, more recently, GATA3 in Tregs has been described; both are instrumental to regulate respectively Th1 (Koch et al., 2009) and Th2 (Kalekar et al., 2019) responses.

It has been proposed that, in immune driven conditions the plastic properties of Tregs could contribute to the disease pathogenesis, if FOXP3 expression is lost (“Treg instability”) and a pro-inflammatory gene module overrides the regulatory programme. High levels of IL-6 and IL-1 are able to overcome Foxp3 control of the ROR-γt programme, inducing IL-17 expression (Yang et al., 2008). In an animal model of arthritis, in fact, in the presence of high levels of IL-6 Tregs have shown to transdifferentiate into pathogenic cells (Komatsu et al., 2014). However, transdifferentiation to or from Tregs has been observed in vivo in murine fate mapping models (Zhou et al., 2009). This occurrence has not been demonstrated in human autoimmune diseases yet.

1.2.4 Tissue-specificity of Tregs

Tissue-resident T cells are an emerging concept in immunology. The hypothesis that Tregs could exert specialized regulatory immune functions in the tissues, similarly to what observed for other tissue resident cells, is even more recent (Panduro et al., 2016).

Although specialized Tregs have been described in many non lymphoid tissues such as the skeletal muscle and the adipose tissue (Cipolletta et al., 2012), a brief overview will be given on tissue Tregs colonizing two organs often affected by SpA: the gut, and the joint.

A large barrier tissue at the functional forefront between immune response and tolerance, the gut mucosa represents an example of site where T cell regulatory responses have evolved in response to the environment (Whibley et al., 2019). In the mouse intestine, two well characterised Treg subsets exist: one, presumed to be of thymic origin, expresses the TF *Gata3* and promotes intestinal tolerance via IL-33 (Schiering et al., 2014), the other expresses the Th17 master TF ROR-γt and is induced by intestinal microbiota (Ohnmacht et al., 2015; Sefik et al., 2015). The latter is a stable subset, as shown by the hypomethylation of TSDR, and exerts mucosal tolerance functions (Yang et al., 2016) towards type 2 responses (Ohnmacht et al., 2015), or controls pathogenic Th17 responses triggered by pathobiont (Xu et al., 2018), via cMaf, a master regulator for IL-10. IL-10 controls Th17 pathology (Huber et al., 2011) as shown by deletion of *Maf* or *Il10r* which exacerbates mucosal inflammation often driven by pathogenic Th17 cells (Chaudhry et al., 2011; Xu et al., 2018).

Whether correspondent Tregs subset are present in the human gut has been addressed only recently: Tregs with Th17 characteristics, responsive to retinoic acid and involved in tissue repair, have been identified in patients with Crohn's disease (Povoleri et al., 2018). In one report within the Human Cell Atlas project, the lymphoid landscape of the colon identified three subsets of Tregs: a lymphoid-tissue-like cluster, a non-lymphoid tissue like, and a group of cells expressing the *KLRB1* gene (James et al., 2020). Certainly IL-10 has important regulatory function also in the human intestine, as confirmed by genetic mutations of *IL10RA* and *IL10RB,* associated with severe, early-onset inflammatory bowel disease (Glocker et al., 2009).

The synovial fluid in the course of arthritis is a complex inflammatory environment, where T cells interact with organ-specific resident cell populations such as synovial fibroblasts or other activated immune cells (eg macrophages and DCs), which provide both cell-dependent and soluble signals. How the synovial environment in the course of arthritis can influence gene regulation in Tregs is a largely underexplored area. Specific Treg subsets and described functional alterations affecting Treg function in the SF will be described in 1.3.2.6.

Tissue Tregs do not differ from peripheral blood cells exclusively in their activation status or the expression of a specific TF. Integrating chromatin accessibility and single cell RNAseq data of tissue Tregs from different organs and the spleen, DiSpirito et al., 2018 showed the existence of tissue-restricted areas of open chromatin that are activated on top of regions already accessible in the spleen Whether there is a tissue-specificity in the suppressive functions is an important outstanding question.

1.2.5 Mechanisms of suppression

Tregs mediate their suppressive functions integrating a series of mechanisms involving cell contact, secreted factors and modification of the surrounding environment. The T cell suppressive armamentarium is comprising a vast number of molecular mechanisms, ranging from cell surface proteins (CTLA-4, CD25, TIGIT), to immunoregulatory cytokines (IL-10, TGF-β, and IL-35) and intracellular peptides (granzyme, cyclic AMP) (reviewed in Schmidt et al., 2012). Some of these markers, constitutively expressed on Tregs, are essential for maintaining self-tolerance: deficiency of CTLA-4, CD25 or IL-2 all cause severe autoimmune or inflammatory disease, often fatal.

CTLA-4 on Tregs downregulates the expression of CD80 and CD86 by antigen-presenting cells (APCs), competing with CD28 for CD80/CD86 binding consequently depriving T effectors cells of needed costimulatory signals (Wing et al., 2008). Furthermore, CTLA-4 removes the CD80 and CD86 molecules from the cell surface of APCs by transendocytosis (Qureshi et al., 2011). IL-2 is absorbed by Tregs, owing to their high expression of CD25 and the high affinity heterotrimeric IL-2 receptor stably expressed on their surface, outcompeting T effector cells for a cue for their expansions and differentiation (Pandiyan et al., 2007).

The two mechanisms above are regulated by FOXP3 (Wu et al., 2006), while others may be adopted by Tregs as additional instruments of immune regulation, particularly at sites of tissue inflammation (Wing and Sakaguchi, 2012). For example, IL-10 expression is not a prerogative of Tregs but it is acquired in the tissue. Treg-conditional IL-10 deletion produces tissue pathology

(colitis) but not spontaneous, systemic autoimmune disease, suggesting that there is a hierarchy of suppressive markers (Rubtsov et al., 2008). Further studies are needed to identify which mechanisms Tregs employ to regulate different responder cells and in which inflammatory sites.

1.2.6 Treg antigen specificity

As explained, the T cells that show intermediate or high affinity towards the antigen are programmed to become Tregs, while those with low antigen affinity are become conventional T cells. The result is that the TCR repertoire in Tregs is more skewed towards self-reactive peptides compared to any other $CD4^+$ population (Romagnoli et al., 2002). The tTreg population, in particular, is thought to be largely autoreactive, but in a TCRβ transgenic mouse experiment, it was shown that the TCR repertoires of Tregs and autoreactive Teffs are partially overlapping (Hsieh et al., 2006).

Tregs that are not instructed in the thymus but in the periphery, recognize self peptides more frequently than conventional T cells. In reality, Tregs specific for exogenous antigens have been described: both pTregs (Lathrop et al., 2011), and, surprisingly, tTregs (Cebula et al., 2013) can instruct regulatory responses against intestinal bacteria in mice, and similarly against viral antigens (Ebinuma et al., 2008) or aeroantigens in human allergies (Bacher et al., 2016), challenging the dogma that Tregs are exclusively autoreactive. It is possible that tTregs mainly recognise self-antigens, and that the pTreg TCR repertoire includes both self and foreign epitopes, comprising of both innocuous environmental or commensal-derived antigens. Reports of Treg clonal

expansions are constrained by the relative scarcity of Tregs compared to other $CD4^+$ cells, yet the comprehension of clonal restricted regulatory responses could help designing antigen-specific modulation for Treg cell-based therapy in autoimmune diseases where an autoantigen has been already identified.

1.2.7 Tregs in immune-mediated diseases

Since their description as the main regulatory subset of the immune system, considerable effort has been put to demonstrate an association between Tregs and immune driven diseases (Miyara et al., 2011). Despite inconsistencies in the markers employed for their identification, numerous reports have described functional or numerical anomalies of circulating Tregs in many immune mediated diseases, including inflammatory arthritides (see 1.3.2.6).

Whether a quantitative or qualitative Treg anomaly is causative of an immune-mediated condition, or is instead the consequence of it, remains difficult to prove. Furthermore, concomitant over-activation and resistance of effector cells to Treg-mediated suppression are often described in immune-driven diseases. Genome-wide association studies have shown that SNPs associated to autoimmune diseases, including inflammatory arthritides, can localize in enhancer regions of genes with regulatory functions such as *IL2RA* and *CTLA4* (Todd et al., 2007; Brown et al., 2016; Okada et al., 2019) . Mapping the effects of Treg-associated immune variants on gene expression and chromatin status has been attempted only very recently (Bossini-Castillo et al., 2019). It is possible that certain genetic variations could be of relevance only

during organ pathology, or in one specific tissue-resident subpopulation of Tregs. In asthma, for example, a disease-causing polymorphism of *IL4R* was proposed as causing pathogenic conversion of Treg to Th17, which worsened airway inflammation (Massoud et al., 2016).

1.2.8 Treg-based therapies

Owing to their ability of induce tolerance and to regulate excessive inflammatory responses, therapies that promote Tregs are considered a viable strategy for treating immune driven diseases. Adoptive cell therapy with antigen-specific or polyclonal Tregs is being trialed in several autoimmune conditions. In it, purified circulating Tregs from a patient are expanded in vitro with polyclonal stimuli such as TCR and CD28 and/or IL-2, and transferred back to the patient (Hippen et al., 2011; Bluestone et al., 2015). Alloantigens can be added if the aim is expanding antigen-specific Tregs before reinjection in patients. The ability of IL-2 to induce Tregs proliferation can be also used directly in vivo: the injection of low doses of rhIL-2 has been used to successfully enhance regulatory responses in autoimmune diseases (Todd et al., 2016; Humrich et al., 2019). Going forward, a strategy to obtain antigen-specific Tregs could be engineering them to express a chimeric antigen receptor, or homing receptors that would mediate trafficking to the sites of organ autoimmunity (Zhang et al., 2018).

While adoptive Treg transfer for the treatment of autoimmune diseases is an emerging, although promising, experimental approach, therapies that mirror certain Treg functions are already in clinical use. The discovery of CTLA-4 and its modulation of the CD80/86 co-stimulatoy signal led to the development of

abatacept, a CTLA-4/Ig fusion protein, currently in widespread clinical use in RA (Westhovens et al., 2009).

Conversely, a high Treg number is detrimental when a strong immune response against a certain antigen is desired. The number of Tregs in the tumor microenvironment, in fact, correlates with disease progression (Togashi et al., 2019). In oncology, the state-of-the-art approach is to inhibit the regulatory responses in order to reinforce antitumor immune surveillance. Immunotherapies, based on the inhibition of the immune checkpoints (such as CTLA-4, PD-1 and LAG-3) interfere with the regulatory receptors expressed by conventional $CD4^+$ and $CD8^+$ cells upon exhaustion and/or repetitive exposure to an antigen (Havel et al., 2019), and simultaneously deplete Tregs (Arce Vargas et al., 2018).

1.3 THE SPONDYLOARTHROPATHIES (SpA)

SpA is a collective term that defines a spectrum of chronic immune-mediated arthritic conditions with unifying clinical, genetic and pathophysiological features. The main pathogenic event in SpA is inflammation of different musculoskeletal structures, which presents with pain, tenderness or stiffness of the joints, the tendons and the axial skeleton. If untreated, the persisting inflammation leads to structural changes and deformity.

Historically, the SpA classification includes five conditions, named after one characterizing clinical feature or its etiology: ankylosing spondylitis (AS), undifferentiated SpA, reactive arthritis, psoriatic arthritis (PsA), juvenile SpA, and inflammatory bowel diseases-associated arthritis (Sieper et al., 2009). These conditions share numerous characteristics, such as the high prevalence of the allele HLA-B27, the absence of the rheumatoid factor and overlapping clinical manifestations, together with a significant familial recurrence.

This research was conducted on two forms of SpA: Ankylosing Spondylitis (AS) and Psoriatic Arthritis (PsA), whose clinical features and pathogenesis will be described.

1.3.1 Clinical manifestations

AS is a common chronic immune-mediated disease characterized by inflammation of the axial skeleton, with early involvement of the sacro-iliac joints. It usually presents with chronic back pain that appears typically before the age of 45, characterised by insidious onset and improvement with exercise. It is often associated with one or more articular features, including peripheral joint synovitis, enthesitis (inflammation of the tendon insertion site) and dactylitis (inflammation of a whole digit caused by flexor tenosynovitis) (Taurog et al., 2016). In AS, inflammation likely originates at the enthesis. Through mechanisms that are still poorly understood, the inflammation leads to erosion and bone proliferation. If untreated, these events lead to ossification of the vertebral ligaments, causing loss of spinal flexibility, deformity and severe disability.

Psoriatic arthritis (PsA) is characterised by synovitis of peripheral joints. The pattern of distribution of the affected joints is very heterogeneous: the inflammation may involve both axial and peripheral joints, often as a polyarthritis or as an oligoarthritis. Approximately 15% of patients with PsA will have psoriasis. Importantly, in PsA the same sequence of inflammation, erosion and bone production in entheseal sites is also seen. Enthesitis, tenosynovitis, and dactylitis also are commonly present.

Both AS and PsA are associated with extra-articular manifestations, with uveitis the most frequent, followed by inflammatory bowel disease.

1.3.2 Pathogenesis of AS and PsA *

1.3.2.1 Immune associated genetics risk in AS and PsA

AS has long been associated with inheritance of the Human Leukocyte Antigen (HLA) allele B27 (Schlosstein et al., 1973), representing one of the strongest genetic associations of any common human disease. Heterozygote HLA-B27 carriage results in an increased odds ratio for AS of approximately 50, while homozygosity has an odds ratio of around 100. The concordance rate in monozygotic twins is 63% and the risk in first degree relative is 8.2% (Brown et al., 2000). Molecular typing has now shown that many closely related forms of HLA-B27 exist, differing at a few amino acid residues only. Nearly 60 subtypes of HLA-B27 have been identified. However, associations with disease are not

* Content from paragraphs 1.3.2.1 to 1.3.2.3 has been published (Simone et al., 2018). The material here reported has been produced by myself, with the publication joint authors providing critical reading. They have given me permission to include the material in this thesis.

clear for many of the subtypes. The subtypes from B*2702 through to B*2710, B*2714, B*2715, B*2719 and B*2730 all have proven associations with spondyloarthropathies, with B*2705 being the commonest in white European individuals. The HLA-B*2706 and HLA-B*2709 subtypes were until recently thought to be protective but a few cases of AS have been reported suggesting that they are not absolutely protective but weakly associated with the development of AS (Cauli et al., 2007). All causative variants produce modification in the biochemical structure, which leads to altered conformation of the HLA heavy chain or to alternative peptide presentation. Even though the majority of patients with AS are HLA-B27 positive, this only accounts for approximately 30% of the total heritability of the disease, which is estimated to be in the region of 90% (as emerged from study on twins) (Bowness, 2015). Thus whilst B27 is the most important single gene by far, it contributes the minority of the total genetic risk. Many of these other genetic variants are shared with other immune-mediated conditions, some of which often seen in overlap with AS. The most recent genome-wide association study has now implicated over 40 genes in providing susceptibility to AS (International Genetics of Ankylosing Spondylitis Consortium (IGAS) et al., 2013).

Genetic variation in a gene encoding endoplasmic reticulum aminopeptidase 1 (*ERAP1*), involved in peptide trimming for presentation on HLA class I. is also associated with AS (Evans et al., 2011). Other important associated genes are involved in the so-called interleukin-17 (IL-17)/interleukin-23 (IL-23) inflammatory axis. The two cytokines are physiologically linked, since IL-23 signalling through the IL-23 receptor (IL-23R) on $CD4^+$ T-helper cells is required for the differentiation and expansion of Th17 cells (McGeachy et al.,

2009). Polymorphisms of the *IL23R* and also of the surrounding regulatory region have been strongly associated with the risk of developing AS (Roberts et al., 2016), IBD and psoriasis, reinforcing the concept of a common pathogenic role involving the IL-17/23 axis. It was later shown that the protective allele coded for a loss of function mutation resulting in defective signalling and decreased Th17 cells (Di Meglio et al., 2011). The IL-23R receptor signals via downstream signalling cascades including Stat3 and Tyk2 (Cho et al., 2006). Polymorphisms in these molecules have also shown disease susceptibility in AS (International Genetics of Ankylosing Spondylitis Consortium (IGAS) et al., 2013). Other polymorphisms observed in AS patients are found in genes with a possible indirect effect on the same pathway (*IL6R* gene), in genes involved in T cell proliferation and survival (*EOMES*, *RUNX3* and *TBX21*), or in the innate immunity response, such as *CARD9* (Pointon et al., 2010).

Psoriasis, and psoriatic arthritis, has also long been known to occur in families, and this has confirmed by family studies (Chandran et al., 2009; Myers et al., 2005). A number of associations with specific HLA allele has been identified, the best studied being (HLA)-B7, B13, HLA-B17, HLA-B57, and HLA-Cw*0602 (Gladman et al., 1986). A further classification can be done, to separate the genes conferring risk of developing PsA compared to cutaneous psoriasis alone, for example HLA-C*06:02 was protective for PsA compared with cutaneous psoriasis. Similarly to what is observed in AS, a significant association with amino acid 97 of HLA-B was associated with PsA risk (Bowes et al., 2015). The exact mechanism of the association between HLA antigens and PsA is not clear. Genome-wide association studies in psoriasis (Nair et al., 2009) confirmed associations with non-HLA genes, such as those associated with interleukin (IL)-

23 signaling (*IL23A*, *IL23R*, *IL12B*), as well as two genes that regulate the NF-κB pathway. Studies of individual genes in PsA have investigated for disease association, these include *CARD15* (Rahman et al., 2003), TNF promoter polymorphisms (Reich et al., 2007), *PTPN22* and many others.

1.3.2.2 Immuno-pathogenesis of AS and PsA

Recent genetic and immunological research have highlighted a key role for Th17 cytokine dysregulation in the aetiology of AS, which together with the genetic data and results of clinical trials using immunotherapeutics, strongly supports the concept of SpA as "type 17"-driven inflammatory disease.

Despite intensive research, the pathogenic role of HLA-B27 remains unclear. Three major theories are the "arthritogenic" peptide theory, the cell-surface homodimers hypothesis, and the misfolded B27 hypothesis (**Figure 1.2**).

The "arthritogenic" peptide theory proposes that HLA-B27 plays a central pathogenic role for presentation of joint-specific peptides to $CD8^+$ cytotoxic T cells. Lines of enquiry looked to identify specific self or environmental peptides presented by HLA-B27 that would activate $CD8^+$ cells via the HLA class I pathway. Although chlamydia-specific $CD8^+$ cells can be detected in joints (using HLA-B27 tetramers) in Chlamydia-triggered reactive arthritis (Appel et al., 2004), no convincing arthritogenic peptides have been identified to date in AS. Furthermore, disease still occurs in the B27 transgenic rat model in the absence $CD8^+$ cells (Taurog et al., 2009).

A second theory for the pathogenesis of HLA-B27 in AS stems from the observation that HLA-B27 can misfold in the endoplasmic reticulum (Mear et al., 1999). This misfolding leads to endoplasmic reticulum (ER)-stress which

activates what is known as unfolded protein response (UPR) leading to the upregulation of IL-23 in dendritic cells (DCs) (Goodall et al., 2010), an occurrence that was observed in the transgenic B27 rat model, where HLA-B27 misfolding in macrophages led to upregulation of IL-23 (DeLay et al., 2009). However, in AS patients, studies of gut biopsies did not show evidence of upregulated unfolded protein response genes transcription, but instead autophagy (the intracellular response seen in macrophages to improperly folded proteins for degradation) (Ciccia et al., 2014). The role of the UPR in HLA-B27 driven inflammation is therefore yet unproven.

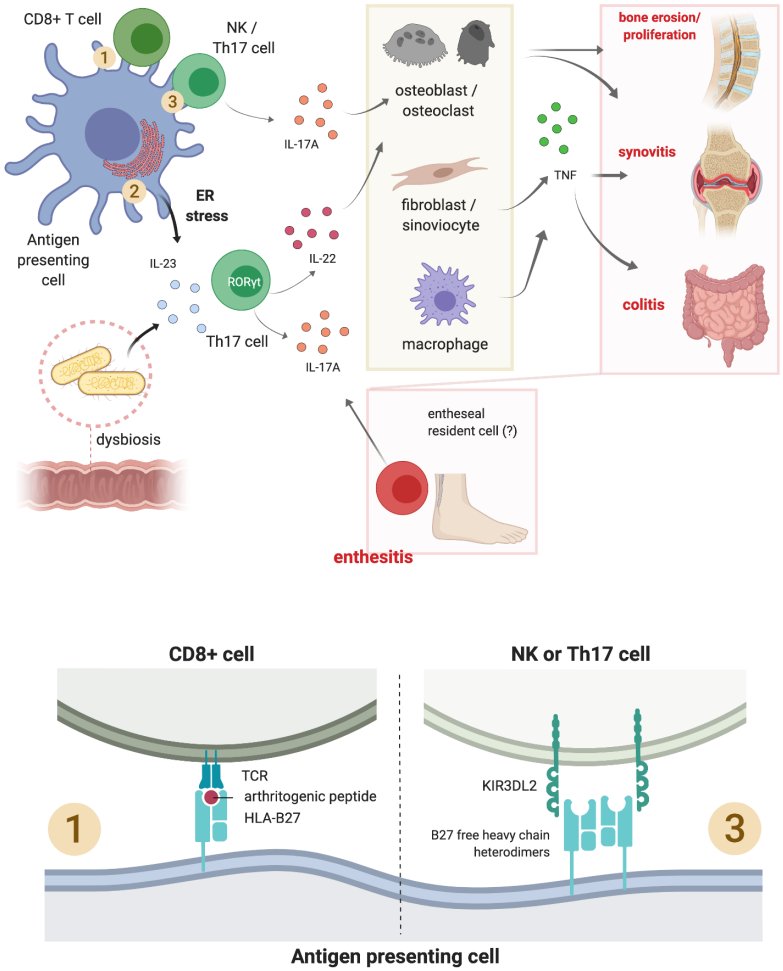

Figure 1.2. Proposed pathogenic mechanisms in ankylosing spondylitis (modified from Simone et al., 2018). The three hypothesis connecting HLA-B27 to the pathogenesis of AS are shown: (1) 'arthritogenic' peptide presentation; (2) misfolded HLA-B27 leading to ER stress or UPR (3) cell-surface homodimers. A recent body of evidences supports the importance of HLA-B27-induced intestinal dysbiosis, resulting in over-expression of the IL-17A/IL-23 axis. This leads to production of IL-17A, IL-22, TNF-α, interferon-γ and other cytokines that target organs and tissues directly or through tissue-resident effector cells.

The third major theory for the pathogenesis of HLA-B27 in AS revolves around the ability of HLA-B27 to aberrantly fold to form homodimers (Allen et al., 1999) or beta-2-microglobulin free heavy chains on the cell surface (Bird et al., 2003). Aberrant forms of HLA-B27 can be recognised in vitro by Killer-Immunoglobulin-like receptors (KIRs) (Kollnberger et al., 2002). These receptors are primarily expressed on NK cells but are also expressed on circulating CD4 T cells (Lanier, 2005). HLA-B27 individuals with AS and HLA-B27 healthy donors have been shown to have a higher frequency of T cells expressing this receptor and these cells are polarised towards a Th17 phenotype (see below), with high levels of IL-17A produced (Bowness et al., 2011). In further work it was shown that this receptor is expressed on $CD4^+$ T cells after activation and i induces transcription of the Th17 TF ROR-γt (Ridley et al., 2016) following direct binding. This body of work linked HLA-B27 with the Th17 immune pathway for the first time.

Lastly, HLA-B27 may have an indirect effect in disease causation through altering the individual's microbiome (Asquith et al., 2019).

Less is known about the pathogenic events that occur in patients not carrying HLA-B27, although interestingly recent genetic evidence, analysing many thousands of patients and controls suggests that the nature of the aminoacid residue position 97 of an individual's HLA class I molecules may be critical for disease predisposition.

In PsA, evidences suggest that the initiating phenomenon could be related to tissue-specific factors and by innate immune mechanisms originating in the skin or in the sites of mechanical stress in the enthesis (McGonagle et al.,

2001), that would trigger a response that involves adaptive immunity cells among which are Th17 $CD4^+$ T cells and $CD8^+$ T cells.

1.3.2.3 Role of T helper 17 and "type 17" immunity

As described, $CD4^+$ T cells are released as naïve $CD4^+$ cells into the circulation and to lymphoid organs, where they differentiate into the different types of effector T cells. Th17 were added to the T helper subset paradigm around 2005 (Harrington et al., 2005b). The key physiological effector function of these cells is thought to be immunity against extracellular bacteria and fungal infections. The effector functions of Th17 are mediated through the release of cytokines such as IL-17A, the signature cytokine of the lineage, and IL-17F, in addition to IL-22. The differentiation of Th17 is driven by a combination of cytokines, such as IL-1β, IL-6, TGF- β and IL-23. Th17 cells show considerable plasticity and heterogeneity, and some cells are more pathogenic than others, in part due to production of additional inflammatory cytokines. In fact IL-17A cytokine production is often coupled with IL-22, IFN-γ and GM-CSF (El-Behi et al., 2011) in the same cell. Recently, genes that confer pathogenicity to murine Th17 cells have been described (Gaublomme et al., 2015). However, the characterisation of human multipotent Th17 is quite recent, including reports of IL-23R+ Th17 cells (Ramesh et al., 2014), akin to pathogenic mouse Th17 cells, Th17 GM-CSF producers, with have a putative pathogenic role in SpA (Al-Mossawi et al., 2017) and previously IFN-γ+ Th17 cells, often found in the inflammatory environment (eg. RA SF) and termed "Th17.1", or "non classical Th1" (Nistala et al., 2010; Basdeo et al., 2017), but the transcriptional determinant of Th17 pathogenicity have not been unveiled. The cytokine repertoire and

transcriptional profile of Th17 cells has been described also in other lymphocyte subsets in AS. CD161-expressing $CD8^+$ T cells (Gracey et al., 2016), $\gamma\delta$ T-cells (Kenna et al., 2012) and innate lymphoid cells (ILCs) (Cua and Tato, 2010) have shown to make IL-17A. The possible contribution of these cells subsets to the pathogenesis of AS, besides their production of IL-17A, has been explored only very recently.

In PsA, the pattern of proinflammatory cytokines observed in the peripheral blood, in the synovial and in synovial fluid is similar to that observed in AS, with Th17 increased both in $CD4^+$, often able to produce multiple inflammatory cytokines (Wade et al., 2019) and $CD8^+$ (the so called Tc17) (Steel et al., 2020). Increase of other type 17 cells, such as group 3 innate lymphoid cells (ILC3) was observed in psoriatic synovial fluid (Leijten et al., 2015) and skin (Villanova et al., 2014), together with natural killer cells (McQueen et al., 1994).

One of the most specific pathological features of all SpA-related conditions is inflammation at the enthesis (the site of attachment of bone into tendon or ligament) (McGonagle et al., 1998). This reason for this peculiar disease localisation remains poorly understood, but it might be triggered by mechanical stress, and that local inflammation can be associated with dysregulation of normal homeostatic repair mechanisms at this site. A possible connection between this site and Th17 responses was suggested by a study that identified murine entheseal cells able to respond to IL-23 and to mediate spinal and peripheral inflammation via IL-17 production (Sherlock et al., 2012). The existence of these cell populations in humans has not yet been established, although other cell types with similar potential of producing IL-17 family cytokines

upon stimulation have been found in the human enthesis (Cuthbert et al., 2017, 2019).

1.3.2.4 Myeloid cells in SpA

Myeloid cells, including DCs and macrophages, sample the antigen, induce T-cell differentiation through cell–cell interactions and modify the environment secreting soluble mediators, among which IL-1β, IL-6, IL-23, all known to induce Th17 responses.

In the B27-TG experimental model (Taurog et al., 1999), DCs were found altered and promoted preferentially Th17 responses. Dysregulated myeloid-derived mediators promoting Th17 included overexpression of IL-23 (DeLay et al., 2009). Strong evidences of pathogenic role of myeloid cells in the human disease are not numerous. DCs from both AS patients and healthy controls' PB released similar levels of IL-23 and IL-12 after toll-like receptor TLR stimulation, while AS macrophages showed augmented response (Zeng et al., 2011). In the tissue, IL-23 expression was elevated in intestinal samples from patients with AS or Crohn's disease (Ciccia et al., 2009), but it was not specified whether the source were infiltrating mononuclear cells, or DCs migrating from the lymph nodes. An intracellular protein found in the neutrophil cytosol, calprotectin, was found elevated in the gut of AS patients and proposed as a surrogate marker for intestinal inflammation (Cypers et al., 2016). More recently, myeloid cells in the spinal enthesis of healthy subjects have been identified as capable to produce IL-23 locally (Bridgewood et al., 2019), while previously a molecule regulating Stat1 signalling was described in the murine enthesis-resident myeloid cells (Wilde et al., 2017).

The actual relevance of IL-23 in the pathogenesis of the human disease is currently debated, in particular whether the Th17 responses seen in SpA are dependent from IL-23. Although blocking with monoclonal antibodies directed against the p40 and p19 subunit proved effective in certain SpA-associated manifestations such as skin psoriasis and enthesitis, its potential has been reconsidered after the failure (Baeten et al., 2018) in improving the axial symptoms of AS, suggesting tissue-related differences in response.

1.3.2.5 Intracellular kinase signalling pathways

In inflammatory disorders, targeting intracellular signalling pathway leading to cytokine production and release has attracted great therapeutic interest. There is an argument for treating SpA patients with small molecule inhibitors of these pathways, considering that several disease driving cytokines are controlled by this pathway, and that genetic variants of signalling intermediates have been described in AS and PsA. In a series of in vitro experiments on SpA patient-derived PBMCs, JAK inhibitors were effective in suppressive inflammatory responses, including IL-17A production (Hammitzsch et al., 2018). While tofacitinib (a JAK1/3 inhibitor) has shown little efficacy in a placebo-controlled trial in AS (van der Heijde et al., 2017), it is approved in PsA (Gladman et al., 2017). Very recently, an inhibitor of TYK2, an intracellular mediator of IL-23 signalling (together with mediating signal from the type 1 IFN receptor, IL-10 family receptors and IL-12R), has shown promise in an experimental model of SpA (Gracey et al., 2020). There is still remarkable interest in identifying new targets for small molecules, although more research is needed to identify which

pathways are crucial in SpA pathogenesis, and how the genetic variants associated to the disease (*STAT3*, *TYK2*) affect them functionally.

1.3.2.6 Regulatory T cells (Tregs) in SpA

The best studied SpA experimental model, the B27-TG rat, reproduces clinical but also biological aspects of the human disease, such as the overexpression of Th17 cells (Glatigny et al., 2012). A defect of regulatory T cells was also observed, with Tregs being characterised by a higher IL-17/IL-10 ratio (Araujo et al., 2014).

In humans, SpA patients have been reported to have similar frequencies of $CD4^+CD25^+$ Tregs in peripheral blood compared to healthy control in two studies (Appel et al., 2011; Cao et al., 2004), whereas another study reported reduced number of Tregs compared with HLA-B27-positive healthy donors. Currently, there is no overall consensus regarding Tregs in the peripheral circulation, and a recent metanalysis (Lai et al., 2019), noted how, in the various reports published so far in AS, different flow cytometric parameters have been used to define Tregs. In the synovial fluid of AS patients, a significant increase in Tregs was found compared with peripheral blood (Appel et al., 2011), potentially indicating recruitment of Tregs to this site of inflammation. Synovial Tregs preserved their suppressive activity and effectively inhibited proliferation of effector T cells (Cao et al., 2004). Little is known about the composition of Tregs in the SF and tissue during an SpA flare, or how the tissue microenvironment influences their phenotype and functionality.

In a study focusing on another organ affected by SpA, the terminal ileum, a high number of $CD4^+$ $CD25^+$ $CD127^{low}$ Tregs was identified (Ciccia et al., 2010).

The majority of these cells were able to produce IL-10, suggesting a putative role in the regulation of intestinal inflammation.

Few more studies reporting Tregs features in other inflammatory arthritic conditions are available. A phenotypic and functional analysis of Tregs in RA (Walter et al., 2016) did not identify intrinsic defects, whereas the description of a dysregulated Treg subset expressing CD161 Tregs in Juvenile Idiopatic Arthritis revealed the existence of Tregs with inflammatory characteristics in the SF (Pesenacker et al., 2013), and a similar phenotype was described in RA (Afzali et al., 2013). An altered post-transcriptional control of *FOXP3* secondary to inflammatory mediators (eg TNF) in the microenvironment was proposed as explanation for the Treg defect in RA (Nie et al., 2013). Specific anti-arthritic treatments seem to restore the efficacy of Treg suppression, as proposed for TNF inhibitors (Nguyen and Ehrenstein, 2016), and methotrexate (Cribbs et al., 2015).

1.4 NOVEL APPROACHES TO IMMUNOPHENOTYPE ANALYSIS IN HUMAN DISEASES

1.4.1 High resolution proteomics with flow and mass cytometry

Aimed at the characterization of cell populations based on the identification of surface and intracellular protein markers, fluorescence-activated cell sorting (FACS) is a widely used tool for studies of the phenotype and function of immune cells. By evaluating several cell markers using flurochrome-tagged antibodies together, different cell populations can be identified and enumerated with a single experiment, offering characterization of vast areas of

immune system in the course of the disease. Further aadvancements have made possible to define, thanks to the detection of intracellular proteins and functional readouts, dynamic cell states together with distinct cell types. Lately, mass cytometry, a cytometry platform that uses antibodies conjugated to metal isotopes instead of fluorescent dyes, has expanded the number of parameters simultaneously detected, allowing higher-dimensional phenotypic and functional analysis of single cells.

A limitation of flow and mass cytometry is the variation across batches and laboratories. Significant variation can also be attributed to gating. In order to overcome limitations arising from manual analysis, automated methods for visualisation and analysis of high dimensional data have been developed (Kimball et al., 2018).

Secondly, the number of analytes that can be detected with flow and mass cytometry is still limited compared to the cellular proteome. Furthermore, cell membrane markers are useful to classify cell types, but only partially capture the complexity of cellular processes and the diversity of states. Sequencing the messenger RNA pool, or the transcriptome, provides the best approximation of the full range of functional proteins in the cell.

1.4.2 Single cell transcriptomics

In the recent years, remarkable advancements in microfluidics technologies, cell capture and RNA amplification have rendered the characterisation of a complex, heterogeneous population of immune cells finally possible. Thanks to single cell RNA sequencing technologies, researchers can

now profile the transcriptome of individual cells at unprecedented detail without any pre-existing assumption or expectance of pre-selected markers. Furthermore, the improved capture efficiency allows detailed catalogue of the cells found in small samples that have been traditionally difficult to analyse, such as tissues biopsies. This has spurred to the creation of collaborative cell atlases, among which the Human Cell Atlas (Regev et al., 2017).

A further advancement is a multimodal approach, or multiomics, that is to perform different assays in parallel on the same cell (for example protein and mRNA expression (Macaulay et al., 2017)): the additional layer provides information about the RNA status and of the visible phenotype of the cell at the same time, and helps offering a more comprehensive view of the cell.

1.4.3 T-cell receptor sequencing

One fundamental aspect of the characterisation of immune responses is the determination of the TCR repertoire. As the TCR does not mutate after the T cell egresses the thymus, the CDR3 region can serve as a molecular tag for tracing and identifying T cell with identical aminoacid sequence. Messenger RNA species coding for specific CDR3 regions can be in fact amplified and sequenced just like any normal mRNA. Single-cell methods provide both CDR3 sequences and the composition of the TCR chain pairs, both elements necessary to accurately define clonotypes and impute antigen specificity. In conditions where a clonal expansion is seen, such as autoimmune diseases and cancer, this allows to define T cell receptor diversity and to discover clonal expansion in specific organs. Recent adaption of single cell protocols, such as the 5’ technology by 10x

Genomics (which barcodes the 5’ end of the mRNA molecule to provide improved coverage of the CDR3 region) pair TCR information with gene expression matrices, permitting simultaneous profiling of the cell transcriptional program and its immune repertoire.

1.5 THESIS AIMS

1.5.1 To describe the frequency and the phenotype of Tregs in SpA patients compared to controls, both in the peripheral blood and synovial fluid

1.5.2 To define the single cell gene expression landscape of Tregs in the peripheral blood and synovial fluid in patients with active SpA, and to identify clonally restricted regulatory responses

1.5.3 To characterise tissue- and disease-specific Treg subsets revealed by the unsupervised analysis in order to identify novel mechanisms of suppression with therapeutic potential

1.5.4 To evaluate the in vitro efficacy of a novel Mitogen-Activated Protein Kinase (MAPK)-associated Kinase 2 antagonist in suppressing the inflammatory T cell responses

1.6 REFERENCES

Cauli, A., Vacca, A., Mameli, A., Passiu, G., Fiorillo, M.T., Sorrentino, R., Mathieu., A (2007). A Sardinian patient with ankylosing spondylitis and HLA-B*2709 co-occurring with HLA-B*1403 (Arthritis Rheum).

Afzali, B., Mitchell, P.J., Edozie, F.C., Povoleri, G.A.M., Dowson, S.E., Demandt, L., Walter, G., Canavan, J.B., Scotta, C., Menon, B., et al. (2013). CD161 expression characterizes a subpopulation of human regulatory T cells that produces IL-17 in a STAT3-dependent manner: Cellular immune response. European Journal of Immunology *43*, 2043–2054.

Allen, R.L., O'Callaghan, C.A., McMichael, A.J., and Bowness, P. (1999). Cutting edge: HLA-B27 can form a novel beta 2-microglobulin-free heavy chain homodimer structure. J. Immunol. *162*, 5045–5048.

Al-Mossawi, M.H., Chen, L., Fang, H., Ridley, A., Wit, J., Yager, N., Hammitzsch, A., Pulyakhina, I., Fairfax, B.P., Simone, D., et al. (2017). Unique transcriptome signatures and GM-CSF expression in lymphocytes from patients with spondyloarthritis. Nature Communications *8*, 1510.

Appel, H., Kuon, W., Kuhne, M., Wu, P., Kuhlmann, S., Kollnberger, S., Thiel, A., Bowness, P., and Sieper, J. (2004). Use of HLA-B27 tetramers to identify low-frequency antigen-specific T cells in Chlamydia-triggered reactive arthritis. Arthritis Res. Ther. *6*, R521-534.

Appel, H., Wu, P., Scheer, R., Kedor, C., Sawitzki, B., Thiel, A., Radbruch, A., Sieper, J., and Syrbe, U. (2011). Synovial and peripheral blood CD4+FoxP3+ T cells in spondyloarthritis. J. Rheumatol. *38*, 2445–2451.

Araujo, L.M., Fert, I., Jouhault, Q., Labroquère, K., Andrieu, M., Chiocchia, G., and Breban, M. (2014). Increased Production of Interleukin-17 Over Interleukin-10 by Treg Cells Implicates Inducible Costimulator Molecule in Experimental Spondyloarthritis: Imbalanced Production of IL-10 and IL-17 by Treg Cells from HLA-B27-Transgenic Rats. Arthritis & Rheumatology *66*, 2412–2422.

Arce Vargas, F., Furness, A.J.S., Litchfield, K., Joshi, K., Rosenthal, R., Ghorani, E., Solomon, I., Lesko, M.H., Ruef, N., Roddie, C., et al. (2018). Fc Effector Function Contributes to the Activity of Human Anti-CTLA-4 Antibodies. Cancer Cell *33*, 649-663.e4.

Asquith, M., Sternes, P.R., Costello, M.-E., Karstens, L., Diamond, S., Martin, T.M., Li, Z., Marshall, M.S., Spector, T.D., Cao, K.-A. le, et al. (2019). HLA Alleles Associated With Risk of Ankylosing Spondylitis and Rheumatoid Arthritis Influence the Gut Microbiome. Arthritis & Rheumatology *71*, 1642–1650.

Bacher, P., Heinrich, F., Stervbo, U., Nienen, M., Vahldieck, M., Iwert, C., Vogt, K., Kollet, J., Babel, N., Sawitzki, B., et al. (2016). Regulatory T Cell Specificity Directs Tolerance versus Allergy against Aeroantigens in Humans. Cell *167*, 1067-1078.e16.

Baecher-Allan, C., Brown, J.A., Freeman, G.J., and Hafler, D.A. (2001). CD4+CD25high regulatory cells in human peripheral blood. J Immunol *167*, 1245–1253.

Baeten, D., Østergaard, M., Wei, J.C.-C., Sieper, J., Järvinen, P., Tam, L.-S., Salvarani, C., Kim, T.-H., Solinger, A., Datsenko, Y., et al. (2018). Risankizumab, an IL-23 inhibitor, for ankylosing spondylitis: results of a randomised, double-blind, placebo-controlled, proof-of-concept, dose-finding phase 2 study. Annals of the Rheumatic Diseases *77*, 1295–1302.

Basdeo, S.A., Cluxton, D., Sulaimani, J., Moran, B., Canavan, M., Orr, C., Veale, D.J., Fearon, U., and Fletcher, J.M. (2017). Ex-Th17 (Nonclassical Th1) Cells Are Functionally Distinct from Classical Th1 and Th17 Cells and Are Not Constrained by Regulatory T Cells. The Journal of Immunology *198*, 2249–2259.

Bird, L.A., Peh, C.A., Kollnberger, S., Elliott, T., McMichael, A.J., and Bowness, P. (2003). Lymphoblastoid cells express HLA-B27 homodimers both intracellularly and at the cell surface following endosomal recycling. Eur. J. Immunol. *33*, 748–759.

Bluestone, J.A., Buckner, J.H., Fitch, M., Gitelman, S.E., Gupta, S., Hellerstein, M.K., Herold, K.C., Lares, A., Lee, M.R., Li, K., et al. (2015). Type 1 diabetes immunotherapy using polyclonal regulatory T cells. Sci Transl Med *7*, 315ra189.

Bossini-Castillo, L., Glinos, D.A., Kunowska, N., Golda, G., Lamikanra, A., Spitzer, M., Soskic, B., Cano-Gamez, E., Smyth, D.J., Cattermole, C., et al. (2019). Immune disease variants modulate gene expression in regulatory CD4+ T cells and inform drug targets. BioRxiv 654632.

Bowes, J., Budu-Aggrey, A., Huffmeier, U., Uebe, S., Steel, K., Hebert, H.L., Wallace, C., Massey, J., Bruce, I.N., Bluett, J., et al. (2015). Dense genotyping of immune-related susceptibility loci reveals new insights into the genetics of psoriatic arthritis. Nature Communications *6*, 6046.

Bowness, P. (2015). HLA-B27. Annual Review of Immunology *33*, 29–48.

Bowness, P., Ridley, A., Shaw, J., Chan, A.T., Baeza, I.W., Fleming, M., Cummings, F., McMichael, A., and Kollnberger, S. (2011). Th17 cells expressing KIR3DL2+ and responsive to HLA-B27 homodimers are increased in Ankylosing Spondylitis. J Immunol *186*, 2672–2680.

Bridgewood, C., Watad, A., Russell, T., Palmer, T.M., Marzo-Ortega, H., Khan, A., Millner, P.A., Dunsmuir, R., Rao, A., Loughenbury, P., et al. (2019). Identification of myeloid cells in the human enthesis as the main source of local IL-23 production. Annals of the Rheumatic Diseases *78*, 929–933.

Brown, M.A., Laval, S.H., Brophy, S., and Calin, A. (2000). Recurrence risk modelling of the genetic susceptibility to ankylosing spondylitis. Ann. Rheum. Dis. *59*, 883–886.

Brown, M.A., Kenna, T., and Wordsworth, B.P. (2016). Genetics of ankylosing spondylitis--insights into pathogenesis. Nat Rev Rheumatol *12*, 81–91.

Brunkow, M.E., Jeffery, E.W., Hjerrild, K.A., Paeper, B., Clark, L.B., Yasayko, S.A., Wilkinson, J.E., Galas, D., Ziegler, S.F., and Ramsdell, F. (2001). Disruption of a new

forkhead/winged-helix protein, scurfin, results in the fatal lymphoproliferative disorder of the scurfy mouse. Nat. Genet. *27*, 68–73.

Burchill, M.A., Yang, J., Vogtenhuber, C., Blazar, B.R., and Farrar, M.A. (2007). IL-2 receptor beta-dependent STAT5 activation is required for the development of Foxp3+ regulatory T cells. J. Immunol. *178*, 280–290.

Cao, D., van Vollenhoven, R., Klareskog, L., Trollmo, C., and Malmström, V. (2004a). CD25brightCD4+ regulatory T cells are enriched in inflamed joints of patients with chronic rheumatic disease. Arthritis Res. Ther. *6*, R335-346.

Cao, D., van Vollenhoven, R., Klareskog, L., Trollmo, C., and Malmström, V. (2004b). CD25brightCD4+ regulatory T cells are enriched in inflamed joints of patients with chronic rheumatic disease. Arthritis Res. Ther. *6*, R335-346.

Cebula, A., Seweryn, M., Rempala, G.A., Pabla, S.S., McIndoe, R.A., Denning, T.L., Bry, L., Kraj, P., Kisielow, P., and Ignatowicz, L. (2013). Thymus-derived regulatory T cells contribute to tolerance to commensal microbiota. Nature *497*, 258–262.

Chandran, V., Schentag, C.T., Brockbank, J.E., Pellett, F.J., Shanmugarajah, S., Toloza, S.M.A., Rahman, P., and Gladman, D.D. (2009). Familial aggregation of psoriatic arthritis. Ann. Rheum. Dis. *68*, 664–667.

Chaudhry, A., Rudra, D., Treuting, P., Samstein, R.M., Liang, Y., Kas, A., and Rudensky, A.Y. (2009). CD4+ regulatory T cells control TH17 responses in a Stat3-dependent manner. Science *326*, 986–991.

Chaudhry, A., Samstein, R.M., Treuting, P., Liang, Y., Pils, M.C., Heinrich, J.-M., Jack, R.S., Wunderlich, F.T., Brüning, J.C., Müller, W., et al. (2011). Interleukin-10 signaling in regulatory T cells is required for suppression of Th17 cell-mediated inflammation. Immunity *34*, 566–578.

Cho, M.-L., Kang, J.-W., Moon, Y.-M., Nam, H.-J., Jhun, J.-Y., Heo, S.-B., Jin, H.-T., Min, S.-Y., Ju, J.-H., Park, K.-S., et al. (2006). STAT3 and NF-κB Signal Pathway Is Required for IL-23-Mediated IL-17 Production in Spontaneous Arthritis Animal Model IL-1 Receptor Antagonist-Deficient Mice. The Journal of Immunology *176*, 5652–5661.

Ciccia, F., Bombardieri, M., Principato, A., Giardina, A., Tripodo, C., Porcasi, R., Peralta, S., Franco, V., Giardina, E., Craxi, A., et al. (2009). Overexpression of interleukin-23, but not interleukin-17, as an immunologic signature of subclinical intestinal inflammation in ankylosing spondylitis. Arthritis Rheum. *60*, 955–965.

Ciccia, F., Accardo-Palumbo, A., Giardina, A., Di Maggio, P., Principato, A., Bombardieri, M., Rizzo, A., Alessandro, R., Ferrante, A., Principe, S., et al. (2010). Expansion of intestinal CD4+CD25(high) Treg cells in patients with ankylosing spondylitis: a putative role for interleukin-10 in preventing intestinal Th17 response. Arthritis Rheum. *62*, 3625–3634.

Ciccia, F., Accardo-Palumbo, A., Rizzo, A., Guggino, G., Raimondo, S., Giardina, A., Cannizzaro, A., Colbert, R.A., Alessandro, R., and Triolo, G. (2014). Evidence that autophagy, but not the unfolded protein response, regulates the expression of IL-23

in the gut of patients with Ankylosing Spondylitis and subclinical gut inflammation. Ann Rheum Dis *73*, 1566–1574.

Cipolletta, D., Feuerer, M., Li, A., Kamei, N., Lee, J., Shoelson, S.E., Benoist, C., and Mathis, D. (2012). PPAR-γ is a major driver of the accumulation and phenotype of adipose tissue Treg cells. Nature *486*, 549–553.

Cribbs, A.P., Kennedy, A., Penn, H., Amjadi, P., Green, P., Read, J.E., Brennan, F., Gregory, B., and Williams, R.O. (2015). Methotrexate Restores Regulatory T Cell Function Through Demethylation of the FoxP3 Upstream Enhancer in Patients With Rheumatoid Arthritis: MTX RESTORATION OF Treg CELL SUPPRESSION IN RA. Arthritis & Rheumatology *67*, 1182–1192.

Cua, D.J., and Tato, C.M. (2010). Innate IL-17-producing cells: the sentinels of the immune system. Nature Reviews Immunology *10*, 479–489.

Cuthbert, R.J., Fragkakis, E.M., Dunsmuir, R., Li, Z., Coles, M., Marzo-Ortega, H., Giannoudis, P.V., Jones, E., El-Sherbiny, Y.M., and McGonagle, D. (2017). Brief Report: Group 3 Innate Lymphoid Cells in Human Enthesis. Arthritis & Rheumatology (Hoboken, N.J.) *69*, 1816–1822.

Cuthbert, R.J., Watad, A., Fragkakis, E.M., Dunsmuir, R., Loughenbury, P., Khan, A., Millner, P.A., Davison, A., Marzo-Ortega, H., Newton, D., et al. (2019). Evidence that tissue resident human enthesis γδT-cells can produce IL-17A independently of IL-23R transcript expression. Ann. Rheum. Dis. *78*, 1559–1565.

Cypers, H., Varkas, G., Beeckman, S., Debusschere, K., Vogl, T., Roth, J., Drennan, M.B., Lavric, M., Foell, D., Cuvelier, C.A., et al. (2016). Elevated calprotectin levels reveal bowel inflammation in spondyloarthritis. Annals of the Rheumatic Diseases *75*, 1357–1362.

DeLay, M.L., Turner, M.J., Klenk, E.I., Smith, J.A., Sowders, D.P., and Colbert, R.A. (2009). HLA-B27 Misfolding and the Unfolded Protein Response Augment IL-23 Production and are Associated with Th17 Activation in Transgenic Rats. Arthritis Rheum *60*, 2633–2643.

Di Meglio, P., Di Cesare, A., Laggner, U., Chu, C.-C., Napolitano, L., Villanova, F., Tosi, I., Capon, F., Trembath, R.C., Peris, K., et al. (2011). The IL23R R381Q gene variant protects against immune-mediated diseases by impairing IL-23-induced Th17 effector response in humans. PLoS ONE *6*, e17160.

DiSpirito, J.R., Zemmour, D., Ramanan, D., Cho, J., Zilionis, R., Klein, A.M., Benoist, C., and Mathis, D. (2018). Molecular diversification of regulatory T cells in nonlymphoid tissues. Sci Immunol *3*.

Ebinuma, H., Nakamoto, N., Li, Y., Price, D.A., Gostick, E., Levine, B.L., Tobias, J., Kwok, W.W., and Chang, K.-M. (2008). Identification and In Vitro Expansion of Functional Antigen-Specific CD25+ FoxP3+ Regulatory T Cells in Hepatitis C Virus Infection. Journal of Virology *82*, 5043–5053.

El-Behi, M., Ciric, B., Dai, H., Yan, Y., Cullimore, M., Safavi, F., Zhang, G.-X., Dittel, B.N., and Rostami, A. (2011). The encephalitogenicity of T(H)17 cells is dependent

on IL-1- and IL-23-induced production of the cytokine GM-CSF. Nat. Immunol. *12*, 568–575.

Evans, D.M., Spencer, C.C.A., Pointon, J.J., Su, Z., Harvey, D., Kochan, G., Oppermann, U., Opperman, U., Dilthey, A., Pirinen, M., et al. (2011). Interaction between ERAP1 and HLA-B27 in ankylosing spondylitis implicates peptide handling in the mechanism for HLA-B27 in disease susceptibility. Nat. Genet. *43*, 761–767.

Fontenot, J.D., Gavin, M.A., and Rudensky, A.Y. (2003). Foxp3 programs the development and function of CD4+CD25+ regulatory T cells. Nat. Immunol. *4*, 330–336.

Fontenot, J.D., Rasmussen, J.P., Williams, L.M., Dooley, J.L., Farr, A.G., and Rudensky, A.Y. (2005). Regulatory T cell lineage specification by the forkhead transcription factor foxp3. Immunity *22*, 329–341.

Gagliani, N., Magnani, C.F., Huber, S., Gianolini, M.E., Pala, M., Licona-Limon, P., Guo, B., Herbert, D.R., Bulfone, A., Trentini, F., et al. (2013). Coexpression of CD49b and LAG-3 identifies human and mouse T regulatory type 1 cells. Nature Medicine *19*, 739–746.

Gaublomme, J.T., Yosef, N., Lee, Y., Gertner, R.S., Yang, L.V., Wu, C., Pandolfi, P.P., Mak, T., Satija, R., Shalek, A.K., et al. (2015). Single-Cell Genomics Unveils Critical Regulators of Th17 Cell Pathogenicity. Cell *163*, 1400–1412.

Gladman, D., Rigby, W., Azevedo, V.F., Behrens, F., Blanco, R., Kaszuba, A., Kudlacz, E., Wang, C., Menon, S., Hendrikx, T., et al. (2017). Tofacitinib for Psoriatic Arthritis in Patients with an Inadequate Response to TNF Inhibitors. New England Journal of Medicine *377*, 1525–1536.

Gladman, D.D., Anhorn, K.A., Schachter, R.K., and Mervart, H. (1986). HLA antigens in psoriatic arthritis. J. Rheumatol. *13*, 586–592.

Glatigny, S., Fert, I., Blaton, M.A., Lories, R.J., Araujo, L.M., Chiocchia, G., and Breban, M. (2012). Proinflammatory Th17 cells are expanded and induced by dendritic cells in spondylarthritis-prone HLA-B27-transgenic rats. Arthritis Rheum. *64*, 110–120.

Glocker, E.-O., Kotlarz, D., Boztug, K., Gertz, E.M., Schäffer, A.A., Noyan, F., Perro, M., Diestelhorst, J., Allroth, A., Murugan, D., et al. (2009). Inflammatory bowel disease and mutations affecting the interleukin-10 receptor. N. Engl. J. Med. *361*, 2033–2045.

Goodall, J.C., Wu, C., Zhang, Y., McNeill, L., Ellis, L., Saudek, V., and Gaston, J.S.H. (2010). Endoplasmic reticulum stress-induced transcription factor, CHOP, is crucial for dendritic cell IL-23 expression. PNAS *107*, 17698–17703.

Gracey, E., Qaiyum, Z., Almaghlouth, I., Lawson, D., Karki, S., Avvaru, N., Zhang, Z., Yao, Y., Ranganathan, V., Baglaenko, Y., et al. (2016). IL-7 primes IL-17 in mucosal-associated invariant T (MAIT) cells, which contribute to the Th17-axis in ankylosing spondylitis. Annals of the Rheumatic Diseases *75*, 2124–2132.

Gracey, E., Hromadová, D., Lim, M., Qaiyum, Z., Zeng, M., Yao, Y., Srinath, A., Baglaenko, Y., Yeremenko, N., Westlin, W., et al. (2020). TYK2 inhibition reduces type 3 immunity and modifies disease progression in murine spondyloarthritis. J Clin Invest *130*, 1863–1878.

Hammitzsch, A., Chen, L., Wit, J. de, Al-Mossawi, M.H., Ridley, A., Sekine, T., Simone, D., Doig, K., Skapenko, A., and Bowness, P. (2018). Inhibiting ex-vivo Th17 responses in Ankylosing Spondylitis by targeting Janus kinases. Scientific Reports *8*, 15645.

Harrington, L.E., Hatton, R.D., Mangan, P.R., Turner, H., Murphy, T.L., Murphy, K.M., and Weaver, C.T. (2005a). Interleukin 17-producing CD4+ effector T cells develop via a lineage distinct from the T helper type 1 and 2 lineages. Nat. Immunol. *6*, 1123–1132.

Harrington, L.E., Hatton, R.D., Mangan, P.R., Turner, H., Murphy, T.L., Murphy, K.M., and Weaver, C.T. (2005b). Interleukin 17-producing CD4+ effector T cells develop via a lineage distinct from the T helper type 1 and 2 lineages. Nat. Immunol. *6*, 1123–1132.

Havel, J.J., Chowell, D., and Chan, T.A. (2019). The evolving landscape of biomarkers for checkpoint inhibitor immunotherapy. Nat Rev Cancer *19*, 133–150.

van der Heijde, D., Deodhar, A., Wei, J.C., Drescher, E., Fleishaker, D., Hendrikx, T., Li, D., Menon, S., and Kanik, K.S. (2017). Tofacitinib in patients with ankylosing spondylitis: a phase II, 16-week, randomised, placebo-controlled, dose-ranging study. Annals of the Rheumatic Diseases annrheumdis–2016.

Hippen, K.L., Merkel, S.C., Schirm, D.K., Sieben, C.M., Sumstad, D., Kadidlo, D.M., McKenna, D.H., Bromberg, J.S., Levine, B.L., Riley, J.L., et al. (2011). Massive ex vivo expansion of human natural regulatory T cells (T(regs)) with minimal loss of in vivo functional activity. Sci Transl Med *3*, 83ra41.

Hori, S., Nomura, T., and Sakaguchi, S. (2003). Control of regulatory T cell development by the transcription factor Foxp3. Science *299*, 1057–1061.

Hsieh, C.-S., Zheng, Y., Liang, Y., Fontenot, J.D., and Rudensky, A.Y. (2006). An intersection between the self-reactive regulatory and nonregulatory T cell receptor repertoires. Nat. Immunol. *7*, 401–410.

Huber, S., Gagliani, N., Esplugues, E., O'Connor, W., Huber, F.J., Chaudhry, A., Kamanaka, M., Kobayashi, Y., Booth, C.J., Rudensky, A.Y., et al. (2011). Th17 cells express interleukin-10 receptor and are controlled by $Foxp3^{-}$ and Foxp3+ regulatory CD4+ T cells in an interleukin-10-dependent manner. Immunity *34*, 554–565.

Humrich, J.Y., Spee-Mayer, C. von, Siegert, E., Bertolo, M., Rose, A., Abdirama, D., Enghard, P., Stuhlmüller, B., Sawitzki, B., Huscher, D., et al. (2019). Low-dose interleukin-2 therapy in refractory systemic lupus erythematosus: an investigator-initiated, single-centre phase 1 and 2a clinical trial. The Lancet Rheumatology *1*, e44–e54.

International Genetics of Ankylosing Spondylitis Consortium (IGAS), Cortes, A., Hadler, J., Pointon, J.P., Robinson, P.C., Karaderi, T., Leo, P., Cremin, K., Pryce, K.,

Harris, J., et al. (2013). Identification of multiple risk variants for ankylosing spondylitis through high-density genotyping of immune-related loci. Nat. Genet. *45*, 730–738.

Ivanov, I.I., McKenzie, B.S., Zhou, L., Tadokoro, C.E., Lepelley, A., Lafaille, J.J., Cua, D.J., and Littman, D.R. (2006). The orphan nuclear receptor RORgammat directs the differentiation program of proinflammatory IL-17+ T helper cells. Cell *126*, 1121–1133.

James, K.R., Gomes, T., Elmentaite, R., Kumar, N., Gulliver, E.L., King, H.W., Stares, M.D., Bareham, B.R., Ferdinand, J.R., Petrova, V.N., et al. (2020). Distinct microbial and immune niches of the human colon. Nature Immunology *21*, 343–353.

Kalekar, L.A., Cohen, J.N., Prevel, N., Sandoval, P.M., Mathur, A.N., Moreau, J.M., Lowe, M.M., Nosbaum, A., Wolters, P.J., Haemel, A., et al. (2019). Regulatory T cells in skin are uniquely poised to suppress profibrotic immune responses. Science Immunology *4*.

Karwacz, K., Miraldi, E.R., Pokrovskii, M., Madi, A., Yosef, N., Wortman, I., Chen, X., Watters, A., Carriero, N., Awasthi, A., et al. (2017). Critical role of IRF1 and BATF in forming chromatin landscape during type 1 regulatory cell differentiation. Nature Immunology *18*, 412–421.

Kenna, T.J., Davidson, S.I., Duan, R., Bradbury, L.A., McFarlane, J., Smith, M., Weedon, H., Street, S., Thomas, R., Thomas, G.P., et al. (2012). Enrichment of circulating interleukin-17–secreting interleukin-23 receptor–positive γ/δ T cells in patients with active ankylosing spondylitis. Arthritis & Rheumatism *64*, 1420–1429.

Kim, B.-S., Lu, H., Ichiyama, K., Chen, X., Zhang, Y.-B., Mistry, N.A., Tanaka, K., Lee, Y., Nurieva, R., Zhang, L., et al. (2017). Generation of RORγt+ antigen-specific T regulatory 17 (Tr17) cells from Foxp3+ precursors in autoimmunity. Cell Rep *21*, 195–207.

Kimball, A.K., Oko, L.M., Bullock, B.L., Nemenoff, R.A., Dyk, L.F. van, and Clambey, E.T. (2018). A Beginner's Guide to Analyzing and Visualizing Mass Cytometry Data. The Journal of Immunology *200*, 3–22.

Kitagawa, Y., Ohkura, N., Kidani, Y., Vandenbon, A., Hirota, K., Kawakami, R., Yasuda, K., Motooka, D., Nakamura, S., Kondo, M., et al. (2017). Guidance of regulatory T cell development by Satb1-dependent super-enhancer establishment. Nat. Immunol. *18*, 173–183.

Knight, J.C. (2013). Genomic modulators of the immune response. Trends Genet *29*, 74–83.

Koch, M.A., Tucker-Heard, G., Perdue, N.R., Killebrew, J.R., Urdahl, K.B., and Campbell, D.J. (2009). The transcription factor T-bet controls regulatory T cell homeostasis and function during type 1 inflammation. Nat. Immunol. *10*, 595–602.

Kollnberger, S., Bird, L., Sun, M.-Y., Retiere, C., Braud, V.M., McMichael, A., and Bowness, P. (2002). Cell-surface expression and immune receptor recognition of HLA-B27 homodimers. Arthritis Rheum. *46*, 2972–2982.

Komatsu, N., Okamoto, K., Sawa, S., Nakashima, T., Oh-hora, M., Kodama, T., Tanaka, S., Bluestone, J.A., and Takayanagi, H. (2014). Pathogenic conversion of Foxp3+ T cells into TH17 cells in autoimmune arthritis. Nat. Med. *20*, 62–68.

Lai, N.-L., Zhang, S.-X., Wang, J., Zhang, J.-Q., Wang, C.-H., Gao, C., and Li, X.-F. (2019). The Proportion of Regulatory T Cells in Patients with Ankylosing Spondylitis: A Meta-Analysis. J Immunol Res *2019*, 1058738.

Lanier, L.L. (2005). NK cell recognition. Annu. Rev. Immunol. *23*, 225–274.

Lathrop, S.K., Bloom, S.M., Rao, S.M., Nutsch, K., Lio, C.-W., Santacruz, N., Peterson, D.A., Stappenbeck, T.S., and Hsieh, C.-S. (2011). Peripheral education of the immune system by colonic commensal microbiota. Nature *478*, 250–254.

Leijten, E.F.A., van Kempen, T.S., Boes, M., Michels-van Amelsfort, J.M.R., Hijnen, D., Hartgring, S.A.Y., van Roon, J.A.G., Wenink, M.H., and Radstake, T.R.D.J. (2015). Brief report: enrichment of activated group 3 innate lymphoid cells in psoriatic arthritis synovial fluid. Arthritis & Rheumatology (Hoboken, N.J.) *67*, 2673–2678.

Lio, C.-W.J., and Hsieh, C.-S. (2008). A two-step process for thymic regulatory T cell development. Immunity *28*, 100–111.

Liu, W., Putnam, A.L., Xu-yu, Z., Szot, G.L., Lee, M.R., Zhu, S., Gottlieb, P.A., Kapranov, P., Gingeras, T.R., de St. Groth, B.F., et al. (2006). CD127 expression inversely correlates with FoxP3 and suppressive function of human CD4 $^{+}$ T reg cells. The Journal of Experimental Medicine *203*, 1701–1711.

Macaulay, I.C., Ponting, C.P., and Voet, T. (2017). Single-Cell Multiomics: Multiple Measurements from Single Cells. Trends in Genetics *33*, 155–168.

Massoud, A.H., Charbonnier, L.-M., Lopez, D., Pellegrini, M., Phipatanakul, W., and Chatila, T.A. (2016). An asthma-associated IL4R variant exacerbates airway inflammation by promoting conversion of regulatory T cells to TH17-like cells. Nat. Med. *22*, 1013–1022.

McGeachy, M.J., Chen, Y., Tato, C.M., Laurence, A., Joyce-Shaikh, B., Blumenschein, W.M., McClanahan, T.K., O'Shea, J.J., and Cua, D.J. (2009). The interleukin 23 receptor is essential for the terminal differentiation of interleukin 17-producing effector T helper cells in vivo. Nat. Immunol. *10*, 314–324.

McGonagle, D., Gibbon, W., and Emery, P. (1998). Classification of inflammatory arthritis by enthesitis. Lancet *352*, 1137–1140.

McGonagle, D., Stockwin, L., Isaacs, J., and Emery, P. (2001). An enthesitis based model for the pathogenesis of spondyloarthropathy. additive effects of microbial adjuvant and biomechanical factors at disease sites. The Journal of Rheumatology *28*, 2155–2159.

McQueen, F.M., Skinner, M.A., Krissansen, G.W., Robinson, E., and Tan, P.L. (1994). Natural killer cell function and expression of beta 7 integrin in psoriatic arthritis. J. Rheumatol. *21*, 2266–2273.

Mear, J.P., Schreiber, K.L., Münz, C., Zhu, X., Stevanović, S., Rammensee, H.-G., Rowland-Jones, S.L., and Colbert, R.A. (1999). Misfolding of HLA-B27 as a Result of Its B Pocket Suggests a Novel Mechanism for Its Role in Susceptibility to Spondyloarthropathies. The Journal of Immunology *163*, 6665–6670.

Miyara, M., Yoshioka, Y., Kitoh, A., Shima, T., Wing, K., Niwa, A., Parizot, C., Taflin, C., Heike, T., Valeyre, D., et al. (2009). Functional Delineation and Differentiation Dynamics of Human CD4+ T Cells Expressing the FoxP3 Transcription Factor. Immunity *30*, 899–911.

Miyara, M., Gorochov, G., Ehrenstein, M., Musset, L., Sakaguchi, S., and Amoura, Z. (2011). Human FoxP3+ regulatory T cells in systemic autoimmune diseases. Autoimmun Rev *10*, 744–755.

Myers, A., Kay, L.J., Lynch, S.A., and Walker, D.J. (2005). Recurrence risk for psoriasis and psoriatic arthritis within sibships. Rheumatology (Oxford) *44*, 773–776.

Nair, R.P., Duffin, K.C., Helms, C., Ding, J., Stuart, P.E., Goldgar, D., Gudjonsson, J.E., Li, Y., Tejasvi, T., Feng, B.-J., et al. (2009). Genome-wide scan reveals association of psoriasis with IL-23 and NF-kappaB pathways. Nat. Genet. *41*, 199–204.

Ng, W.F., Duggan, P.J., Ponchel, F., Matarese, G., Lombardi, G., Edwards, A.D., Isaacs, J.D., and Lechler, R.I. (2001). Human CD4(+)CD25(+) cells: a naturally occurring population of regulatory T cells. Blood *98*, 2736–2744.

Nguyen, D.X., and Ehrenstein, M.R. (2016). Anti-TNF drives regulatory T cell expansion by paradoxically promoting membrane TNF–TNF-RII binding in rheumatoid arthritis. The Journal of Experimental Medicine *213*, 1241–1253.

Nie, H., Zheng, Y., Li, R., Guo, T.B., He, D., Fang, L., Liu, X., Xiao, L., Chen, X., Wan, B., et al. (2013). Phosphorylation of FOXP3 controls regulatory T cell function and is inhibited by TNF-α in rheumatoid arthritis. Nat. Med. *19*, 322–328.

Nistala, K., Adams, S., Cambrook, H., Ursu, S., Olivito, B., de Jager, W., Evans, J.G., Cimaz, R., Bajaj-Elliott, M., and Wedderburn, L.R. (2010). Th17 plasticity in human autoimmune arthritis is driven by the inflammatory environment. Proceedings of the National Academy of Sciences *107*, 14751–14756.

Ohkura, N., Hamaguchi, M., Morikawa, H., Sugimura, K., Tanaka, A., Ito, Y., Osaki, M., Tanaka, Y., Yamashita, R., Nakano, N., et al. (2012). T cell receptor stimulation-induced epigenetic changes and Foxp3 expression are independent and complementary events required for Treg cell development. Immunity *37*, 785–799.

Ohnmacht, C., Park, J.-H., Cording, S., Wing, J.B., Atarashi, K., Obata, Y., Gaboriau-Routhiau, V., Marques, R., Dulauroy, S., Fedoseeva, M., et al. (2015). The microbiota regulates type 2 immunity through ROR t+ T cells. Science *349*, 989–993.

Okada, Y., Eyre, S., Suzuki, A., Kochi, Y., and Yamamoto, K. (2019). Genetics of rheumatoid arthritis: 2018 status. Annals of the Rheumatic Diseases *78*, 446–453.

Pandiyan, P., Zheng, L., Ishihara, S., Reed, J., and Lenardo, M.J. (2007). CD4+CD25+Foxp3+ regulatory T cells induce cytokine deprivation-mediated apoptosis of effector CD4+ T cells. Nat. Immunol. *8*, 1353–1362.

Panduro, M., Benoist, C., and Mathis, D. (2016). Tissue Tregs. Annu. Rev. Immunol. *34*, 609–633.

Park, H., Li, Z., Yang, X.O., Chang, S.H., Nurieva, R., Wang, Y.-H., Wang, Y., Hood, L., Zhu, Z., Tian, Q., et al. (2005). A distinct lineage of CD4 T cells regulates tissue inflammation by producing interleukin 17. Nat. Immunol. *6*, 1133–1141.

Pesenacker, A.M., Bending, D., Ursu, S., Wu, Q., Nistala, K., and Wedderburn, L.R. (2013). CD161 defines the subset of FoxP3+ T cells capable of producing proinflammatory cytokines. Blood *121*, 2647–2658.

Pointon, J.J., Harvey, D., Karaderi, T., Appleton, L.H., Farrar, C., Stone, M.A., Sturrock, R.D., Brown, M.A., and Wordsworth, B.P. (2010). Elucidating the chromosome 9 association with AS; CARD9 is a candidate gene. Genes & Immunity *11*, 490–496.

Polansky, J.K., Kretschmer, K., Freyer, J., Floess, S., Garbe, A., Baron, U., Olek, S., Hamann, A., von Boehmer, H., and Huehn, J. (2008). DNA methylation controls Foxp3 gene expression. Eur. J. Immunol. *38*, 1654–1663.

Pot, C., Apetoh, L., and Kuchroo, V.K. (2011). Type 1 regulatory T cells (Tr1) in autoimmunity. Seminars in Immunology *23*, 202–208.

Povoleri, G.A.M., Nova-Lamperti, E., Scottà, C., Fanelli, G., Chen, Y.-C., Becker, P.D., Boardman, D., Costantini, B., Romano, M., Pavlidis, P., et al. (2018). Human retinoic acid–regulated CD161 + regulatory T cells support wound repair in intestinal mucosa. Nature Immunology 1.

Qureshi, O.S., Zheng, Y., Nakamura, K., Attridge, K., Manzotti, C., Schmidt, E.M., Baker, J., Jeffery, L.E., Kaur, S., Briggs, Z., et al. (2011). Trans-endocytosis of CD80 and CD86: a molecular basis for the cell-extrinsic function of CTLA-4. Science *332*, 600–603.

Rahman, P., Bartlett, S., Siannis, F., Pellett, F.J., Farewell, V.T., Peddle, L., Schentag, C.T., Alderdice, C.A., Hamilton, S., Khraishi, M., et al. (2003). CARD15: a pleiotropic autoimmune gene that confers susceptibility to psoriatic arthritis. Am. J. Hum. Genet. *73*, 677–681.

Ramesh, R., Kozhaya, L., McKevitt, K., Djuretic, I.M., Carlson, T.J., Quintero, M.A., McCauley, J.L., Abreu, M.T., Unutmaz, D., and Sundrud, M.S. (2014). Pro-inflammatory human Th17 cells selectively express P-glycoprotein and are refractory to glucocorticoids. The Journal of Experimental Medicine *211*, 89–104.

Regev, A., Teichmann, S.A., Lander, E.S., Amit, I., Benoist, C., Birney, E., Bodenmiller, B., Campbell, P., Carninci, P., Clatworthy, M., et al. (2017). The Human Cell Atlas. BioRxiv 121202.

Reich, K., Hüffmeier, U., König, I.R., Lascorz, J., Lohmann, J., Wendler, J., Traupe, H., Mössner, R., Reis, A., and Burkhardt, H. (2007). TNF polymorphisms in psoriasis:

association of psoriatic arthritis with the promoter polymorphism TNF*-857 independent of the PSORS1 risk allele. Arthritis Rheum. *56*, 2056–2064.

Ridley, A., Hatano, H., Wong-Baeza, I., Shaw, J., Matthews, K.K., Al-Mossawi, H., Ladell, K., Price, D.A., Bowness, P., and Kollnberger, S. (2016). Activation-Induced Killer Cell Immunoglobulin-like Receptor 3DL2 Binding to HLA-B27 Licenses Pathogenic T Cell Differentiation in Spondyloarthritis. Arthritis & Rheumatology (Hoboken, N.J.) *68*, 901–914.

Roberts, A.R., Vecellio, M., Chen, L., Ridley, A., Cortes, A., Knight, J.C., Bowness, P., Cohen, C.J., and Wordsworth, B.P. (2016). An ankylosing spondylitis-associated genetic variant in the IL23R-IL12RB2 intergenic region modulates enhancer activity and is associated with increased Th1-cell differentiation. Ann Rheum Dis *75*, 2150–2156.

Romagnoli, P., Hudrisier, D., and van Meerwijk, J.P.M. (2002). Preferential recognition of self antigens despite normal thymic deletion of CD4(+)CD25(+) regulatory T cells. J. Immunol. *168*, 1644–1648.

Rubtsov, Y.P., Rasmussen, J.P., Chi, E.Y., Fontenot, J., Castelli, L., Ye, X., Treuting, P., Siewe, L., Roers, A., Henderson, W.R., et al. (2008). Regulatory T cell-derived interleukin-10 limits inflammation at environmental interfaces. Immunity *28*, 546–558.

Sakaguchi, S., Sakaguchi, N., Asano, M., Itoh, M., and Toda, M. (1995). Immunologic self-tolerance maintained by activated T cells expressing IL-2 receptor alpha-chains (CD25). Breakdown of a single mechanism of self-tolerance causes various autoimmune diseases. J. Immunol. *155*, 1151–1164.

Schiering, C., Krausgruber, T., Chomka, A., Fröhlich, A., Adelmann, K., Wohlfert, E.A., Pott, J., Griseri, T., Bollrath, J., Hegazy, A.N., et al. (2014). The Alarmin IL-33 Promotes Regulatory T Cell Function in the Intestine. Nature *513*, 564–568.

Schlosstein, L., Terasaki, P.I., Bluestone, R., and Pearson, C.M. (1973). High Association of an HL-A Antigen, W27, with Ankylosing Spondylitis. New England Journal of Medicine *288*, 704–706.

Schmidt, A., Oberle, N., and Krammer, P.H. (2012). Molecular mechanisms of treg-mediated T cell suppression. Front Immunol *3*, 51.

Sefik, E., Geva-Zatorsky, N., Oh, S., Konnikova, L., Zemmour, D., McGuire, A.M., Burzyn, D., Ortiz-Lopez, A., Lobera, M., Yang, J., et al. (2015). MUCOSAL IMMUNOLOGY. Individual intestinal symbionts induce a distinct population of RORγ^{+} regulatory T cells. Science *349*, 993–997.

Sherlock, J.P., Joyce-Shaikh, B., Turner, S.P., Chao, C.-C., Sathe, M., Grein, J., Gorman, D.M., Bowman, E.P., McClanahan, T.K., Yearley, J.H., et al. (2012). IL-23 induces spondyloarthropathy by acting on ROR-γt+ CD3+CD4−CD8− entheseal resident T cells. Nature Medicine *18*, 1069–1076.

Shevach, E.M., and Thornton, A.M. (2014). tTregs, pTregs, and iTregs: Similarities and Differences. Immunol Rev *259*, 88–102.

Shimizu, J., Yamazaki, S., Takahashi, T., Ishida, Y., and Sakaguchi, S. (2002). Stimulation of CD25(+)CD4(+) regulatory T cells through GITR breaks immunological self-tolerance. Nat. Immunol. *3*, 135–142.

Sieper, J., Rudwaleit, M., Baraliakos, X., Brandt, J., Braun, J., Burgos-Vargas, R., Dougados, M., Hermann, K.-G., Landewé, R., Maksymowych, W., et al. (2009). The Assessment of SpondyloArthritis international Society (ASAS) handbook: a guide to assess spondyloarthritis. Ann. Rheum. Dis. *68 Suppl 2*, ii1-44.

Simone, D., Al Mossawi, M.H., and Bowness, P. (2018). Progress in our understanding of the pathogenesis of ankylosing spondylitis. Rheumatology (Oxford) *57*, vi4–vi9.

Steel, K.J.A., Srenathan, U., Ridley, M., Durham, L.E., Wu, S.-Y., Ryan, S.E., Hughes, C.D., Chan, E., Kirkham, B.W., and Taams, L.S. (2020). Polyfunctional, Proinflammatory, Tissue-Resident Memory Phenotype and Function of Synovial Interleukin-17A+CD8+ T Cells in Psoriatic Arthritis. Arthritis & Rheumatology (Hoboken, N.J.) *72*, 435–447.

Suri-Payer, E., Amar, A.Z., Thornton, A.M., and Shevach, E.M. (1998). CD4+CD25+ T cells inhibit both the induction and effector function of autoreactive T cells and represent a unique lineage of immunoregulatory cells. J. Immunol. *160*, 1212–1218.

Szabo, S.J., Kim, S.T., Costa, G.L., Zhang, X., Fathman, C.G., and Glimcher, L.H. (2000). A novel transcription factor, T-bet, directs Th1 lineage commitment. Cell *100*, 655–669.

Szabo, S.J., Sullivan, B.M., Stemmann, C., Satoskar, A.R., Sleckman, B.P., and Glimcher, L.H. (2002). Distinct effects of T-bet in TH1 lineage commitment and IFN-gamma production in CD4 and CD8 T cells. Science *295*, 338–342.

Tai, X., Cowan, M., Feigenbaum, L., and Singer, A. (2005). CD28 costimulation of developing thymocytes induces Foxp3 expression and regulatory T cell differentiation independently of interleukin 2. Nat. Immunol. *6*, 152–162.

Taurog, J.D., Maika, S.D., Satumtira, N., Dorris, M.L., McLean, I.L., Yanagisawa, H., Sayad, A., Stagg, A.J., Fox, G.M., Lê O'Brien, A., et al. (1999). Inflammatory disease in HLA-B27 transgenic rats. Immunol. Rev. *169*, 209–223.

Taurog, J.D., Dorris, M.L., Satumtira, N., Tran, T.M., Sharma, R., Dressel, R., van den Brandt, J., and Reichardt, H.M. (2009). Spondylarthritis in HLA-B27/human beta2-microglobulin-transgenic rats is not prevented by lack of CD8. Arthritis Rheum. *60*, 1977–1984.

Taurog, J.D., Chhabra, A., and Colbert, R.A. (2016). Ankylosing Spondylitis and Axial Spondyloarthritis. New England Journal of Medicine *374*, 2563–2574.

Todd, J.A., Walker, N.M., Cooper, J.D., Smyth, D.J., Downes, K., Plagnol, V., Bailey, R., Nejentsev, S., Field, S.F., Payne, F., et al. (2007). Robust associations of four new chromosome regions from genome-wide analyses of type 1 diabetes. Nat Genet *39*, 857–864.

Todd, J.A., Evangelou, M., Cutler, A.J., Pekalski, M.L., Walker, N.M., Stevens, H.E., Porter, L., Smyth, D.J., Rainbow, D.B., Ferreira, R.C., et al. (2016). Regulatory T Cell Responses in Participants with Type 1 Diabetes after a Single Dose of Interleukin-2: A Non-Randomised, Open Label, Adaptive Dose-Finding Trial. PLOS Medicine *13*, e1002139.

Togashi, Y., Shitara, K., and Nishikawa, H. (2019). Regulatory T cells in cancer immunosuppression — implications for anticancer therapy. Nature Reviews Clinical Oncology *16*, 356–371.

Villanova, F., Flutter, B., Tosi, I., Grys, K., Sreeneebus, H., Perera, G.K., Chapman, A., Smith, C.H., Di Meglio, P., and Nestle, F.O. (2014). Characterization of innate lymphoid cells in human skin and blood demonstrates increase of NKp44+ ILC3 in psoriasis. J. Invest. Dermatol. *134*, 984–991.

Wade, S.M., Canavan, M., McGarry, T., Low, C., Wade, S.C., Mullan, R.H., Veale, D.J., and Fearon, U. (2019). Association of synovial tissue polyfunctional T-cells with DAPSA in psoriatic arthritis. Ann. Rheum. Dis. *78*, 350–354.

Walter, G.J., Fleskens, V., Frederiksen, K.S., Rajasekhar, M., Menon, B., Gerwien, J.G., Evans, H.G., and Taams, L.S. (2016). Phenotypic, Functional, and Gene Expression Profiling of Peripheral CD45RA+ and CD45RO+ CD4+CD25+CD127 ^{low} Treg Cells in Patients With Chronic Rheumatoid Arthritis: PERIPHERAL Treg CELLS IN CHRONIC RA. Arthritis & Rheumatology *68*, 103–116.

Weiss, J.M., Bilate, A.M., Gobert, M., Ding, Y., Curotto de Lafaille, M.A., Parkhurst, C.N., Xiong, H., Dolpady, J., Frey, A.B., Ruocco, M.G., et al. (2012). Neuropilin 1 is expressed on thymus-derived natural regulatory T cells, but not mucosa-generated induced Foxp3+ T reg cells. J Exp Med *209*, 1723–1742.

Westhovens, R., Robles, M., Ximenes, A.C., Nayiager, S., Wollenhaupt, J., Durez, P., Gomez-Reino, J., Grassi, W., Haraoui, B., Shergy, W., et al. (2009). Clinical efficacy and safety of abatacept in methotrexate-naive patients with early rheumatoid arthritis and poor prognostic factors. Ann. Rheum. Dis. *68*, 1870–1877.

Whibley, N., Tucci, A., and Powrie, F. (2019). Regulatory T cell adaptation in the intestine and skin. Nat. Immunol. *20*, 386–396.

Wilde, K.D., Martens, A., Lambrecht, S., Jacques, P., Drennan, M.B., Debusschere, K., Govindarajan, S., Coudenys, J., Verheugen, E., Windels, F., et al. (2017). A20 inhibition of STAT1 expression in myeloid cells: a novel endogenous regulatory mechanism preventing development of enthesitis. Annals of the Rheumatic Diseases *76*, 585–592.

Wildin, R.S., Ramsdell, F., Peake, J., Faravelli, F., Casanova, J.L., Buist, N., Levy-Lahad, E., Mazzella, M., Goulet, O., Perroni, L., et al. (2001). X-linked neonatal diabetes mellitus, enteropathy and endocrinopathy syndrome is the human equivalent of mouse scurfy. Nat. Genet. *27*, 18–20.

Wing, J.B., and Sakaguchi, S. (2012). Multiple treg suppressive modules and their adaptability. Front Immunol *3*, 178.

Wing, K., Onishi, Y., Prieto-Martin, P., Yamaguchi, T., Miyara, M., Fehervari, Z., Nomura, T., and Sakaguchi, S. (2008). CTLA-4 control over Foxp3+ regulatory T cell function. Science *322*, 271–275.

Wu, Y., Borde, M., Heissmeyer, V., Feuerer, M., Lapan, A.D., Stroud, J.C., Bates, D.L., Guo, L., Han, A., Ziegler, S.F., et al. (2006). FOXP3 Controls Regulatory T Cell Function through Cooperation with NFAT. Cell *126*, 375–387.

Li, X., Kang, N., Zhang, X., Dong, X., Wei, W., Cui, L., Ba, D., He W. (2011). Generation of human regulatory gammadelta T cells by TCRgammadelta stimulation in the presence of TGF-beta and their involvement in the pathogenesis of systemic lupus erythematosus (J Immunol).

Xu, M., Pokrovskii, M., Ding, Y., Yi, R., Au, C., Harrison, O.J., Galan, C., Belkaid, Y., Bonneau, R., and Littman, D.R. (2018). c-MAF-dependent regulatory T cells mediate immunological tolerance to a gut pathobiont. Nature 554, 373-377.

Yadav, M., Louvet, C., Davini, D., Gardner, J.M., Martinez-Llordella, M., Bailey-Bucktrout, S., Anthony, B.A., Sverdrup, F.M., Head, R., Kuster, D.J., et al. (2012). Neuropilin-1 distinguishes natural and inducible regulatory T cells among regulatory T cell subsets in vivo. Journal of Experimental Medicine *209*, 1713–1722.

Yang, B.-H., Hagemann, S., Mamareli, P., Lauer, U., Hoffmann, U., Beckstette, M., Föhse, L., Prinz, I., Pezoldt, J., Suerbaum, S., et al. (2016). Foxp3+ T cells expressing RORγt represent a stable regulatory T-cell effector lineage with enhanced suppressive capacity during intestinal inflammation. Mucosal Immunology *9*, 444–457.

Yang, X.O., Nurieva, R., Martinez, G.J., Kang, H.S., Chung, Y., Pappu, B.P., Shah, B., Chang, S.H., Schluns, K.S., Watowich, S.S., et al. (2008). Molecular antagonism and plasticity of regulatory and inflammatory T cell programs. Immunity *29*, 44–56.

Zeng, L., Lindstrom, M.J., and Smith, J.A. (2011). Ankylosing spondylitis macrophages produce greater interleukin-23 in response to lipopolysaccharide without significant Unfolded Protein Response induction. Arthritis Rheum *63*, 3807–3817.

Zhang, Q., Lu, W., Liang, C.-L., Chen, Y., Liu, H., Qiu, F., and Dai, Z. (2018). Chimeric Antigen Receptor (CAR) Treg: A Promising Approach to Inducing Immunological Tolerance. Front. Immunol. *9*.

Zheng, W., and Flavell, R.A. (1997). The transcription factor GATA-3 is necessary and sufficient for Th2 cytokine gene expression in CD4 T cells. Cell *89*, 587–596.

Zhou, X., Bailey-Bucktrout, S.L., Jeker, L.T., Penaranda, C., Martínez-Llordella, M., Ashby, M., Nakayama, M., Rosenthal, W., and Bluestone, J.A. (2009). Instability of the transcription factor Foxp3 leads to the generation of pathogenic memory T cells in vivo. Nat. Immunol. *10*, 1000–1007.

2 Materials and methods

2.1 PATIENT AND CONTROL RECRUITMENT

Patients with SpA and healthy controls were recruited during clinical care between those attending the Rheumatology Unit of the Nuffield Orthopaedic Centre. Informed consent was obtained for the collection of blood and synovial fluid and demographic and clinical data. Synovial fluid samples were obtained from knee joint aspiration performed for therapeutic reasons. The study was approved by the South Central – Oxford C Research Ethics Committee (IFIA, Immune Function in Inflammatory Arthritis: ethics reference 06/Q1606/139).

2.2 LABORATORY METHODS AND MATERIALS

2.2.1 Mononuclear cell separation from peripheral blood and synovial fluid

Venous blood and synovial fluid were collected in 10 ml tubes containing sodium heparin (BD Vacutainer). Samples were centrifuged to remove plasma and synovial fluid supernatant. The remaining volumes were diluted at a concentration of 1:1 (or 1:2 for synovial fluid) with RPMI 1640 culture medium with the addition of Penicillin 100 U/ml, Streptomycin 100 ug/ml (hereafter called R0), and the mononuclear cells separated by density centrifugation: a maximum of 35 ml of diluted blood/synovial fluid was layered over 15 ml Histopaque (Sigma) in a 50ml falcon tube (BD Falcon), then spun for 20 minutes with no brake. The resulting cell interface, containing the mononuclear cells, was then collected and resuspended in R10 medium, that is R0 supplemented with 10% Fetal Bovine Serum (FBS, Sigma), L-Glutamine 2mM (Gibco), Penicillin 100 U/ml, Streptomycin 100 ug/ml (Gibco) and washed twice by recentrifugation. After staining a small volume aliquot with Trypan Blue (Sigma), cells were counted with the help of a hemocytometer under a light microscope.

2.2.2 Cryopreservation and thawing of mononuclear cells

For medium or long term storage, PBMC or SFMC were centrifuged at 1800 rpm (revolutions per minute) for 5 minutes then suspended in freezing medium (10% DMSO in 90% FBS), at a density of 10^8 cells/ml, in 2 ml cryovials (Grenier Bio One) before being placed in pre-chilled freezing container (Mr Frosty, Nalgene) into a -80 C freezer. For longer-term storage, the vials were transferred to a liquid nitrogen tank.

To recover the frozen PBMC and SFMC, the cryovials were placed at 37°C (in a water bath) to allow thawing of the freezing medium. The content was then transferred to a falcon tube and washed twice with warm R10 by centrifugation. Cells were then counted and used as desired.

2.2.3 Cytokine Bead Array (CBA)

CBA (BD Biosciences) is a flow cytometry application that allows quantification of multiple soluble proteins simultaneously. The analytes are captured by specific phycoerythrin (PE)-conjugated antibodies and by beads of known size and fluorescence, creating “sandwich” complexes. When analysing the sample using flow cytometry, the intensity of PE fluorescence of each sandwich complex reveals the concentration of that protein (against a mix of standards of known concentration)

In this thesis, CBA was used to determine the concentrations of the cytokines IL-17A, IL-17F, IFN-γ, GM-CSF, IL-6 in the culture supernatant after cell based

experiments. CBA was performed according to manufacturers' protocol, except reducing the concentration of the reagents to 25% of the recommended (after protocol optimisation, for reasons of costs). The assay was performed in 96 round-bottom plates. In short, 0.25 μl of cytokine-specific CBA beads were added to 50 μl CBA Wash Buffer per each well, and mixed with 100 μl of the sample. After a one-hour incubation in the dark, 0.25 μl anti-cytokine PE-conjugated antibodies, previously dissolved in 50 μl CBA Wash, were added to the plate, incubated for a further hour, then washed to remove unbound beads and antibodies, and analysed on the flow cytometer.

2.2.4 Magnetic activated cell sorting (MACS) and enrichment

$CD4^+$ isolation was performed using the CD4+ T cell isolation kit II (Miltenyi Biotec), that works by a process of negative magnetic selection. The protocol followed the manufacturer's instructions. In brief, PBMCs or SFMCs were suspended in MACS buffer (PBS, 2mM EDTA, 2% bovine serum albumin, all Sigma) at a density of 10^7 cells/ 40 μl, and then rested with 10 μl of a cocktail of biotin-conjugated antibodies on ice for 10 minutes. Following incubation, 30 μl MACS buffer and □0 μl anti-biotin microbeads were added and the mix rested for further 15 minutes at 4°C. Cells were washed and resuspended in MACS buffer in a volume not inferior to 500 μl. LS columns mounted on a magnet (Miltenyi Biotec) were used for isolation. After rinsing the column, the cell suspension was applied to the column, which was washed three times with the buffer. The eluted

cells, containing the untouched CD4+ cells at a purity of approximately 95%, were washed with MACS buffer and used for subsequent experiments.

For $CD14^+$ magnetic isolation, a positive selection kit (CD14 Microbeads, Miltenyi Biotec) was used. PBMCs were prepared as explained above. For 10^7 cells, cells were suspended in 80 μl of MACS buffer, and 20 μl of CD14-microbeads were added, and the mix incubated for 15 minutes at 4°C. After the washing steps and the column preparation detailed above, the mix was applied to the column. The CD14+ cells, retained in the magnet, were flushed out in 5 ml buffer with the aid of a syringe plunger. Purity of 85-95% was achieved.

2.2.5 Fluorescence staining and flow cytometry analysis

For flow cytometry, samples were prepared washing cells twice in FACS wash (PBS with the addition of 2% FBS) in 96 well U-bottom plates (Corning) or round-bottom polystyrene tubes (BD Biosciences). Typically 0.2-0.5 x 10^6 cells per well or tube were stained. Staining reagents, including flourochrome-conjugated antibodies and/or fixable dyes (2.2.5.1-4) were dissolved in FACS Wash (in a volume of 50 μl of for a number of cells up to 10^7) and the mix added to the cell pellet, mixing thoroughly. Before using them in experiments, antibodies were regularly tested for optimal concentration and, where indicated, isotype controls were used for comparison to estimate background staining.

Cells were then incubated for 20 minutes 4°C, in the dark. In the case of surface staining mixes that included an antibody for LAG-3, incubation was performed at 37°C. Cells were then washes twice with 200 μl FACS wash and resuspended in 200 μl FACS fix (PBS with the addition of 3%

paraformaldehyde) before acquisition.

In case detection of intracellular proteins was desired, after completing the staining for surface markers as described above, cells were permeabilised by resuspending them in a fixation/permeabilization solution (Cytofix/Cytoperm, BD Biosciences) at root temperature for 30 minutes, then washed twice in 200 μl Permwash buffer (BD Biosciences), and finally fixed in FACS fix before being analysed. When staining for Foxp3, a variation of the intracellular staining protocol was adopted, using, instead of Cytofix/Cytoperm and Permwash, the equivalent products in the FOXP3 / TF Staining Buffer Set (Thermofisher). For the detection of intracellular cytokines in T cells, unless otherwise specified, cells were stimulated with 100 ng/ml PMA and 1 μg/ml Ionomycin, together with Monensin (GolgiStop) 1:1500 and Brefeldin A (GolgiPlug) 1:1000 (both BD Biosciences) for four hours at 37°C before the staining.

Sample acquisition was performed on a BD LSR Fortessa flow cytometer. Calibration and setup was done daily with BD FACSDiva CS&T Beads (eBioscience). Compensation was performed using single stained One Comp eBeads (eBioscence), or, for the Viability dye, primary cells. Result were analysed on the FlowJo software (v. 10.6.2, Treestar).

The following antibodies were used, either in staining panels for immunophenotyping experiments, or singularly.

2.2.5.1 Treg phenoyping panel

Antibody	Fluorochrome	Clone	Concentration	Manufacturer
CD3	Brilliant Violet 785	OKT3	1/50	Biolegend
CD4	APC	RPA-T4	1/50	Biolegend
CD25	PE	BC96	1/50	Biolegend
CD127	Brilliant Violet 605	A019D5	1/50	Biolegend
Viability Dye	eFluor780		1/500	Thermofisher
Foxp3 *	Brilliant Violet 421	PCH101	1/50	Invitrogen
IFN-γ *	Alexa Fluor 7007	B27	1/100	Biolegend
IL-17A *	FITC	BL168	1/50	Biolegend
GM-CSF *	PerCP/Cy5.5	BVD2-21C11	1/50	Biolegend

2.2.5.2 Trafficking markers panel

Antibody	Fluorochrome	Clone	Concentration	Manufacturer
CD3	PerCP/Cy5.5	OKT3	1/50	Biolegend
CD4	Alexa Fluor 700	RPA-T4	1/50	Biolegend
CD25	PE	BC96	1/50	Biolegend
CD127	Brilliant Violet 711	A019D5	1/50	Biolegend
CD161	FITC	HP-3G10	1/50	Biolegend
CCR4	Brilliant Violet 605	L291H4	1/100	Biolegend
CCR6	PE/Cy7	G034E3	1/50	Biolegend
CCR7	APC	G043H7	1/50	Biolegend
CCR9	Pe/Dazzle	L053E8	1/50	Biolegend
CXCR3	Brilliant Violet 785	G025H7	1/50	Biolegend
CD45RA	Brilliant Violet 510	HI100	1/50	Biolegend
Viability Dye	eFluor780		1/500	Thermofisher
Foxp3 *	Brilliant Violet 421	PCH101	1/50	Thermofisher

2.2.5.3 Antibodies used for characterisation of functional markers

Antibody	Fluorochrome	Clone	Concentration	Manufacturer
CD137	PE	4B-41	1/50	Biolegend
CD45RA	PerCP/Cy5.5	HI100	1/50	Biolegend
CTLA-4 *	APC	L3D10	1/50	Biolegend
CD27	Brilliant Violet 510	O323	1/50	Biolegend
LAG-3	PE	FAB2319P	1/50	R&D
Granzyme B *	Pe/Dazzle	QA1602	1/50	Biolegend
Granzyme K *	FITC	24C3	1/50	ImmunoTools
Viability Dye	eFluor780		1/500	Thermofisher
Foxp3 *	Brilliant Violet 421	PCH101	1/50	Thermofisher

* Intracellular staining

2.2.5.4 Antibodies used for characterisation of monocyte activation

Antibody	Fluorochrome	Clone	Concentration	Manufacturer
CD14	APC	M5E2	1/50	Biolegend
HLA-DR	PerCP-Cy5.5	L243	1/50	Biolegend
CD80	Brilliant Violet 650	2D10	1/50	Biolegend
CD86	FITC	BU63	1/50	Biolegend
CX3CR1	PE	K0124E1	1/50	Biolegend
CD16	PE/Cy7	3G8	1/50	Biolegend
CD40	Brilliant Violet 421	5C3	1/50	Biolegend
IL-12/23 p40 *	PE	C8.6	1/100	Thermofisher
TNF *	Brilliant Violet 650	MAb11	1/50	Biolegend
Viability Dye	eFluor780		1/500	Thermofisher

2.2.5.5 Antibodies for FACS sorting for single cell RNAseq and cell

Antibody	Fluorochrome	Clone	Concentration	Manufacturer
CD3	PerCP-Cy5.5	OKT3	1/50	Biolegend
CD4	PE/Dazzle	RPA-T4	1/50	Biolegend
CD8a	PE	RPA-T8	1/50	Biolegend
CD45RA	PE/Dazzle	HI100	1/50	Biolegend
CD25	PE	BC96	1/50	Biolegend
CD127	PE/Cy7	A019D5	1/50	Biolegend
Viability Dye	eFluor520		1/250	Thermofisher

2.2.6 Fluorescence activated cell sorting

PBMC and SFMC, isolated as explained, were suspended in FACS sorting buffer (RPMI without phenol red + 2% BSA + 2mM EDTA + Hepes 25mM) at a density of 3 x 10^7 per ml or less. Appropriate amount of antibodies was added and the samples incubated for 30 minutes in the dark. Cells were washed with FACS sorting buffer and resuspended after being put through a 35 μm nylon mesh cell strainer of 5 ml polystyrene tubes (BD Biosciences) to discard cell clumps. A Sony SH800 sorter was used to sort live cells. Before acquisition, single stain controls were used to compensate.

Sorted cells were collected in 5 ml polystyrene tubes kept at 4°C in the sorter collection chamber, or with 1.5 ml Eppendorf tubes filled with 0.75 ml previous half-filled with FACS collection buffer (similar to FACS sorting buffer, with 4% BSA instead of 2%, and no EDTA) if cells were to be used in RNA sequencing, and normal FACS sorting buffer for in vitro functional assays.

2.2.7 Single cell 10x droplet-based RNA processing

2.2.7.1 Cell preparation and sorting

Sorting of the PsA samples was performed by Dr Hussein al Mossawi and Dr Nicole Yager. Samples were processed ex vivo: after cell isolation by density gradient centrifugation, three paired PBMC and SFMC samples from three PsA patients were stained with the following antibodies: CD3-FITC (SK7), CD4-APC (RPA-T4), CD8a-PE (RPA-T8), CD45RA-BV421 (HI100) (all from Biolegend), together with Fixable Viability Dye eFluor780 (eBioscience) on a BD FACS Aria. Memory (CD45RA-) CD4+ CD8- and CD8+CD4- cells were sorted in a 1:1 ratio from both blood and synovial fluid of patients. It was chosen to define memory T cells based on the lack of expression of the naïve marker CD45RA, rather then the expression of CD45RO, although we were aware that we could potentially miss memory T cells that regain CD45RA expression (eg. the so called T effector memory RA, or TEMRA) (Willinger et al., 2005). Further details on the PsA sample processing in Penkava et al., 2020.

Cell sorting of the AS samples was performed by myself with the help of Dr Frank Penkava, following the protocol illustrated in 2.2.6. PBMCs and SFMCs were separated in two aliquots and stained with two different antibody mixes: CD3-PerCP-Cy5.5, CD8a-PE, CD4-PE/Dazzle, CD45RA-PE/Dazzle and CD25-PE, CD127-PE/Cy7, CD3-PerCP-Cy5.5, CD45RA-PE/Dazzle. Dead cell exclusion was done with Fixable Viability Dye eFluor520 (eBioscience). Cells were then acquired and $CD3^-$, memory Tregs, memory $CD4^+$ and memory $CD8^+$ sorted into four tubes, using the sorting strategy illustrated in **Figure 4.12**. After sorting, each subset was stained separately with Fc blocker (concentration 1:20) (TruStain FcX, Biolegend, step performed to prevent unspecific binding with Fc portion of the oligonucleotide-tagged antibodies), rested for 15 minutes, than washed, and then resuspended in buffer to be stained with assigned oligonucleotide-tagged antibodies (concentration 1:200) (TotalSeq C, Biolegend). Cells were washed two more times, then resuspended in FACS collection buffer and kept cold until use.

2.2.7.2 RNA gene expression reaction

After counting viable cells with TC10™ Automated Cell Counter, cells were loaded into 10x Chip and the standard 10x Chromium protocol for the 5' chemistry, which allows concurrent TCR and gene expression profiling of the same cell, was followed according to the manufacturer's instructions.

Cell processing, execution of the 10x protocol including library preparation and sequencing were carried out according to manufacture by the Oxford Genomics Centre Core Facility at the Wellcome Centre for Human Genetics. Standard short-read sequencing of the 10x barcoded library was performed on an Illumina sequencer.

Aiming at sequencing at least 50,000 total cells and expecting a capture efficiency of approximately 30%, approximately 45,000 cells from each of the hashed samples 2, 3, and 4 (Tregs, $CD4^+$ and $CD8^+$) and 15,000 from hashed sample 1 ($CD3^-$) from each sample of origin (PB and SF) were loaded on the 10x chip. The total time taken between the sample acquisition to the RNA library generation was approximately 4 hours.

2.2.7.3 TCR alpha and beta chain reaction

In the 5' 10x Chromium Immune Repertoire technology the enrichment primers are located near the 5' end of the C-region in order to provide batter coverage of the full length V(D)J sequence. The barcoded cDNA molecules from full length V(D)J transcripts are generated in parallel with the rest of the transcriptome. This allows clonotyping, alpha and beta chain pairing and importantly, thanks to the barcoding, attribution to the cell of origin.

2.2.7.4 Sequencing

The oligo-tagged library generated was subsequently sequenced on an Illumina HiSeq 4000 sequencer. Pooled samples were sequenced at a read depth of approximately 30,000 reads per cell for gene expression libraries and 8,500 reads per cell for V(D)J enriched T cell libraries.

2.2.8 Cell-based assays

2.2.8.1 T cell stimulation and culture

PBMCs or isolated $CD4^+$ were plated at a density of 2 x 10^6 cells per milliliter in R10 medium, generally in a volume of 200μl medium in 96-well round-bottom or flat-bottom plate. According to the culture plate used, cells were activated with either soluble anti-CD2, -CD3, -CD28-coated beads (T cell activation/expansion kit, Miltenyi Biotec) at a density of 1:5 bead:cell ratio (experiments in **Chapter 6**), or with plate-bound anti-CD3 (OKT3, 1 μg/ml, Biolegend, added at least 12 hours before cell seeding) and soluble anti-CD28 (CD28.2, 1 μg/ml, Thermofisher) (experiments in **Chapter 5**). For consistency and optimization

2.2.8.2 Monocyte LPS stimulation

PBMCs or isolated CD14+ cells were plated at a concentration of 0.5 x 10^6 cells per well in 96-well round-bottom plate. LPS (LPS-EB, Invivogen) was added at a dose 10 ng/ml. After LPS stimulation, cells were kept in culture overnight. When determination of intracellular cytokine production was desired, brefeldin was added four hours after LPS stimulation.

For experiments that evaluated the effect of LAG-3 ligation on APCs, a recombinant human LAG-3 IgG1 Fc chimera protein (R&D) at a concentration of 2.5 μg/ml was used. As control conditions, a recombinant human IgG1 Fc controls and an anti-human HLA class II (anti-DQ, -DR- DP) (clone Tu39, BD Biosciences) also at 2.5 μg/ml were used. The reagents were added in culture 2 hours before the addition of LPS.

2.2.8.3 Antigen stimulation assay

PBMCs were cultured in 96 well flat-bottom plates at a density of 0.5 x 10^6 cells/well in R10 medium with the following microbial lysates or other stimuli: heat-killed *Salmonella typhimurium* (1:10000, Invivogen), heat-killed *Candida albicans* (1:10000, Invivogen), LPS-EB (10 ng/ml, Invivogen), SEB (1 μg/ml, Sigma) for 16 hours. Control conditions consisted in plate-bound anti-CD3 (1 μg/ml) + soluble anti-CD28 (1 μg/ml). Cells were then harvested, washed and stained with fluorochrome-conjugated antibodies.

2.2.8.4 MK2 inhibition assay

Cells were treated with vehicle (0.1% DMSO) or the MK2 inhibitor (MK2i) CC786012, provided by Celgene (reconstituted in DMSO on receipt and stored at -80°C until used). T cells were activated with activation beads (as explained above) in the presence of cytokines. To determine effect of MK2i on cell division, a CFSE-based proliferation assay was used. Cells were suspended in PBS at a concentration of 10^6 cells/ml and stained with CFSE 5 μM (Celltrace, Thermofisher) for 30 minutes at 37°C in the dark. The reaction was quenched adding five times the original staining volume R10, then cells were the incubated for 5 more minutes. Cells were pelleted after centrifugation to remove the supernatant containing the unbound dye, washed, and counted before being cultured for the uses desired. Proliferation was analyzed with the Proliferation Modeling tool on FlowJo.

To evaluate the cell metabolic fitness in response to MK2i, the colorimetric method PrestoBlue Cell Viability (Thermofisher) was used: 10 μl of PrestoBlue were added to a volume of 90 μl containing cells and culture medium, then rested for three hours. The fluorescence of the analyte, a read of the redox potential of the cell and, more extensively, of its mitochondrial function, was measured on a plate reader.

In experiments performed to evaluate the MK2i effect on cytokine production, 0.2 x 10^6 cells were cultured in 200 μl R10 and stimulated with activation beads and recombinant human IL-2 (100 UI/ml) ("neutral conditions"). "Th17-polarising conditions" were obtained adding IL-1β (20 ng/ml), IL-6 (20 ng/ml), IL-23 (20 ng/ml) (all purchased from Peptrotech).

2.3 ANALYTICAL METHODS AND RESOURCES

2.3.1 scRNA-seq data mapping and pre-processing

Demultiplexing of the Illumina files and generation of fastq files containing the scRNA-seq data were done using the "*mkfastq*" function in the Cell Ranger software package (10x Genomics, v. 2.1, and subsequently v. 3.0). Alignment of scRNA-seq reads to the human reference genome (GRCh38) and transcript quantification were performed using the "*count*" function in Cell Ranger. The V(D)J single cell sequences were similarly mapped and quantified against the GRCh38 reference. The generated consensus annotation files for

each patient and sample type (blood or SF) were then used to construct clonality tables and input files for further downstream analysis.

Downstream analysis of the count matrices was carried out using R and the package Seurat (v. 3.0).

2.3.2 Quality control (QC)

Outlier cells potentially representing low-quality cells or multiple cell captures were removed by excluding barcodes with very low or high library sizes. Thus, cells with either 10% mitochondrial genes, and > 25,000 log-normalized UMIs [*] were removed. Based on the distribution of gene numbers per cell, further thresholds were set: cells with <500 or >3500 genes were discarded from the PsA dataset, and cells with < 250 or >4000 genes from the AS dataset. Cells were further filtered to exclude cells having both *CD4* and *CD8A* gene expression (given the sorting strategy used).

2.3.3 Data processing, visualisation and statistical analysis

2.3.3.1 Harmonisation of gene expression data across samples and different experiments

The analytical strategy used to integrate datasets from different samples and across different experiments uses the Seurat v.3 pipeline (Stuart et al., 2019). The Seurat command "*SCTransform*", was used to log-normalise and

[*] UMI: unique molecular identifier. In 10x Chromium, each input RNA molecule is tagged with a UMI (an oligo sequence) that is used during data analysis to account for PCR amplification bias.

scale the data and to identify variable features in each sample separately. Then, samples were harmonised and integrated to identify shared cell states that are present across different datasets. First, 3000 ‘anchors’ (pairwise gene correspondences between individual cells that have high probability to represent correspondent cell types or biological states) were determined for each pair of samples, then samples were integrated in one object. TCR genes were deliberately excluded from the ‘anchors’, in order to prevent correspondences across cells or clusters based on shared TCR gene loci.

When integrating datasets from different conditions or technologies (like in 4.3.4) removal of unwanted sources of variation across datasets (eg. read depth or mitochondrial mapping percentage) was included in the integration workflow.

A scheme of the computational workflow adopted for the AS single cell dataset is shown in **Figure 4.14**.

2.3.3.2 Dimensionality reduction and clustering

The function “*RunPCA*” was performed on the integrated assay to compute the 30 principal components (PC) based on Seurat elbow plot. Clustering was performed with the functions “*FindNeighbours*” and “*FindClusters*” on the basis of the PCs identified. The resulting clusters were visualized with Uniform Manifold Approximation and Projection (UMAP) to provide dimensionality reduction.

2.3.3.3 Sample demultiplexing

The AS sample was analysed following the CITE-seq pipeline (Stoeckius et al., 2018), which allows simultaneous quantification of the cell transcriptome and of selected surface epitopes. The Seurat demultiplexing function ("*HTODemux"*) was used to deconvolute the hashing library. A negative binomial distribution for each HTO (hashtag oligonucleotide) was calculated and the 0.99 quantile of this distribution was used as a threshold to classify each cell as positive or negative for each HTO. Cells that were positive for more than one HTO are annotated as doublets, with further adjustment based on the log-fold change between the top and second-most abundant HTOs.

2.3.3.4 Differential gene expression and functional profilling

Pairwise differential gene expression comparisons were made across cell clusters or conditions. Differential expression analysis was performed using negative binomial generalized linear model implemented in Seurat, through the command "FindMarkers". Wilcoxon rank-sum test was used to determine differences.

To perform statistical analysis of functional profiles the R package Clusterprofiler was used. Genes with significant differential expression for each pairwise comparison were used as input for the pathway analysis, using the Gene Ontology (Ashburner et al., 2000) or the Reactome Pathway (Fabregat et al., 2018) repositories.

2.3.3.5 TCR mapping

After TCR reconstruction, the proportion of cells having the same clone was compared between sample types for each clone using a Fisher's exact test with Benjamini and Hochberg correction for multiple comparisons. A clone was defined based on the amino acid sequence of complementary determining region 3 (CDR3) of both alpha and beta chains. Cells were filtered to exclude potential multiples, defined as cells with greater than one β chain or 2 α chains. This analysis was performed by Dr Frank Penkava.

2.3.3.6 Statistical analysis and graphical representation

Statistical analysis was performed using the software GraphPad Prism 8.4. Data are presented in the form of bar plots (mean standard error of the mean) or box plots (minimum maximum and interquartile range). Statistical analysis on the scRNA-seq data was performed using the R “Stats” package or the built-in statistical tools for each R package used.

In heat maps, generated with the R packages “Seurat” or “pheatmap”, the marker expression was shown as row-based scaled z-scores for that identity.

Dimensionality reduction of flow cytometry data and t-SNE plot generatin was obtained with the “t-SNE” plugin on FlowJo 10, selecting standard parameters for that release. When the analysis was run on a group of samples, the events in each single flow cytometry files were first downsampled to the lowest common denominator in the dataset to ensure each sample was represented by an equal number of cells, then merged before running the tSNE (t-distributed Stochastic Neighbor Embedding) command.

2.3.3.7 Illustrations

The illustrations have been generated by myself on the Biorender webtool.

2.4 REFERENCES

Ashburner, M., Ball, C.A., Blake, J.A., Botstein, D., Butler, H., Cherry, J.M., Davis, A.P., Dolinski, K., Dwight, S.S., Eppig, J.T., et al. (2000). Gene Ontology: tool for the unification of biology. Nat Genet *25*, 25–29.

Fabregat, A., Jupe, S., Matthews, L., Sidiropoulos, K., Gillespie, M., Garapati, P., Haw, R., Jassal, B., Korninger, F., May, B., et al. (2018). The Reactome Pathway Knowledgebase. Nucleic Acids Res. *46*, D649–D655.

Penkava, F., Velasco-Herrera, M.D.C., Young, M.D., Yager, N., Nwosu, L.N., Pratt, A.G., Lara, A.L., Guzzo, C., Maroof, A., Mamanova, L., et al. (2020). Single-cell sequencing reveals clonal expansions of pro-inflammatory synovial CD8 T cells expressing tissue-homing receptors in psoriatic arthritis. Nature Communications *11*, 4767.

Stoeckius, M., Zheng, S., Houck-Loomis, B., Hao, S., Yeung, B.Z., Mauck, W.M., Smibert, P., and Satija, R. (2018). Cell Hashing with barcoded antibodies enables multiplexing and doublet detection for single cell genomics. Genome Biol *19*.

Willinger, T., Freeman, T., Hasegawa, H., McMichael, A.J., and Callan, M.F.C. (2005). Molecular Signatures Distinguish Human Central Memory from Effector Memory CD8 T Cell Subsets. J Immunol *175*, 5895–5903.

3 Immunophenotypic analysis of Regulatory T cells in Spondyloarthropathy

3.1 INTRODUCTION

In SpA numerous lines of evidence indicate that effector T cells (including Th17) (Ranganathan et al., 2017) are more active or express higher levels of inflammatory cytokines, yet no clear consensus exist about whether the regulatory arm of immunity, represented by Tregs, is intrinsically defective, transiently disabled or normal in the course of the disease. Very few studies focusing on the regulatory T cells' phenotype have been published in the SpA field (Cao et al., 2004a; Appel et al., 2011).

Whether circulating Tregs in SpA have a preferential migratory capacity that favours homing to specific inflammatory sites is an unanswered question. The expression of CCR7 on $CD4^+$ cells mediates the homing to secondary lymphoid organs during antigen-specific responses (Schneider et al., 2007), while CCR9 is a gut trophic chemokine receptor for different T cell subsets (Uehara et al., 2002) and CXCR3, CCR4 and CCR6 mediate trafficking to inflamed tissues in response to chemotactic inflammatory signals (Sallusto et al., 1998; Acosta-

Rodriguez et al., 2007). The expression of these markers, which might constitute an important functional element for Tregs to co-localize effectively with effector T cells and exert suppressive functions (Duhen et al., 2012), will be evaluated in this chapter .

3.2 AIM

The aim of this chapter is to describe the frequency and the phenotype of Tregs in SpA patients and controls, both in the peripheral blood and synovial fluid, with particular focus on differential expression patterns of selected functional and trafficking molecules.

3.3 RESULTS

3.3.1 Frequency and phenotype of Tregs in peripheral blood and synovial fluid of SpA patients

To study Tregs I analysed samples obtained from patients and controls whose characteristics shown in **Table 3.1**. After mononuclear cell separation, surface and intracellular staining and flow cytometric acquisition as detailed in **Methods,** the total Treg frequency, classified as shown in **Figure 3.1** (single, live cells that were $CD3^+$ $CD4^+$ $CD25^+$ $CD127^{low}$)**,** was not different to controls in the peripheral blood. An increased frequency compared to matched PB was observed in the SF (**Figure 3.2A, B**), where they presented enhanced expression

of Foxp3 and CD25. Importantly, the vast majority of Tregs in the SF appeared negative for CD45RA. This indicates that Tregs in the SF are relatively expanded compared to the PB, and are characterized by an activated, memory phenotype **(Figure 3.2C, D)**.

	HC (n=21)	AS (n=32)	PsA (n=20)
Age (years), mean ± *SD	45.5 ± 11.0	44.6 ± 14.9	49.3 ± 13.9
Sex, male (%)	8 (38.1)	23 (71.8)	14 (70.0)
HLA-B27+ number (%)	N/A	26 (81.2) #	n/a
TREATMENT NSAIDs **csDMARDS TNF-inhibitors	 - - -	 15 6 (1 §) 12	 1 17 (4 §) 6
DISEASE ACTIVITY SCORE, mean ± SD BASDAI	 N/A	 4.5 ± 2.4 *	 -
CRP, mean ± SD	N/A	13.6± 31.3	17.0 ± 27.9

Table 3.1. Demographic and clinical characteristics of the AS, PsA and HC subjects studied. **SD*: standard deviation; **NSAIDs: Non steroidal anti-inflammatory drugs; *csDMARDS*: conventional synthetic disease modifying anti-rheumatic drugs. BASDAI: Bath Ankylosing Spondylitis Disease Activity Index; CRP: C-reactive protein. # available in 29 subjects; § in combination with a TNFi; * available in 31 subjects. Disease activity measurements and treatment status intended at the time of the sampe.

3.3.2 Analysis of trafficking markers in the memory compartment shows heterogeneity mirroring the T helper classification

PBMCs were then stained with a multicolor flow cytometry panel, which included chemokine receptors (2.2.5.2**)**. To visualize the distribution of said markers, Treg flow cytometric data from nine AS patients were merged and visualized in a bidimensional tSNE plot (see 2.3.3.6).

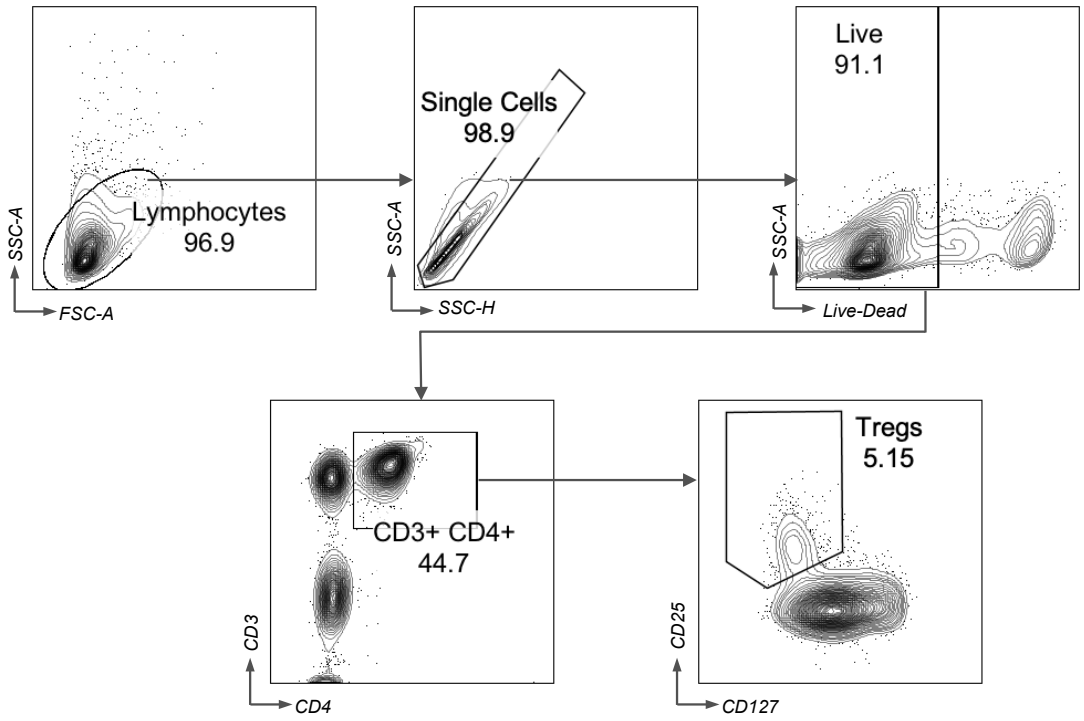

Figure 3.1. Gating strategy for the identification of Tregs in the peripheral blood. Tregs are defined as $CD3^+$ $CD4^+$ $CD25^+$ $CD127^{low}$. Within this population, 74.3% (range 58.7-86.9) of the cells are $Foxp3^+$.

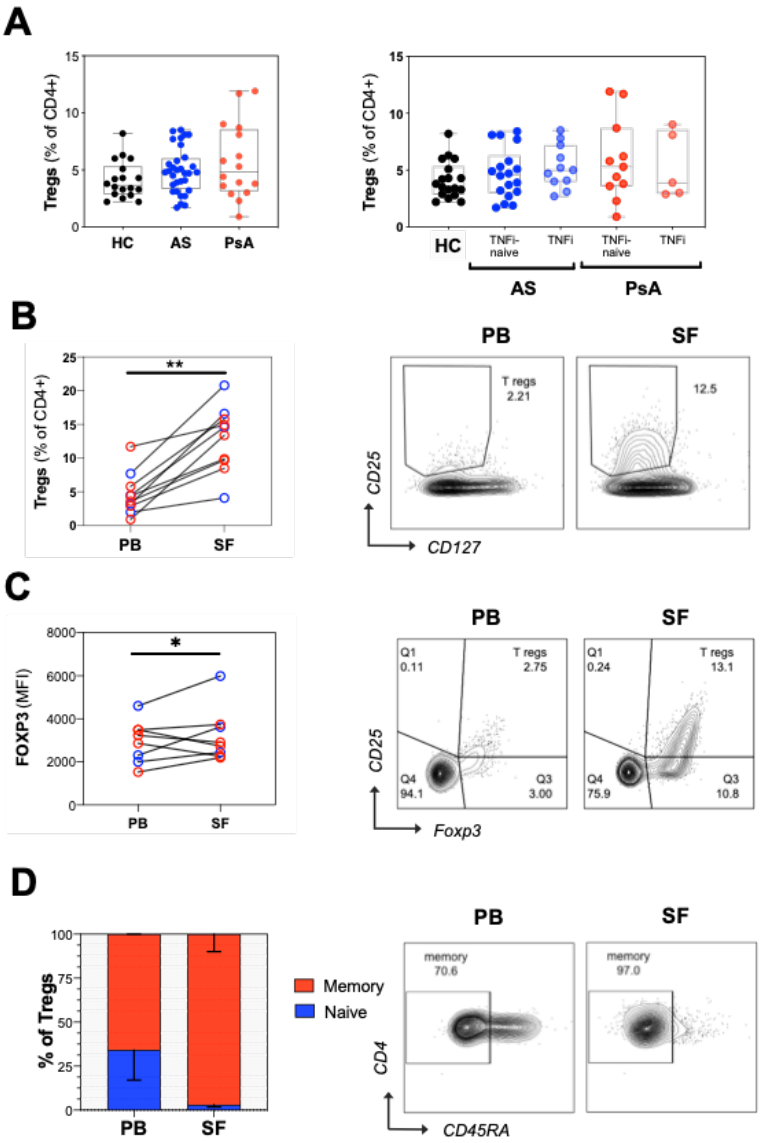

Figure 3.2. Regulatory T cells in peripheral blood of SpA patients are unchanged in frequency compared to HC, but are increased in SF, where they show an activated phenotype. (A) Relative frequency of Tregs ($CD4^+$ $CD25^+$ $CD127^{low}$) in the blood of healthy controls and patients, classified by treatment. (HC n= 18, AS n=32, PsA n=16). **(B-C)** Treg frequency and Foxp3 expression in paired PB and SF samples from SpA patients (n=8, blue dots: AS, red dots: PsA) and example flow cytometry plots. **(D)** Memory/naïve Tregs proportion in PB and SF (based on the expression of CD45RA) (mean of n=3) and example flow cytometry plots gated on live singlet $CD3^+$ $CD4^+$ $CD25^+$ $CD127^{low}$ events. * p≤0.05, ** p≤0.01 (paired t-test).

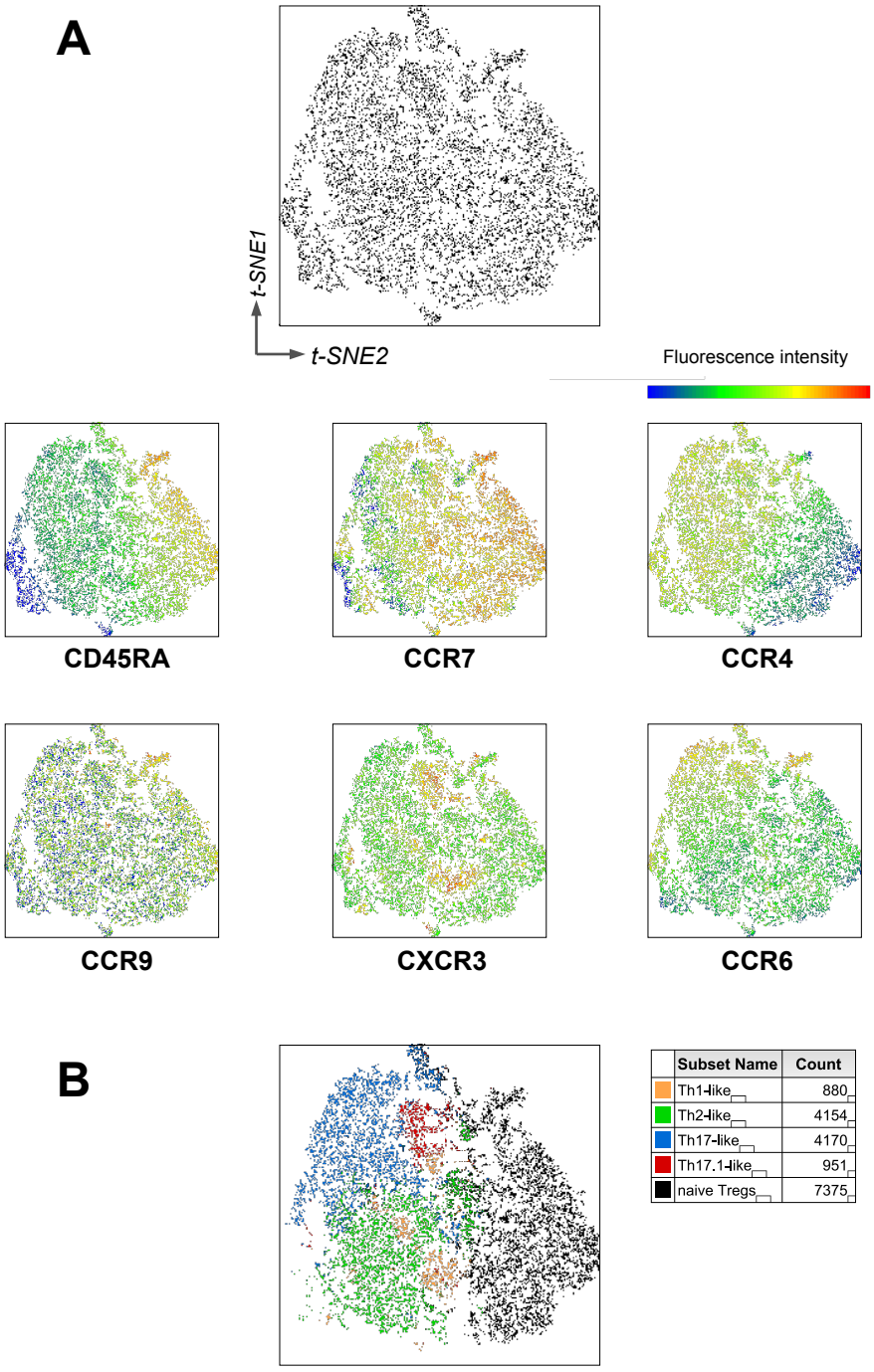

Figure 3.3. Dimensionality reduction allows visualization of Treg trafficking marker heterogeneity. (A) tSNE (t-distributed Stochastic Neighbor Embedding) plot of PB Tregs from n=9 AS patients (18,000 cells), stained with 13 flow cytometry markers including chemokine receptors, with color heatmaps of selected markers (see 2.3.3.6). **(B)** Manually-gated memory T helper-like Tregs (live singlet $CD3^+$ $CD4^+$ $CD25^+$ $CD127^{low}$ $CD45RA^-$) (see **Figure 3.4**) overlaid onto the tSNE space reveal their localization on the bidimensional space.

The distribution of the markers showed a naïve-to-memory gradient (CD45RA), the presence of a small cluster of Tregs expressing CCR9 and considerable areas of overlap for the remaining markers (**Figure 3.3A**), whose distribution did not coincide with a distinct area of the plot.

Using traditional manual gating based on bimodal marker expression, the combination of CCR6, CXCR3 and CCR4 expression within the memory compartment allowed the identification in the circulation of four Treg phenotypes mirroring the four Th cell subsets (**Figure 3.4A**). The majority of memory Tregs was CCR4+, with differential expression of CXCR3 and CCR6. The relative frequencies of the four subsets showed little differences between patients and controls in the PB (**Figure 3.4B**), with the exception of a small increase in Th17/1-like Tregs in PsA. Interestingly, in the SF, in three paired samples, the relative percentage of Th2-like Tregs was increased compared to PB, in parallel with a downregulation of CCR6 and CXCR3 (**Figure 3.4C**).

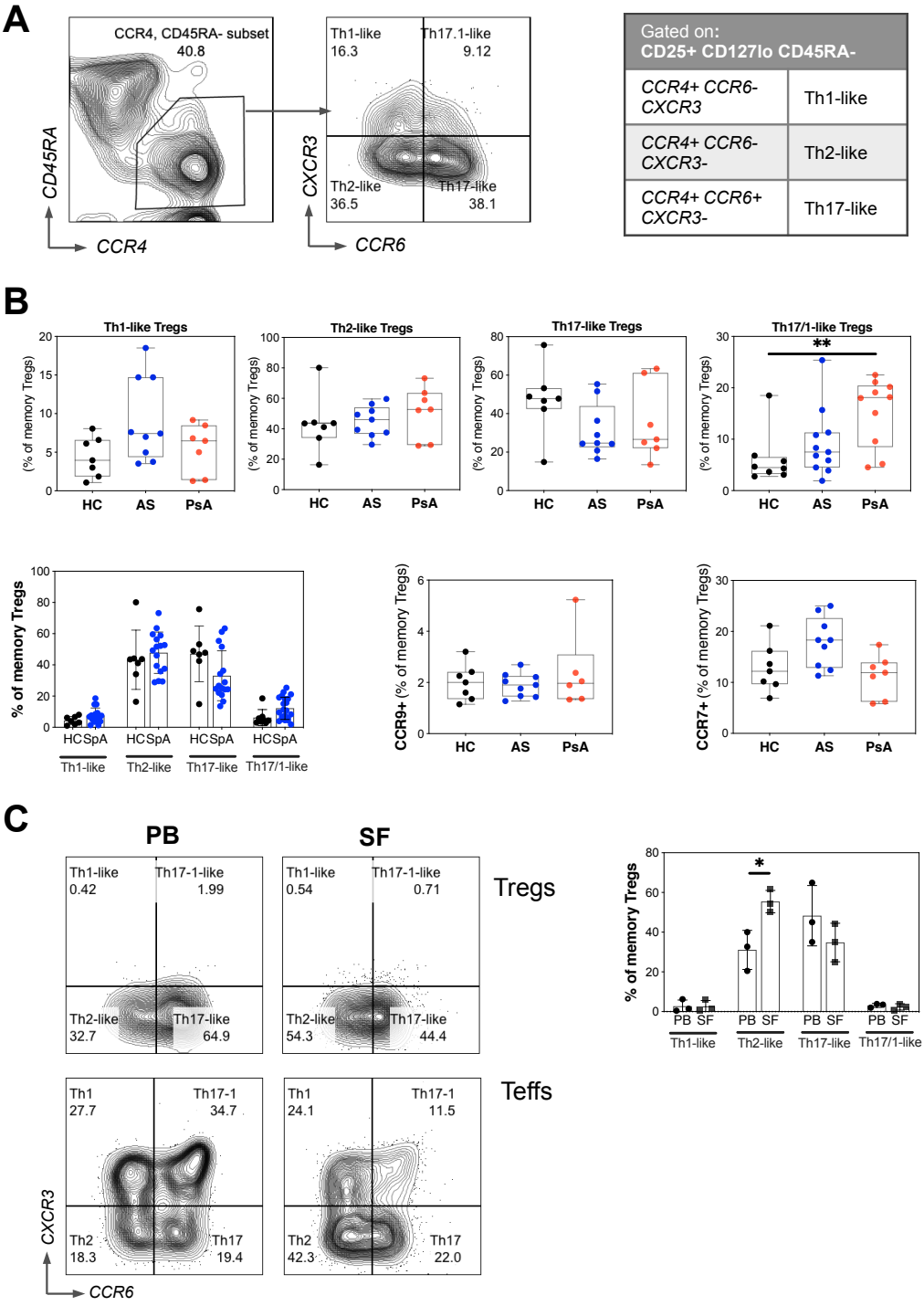

Figure 3.4. Differential expression of trafficking markers identifies four Th-like Treg phenotypes in the peripheral blood and synovial fluid. **(A)** CCR4, CXCR3, and CCR6 expression in memory CD4^{+} CD25^{+} CD127^{low} CD45RA^{-} Tregs. Four Th-like lineages are identified: Th2, Th17, Th1, and Th1/17-like Tregs. **(B)** Frequency of Th-like subsets (defines as in **A**) and of CCR7 and CCR9-expressing memory Tregs (CD4^{+} CD25^{+} CD127^{low} CD45RA^{-}) in HC (n=7-8) compared to SpA (AS n=9, PsA n=7) **(C)** Expression of CCR6 and CXCR3 in CD4^{+} CD25^{+} CD127^{low} CD45RA^{-} in paired PB and SF samples (n=3). * p≤0.05 ** p≤0.01 (One-way ANOVA).

3.3.3 Analysis of markers associated with regulatory function

The following analysis was focused on selected T cell functional and activation markers. Because some were not exclusive of Tregs but also expressed on effector T cells upon exhaustion or activation (eg. CTLA-4, TIGIT), or on non-T helper subsets (eg Granzyme B, CD27), the distribution in memory and naïve T effectors was also assessed. The ex vivo expression of CTLA-4, TIGIT, and of the transcription factor Helios confirmed to be higher on Tregs (**Figure 3.5A**). CD27, a costimulatory marker associated with Treg stability upon in vitro expansion, was elevated in naïve T cells, coherently with its requirement for acquisition of T cell memory (Hendriks et al., 2000). However, at population level in PB, the expression of these markers was not different in patients and controls (**Figure 3.5B**).

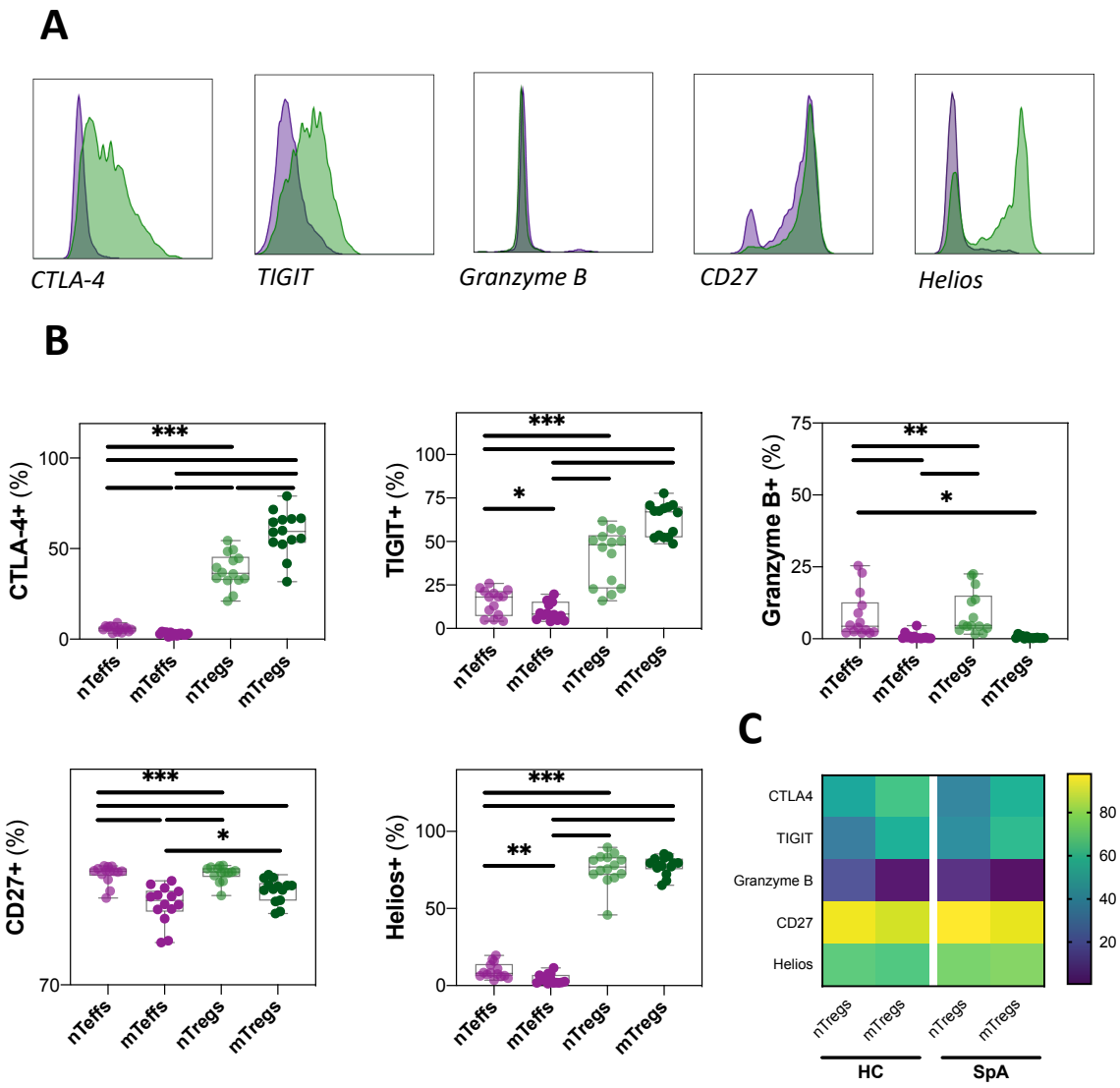

Figure 3.5. Differential expression of immunoregulatory molecules on selected CD4+ T cells subsets from PBMCs. **(A)** Example staining for each of the markers in one PsA PB sample. After gating on live singlet CD3+ CD4+ cells, Tregs (green) are $CD25^{+}$ $CD127^{low}$ and Teffs (purple) $CD25^{-}$ $CD127^{+}$ **(B)** CTLA-4, TIGIT, Granzyme B, CD27, Helios positive cells gated on nTeffs ($CD3^{+}$ $CD4^{+}$ $CD25^{-}$ $CD127^{+}$ $CD45RA^{+}$), mTeffs ($CD3^{+}$ $CD4^{+}$ $CD25^{-}$ $CD127^{+}$ $CD45RA^{-}$), nTregs ($CD3^{+}$ $CD4^{+}$ $CD25^{+}$ $CD127^{low}$ $CD45RA^{+}$), mTregs ($CD3^{+}$ $CD4^{+}$ $CD25^{+}$ $CD127^{low}$ $CD45RA^{-}$) (n=14 SpA). **(C)** Heatmap showing percentage of positive cells in HC (n=4) and SpA (n=14). * p≤0.05, ** p≤0.01, *** p≤0.01 (One-way ANOVA).

3.3.4 Intracellular staining of Tregs shows increased IL-17A production in SpA, associated with the expression of CD161

Figure 3.6A and **B** show that a higher number of Tregs in the PB of SpA patients is able to produce IL-17A upon stimulation, and this feature is strictly associated with the expression of CD161, consistent with previous reports (Pesenacker et al., 2013). CD161+ Tregs were not increased in the peripheral blood of SpA patients. I then investigater whether an imbalance in the T effector/Treg ratio could be observed across type 17 immune subsets. The ratio $CD161^+$ Teffs/$CD161^+$ Tregs was not altered in SpA and neither was the Th17 Teff/Th17-like Treg ratio, but the global Th17/Treg ratio was increased in AS and PsA (**Figure 3.6C, D**). This could suggest that in the PB these specialised Treg subsets are present in equal proportion in healthy and patients, but the capacity of produce IL-17A by Tregs in the course of the disease might indicate a skewing towards inflammatory responses.

3.3.5 Treatment with TNF inhibitors causes mild phenotypic changes in Tregs

I stained matched PBMC samples from eight patients before commencement of TNF inhibitor treatment and three months after. All patients showed clinical response to treatment. No difference was seen in Treg frequency, neither in the proportion of memory cells within Tregs. A small increase in Foxp3 expression was observed. When studying the Teff/Treg ratio within the Th17, Th17-1 and CD161+ subgroups, no significant variation was seen after the treatment (**Figure 3.7**).

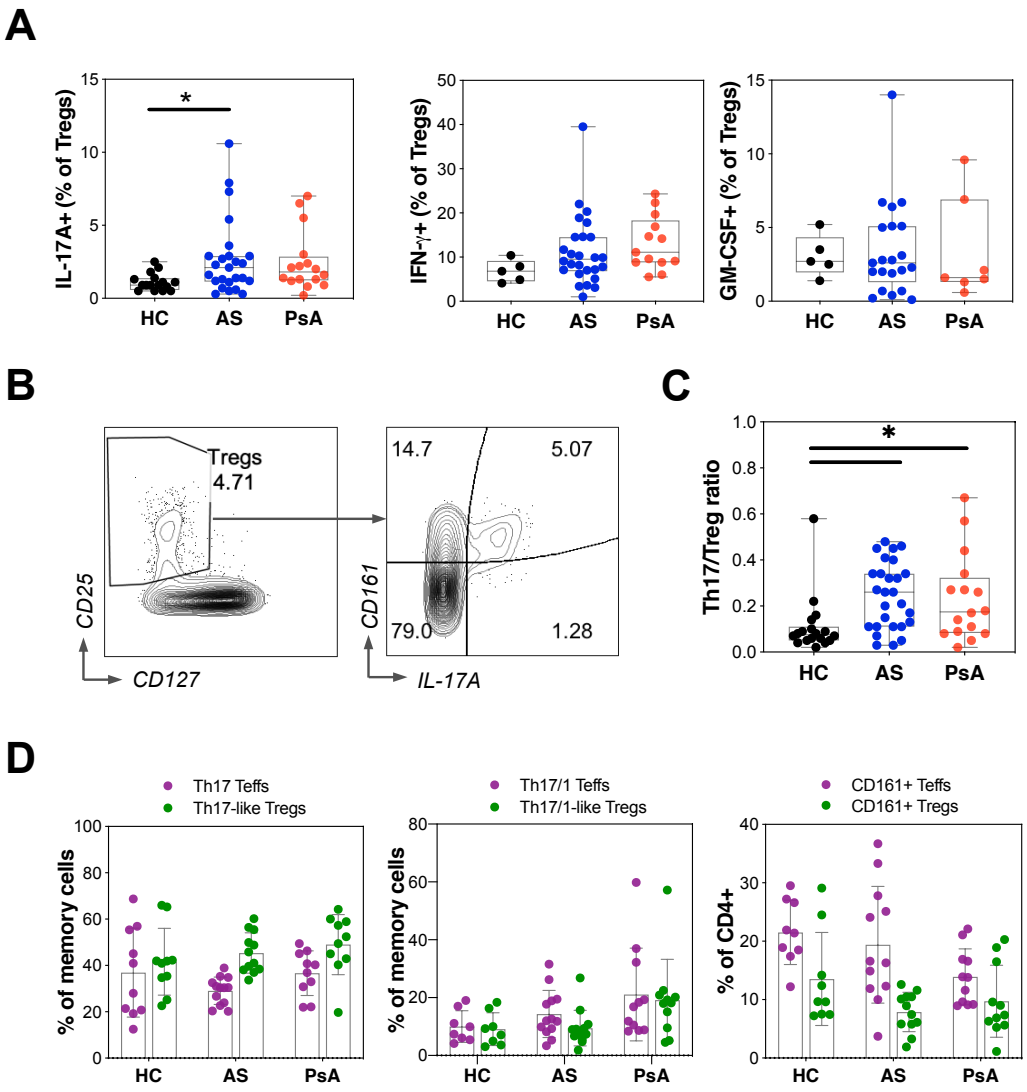

Figure 3.6. IL-17A production by PB Tregs, associated with CD161 expression, is increased in AS. **(A)** Percentage of PB Tregs producing inflammatory cytokines upon stimulation. **(B)** CD161^{+} Tregs are the principal IL-17A-producing subset. **(C)** Th17/Treg ratio (calculated as IL-17A^{+} Teffs / total Tregs) in HC and SpA. **(D)** The ratio Tregs/Teffs in SpA in the Th17, Th17/1 and CD161^{+} subsets (n= 9-11). All T helper subsets in this figure are: CD3^{+} CD4^{+} CD45RA^{-}. Further distinction between Teffs and Tregs is based on CD25 and CD127 expression. * p≤0.05, (One-way ANOVA).

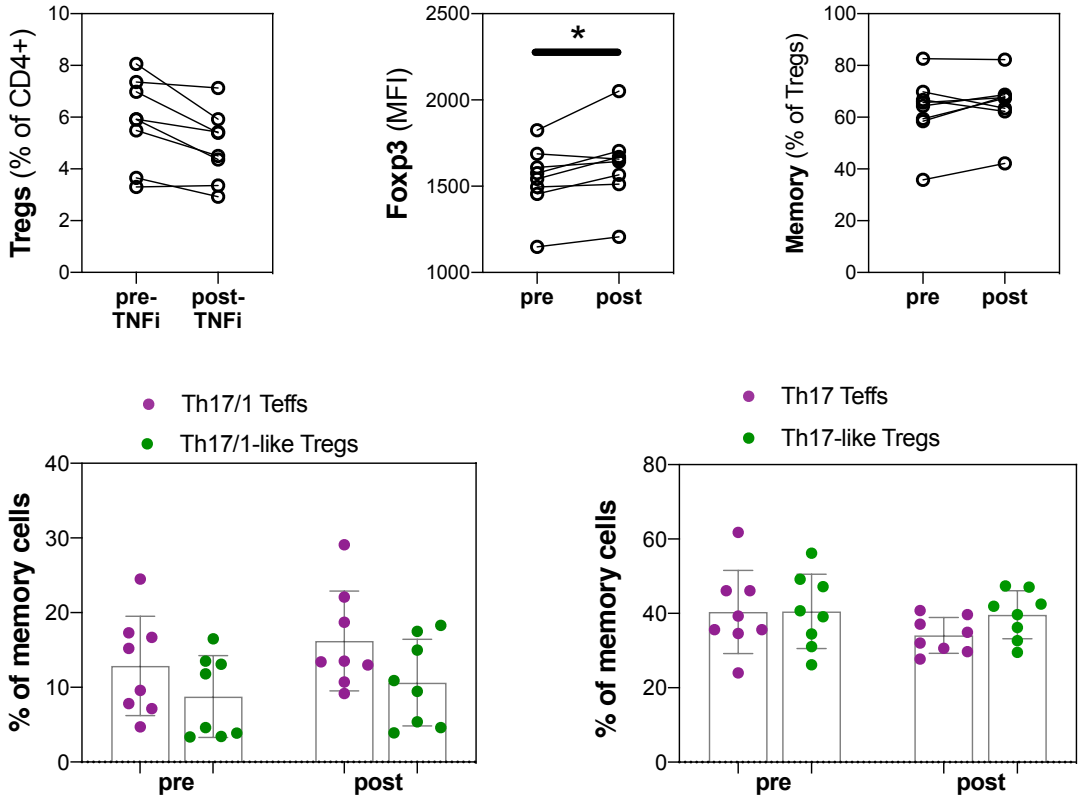

Figure 3.7. TNF inhibitors treatment increases Foxp3 expression on Tregs in AS. (A) A small increase in Foxp3 expression is seen after TNFi treatment, without a significant change in the number of Tregs or the percentage of memory Tregs **(B)** No significant changes in the Teff/Treg ratio within Th17/1 and Th17 subsets are seen after TNFi treatment. n=8. MFI: mean fluorescence intensity.

3.4 DISCUSSION

This immunophenotypic analysis of Tregs in SpA patients showed normal frequency of Tregs in the PB, but increased numbers in the synovial fluid, where Tregs highly expressed markers (CD25, Foxp3) consisted with an “activated” phenotype. Activated Tregs cells have increased ability to migrate to tissue sites, especially in the course of inflammation. This confirms the observation that the number of Tregs, in fact, generally appears to be enriched in inflammation sites during organ specific autoimmune diseases.

The analysis of trafficking markers in Tregs mirrored the T helper subdivision, but did not show the prevalence of a subset compared to healthy controls. Given the strong Th17 signature across different effector subsets in SpA, a prevalence of Th17-like Tregs was expected, yet the presence of a subset of Tregs with potential to secrete IL-17A upon stimulation suggests that Tregs in SpA include a phenotype with a skew towards Th17 effector functions.

In humans, Tregs with potential to produce IL-17A have been described in inflammatory settings, including in the SF during an arthritis flare in juvenile idiopathic arthritis (JIA) (Pesenacker et al., 2013) and in RA (Afzali et al., 2013). I observed that the production of IL-17A upon stimulation was exclusive to CD161-expressing Treg, consistent with previous studies in different arthritides. This cell subset is likely in overlap with the cells here defined Th17-like (CCR4+ CCR6+ CXCR3-). In Halim et al., 2017, Th-like Tregs were indeed able to secrete the correspondent T helper inflammatory cytokines. Interestingly, this did not have an impact on their suppressive capacity in vitro, similarly to what observed for $CD161^{+}$ Tregs: both subpopulations were able to secrete inflammatory cytokines yet maintain suppressive capability. However, the pro-inflammatory consequences of the IL-17A production by these cells in vivo, in particular in the tissue, needs to be considered. In my analysis, a mild expansion of Tregs with a phenotype similar to the so-called Th17/1 was seen. These cells have been described as expanded in the synovial fluid and might represent a subset of plastic Th17 that shift towards Th1 (Nistala et al., 2010). A previous study addressing the distribution of Th-like Tregs in the PB and various organs found that Th2-like Tregs were the most prevalent subset in the peripheral tissues, an observation that the authors explained with a higher chemotactic ability in vitro

towards their ligands. I have observed that Th2-like cells are indeed higher in the SF, but this could be also explained by a downregulation of CXCR3 and CCR6, likely induced by the presence of their ligands in the SF (Yamazaki et al., 2008), increasing the relative percentage of Th2, rather than a Th2 chemotactic signal. However, paired staining of chemokine receptors in PB and SF was only performed in three samples.

In conclusion, I have observed an increased prevalence of Tregs in the SF, mostly with memory features. The PB analysis using conventional surface markers in flow cytometry showed considerable heterogeneity of trafficking molecules, but did not preferentially overexpressed the chemokine receptor signature associated to Th17 effectors. Tregs in SpA appear to have, globally, comparable expression of CTLA-4, TIGIT or CD27 to healthy controls, but have a higher capacity of diverge to inflammatory Th17 responses upon stimulation.

The first limitation of this part of the work is that the immunophenotype analysis has been conducted almost exclusively on peripheral blood, whereas in particular for effector markers such as CTLA-4 and TIGIT, their expression would be expected to be more relevant in the inflammatory sites. Flow cytometry is still limited by the numbers of parameters that can be measured simultaneously for each cell. To immunophenotype Tregs with the named markers, three different multicolor flow cytometry panels were designed: considering the necessity to include the Treg defining markers, the number of additional features available to further characterise the Treg subpopulations is limited. Finally the pre-selection of markers based on the literature or *a priori* expectations biases the analysis and limits its breadth. As a consequence of the low dimensionality of the dataset, a robust unsupervised clustering analysis was not possible. In fact, specific, rarer

Treg subpopulations might present dysregulated or disease-specific signatures that a coarse-grained analysis might miss.

For the reasons above, to further explore the Tregs functional and transcriptional variety, I used single cell transcriptomics.

3.5 REFERENCES

Acosta-Rodriguez, E.V., Rivino, L., Geginat, J., Jarrossay, D., Gattorno, M., Lanzavecchia, A., Sallusto, F., and Napolitani, G. (2007). Surface phenotype and antigenic specificity of human interleukin 17–producing T helper memory cells. Nature Immunology *8*, 639–646.

Afzali, B., Mitchell, P.J., Edozie, F.C., Povoleri, G.A.M., Dowson, S.E., Demandt, L., Walter, G., Canavan, J.B., Scotta, C., Menon, B., et al. (2013). CD161 expression characterizes a subpopulation of human regulatory T cells that produces IL-17 in a STAT3-dependent manner: Cellular immune response. European Journal of Immunology *43*, 2043–2054.

Appel, H., Wu, P., Scheer, R., Kedor, C., Sawitzki, B., Thiel, A., Radbruch, A., Sieper, J., and Syrbe, U. (2011). Synovial and peripheral blood CD4+FoxP3+ T cells in spondyloarthritis. J. Rheumatol. *38*, 2445–2451.

Cao, D., van Vollenhoven, R., Klareskog, L., Trollmo, C., and Malmström, V. (2004). CD25brightCD4+ regulatory T cells are enriched in inflamed joints of patients with chronic rheumatic disease. Arthritis Res. Ther. *6*, R335-346.

Duhen, T., Duhen, R., Lanzavecchia, A., Sallusto, F., and Campbell, D.J. (2012). Functionally distinct subsets of human FOXP3+ Treg cells that phenotypically mirror effector Th cells. Blood *119*, 4430–4440.

Halim, L., Romano, M., McGregor, R., Correa, I., Pavlidis, P., Grageda, N., Hoong, S.-J., Yuksel, M., Jassem, W., Hannen, R.F., et al. (2017). An Atlas of Human Regulatory T Helper-like Cells Reveals Features of Th2-like Tregs that Support a Tumorigenic Environment. Cell Reports *20*, 757–770.

Hendriks, J., Gravestein, L.A., Tesselaar, K., van Lier, R.A.W., Schumacher, T.N.M., and Borst, J. (2000). CD27 is required for generation and long-term maintenance of T cell immunity. Nature Immunology *1*, 433–440.

Nistala, K., Adams, S., Cambrook, H., Ursu, S., Olivito, B., de Jager, W., Evans, J.G., Cimaz, R., Bajaj-Elliott, M., and Wedderburn, L.R. (2010). Th17 plasticity in human autoimmune arthritis is driven by the inflammatory environment. Proceedings of the National Academy of Sciences *107*, 14751–14756.

Pesenacker, A.M., Bending, D., Ursu, S., Wu, Q., Nistala, K., and Wedderburn, L.R. (2013). CD161 defines the subset of FoxP3+ T cells capable of producing proinflammatory cytokines. Blood *121*, 2647–2658.

Ranganathan, V., Gracey, E., Brown, M.A., Inman, R.D., and Haroon, N. (2017). Pathogenesis of ankylosing spondylitis — recent advances and future directions. Nature Reviews Rheumatology *13*, 359–367.

Sallusto, F., Lenig, D., Mackay, C.R., and Lanzavecchia, A. (1998). Flexible programs of chemokine receptor expression on human polarized T helper 1 and 2 lymphocytes. J. Exp. Med. *187*, 875–883.

Schneider, M.A., Meingassner, J.G., Lipp, M., Moore, H.D., and Rot, A. (2007). CCR7 is required for the in vivo function of CD4+ CD25+ regulatory T cells. J. Exp. Med. *204*, 735–745.

Uehara, S., Grinberg, A., Farber, J.M., and Love, P.E. (2002). A role for CCR9 in T lymphocyte development and migration. J. Immunol. *168*, 2811–2819.

Yamazaki, T., Yang, X.O., Chung, Y., Fukunaga, A., Nurieva, R., Pappu, B., Martin-Orozco, N., Kang, H.S., Ma, L., Panopoulos, A.D., et al. (2008). CCR6 Regulates the Migration of Inflammatory and Regulatory T Cells. The Journal of Immunology *181*, 8391–8401.

4 Single cell gene expression analysis in blood and joints of Spondyloarthropathy patients

4.1 INTRODUCTION

The increasing resolution of the tools commonly adopted for immunoprofiling studies has increased awareness of the heterogeneity of Treg cells. In addition to heterogeneity in their surface marker expression, Tregs can adapt to different tissues and inflammatory environments by modifying their transcriptional program. Whether different subsets specialize in distinct suppressive functions has yet to be fully elucidated. As shown in Chapter 3, the conventional methods that rely on a limited number of markers fail to capture this complexity; furthermore, data interpretation can be biased by supervised analysis and *a priori* selection of markers. Finally, molecular adaptation is expected to be found, rather than in the circulation, in the tissues, where Tregs acquire tissue-specific gene signatures (Panduro et al., 2016), that adapt their effector role to the environment found in each organ. Very few studies have

explored the Treg heterogeneity in human tissues with high-resolution tools, especially during pathology, with the partial exception of the tumour immune environment (De Simone et al., 2016; Guo et al., 2018). Finally, there is incomplete understanding of regulatory effector pathways (Schmidt et al., 2012) in response to systemic and local inflammation.

To define the Treg molecular diversity and capture the different states that Treg cells adopt in the course of inflammation in SpA, I used scRNA-seq analysis, which does not rely on pre-existing assumptions on expected cell markers, and it overcomes the problem of averaging RNA expression data in a heterogeneous cell population such as Tregs.

4.2 AIM

This chapter aims to address the following questions:

- What populations of Tregs can be identified in the synovial fluid and peripheral blood in SpA patients using scRNAseq?
- Is there a tissue-specific footprint in Tregs in the synovial fluid?
- Is there predominance of certain T cell clones (as identified by their T cell receptor) in Tregs in the inflamed joint of patients with SpA and what is the transcriptional of clonally expanded Tregs?

Studying Tregs at single cell level and in inflammatory sites has translational potential and clinical returns: the transcriptional program of Tregs in synovial fluid and the preferred effector pathway adopted in that environment remains an unexplored area. For instance, direct evidence suggest that, to inhibit Th17

responses, Tregs adopt specific mechanisms of such as the regulatory immune receptor TIGIT (Joller et al., 2014) (in vitro) or, as shown in the course of experimental colitis, IL-10 (Huber et al., 2011). The identification of differentially expressed effector pathways in the synovial environment can open the possibility of exciting experimentation, in a field in which there is substantial therapeutic unmet need. Leveraging T cell-mediated mechanisms of suppression for therapeutic benefit is in fact an effective strategy already in use in immune mediated diseases, as in the case of abatacept, a CTLA-Ig fusion protein, which is effective in RA (Westhovens et al., 2009).

4.3 RESULTS

4.3.1 Experimental design

To explore the Treg single cell transcriptional landscape, two distinct datasets were analyzed in parallel (**Figure 4.1**). The first one was obtained from sequencing memory CD4+ and memory CD8+ cells sorted from PBMC and SFMCs on the 10x Chromium single cell platform (5' chemistry). Three paired samples were obtained from blood and knee synovial fluid of three PsA patients, naïve to biological drugs. The dataset was generated by Dr Frank Penkava and Dr Hussein Al Mossawi and shared with me for in depth analysis of the Treg subsets. The second dataset was generated by myself: two paired (PB and SF) samples from HLA-B27 positive patients with axial and peripheral involvement, also naïve to biological drugs, were FACS sorted to isolate four immune subsets,

including Tregs. Dr Frank Penkava assisted with the sample processing, cell sorting and read alignment. The two analyses will be presented separately.

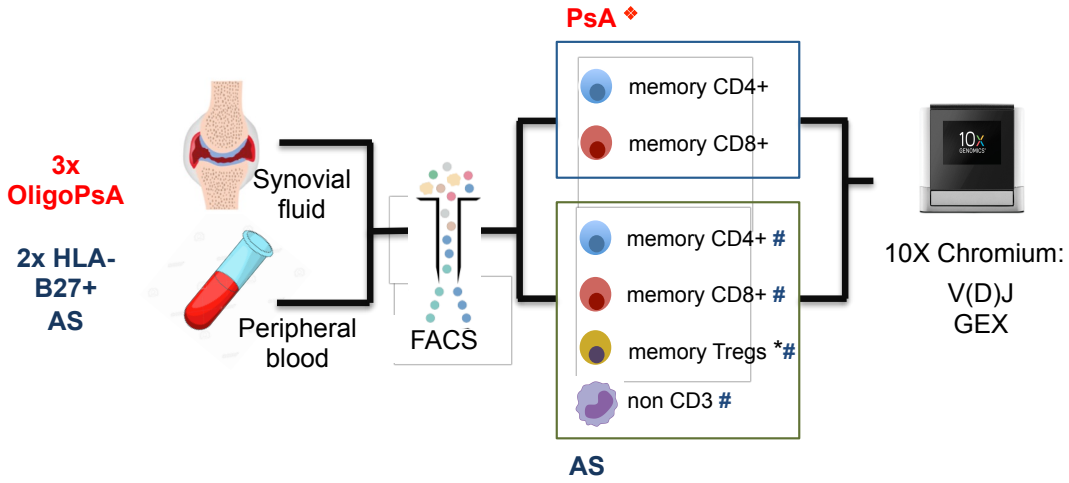

Figure 4.1. Single cell RNA sequencing experiments design. Selected leukocyte populations from paired PBMC and SFMC were obtained from patients with active PsA (n=3) and AS (n=2), all naïve to TNF blockers. Peripheral mononuclear cells were isolated by density gradient centrifugation. Cells were sorted by flow cytometry. Single cells were then encapsulated in nanodroplets according to the 10x Chromium protocol (v.3.0, 5' chemistry). mRNA was reverse transcribed using adapters contained in each droplet. The emulsion was then broken and linear amplification of the reads was performed by in vitro transcription. Libraries were sequenced on an Illumina sequencer.

❖ PsA single cell data generation (sample collection and preparation, cell sorting, reads alignment and dataset set up) performed by Dr Frank Penkava and Dr Hussein al Mossawi with the help of Dr Nicole Yager. AS single cell data generated by myself, with the help of Dr Frank Penkava

* Memory Tregs sorted as $CD3^{+}$ $CD45RA^{-}$ $CD25^{+}$ $CD127^{low}$ (sorting strategy in Figure 4.12)

samples stained with TotalSeq C hashing antibodies

4.3.2 PsA single cell dataset analysis

The PsA dataset included memory CD4+ and memory CD8+, sorted to high purity, then pooled at a 1:1 ratio before being loaded on the 10x Chromium chip. After RNA library generation, sequencing and data mapping, the data matrix was normalized and unsupervised clustering was performed (details in (Penkava et al., 2019)). One distinct cluster, characterized by higher *FOXP3, IL2RA* and *IKZF2* expression representing Tregs, was evident. Thus, the cells belonging to this cluster were subsetted out and the dataset made available to me for downstream analysis.

4.3.2.1 Quality Control

To remove low-quality cells, doublets as well as empty droplets, cells with > 10% mitochondrial genes, < 500 or > 3500 genes, and > 25,000 UMI (unique molecular identifiers, i.e. single transcripts) were removed before the clustering. A total of 3066 Tregs (**Figure 4.2A**) were obtained. In particular, it was chosen to remove cells with high content of RNAs coding for mitochondrially localized proteins because this occurrence is associated to cell stress and death (Ilicic et al., 2016). On average, 4525 unique mRNA molecules representing 1716 genes were detected per single cell, altogether surveying 33,694 genes. All six samples had similar coverage **(Figure 4.2B, C)**. In total, 951 PBMCs and 2115 SFMCs were used for downstream analysis, confirming the observed higher proportion of Tregs within $CD4^+$ cells in the SF (see **Figure 3.2**).

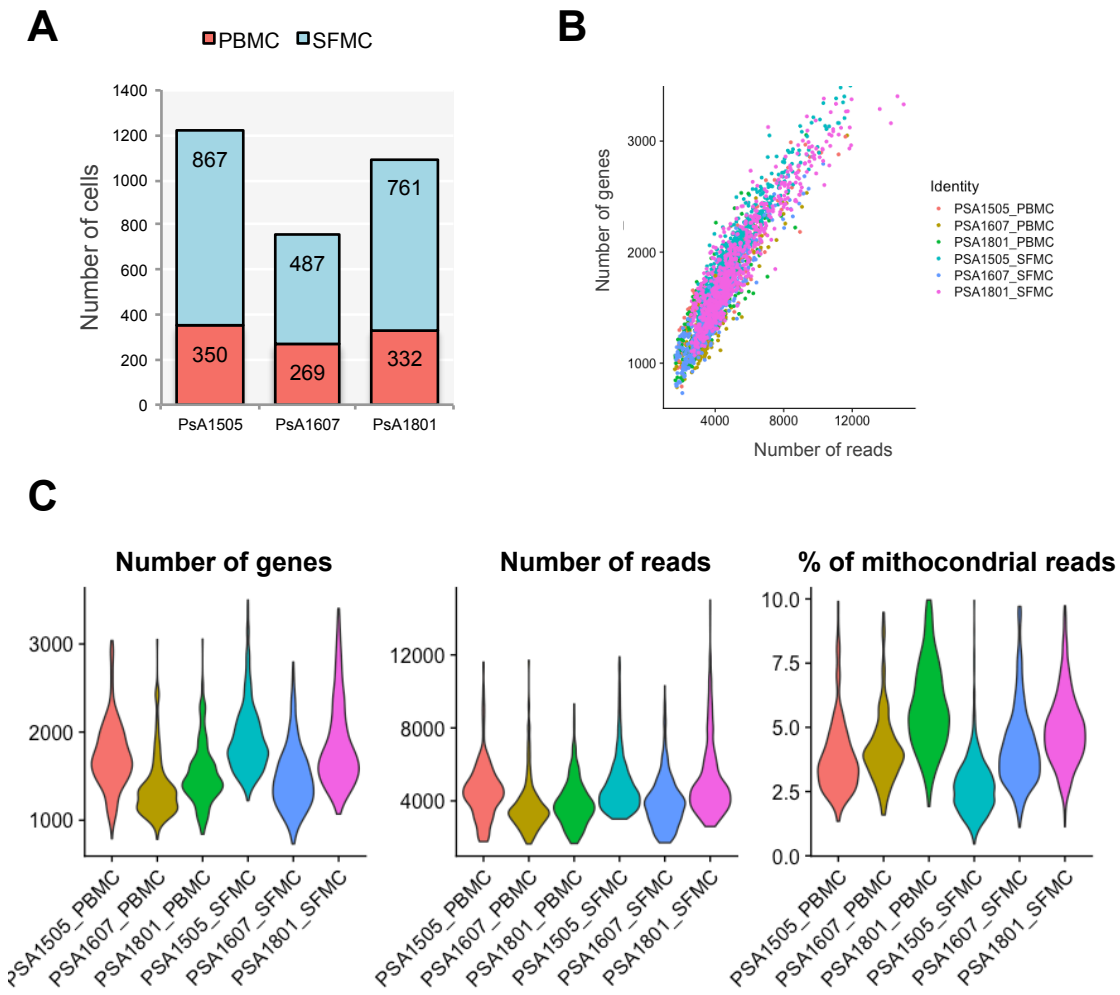

Figure 4.2. Quality control metrics of subsetted Tregs from the PsA dataset. (A) 3,066 Tregs from PB and SF from three patients were identified by the unsupervised clustering analysis on the PsA T cell data set **(B)** Number of genes detected and number of reads per cell **(C)** Violin plots showing data features separated according to the six samples of origin.

4.3.2.2 Clustering

Logarithmic normalization and scaling of the data was performed on the raw count matrices (see 2.3.3) in order to remove pre-existing clustering information. The six samples were then integrated on the basis of the top variable genes to identify common cell types in order to perform comparative analysis. This step crucially corrected for batch effects across experiments. Unsupervised clustering was then performed at a resolution of 0.4 on the basis of 30 principal components. Data displayed as a dimensionally reduced Uniform Manifold Approximation and Projection plot revealed that PsA Tregs clustered in five transcriptionally distinct subsets (**Figure 4.3A)**. Each cluster (**Figure 4.3B**) was made up by cells originating from PB and SF in similar ratios.

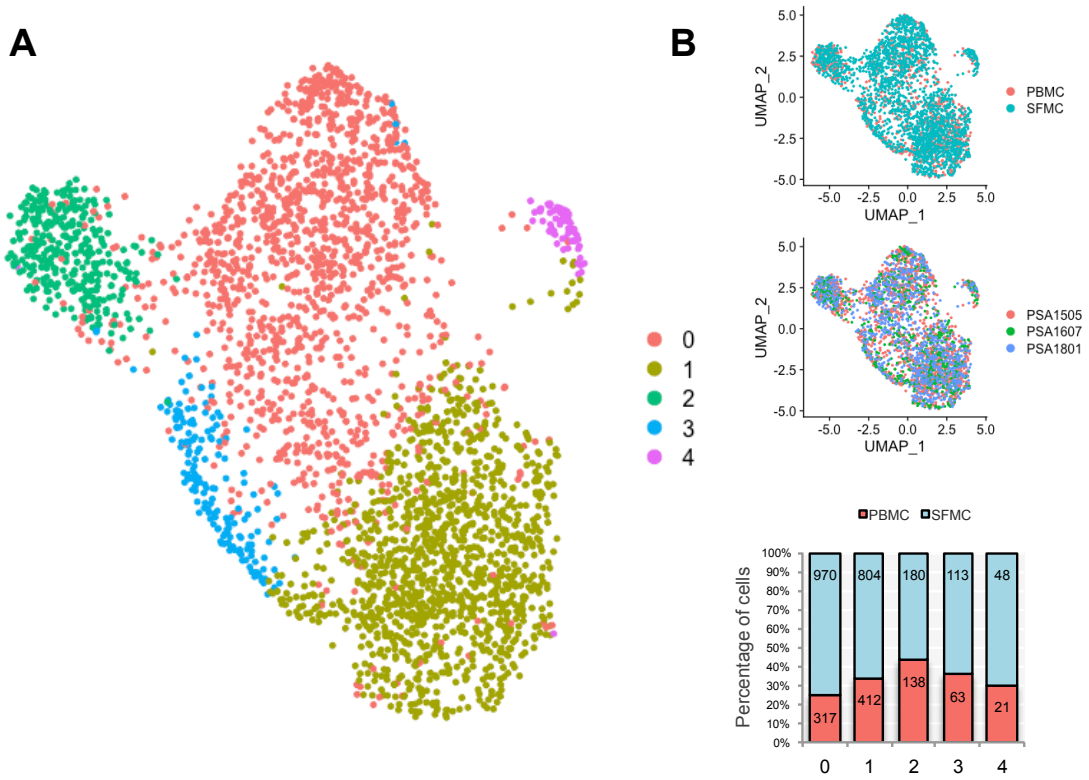

Figure 4.3. UMAP plot of PsA Tregs from three paired PBMC and SFMC samples. (A) after sample integration, five clusters are identified. **(B)** Cells from both PB and SF compose each cluster in similar proportions.

4.3.2.3 Differential gene expression analysis and cluster annotation

To characterise the clusters, differential gene expression analysis was performed on the integrated PB-SF dataset. A heatmap of the top ten differentially expressed genes defining each cluster is shown in **Figure 4.4.** HLA class II-associated genes characterized cluster 0. Cluster 1 was defined by increased expression of genes encoding ribosomal proteins and higher expression of *CCR7*. Cluster 2's highest differentially expressed gene included *PTPRC* (encoding for CD45RA/RO, no further determination of which isoform possible at transcript level) and *CCR4*, Cluster 3 was characterised by expression of *KLRB1* (encoding CD161). Finally, cluster 4 showed, unexpectedly, a distinct signature characterised by *CD8A* and *CD8B* expression and granzyme family genes. Clusters were thus annotated accordingly.

To verify that the clustering algorithm correctly had correctly identified Treg cells, and to exclude contaminations by non Tregs (including Teffs) cells from the PsA dataset, the presence of transcripts identified in a previous published Treg single cell dataset (Zemmour et al., 2018) as "Treg signature genes" was evaluated. These genes were similarly expressed across the different Tregs subsets (**Figure 4.5**), with the partial exception of the cluster characterized by *CCR7* expression, which presented a slightly lower level of *IL2RA* (CD25*)* and *CTLA4*. *IKZF2*, encoding the transcription factor Helios, was virtually absent in the *KLRB1*$^{+}$ cluster and increased in the *CCR4/IKZF2* (Helios)$^{+}$ cluster (log fold change enrichment: 1.4, $p = 2x10^{-54}$). Importantly, the *FOXP3* transcript was detected in 2,302 cells, and *IL2RA* in 1,558 out of the 3,066 composing the dataset. In Zemmour et al., the TNF receptor superfamily genes *TNFRSF4, 9,*

18 and *1B* were identified as part of the Treg signature. In our dataset, their expression, although with some differences (among which the scarcity of *TNFRSF9*, or CD137*)*, seemed also consistently distributed across clusters.

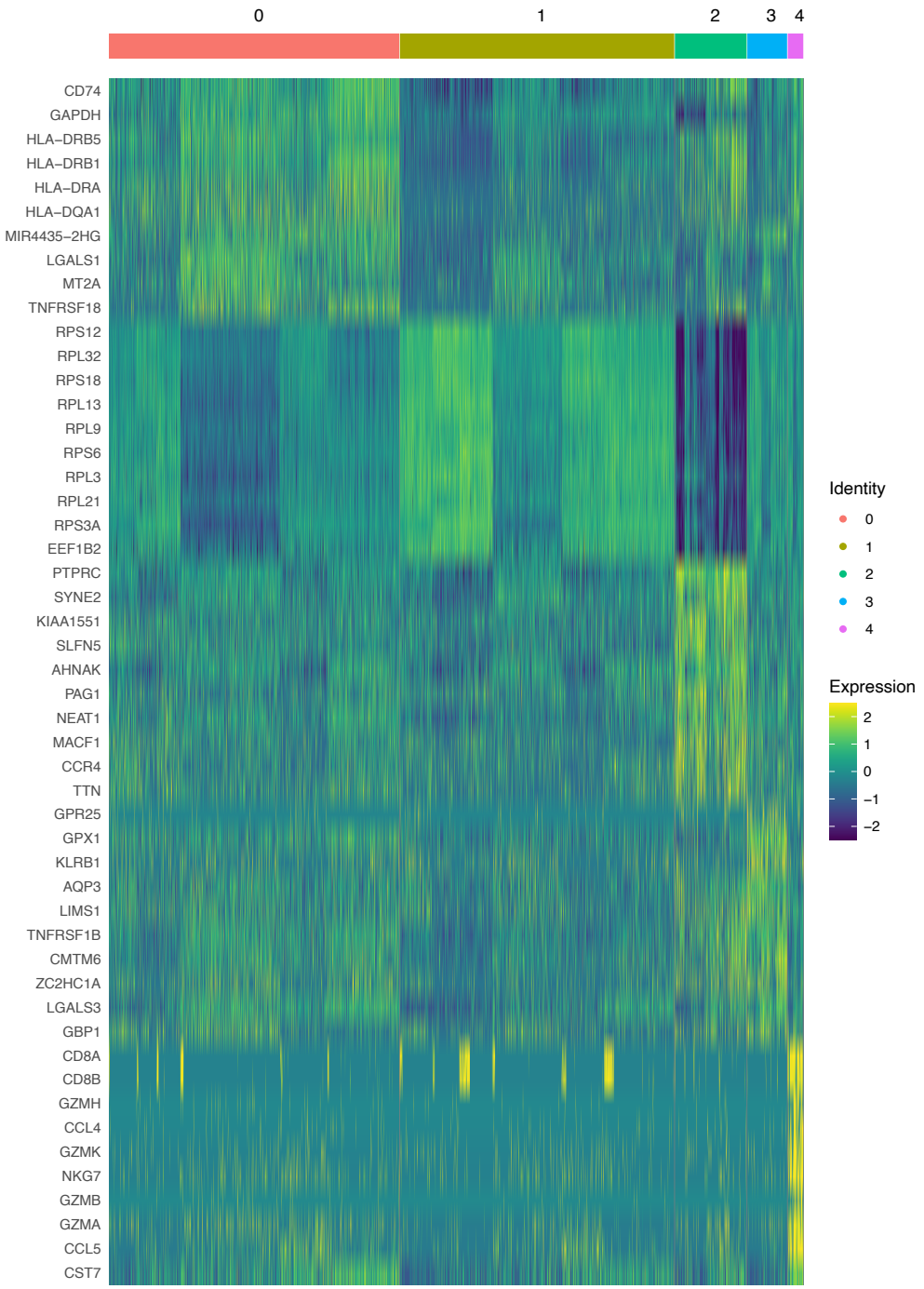

Figure 4.4. Gene heatmap showing the top 10 differentially expressed genes in each cluster. Only genes detected in at least 20% of the cells belonging to the cluster are included. Normalised expression of gene counts.

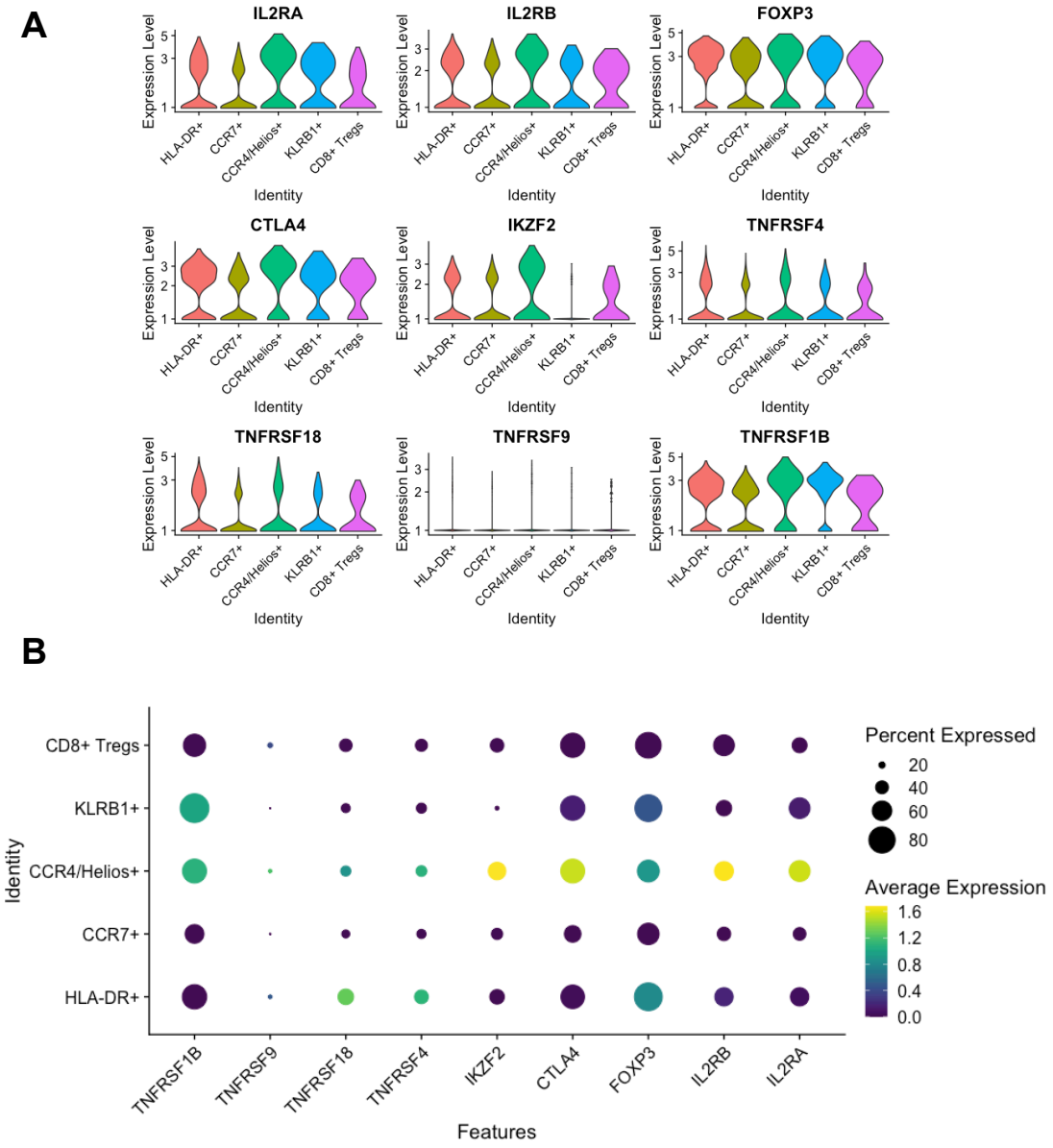

Figure 4.5. Expression of the Treg signature genes across the dataset. **(A)** Violin plots showing count distribution (log scale) for each gene across the clusters. **(B)** Dot Plot: the size of the dot corresponds to the percentage of cells expressing the feature, the color the average expression of the feature.

4.3.2.4 Th17-like cluster

One of the clusters was characterised by *KLRB1*, a gene encoding the C-type lectin-like receptor receptor CD161. This cluster, compared to the other mTregs, showed increased expression of markers indicating a Th17-like phenotype, *KLRB1* included (**Figure 4.6**). The expression of *CCR6*, *IL6R* and *IL1R*, other Th17-associated genes, indicated that the transcriptome of this cluster likely represented the Th17-like Treg phenotype described in Duhen et al., 2012 (characterised as CCR6+ Tregs) (and in 3.3.2), and the phenotype more recently discussed by Duurland et al., 2012. Interestingly, the Th17 master transcription factor *RORC* was also expressed in this cluster. Other top upregulated genes are shown in **Table 4.1**. No transcripts for Th17-associated inflammatory cytokines (eg. *IL17A, IL17F, IL22*) were seen, although they are rarely detected in unstimulated T cells. Among the genes that were downregulated, the coinhibitory receptor *TIGIT* and the TF Helios (*IKZF2*) were the most striking. *FOXP3* expression was not different compared to the average of the other clusters, suggesting a coexistence of *RORC* and *FOXP3*. In terms of effector genes, this cluster had a distinctive IL-10 signature (*IL10*, *MAF*), associated with expression of *LAG3* and *CTLA4*.

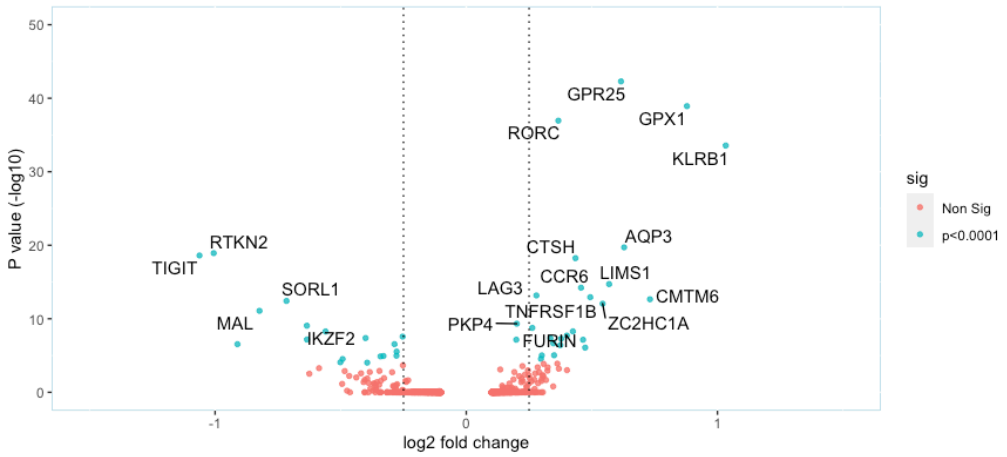

Figure 4.6. Single cell RNAseq analysis of the PsA Treg dataset reveals a regulatory subset with Th17 characteristics. Volcano plot showing differentially expressed genes in the *KLRB1*$^{+}$ cluster compared to all mTregs. Genes with p<1x10^{-10} (Wilcoxon rank sum test) are annotated. Vertical dotted line indicates ±0.25 log-fold change.

Gene	Product	Function(s)
GPR25	Probable G-protein coupled receptor 25	Function unknown. Paralog of *Gpr15* in mice
RORC	ROR-gt	Th17 associated transcription factor
GPX1	Glutathione peroxidase	Antioxidant enzyme
KLRB1	Killer cell lectin-like receptor subfamily B, member 1 (CD161)	Natural killer cell maturation, induction of cytotoxicity
AQP3	Aquaporin 3	Membrane transporter of water and glycerol expressed in keratinocytes
CSTH	Pro-cathepsin H	degradation of proteins in lysosomes
CCR6	C-C chemokine receptor type 6	Trafficking to Th17 sites
LIMS1	LIM and senescent cell antigen-like-containing domain protein 1	Involved in integrin signalling
CMTM6	CKLF Like MARVEL Transmembrane Domain Containing 6	Chemokine-like factor gene superfamily; exact function unknown
FURIN	Furin	Protease
LAG3	Lymphocyte activation gene-3	Trafficking to the sites of inflammation
TNFRSF1B	TNF receptor superfamily 2	Cell survival and immune suppression
PKP4	Plakophillin-4	Component of desmosomal plaque and other adhesion plaques
ZC2HC1A	Zinc finger C2HC domain-containing protein 1A	Function unknown

Table 4.1. Upregulated genes in the KLRB1+ cluster

4.3.2.5 CD8⁺ Treg cluster

Intrigued by the presence of a small *CD8A/CD8B*-expressing cluster within the Treg dataset, differential gene expression analysis was performed. The Treg core set genes, including *FOXP3* and *IL2RA,* were not significantly downregulated in this cluster compared to the CD4+ Treg clusters (**Figure 4.7A**). Very high levels of chemokines *CCL4* and *CCL5,* and of genes associated to cytotoxic functions such as *GZMB*, *GZMH*, *GZMA* and *NKG7* were characteristics of this cluster. Importantly, cells in this cluster did not coexpress *CD4* and *CD8A/B* (**Figure 4.7B**), since cells with detected presence of both transcripts were removed in the QC step because of the sorting strategy used. One hundred and one transcripts were upregulated in this cluster compared to the rest of the Tregs, which made the $CD8^+$ Treg subset the cluster with highest number of genes and transcripts detected (**Figure 4.7C**). To further confirm the regulatory profile of the cluster, I compared it to CD8+ T effectors obtained from the initial mCD4/mCD8 PsA dataset. $CD8^+$ Tregs differed from the $CD8^+$ effector cells for their distinctive regulatory genes (**Figure 4.7D)**. This suggests the coexistence in this cluster of specialised cytotoxic programme and a regulatory transcriptional profile. The presence of the latter resulted in it clustering with the rest of the CD4+ Tregs, reminding that, in unsupervised principal component-based clustering, shared transcription signatures prevail over the expression of lineage markers.

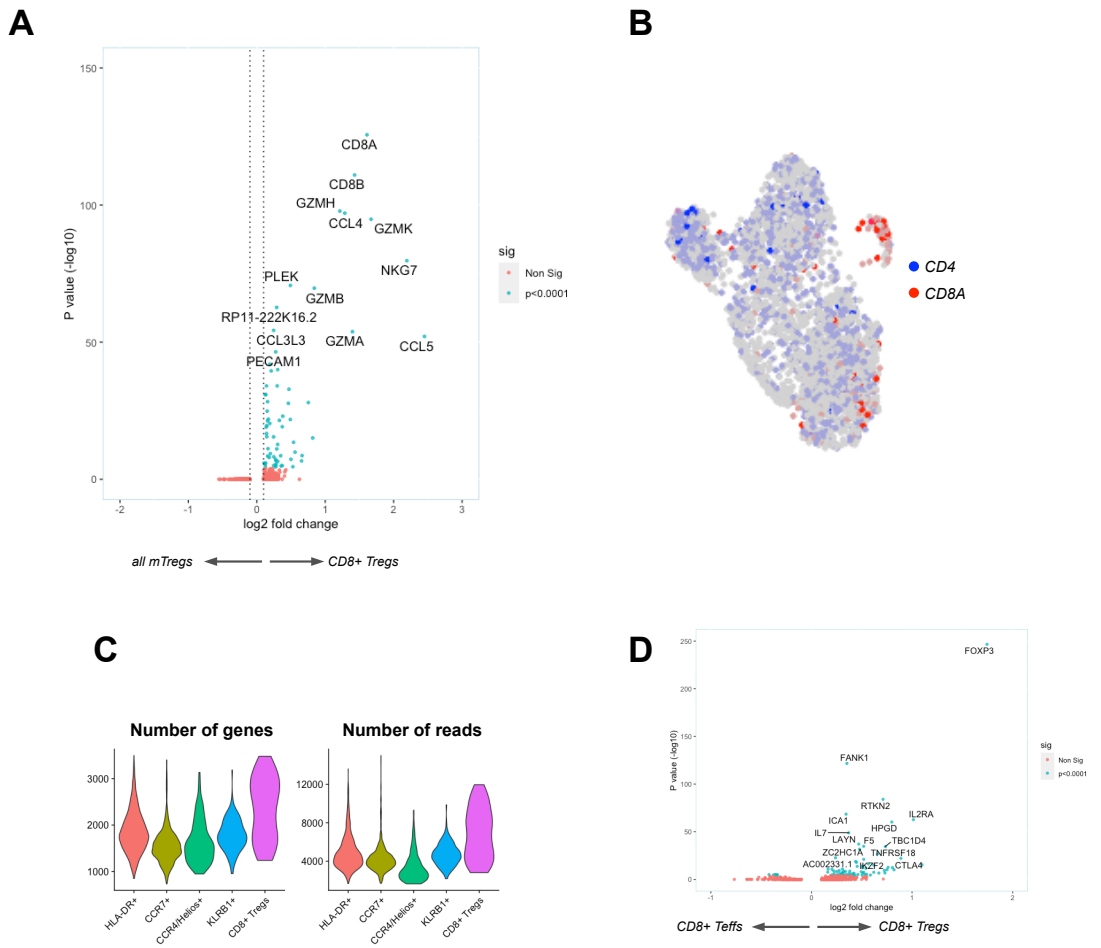

Figure 4.7. Single cell RNAseq analysis of the PsA Treg dataset reveals the presence of a CD8+ Treg cluster. (A) Volcano plot showing differentially expressed genes in CD8 Tregs. p-value according to Wilcoxon Rank Sum test **(B)** Distribution of the *CD4* and *CD8A* transcripts, localizing in distinct areas of the plot **(C)** QC metrics for the 5 clusters: CD8+ Tregs have the highest number of genes and transcripts per cell **(D)** Genes differentially regulated compared to the CD8+ T effector from the initial PsA dataset (Penkava et al., 2019).

4.3.2.6 Treg signature transcripts

Next, in order to identify the genes constituting the Treg signature and to verify the existence of a reciprocal regulation, a differential gene co-expression analysis was performed at the population level. Selected markers encoding regulatory TF or effector markers were selected among the top variable genes,

and the Spearman pairwise correlation was calculated for each pair. The highest positive correlations (**Figure 4.8**) were found across a group of co-regulated genes, which included Treg core TFs (*FOXP3*, *BATF*) and constitutive regulatory functions (*IL2RA*, *CTLA4*). The tightest relationship was between two TNF receptor superfamily genes (*TNFRSF18* and *TNFRSF4*), encoding for two co-stimulatory molecules (GITR and CD134, also known as OX40). Interestingly, little to no correlation was seen between pairs of checkpoint inhibitors such as PD-1, LAG-3 and TIM-3, which are otherwise often co-expressed by tumour infiltrating lymphocytes (Kurtulus et al.; Woo et al., 2012) or during viral infections (Richter et al., 2010).

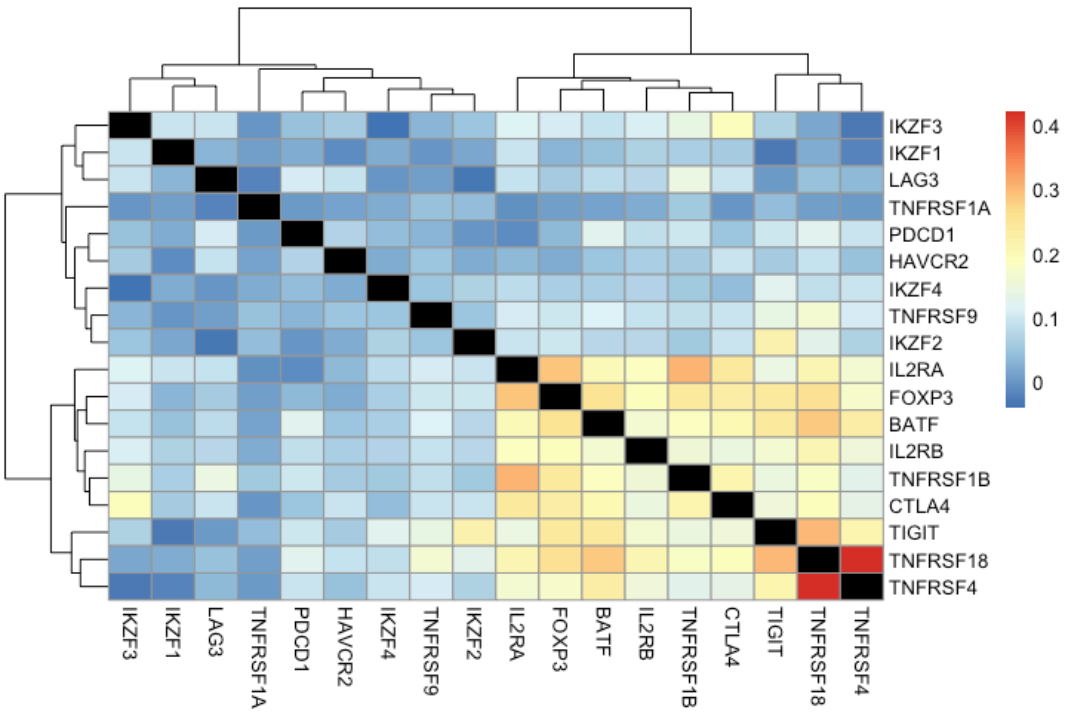

Figure 4.8. Gene correlation heat map for selected Treg markers (including transcription factor and coinhibitory molecules) within the variable gene pool. Gene co-expression by Spearman's rank correlation coefficient.

4.3.2.7 Peripheral blood and synovial fluid signature

The integration of the PB and SF dataset was based on the identification of gene signatures shared in both tissues (see 2.3.3.1). None of the clusters appeared to be exclusive of PB or SF (see **Figure 4.3B**). To verify the presence of tissue-specific differences at gene level, the normalised expression of each detected transcript was compared in the SF and PB. Two hundred and thirty-seven genes were differentially expressed between the two groups, of which 183 enriched in the SF. The top 10 differentially expressed genes in the SF included *FOXP3*, confirming the observation made at protein level (**Figure 3.2**), and *TNFRSF18 (*GITR*)* (**Figure 4.9A**). Annotation of the SF enriched genes using the Gene Ontology (GO) resource showed that SF Tregs' enriched genes were involved in the processes of cell adhesion and cell-cell communication, coherently with the cross talk with non haematopoietic cells such for example as synoviocytes, but also genes involved in type I and II interferon responses (**Figure 4.9B**). Interestingly, *TXNIP*, encoding a Thioredoxin-interacting protein, regulating redox reactions, was the strongest downregulated gene in the SF. SF enriched expressions in the single clusters showed frequent recurrence of the same genes, indicating conserved differences across Treg subsets (**Figure 4.9C**).

When profiling Tregs for their trafficking marker expression (3.3.2), a downregulation of various chemokine receptors was noted in synovial Tregs. The analysis of the same markers at mRNA level in the two sites confirmed the downregulation of *CCR6*, but not of *CXCR3*, in the SF compared to PB. Few cells expressing the gut homing marker *CCR9,* were present but only in the PB. *CCR6*,

was higher in the *RORC*-expressing *KLRB1*$^{+}$ cluster. In other words, the T helper-like classification proposed in previous studies (Duhen et al., 2012; Halim et al., 2017), based on differential expression of chemokine receptors, was not mirrored by the analysis of transcriptional features. In **Figure 4.9D** the expression of the integrin subunit genes, in addition to other important trafficking markers, is also shown.

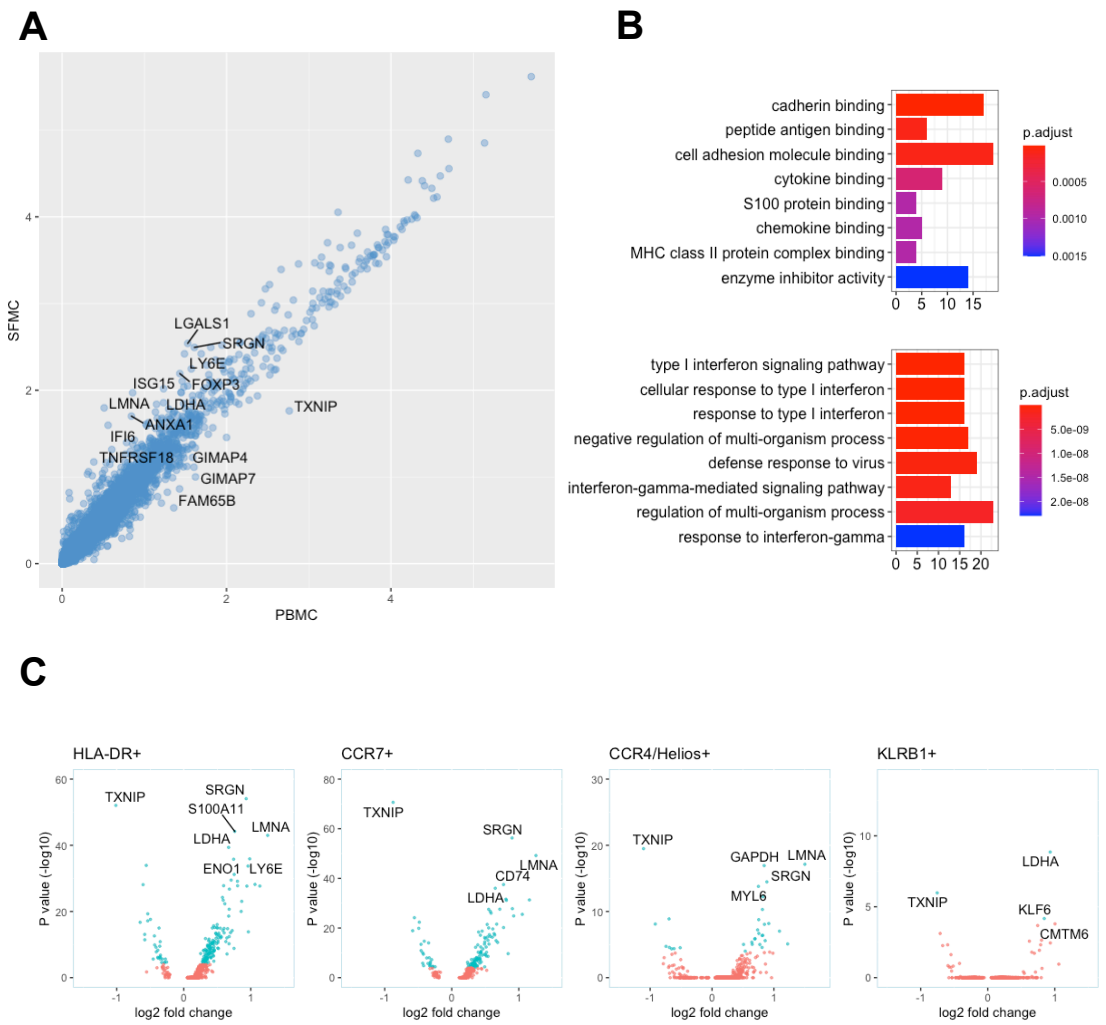

Figure 4.9. PsA synovial fluid gene signature in Tregs (A) Normalised expression of all the genes detected in PB and SF **(B)** Genes enriched in the SF were classified into the Gene Ontogeny (GO) database categories “MF” (molecular function) and “BP” (biological process) to identify enriched categories. The color bar shows the p-value (after Benjamini-Hochberg correction). X axis number

indicates the number of genes differentially expressed belonging for each GO element. **(C)** Tissue differential gene expression for each cluster. In CD8+ Tregs, only two genes were differentially expressed between PB and SF **(D) (next page)** Split plots showing expression of selected trafficking markers, including chemokine receptors and integrin subunits, in PB (red half) and SF (blue).

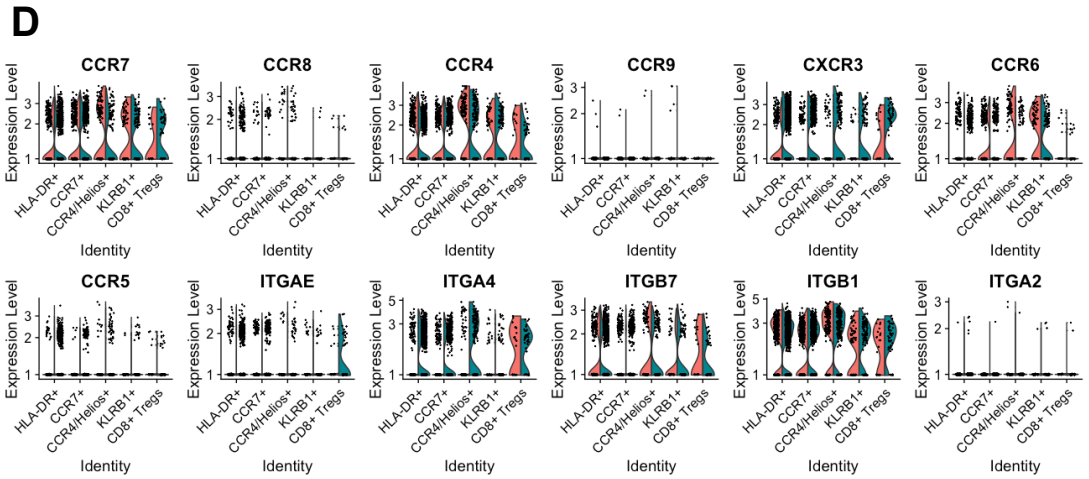

4.3.2.8 Differential expression of inhibitory markers

Tregs can express a vast array of effector molecules to exert their inhibitory functions. The following analysis investigated the frequency and the distribution division of genes relevant to Treg effector functions across the clusters. Average gene expression coupled with hierarchical clustering was used to map these markers (**Figure 4.10A**). CCR4/Helios^{+} cluster was the highest expresser of *IL10*, *TIGIT* and *CTLA4*, whereas CD8+ Tregs had a distinct expression of *GMZB*, *PDCD1* and *TGFB1*. *KLRB1*$^{+}$ cluster showed also a downregulation of *TIGIT*. *LAG3* was prevalently expressed by the KLRB1+ and by the CD8+ Treg cluster. The expression of these markers in the SF was, although at different levels, almost invariably upregulated in the SF compared to the PB, in particular *PDCD1, LAG3, GZMB, HAVCR2* (coding for Tim-3) **(Figure**

4.10B). It was also apparent how the majority of these markers were expressed only in a small percentage of resting Tregs, with the exception of *CTLA4* and *TIGIT*, whose transcripts, present in a higher number of cells, seemed to be constitutive of the Treg. Because of the appearance of TNF receptor superfamily genes as part of the Treg core signature and their enrichment in the synovial fluid, I interrogated their distribution across the clusters and in the PB and SF (**Figure 4.10C**). *TNFRSF18*, encoding for GITR, was particularly upregulated.

4.3.2.9 Treg TCR repertoire analysis

To explore the presence of a restricted clonal diversity in our Treg dataset, the VDJ count matrix containing exact information on TCR sequences was interrogated, making use of the novel 5' chemistry on the 10x Chromium platform, designed to provide simultaneous coverage of both the transcriptome and the TCR α/β variable region in the same single cell.

TCR information on the whole PsA T cell dataset was reconstructed by Dr Frank Penkava: clones were defined by identical TCRα and β nucleotide sequences. A strong clonal enrichment in CD8+ cells in the SF in all three PsA patients, and to a smaller extent in CD4+ cells (details in Penkava et al., 2019). Within the CD4 clones, one of the three patients (PsA1801) presented a number of cells with identical TCR clonotype located in the Treg bidimensional space, identified by α alleles TRAV4 and TRAJ39 and β TRBV28 and TRBJ2-6 with a CDR3 sequence named CASSFNSGANVLTF. This clonotype was found in 43 SF cells, of which 35 were Tregs. No cells sharing this same clonotype were found in the PB. On the UMAP plot, the majority of the clone-sharing cells localised close to each other, prevalently in Cluster 0 (HLA-DR+ Tregs),

suggesting transcriptional similarity (**Figure 4.11AB**), but also potential for a clonal response to switch to a different functional phenotype.

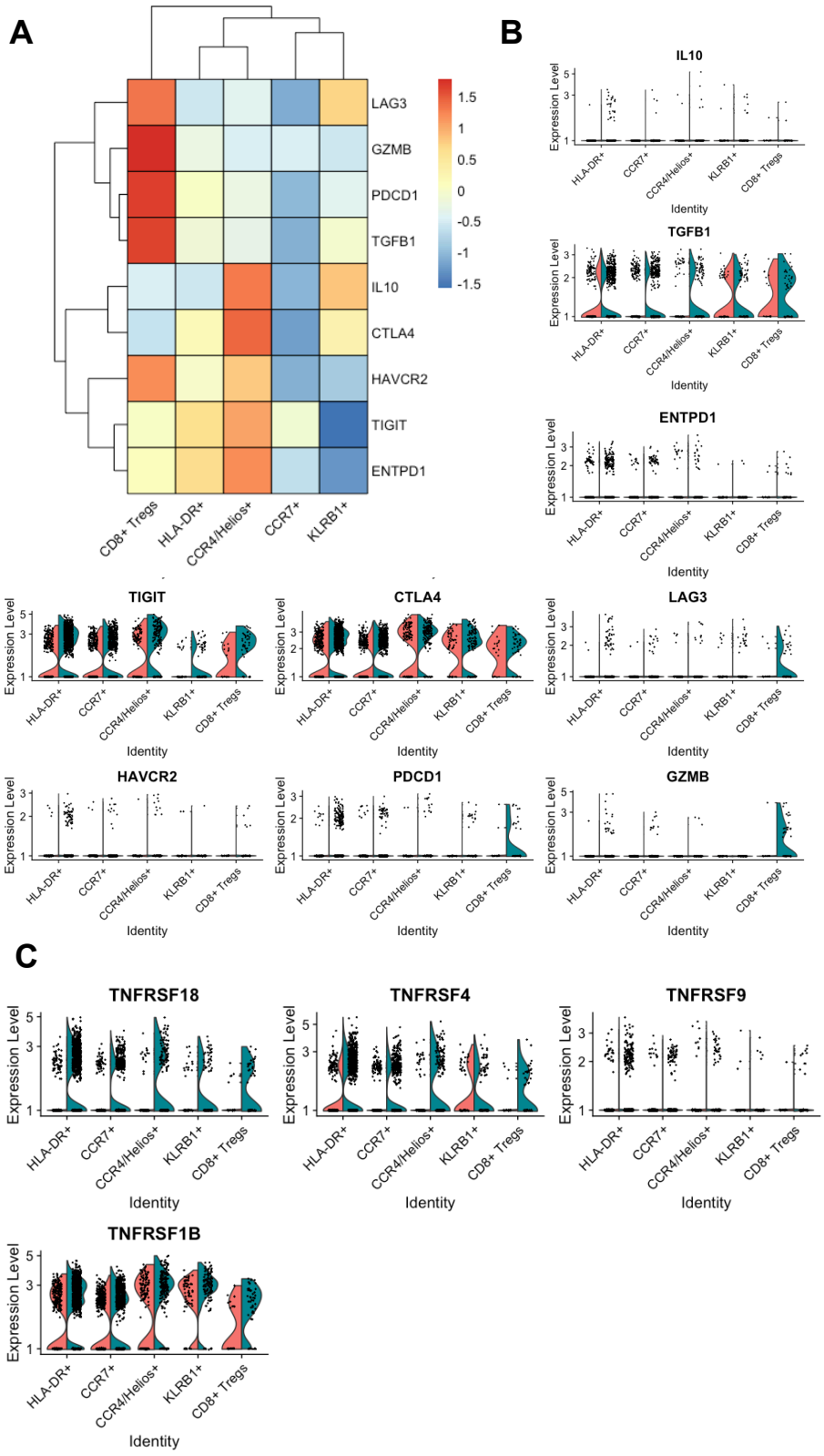

Figure 4.10 (previous page). Distribution of the effector markers in PsA Treg clusters. (A) Average expression of selected suppressive markers (row-based Z-score scaled data). Differential expression of suppressive markers **(B)** and TNF superfamily genes **(C)** in PB (red) and SF (blue), for each cluster. *ENTPD1* encodes CD39.

To verify the transcriptional characteristics of the cells sharing a clonotype, I performed differential gene expression analysis comparing clonal cells versus the rest of the memory Tregs (**Figure 4.11C**). The cells with the shared clonotype overexpressed genes such as *TNFRSF9*, *CCR8*, *IL1R* compared to the rest of the SF Tregs. Genes such as *FOXP3* and *CTLA4* were not differentially expressed, indicating that regulatory genes were preserved.

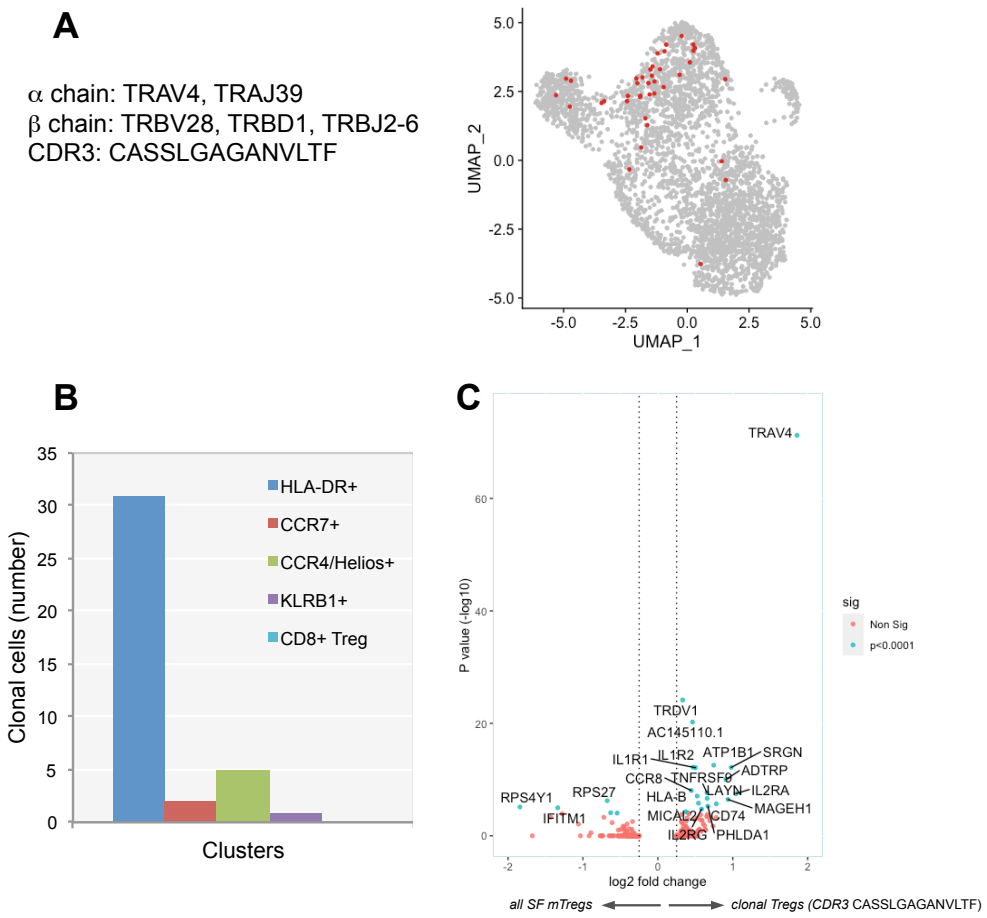

Figure 4.11. Identification and characterization of Treg clonality in the SF. (A) 39 Tregs that express the same TCRα/β CDR3 sequences localise in the same area of the UMAP plot**, (B)** largely corresponding to HLA-DR+ cluster **(C)** differential gene expression of clonal versus non clonal cells

4.3.3 AS single cell dataset analysis

To confirm the findings and validate our observations in a second SpA condition, I decided to carry forward a second single cell experiment on two AS samples. PB and SF cells from two HLA-B27 positive patients with AS, presenting with concomitant active axial disease and peripheral arthritis, were collected.

A different sorting strategy from the PsA single cell experiment was adopted. After mononuclear cells separation by density centrifugation, memory Tregs (defined as $CD3^+$ $CD45RA^-$ $CD25^+$ $CD127^-$) were FACS sorted, together with memory $CD4^+$ and memory $CD8^+$ cells and a smaller subset of $CD3^-$ cells (**Figure 4.12**), included with aim of generating an scRNA library of different immune cells as future resource. I decided not to include the positivity of CD4 in the sorting strategy for Tregs to verify the existence of a $CD8^+$ regulatory subset.

Furthermore, for this experiment we made use of a technology called CITE-seq (Stoeckius et al., 2017). To reduce the number of sequencing runs for reasons of costs, the four cell subsets, after sorting, were labelled with four oligonucleotide-tagged antibodies targeting ubiquitous cell surface antigens (Total-SeqC, Biolegend) before pooling them together prior to loading them onto the Chromium 10x platform. The presence of a specific oligonucleotide sequence (hashing oligonucleotide, HTO) attached to each cell allowed deconvolution of the multiplexed single cell RNA library after cell lysis, preserving the identity of the cell and its origin (in our case, the sorting strategy used) for the downstream analysis. The four cell subsets were pooled together at a ratio of 1:3:3:3 (the $CD3^-$ cells being the smallest fraction).

Given the rare occurrence of peripheral arthritis in HLA-B27+ AS patients and the difficulties encountered to recruit patients with these characteristics, one of the two patient samples (AS02) was obtained from previously cryopreserved PB and SFMCs. Both cell viability before loading onto 10x chip, and quality metrics after sequencing (see examples in **Figure 4.13**) were comparable between the two samples.

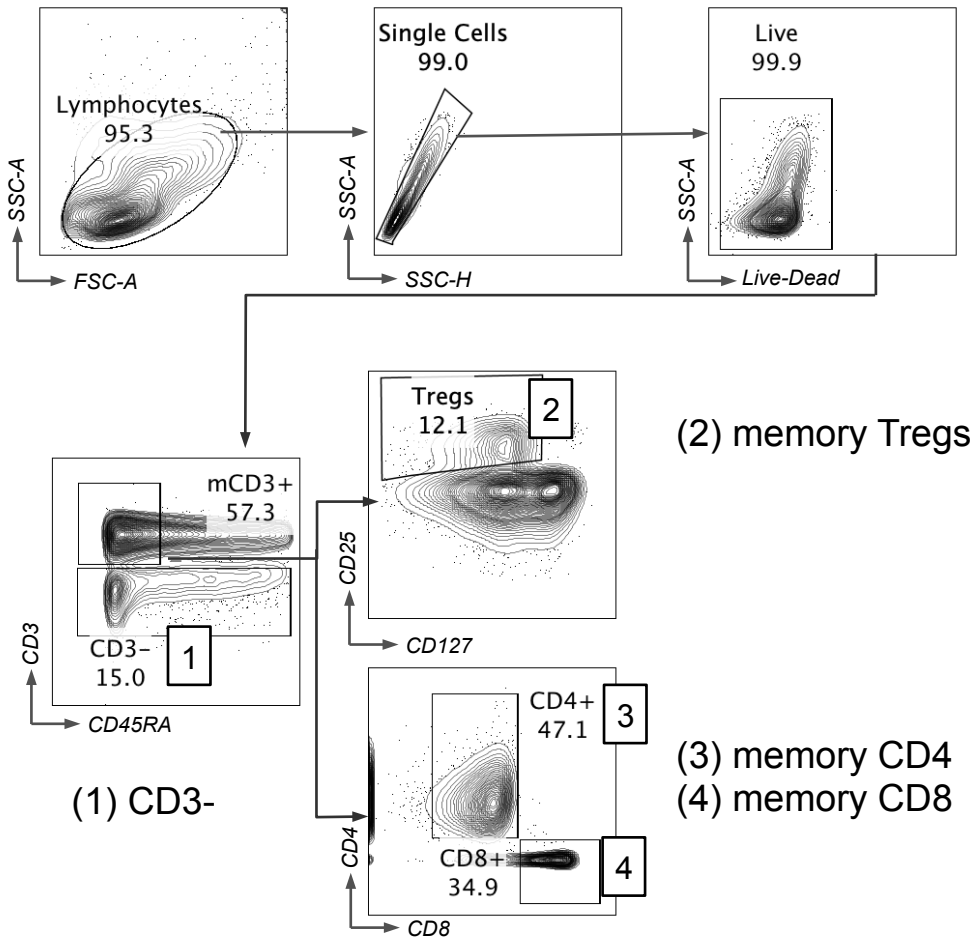

Figure 4.12. Sorting strategy adopted for AS single cell RNAseq experiment. After sorting, the 4 samples were stained with four different hashtag reagents to distinguish between libraries. Here pictured, synovial fluid sample from AS02.

4.3.3.1 Quality control

Approximately 45,000 cells from each sample were loaded onto the 10x Chromium platform. After RNA library generation, sequencing and application of the Cell Ranger analytical pipeline (detailed in 2.3.1), summary metrics from the Cell Ranger automated secondary analysis are shown in **Table 4.2**.

Similarly to what done for the PsA single cell dataset, cells with either 10% mitochondrial genes and cells with > 25,000 log-normalized UMIs were filtered out. On the basis of the gene number distribution, it was decided that the cells

with a number of detected genes lower than 250 and higher 4,000 genes were filtered out (**Figure 4.13**).

Run	Patient	Number of cells	Number of reads (millions)	Mean reads per cell	Median UMI counts per cells	Median genes per cell	Sequencing saturation	Antibody mean reads per cell
1	AS01 PBMC	16507	512.6	31055	3274	1062	74.9%	4946
	AS01 SFMC	18094	501.4	27710	3072	1212	68.2%	4309
2	AS02 PBMC	7959	340.5	42789	2733	1006	86.4%	5201
	AS02 SFMC	16130	584.8	36257	3188	1250	79.7%	3806

Table 4.2. Summary metrics of the two 10x Chromium sequencing runs for each sample. Parameters are calculated by the Cell Ranger automated analysis and refer to 5' gene expression and CITE-seq ("antibody reads").

4.3.3.2 Dimensionality reduction and unsupervised clustering

The resulting matrices (for RNA and HTO expression data) were analysed employing the computational workflow shown in **Figure 4.14**, which follows the Seurat 3 scRNA-seq analysis pipeline (Stuart et al., 2019). Sample integration, data dimensionality reduction and unsupervised clustering methods are explained in **Figure 4.14** and in greater detail in 2.3.3.

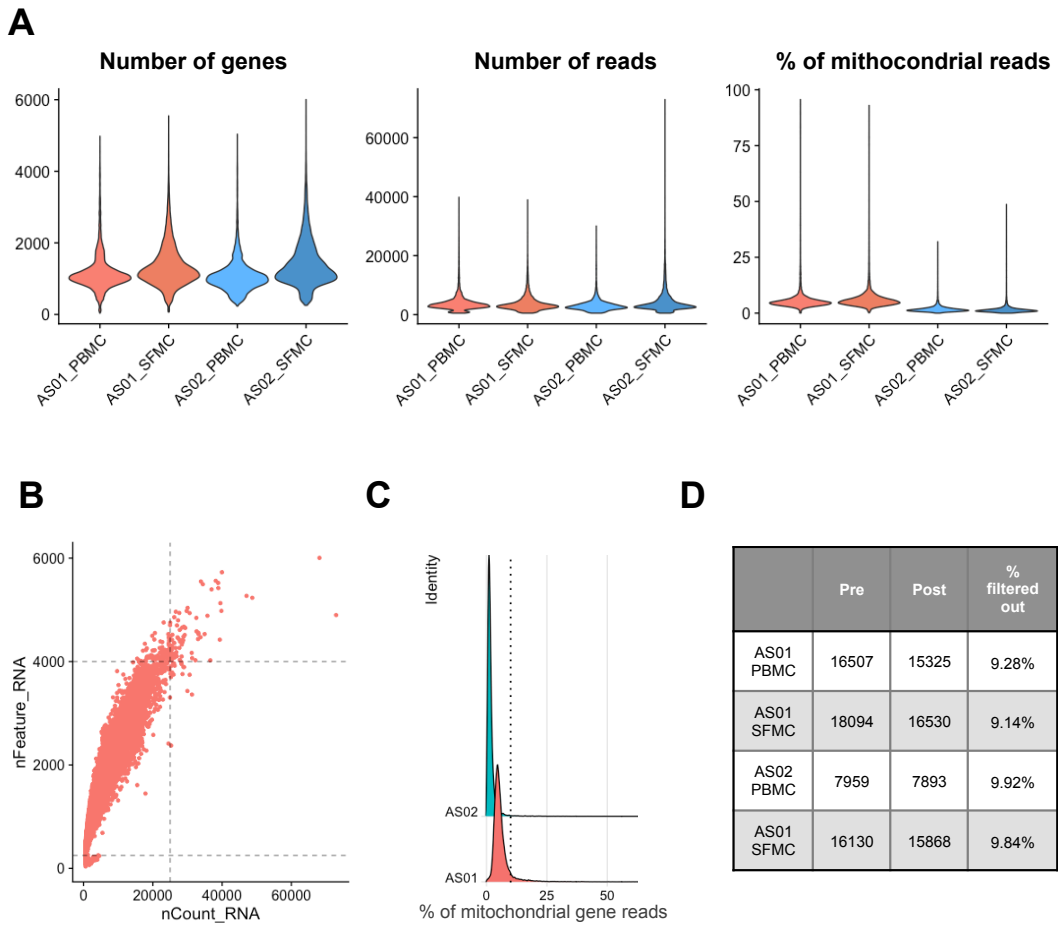

	Pre	Post	% filtered out
AS01 PBMC	16507	15325	9.28%
AS01 SFMC	18094	16530	9.14%
AS02 PBMC	7959	7893	9.92%
AS01 SFMC	16130	15868	9.84%

Figure 4.13. AS single cell RNAseq metrics. (A) Per cell metrics distribution **(B-C)** Cells with > 25,000 UMIs, a number of genes lower than 250 and higher 4,000 and with a proportion of mithocondrial genes >10% were filtered out. Dotted lines indicate said thresholds **(D)** Less than 10% of cells did not pass the QC filters.

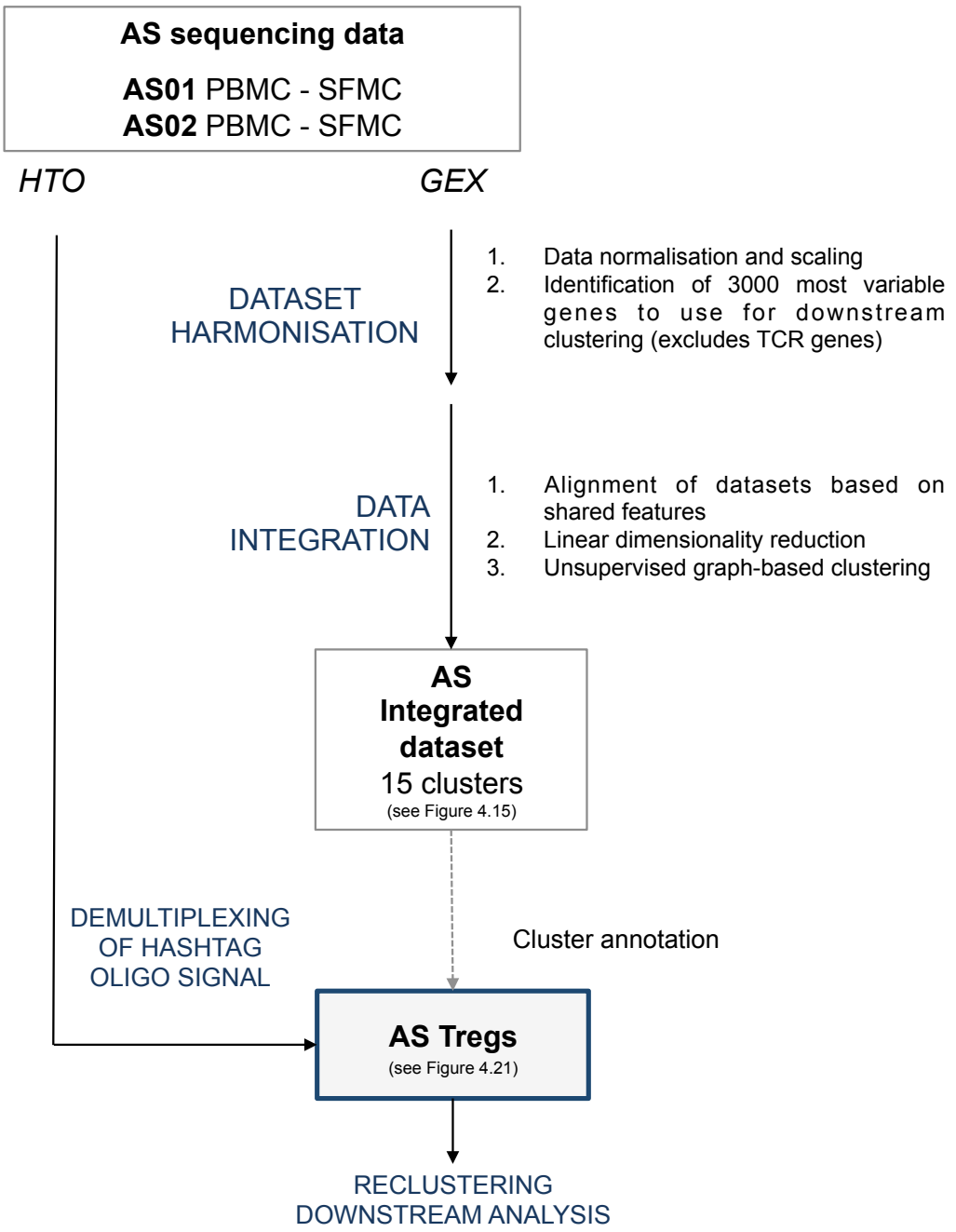

Figure 4.14. AS single cell dataset computational and analytical workflow. GEX = gene expression, HTO = hashtag oligo.

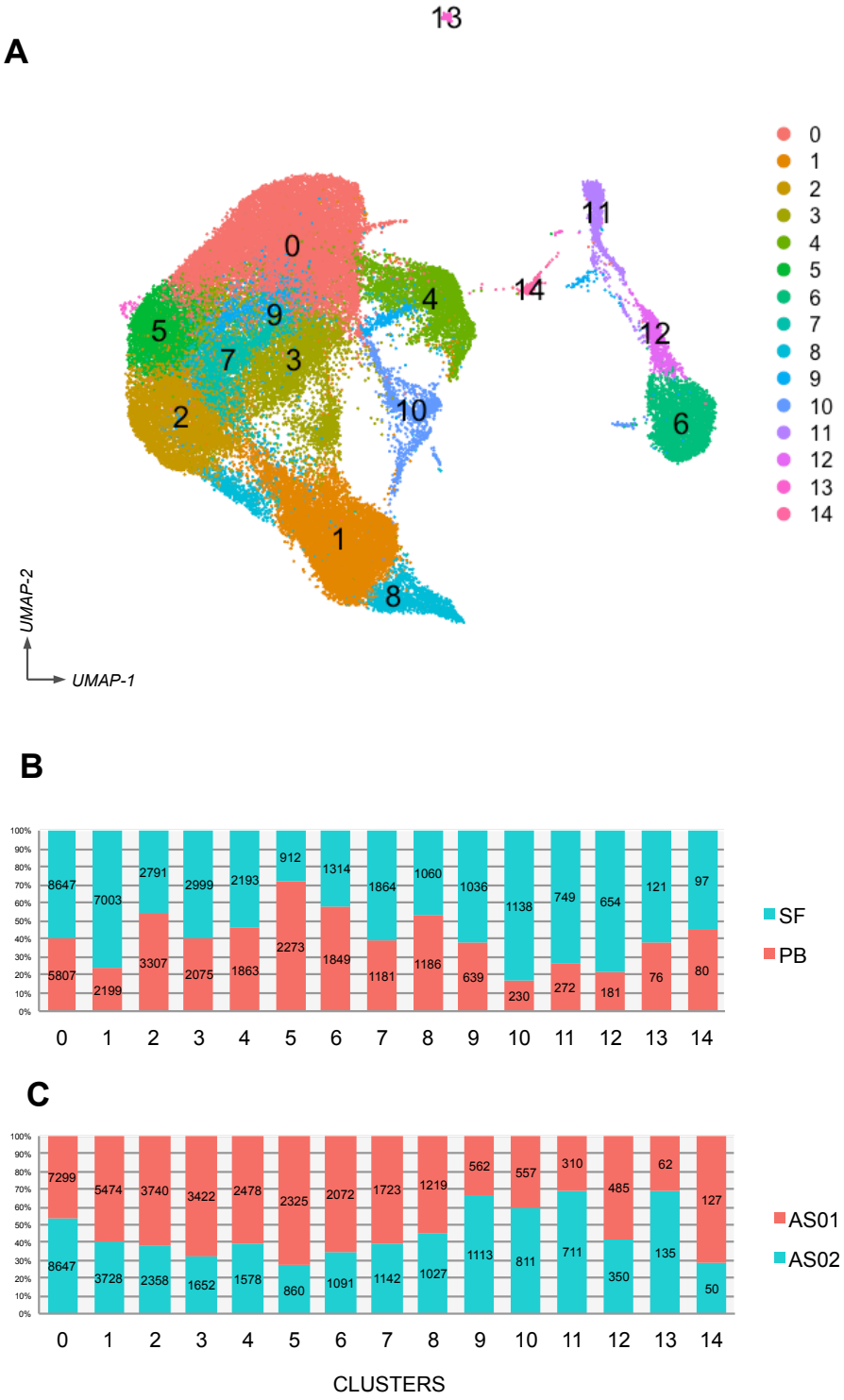

Figure 4.15. UMAP plot (A) showing cell clustering of the AS dataset cells obtained after integrating transcriptomes from memory Tregs, memory CD4$^+$, memory CD8$^+$ and a subset of CD3$^-$ cells (see Figure 4.12). Histograms show relative contribution (percentage) of tissue of origin (**B**) and subject (**C**) for each cluster.

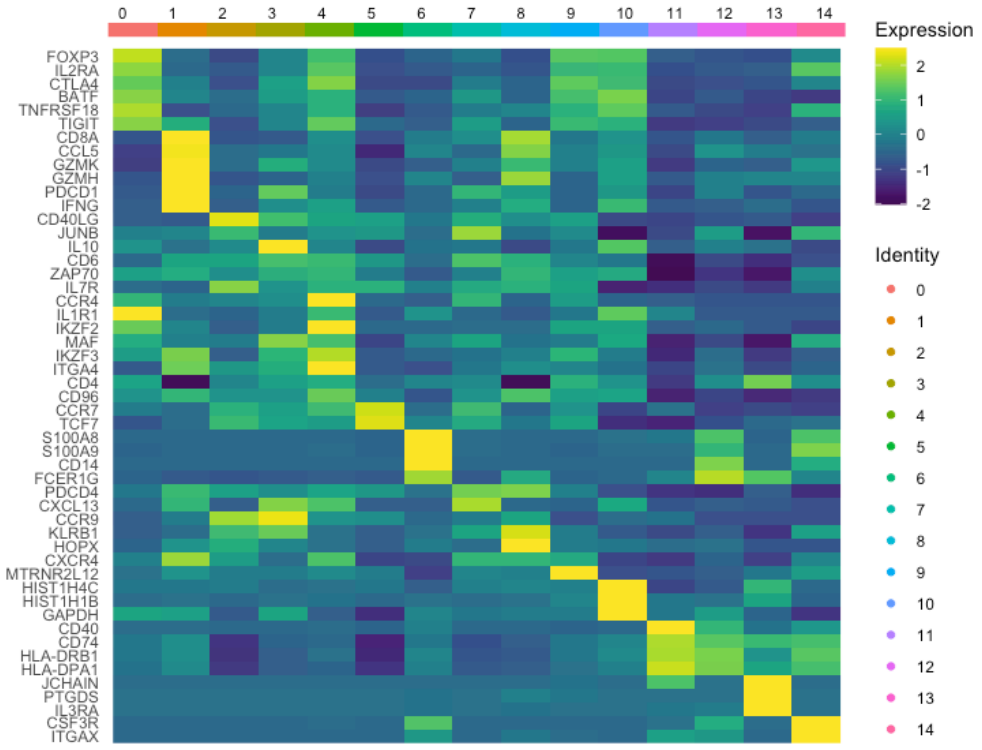

	n. of cells	enriched genes	annotation
0	14454	*FOXP3, IL2RA, CTLA4, BATF, TNFRSF18, TIGIT, IL32, TNFRSF4, CD27*	**Tregs**
1	9201	*CD8A, CCL5, GZMK, GZMH, PDCD1, IFNG, KLRG1, NKG7*	**CD8+**
2	6098	*CD40LG, JUNB, PTGER2, MAL, LTB*	**Activated CD4 (CD154+)**
3	5074	*KLRB1, IL10, ZAP70, CD5, CD6, CCR9*	**CD161+ CD4**
4	4056	*CCR4, IKZF2, MAF, IKZF3, ITGA4, CD4, RORA, PTPRC, CD96*	**CCR4+ CD4**
5	3185	*CCR7, PABPC1, SELL, LEF1, TCF7*	**CCR7+ CD4**
6	3163	*S100A8/9, CD14, FCER1G, CXCL2, IL1B*	**Monocytes**
7	2685	*NR3C1, PDCD4, CXCL13, ZNF331, DUSP2*	**GC-receptor CD4**
8	2246	*KLRB1, HOPX, CCR9, GNLY, KIR3DL1, KLRD1*	**MAIT/MAIT-like CD4**
9	1675	*MTRNR2L12, HIST1H4C, HIST1H1B, GPSM3*	**Humanin+**
10	1368	*MKI67, CDK1, CDK4, FXP3, STMN1*	**Cycling**
11	1021	*CD40, CD74, HLA-DRB1, HLA-DPA1, CST3, LGALS2, CD83*	**HLA-DR+ Monocytes**
12	835	*CD14, FCGR3A, CD1E, CSF1R, IL18, CD68*	**Intermediate Monocytes**
13	197	*JCHAIN, PTGDS, IL3RA, CD36, CD68, JCHAIN*	**pDCs**
14	177	*CSF3R, IGTAX, CD83, TLR2, CD109*	**DCs**

Figure 4.16. Annotation of the 15 cell clusters identified from unsupervised clustering using the top variable genes. Each cluster is annotated based on the genes with highest expression after differential gene expression analysis. Colors encode normalized (Z-scored) gene expression. The table shows number of cells composing each cluster, enriched genes and cluster annotation. Genes shown were selected among the enriched genes for each cluster compared to rest of the dataset and detected in at least 20% of the cluster cells.

The graph-based clustering analysis of the dataset, made of 55,616 cells from two paired samples, yielded 15 clusters (**Figure 4.15A)**: the relative contribution of each patient or tissue of origin to each cluster is shown in **Figure 4.15B, C**. Based on the expression of selected marker genes that included surface markers and transcription factors, the clusters were annotated (**Figure 4.16**).

Five clusters were of myeloid lineage (identifying three monocyte differentiation and activation states, DCs and plasmacytoid DCs respectively), two represented cell states (annotated as “Cycling” and “Humanin+”, the latter being characterised by higher levels of mitochondrial transcripts) and the remaining clusters were T lymphocytes. The $CD4^+$ T cells in particular, which were split into four clusters, localised in contiguous areas of the plot, constituted a continuum rather discrete clusters. One cluster (cluster 0) was characterised by Treg lineage defining genes, but a small number of *FOXP3*- and *IL2RA*-expressing cells were also found in other clusters. To reliably identify and export Tregs for downstream analysis, the barcoding information from our multiplexed samples were deconvoluted.

4.3.3.3 Sample demultiplexing

A known problem with CITE-seq is the data noise originated from unbound antibody encapsulated in the droplets, or binding on other samples when these are pooled together. The distribution of the hashing antibodies over

the UMAP plot (**Figure 4.17**) in our experiment only partially overlays with the awaited expression of the lineage defining genes, with areas of overlap of two or more HTO antibodies, in particular those used to label “memory CD4” and “memory CD8”. A specific function on Seurat, the package I used to analyse single cell data, demultiplexes the HTO data: based on the count distribution of the oligonucleotide reads, it “denoises” the HTO signal using a probabilistic method, and assigns each single cell to its sample of origin (explained in detail in Stoeckius et al., 2017) (**Figure 4.18A**). The four samples were thus demultiplexed. The expression of the genes that emerged from the PsA single cell dataset as distinctive of Tregs confirmed that the cells labelled as “mTreg” indeed captured, with very good accuracy, of the cells expressing Treg lineage genes (**Figure 4.18B-C**).

Therefore, 15,953 cells memory Tregs were subsetted out for in depth downstream analysis.

4.3.3.4 AS Treg reclustering

The Treg cells were reclustered reapplying the same pipeline shown in **Figure 4.14**. Twelve clusters were identified and manually annotated on the basis of the literature about their markers. (**Figure 4.19A**). For further QC check, cells not expressing any transcript for *CD3E*, *CD3G* and *CD3D,* encoding the various CD3 chains, were removed. On examination, two clusters were obviously characterised by genes belonging to myeloid cells (cluster 8 enriched markers: *CD14, CD83, CD68, FCER1G*) or low expression of *FOXP3* (cluster 11 *KLRC1, KLRD1, KLRF1, KIR3DL1*, possibly including gamma delta T cells or NKT cells) (**Figure 4.19B**), and were consequently removed from following analyses. One

further cluster (7) was characterised by low level of *FOXP3* and *IL2RA* (**Figure 4.20**) and the lowest number of genes and reads per cell. One cluster (cluster 1) had also slightly lower expression of *IL2RA* and *FOXP3*, but despite A systematic pathway analysis using the Reactome Knowledgebase (Fabregat et al., 2018), which classifies genes based on their involvement in biomolecular pathways, was run and demonstrated signs of cellular stress, hence it was considered low quality and removed from the analysis. In total, 546 cells were removed because of low quality and 462 because likely non Tregs (indicating a purity for the demultiplexing selection around 97.1%).

4.3.3.5 AS Treg differential gene expression analysis and cluster annotation

The top 10 differentially expressed genes (**Figure 4.21**) guided the cluster annotation. Some differences in the cluster make-up of the AS Tregs compared to the PsA dataset emerged, one being the presence of transitional cell states, such as cycling and high expression of the mitochondrial gene *MTRNR2*, encoding a protein called Humanin, which is probably a consequence of the sorting strategy. Secondly, the higher number of cells allowed the identification of rare clusters previously undetected. Of these two small clusters was strongly characterised by metallothioneins encoding genes, the other presented an interferon response signature.

The biggest 5 clusters had transcriptional profiles very similar to those identified in the PsA dataset. Despite minor differences, I decided to keep the same annotation (“HLA-DR+”, “CCR7+”, “CCR4/Helios+”, “KLRB1+” and “CD8+”).

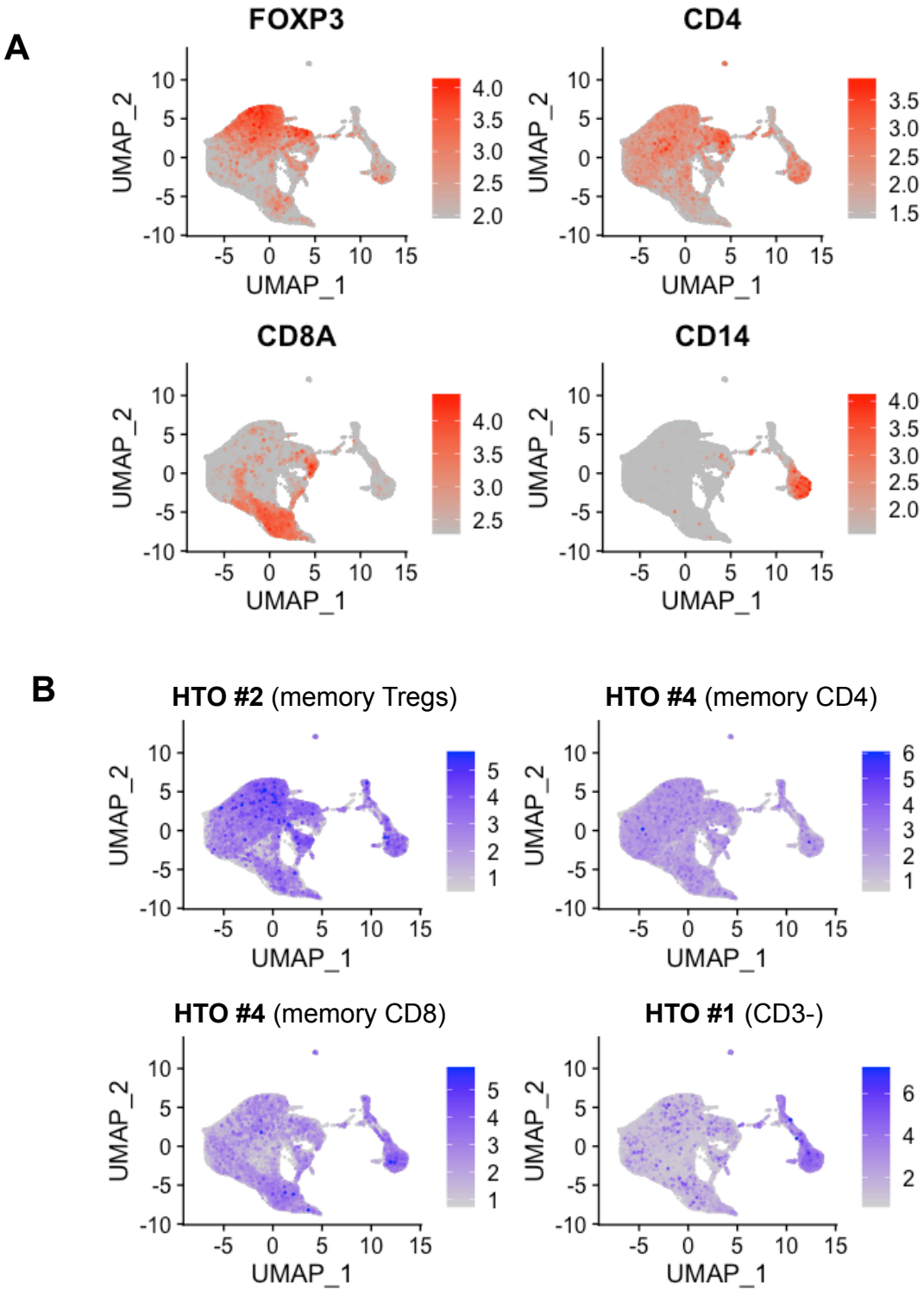

Figure 4.17. Comparison of gene expression and HTO counts distribution in the integrated UMAP plot including PBMC and SFMC cells. UMAP plots highlight cells expressing **(A)** selected lineage-defining genes and **(B)** HTO antibody counts.

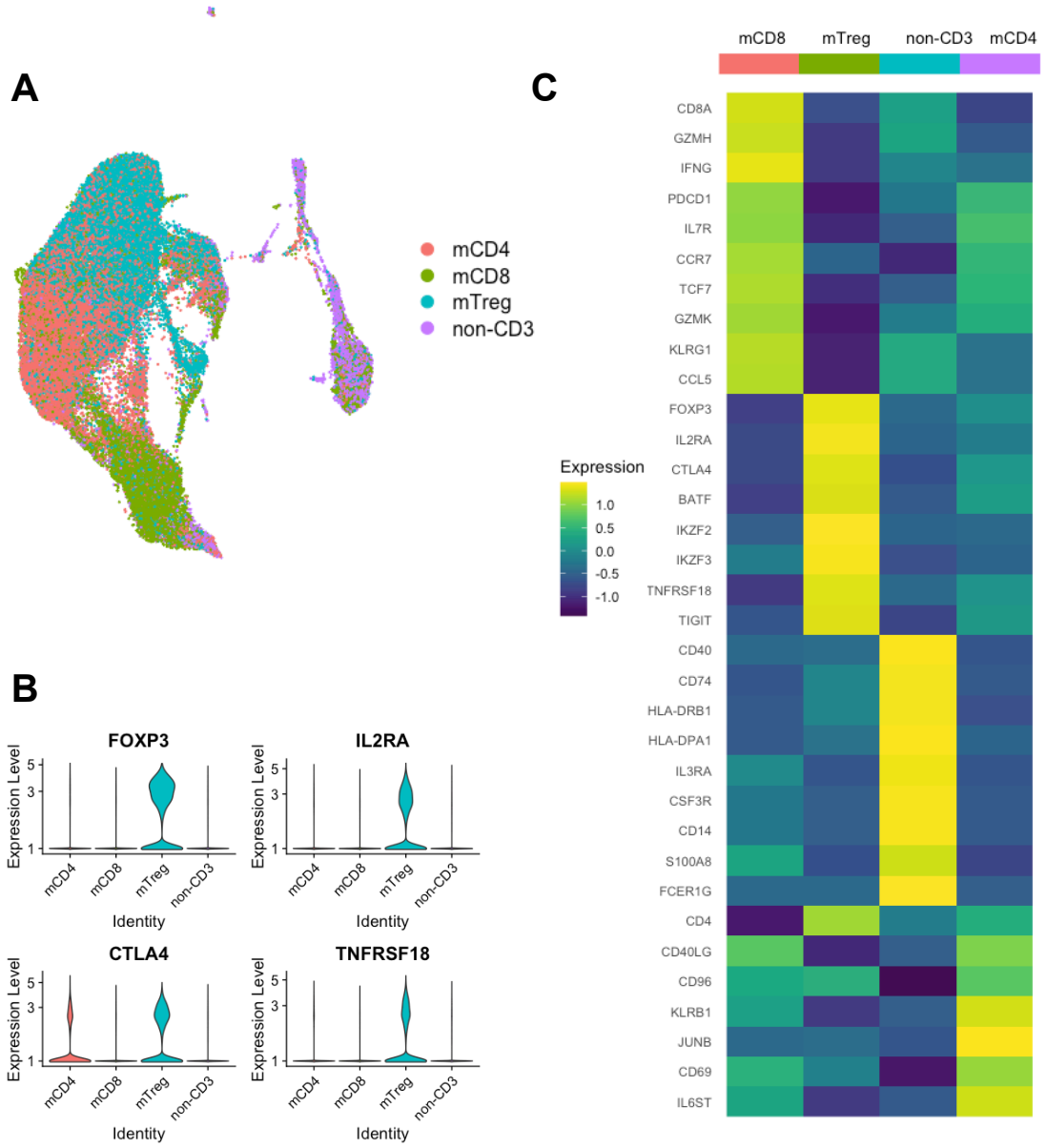

Figure 4.18 Sample demultiplexing. (A) After demultiplexing, cells in the integrated UMAP plot are colored according to group assignment. **(B) (C)** Violin plots and heatmap showing expression of selected genes. “mTreg” cells, as identified after deconvoluting HTO data, express Treg genes. Heatmap colors encode normalized (Z-scored) gene expression.

A

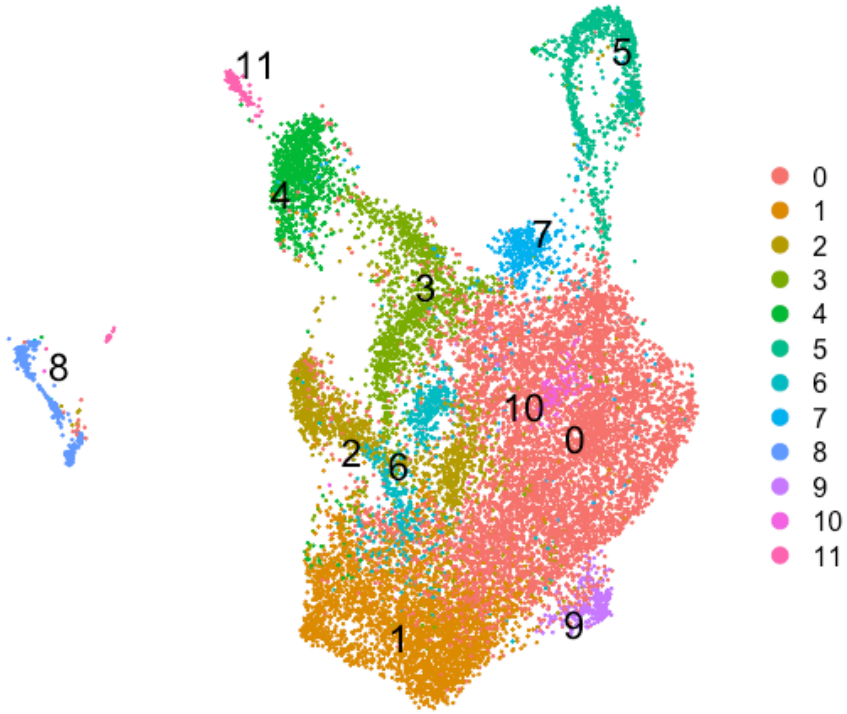

B

cl.	cells	PB	SF	top enriched genes include	annotation
0	6572	1773	4799	*FOXP3, CD27, TNFRSF18, TIGIT*	**HLA-DR+Tregs**
1	3094	1146	1948	*JUNB, MAL, IL7R, PTGER2, CCR7*	**IL7R+**
2	1333	437	896	*PTPRC, CCR4, RORA, IL10RA, IKZF2*	**CCR4/Helios**
3	1176	369	807	*KLRB1, GPR25, GZMA, GZMK, LAG3*	**KLRB1hi**
4	972	127	845	*CD8A/B, CCL4, CCL5, NKG7, GZMK, GZMH*	**CD8+ Tregs**
5	852	145	707	*MKI67, TUBA1B, STMN1, HMGN2*	**Cycling**
6	622	210	412	*MTRNR2L12, MT-CO3*	**Humanin+**
7	*429*	*111*	*318*	*UCP2, LCK, TMBIM6, SKP1*	*ER stress*
8	*316*	*112*	*204*	*CD14, CD68, CST3, S100A8/9, FCER1G*	*Myeloid cells*
9	246	45	201	*IFIT3, IFIT1, ISG15, IFI6*	**IFN response**
10	196	64	132	*MT2A, MT1X, MT1E, MT1F*	**Metallothioneins**
11	*145*	*36*	*109*	*GNLY, GZMB, KLRD1, KLRC1, KIR3DL1*	*Gamma Delta / NKTs*
	15953	**4575**	**11378**		**TOTAL**

Figure 4.19 AS Tregs bidimensional space and cluster annotation. (A) UMAP plot representation of 15,953 AS Tregs from PB and SF, divided in 12 clusters **(B)** Top enriched genes (genes selected among the top 15 genes for each cluster according to average log fold change, Wilcoxon test) and cluster annotation. Cluster 7, 8 and 11 will be discarded for downstream analysis.

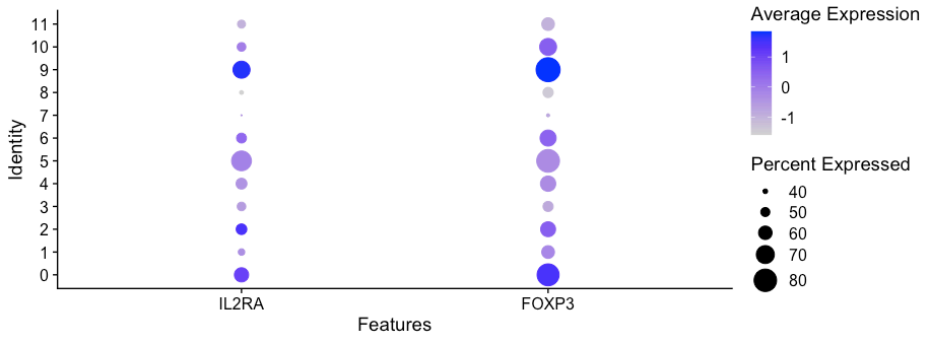

Figure 4.20. Expression of *IL2RA* and *FOXP3* reveals non Treg clusters, that were removed from analysis. Based on average expression and percentage of cells presenting the two genes, cluster 7 (apoptotic or “ER-stress cells”), cluster 8 (“myeloid cells”) and cluster 11 (“Gamma delta/NKT cells”) are considered non Tregs.

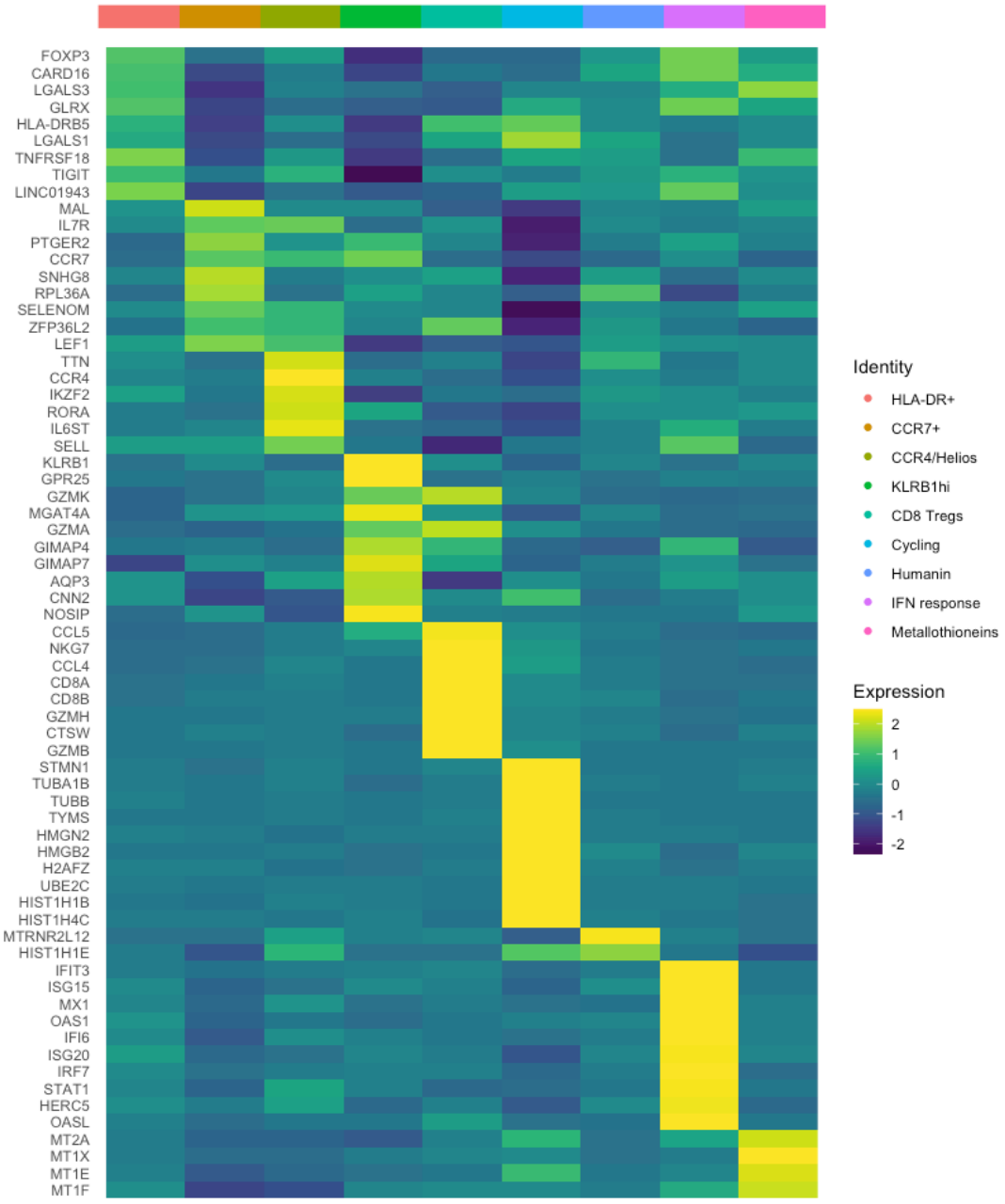

Figure 4.21. Heatmap showing the differentially enriched gene for each cluster. Top 10 genes, at least detected in at least 20% of the cell composing the cluster and with an enrichment of 0.2 log fold change, are shown. Scaled average expression.

4.3.3.6 Specialised regulatory clusters in AS

The gene signatures of clusters “KLRB1+” and “CD8+” described in the PsA Tregs were largely confirmed in the corresponding AS clusters (**Figure 4.22AB**). In the KLRB1+ cluster, *RORC* did not appear among the differentially expressed genes but expression of *LAG3* and *IL10* was instead confirmed. Interestingly, the down regulation of the Helios gene confirmed these cells are likely of non thymic origin. *GPR25*, interestingly associated with AS in a genome-wide association study (International Genetics of Ankylosing Spondylitis Consortium (IGAS) et al., 2013), appeared again as strongly characterising this cluster.

The newly identified clusters 9 and 10 were characterised by genes related to response to interferons and by the expression of metallothioneins, respectively (**Figure 4.22C**). Metallothioneins, a family of metal ion-binding proteins, regulate zinc and copper homeostasis and consequently protect from redox stress. Curiously, one report highlights the ability of the protein MT-1 to suppress inflammation in the experimental model of RA by restoring the Th17/Treg ratio (Sun et al., 2018).

The distribution of effector molecules in the various AS Tregs subset confirms the preferential expression of IL-10 and LAG-3 (together with *HAVCR2*, or TIM-3) by KLRB1+ cells, and of Granzyme B and PD-1 by CD8+ Tregs (**Figure 4.23**).

Finally, the SF signature of AS (**Figure 4.24**) appears similar to PsA. Most of the findings are here replicated, with added upregulation of the genes coding for GITR and OX40, *FOXP3* and *IL2RA*. In this dataset *TIGIT* was also elevated across several clusters, together with the chemokine ligand *CCL5*.

Importantly, interferon response signature genes Among the top downregulated genes, *CCR6*, whose protein expression I previously observed being reduced on the surface SF Tregs (see **Figure 3.4**).

4.3.4 Integration of a healthy control Treg single cell dataset

Remarkable similarities were found in the AS and PsA datasets, from cluster composition to transcriptional identity of the single subsets, to single genes enriched in the SF. To verify if any of these clusters were specific of the synovial environment or disease specific, I compared the generated datasets with a public healthy single cell data obtained from $CD4^+$ $CD25^+$ obtained from the PB of one healthy control (Zheng et al., 2017). This dataset, available on the 10x Chromium public repository, was generated with the 3' chemistry and technology, for this reason an analytical strategy optimised to merge single cell datasets generated with different technologies (Butler et al., 2018) was here employed: the PsA and AS datasets, although obtained with different procedures, did not show notable bias in RNA quality or expression properties, but the read depth for the healthy control dataset was lower, and differences in the sequencing metrics were regressed out (**Figure 4.25A**). Despite the use of a different sorting strategy to obtain the dataset, in a preliminary parallel analysis, the different datasets could be overlaid and shared characteristics could be identified (**Figure 4.25C**). Differential gene expression analysis is underway. This pipeline, allowing across-platform and tissue comparisons, would be of value to compare our data with the increasing number of single cell repositories from healthy tissues made available by consortia such as the Human Cell Atlas.

A

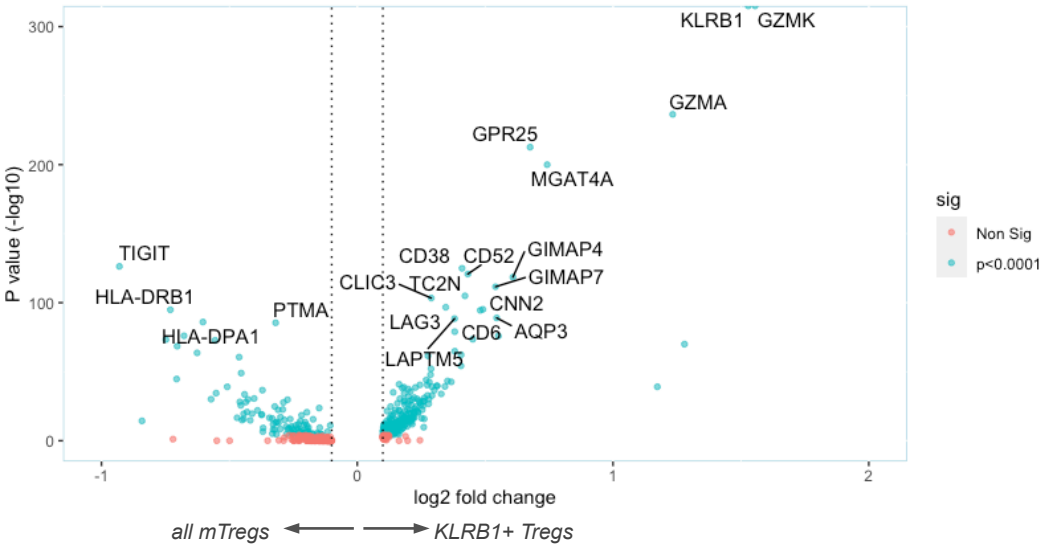
KLRB1
GZMK
GZMA
GPR25
MGAT4A
TIGIT
HLA-DRB1
HLA-DPA1
PTMA
CD38
CD52
GIMAP4
GIMAP7
CLIC3
TC2N
CNN2
LAG3
CD6
AQP3
LAPTM5
P value (-log10)
log2 fold change
all mTregs
KLRB1+ Tregs
sig
Non Sig
p<0.0001

B

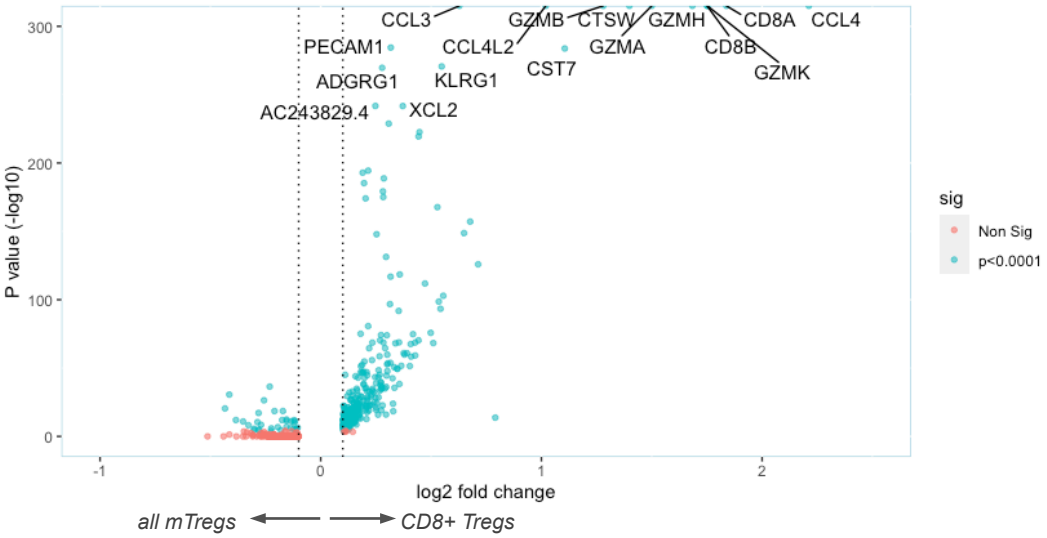
CCL3
GZMB
CTSW
GZMH
CD8A
CCL4
PECAM1
CCL4L2
GZMA
CD8B
CST7
GZMK
ADGRG1
KLRG1
AC243829.4
XCL2
P value (-log10)
log2 fold change
all mTregs
CD8+ Tregs
sig
Non Sig
p<0.0001

C

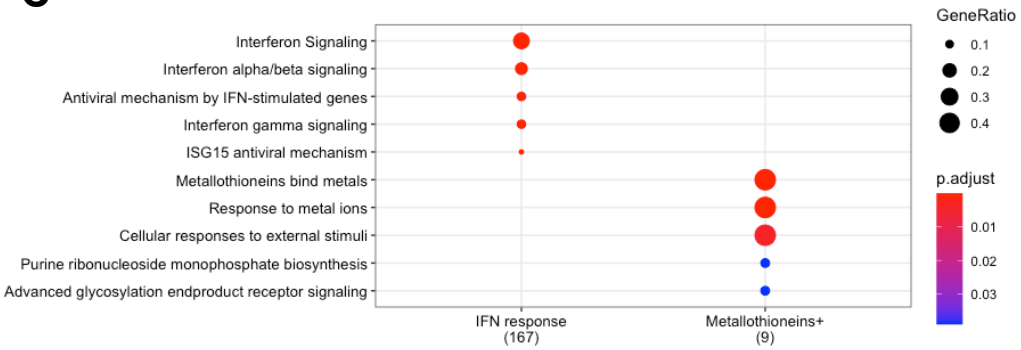
Interferon Signaling
Interferon alpha/beta signaling
Antiviral mechanism by IFN-stimulated genes
Interferon gamma signaling
ISG15 antiviral mechanism
Metallothioneins bind metals
Response to metal ions
Cellular responses to external stimuli
Purine ribonucleoside monophosphate biosynthesis
Advanced glycosylation endproduct receptor signaling
IFN response (167)
Metallothioneins+ (9)
GeneRatio
0.1
0.2
0.3
0.4
p.adjust
0.01
0.02
0.03

Figure 4.22 (previous page). Selected AS Treg clusters with functional specialization. Differential gene expression in KLRB1+ **(A)** and CD8+ Tregs **(B)**. **(C)** Enriched pathways for cluster named "IFN response" and "Metallothioneins+" according to the Reactome pathway knowledgebase. "Gene Ratio" represents the percentage of total differentially expressed gene in the given Reactome term. Dot color represents p value (Fisher's exact test). p-value < $1x10^{-300}$ (**A-B**) are not computed.

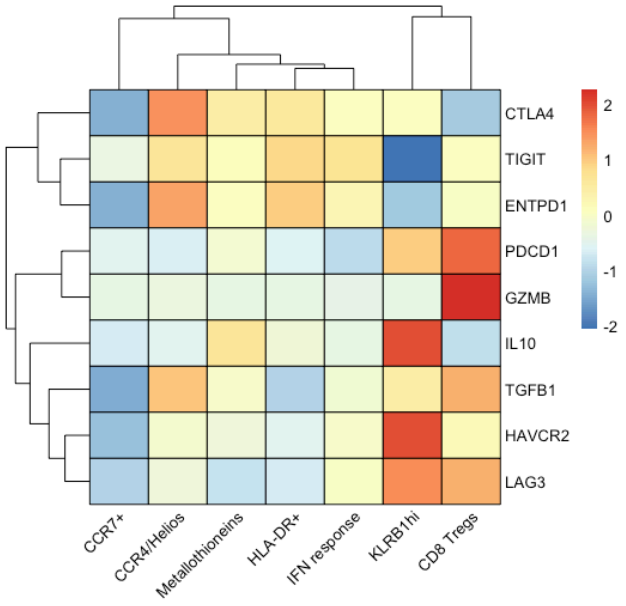

Figure 4.23. Differential expression of selected suppression markers across the different clusters identified in the AS Tregs dataset. Colors represent row-based Z-score of gene average expression.

A

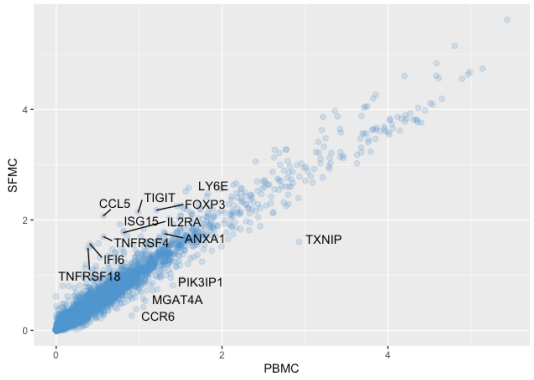

B

	avg_logFC	% PB	% SF	p_val_adj
CCL5	1.429282155	0.069	0.433	< 1E-300
TIGIT	1.157263763	0.322	0.766	< 1E-300
ISG15	1.148940793	0.278	0.734	< 1E-300
IFI6	1.13226466	0.146	0.63	< 1E-300
TNFRSF4	1.108216632	0.171	0.509	< 1E-300
TNFRSF18	1.095669742	0.116	0.539	< 1E-300
MX1	1.092110804	0.143	0.632	< 1E-300
LINC01943	1.062276813	0.156	0.588	< 1E-300
LY6E	0.978379702	0.63	0.918	< 1E-300
FOXP3	0.962868484	0.4	0.784	< 1E-300
CCL5	1.429282155	0.069	0.433	< 1E-300
TXNIP	1.315182616	0.881	0.673	< 1E-300
MGAT4A	0.62913909	0.359	0.175	5.09E-177
S1PR1	0.62688635	0.331	0.11	5.70E-271
PIK3IP1	0.583629123	0.544	0.363	2.39E-185
CCR6	0.576728762	0.3	0.137	8.73E-148

C

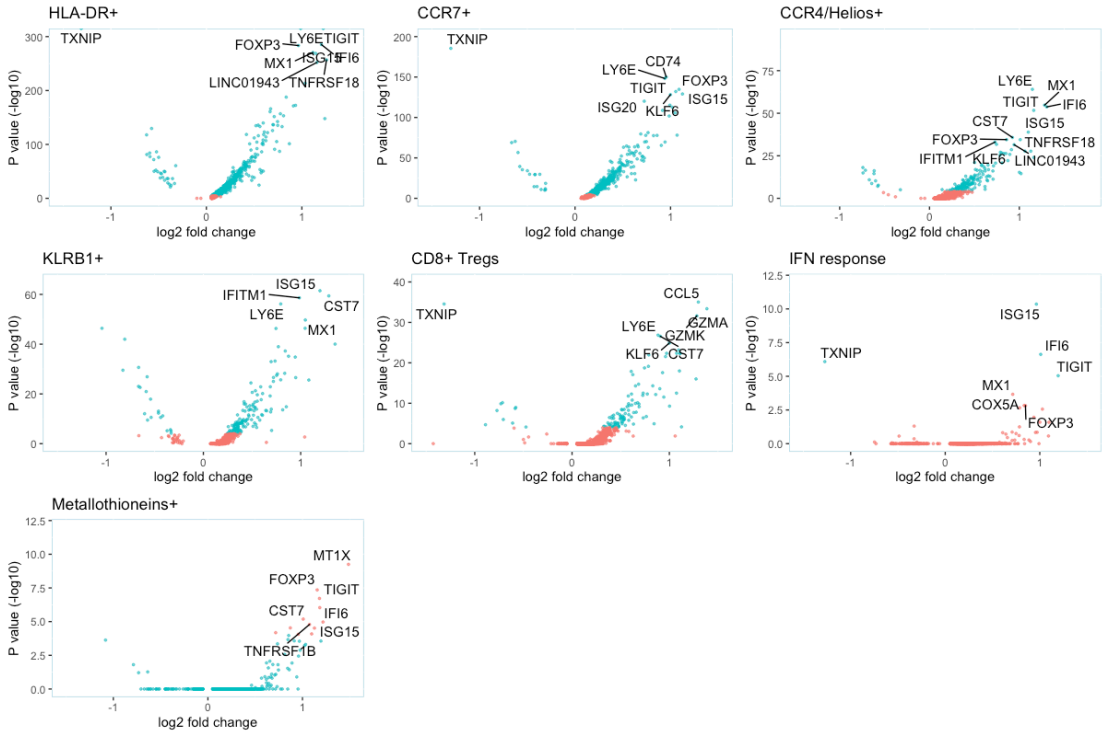

Figure 4.24. Synovial fluid differential gene expression. (A) Scatter plot showing gene expression (log scale) in PB and SF Tregs. **(B)** In light blue: top 10 genes in the SF Tregs compared to PB by average log gold change. In red, top 5 genes enriched in PB. % indicate proportion of cells expressing that gene in each tissue. Only genes detected in at least 10% of the cells are shown. Avg_logFC: average log fold change, p_val_adj: p-value (Wilcoxon rank sum test with Bonferroni correction) **(C)** Volcano plots showing differentially expressed genes in SF (right half) and PB (left half) for each cluster. Blue dots: p<0.0001.

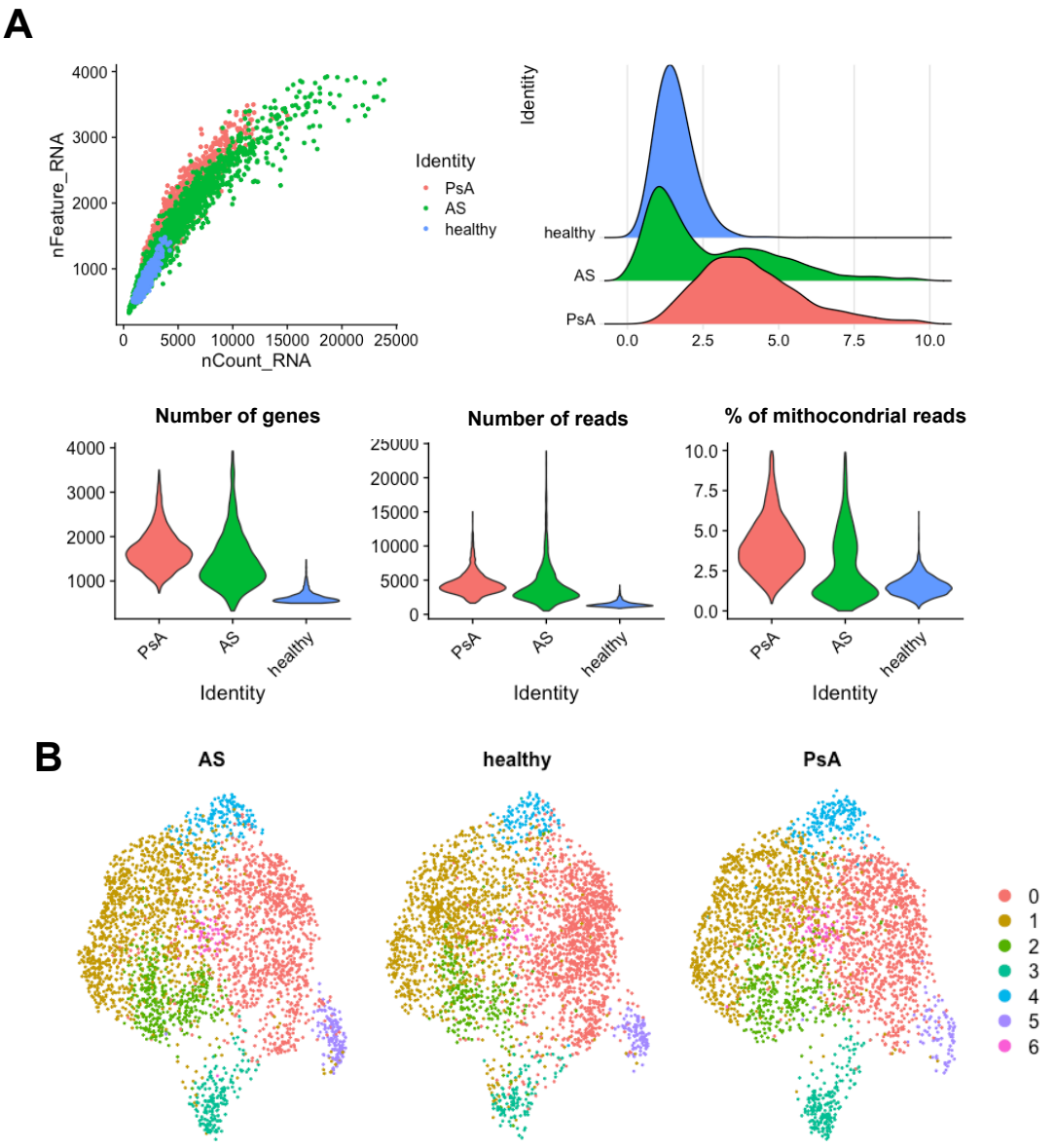

Figure 4.25. Integration of the SpA dataset with a public available Treg repository (A) QC metrics of the three datasets **(B)** After integration and batch correction, integrated UMAP plot with distribution from two AS patients (paired PB/SF), one healthy control (PB) and three PsA (PB/SF).

4.4 DISCUSSION

This chapter focused on the transcriptional profile of Tregs in the course of SpA. The analysis was performed on two datasets, from two SpA conditions: in the first one, Tregs were identified on the basis of their distinctive gene signature after unsupervised clustering on a larger memory T cell dataset from three PsA patients. In the second dataset, barcoded Tregs, previously FACS sorted according to canonical surface markers, were pooled with other immune cells, then identified after sample demultiplexing and analysed separately. Both methods proved accurate in capturing the expected Treg transcriptional identity. Despite some minor differences, the composition of the Treg subsets was very similar. Overlapping subsets were identified independently in the two datasets, suggesting reproducibility of the findings, and similarities in the composition of the regulatory T cell compartment between PsA and AS. All Treg subsets were characterized by the presence of a core of regulatory genes, similarly expressed across the clusters, with specialized modules being expressed in a cluster-specific manner. Importantly, distinct mechanisms of suppression appeared to associate with different subsets, indicating an underappreciated specialization of Tregs effector responses.

Some of the genes that make up the Treg core signature belong to known Treg TFs (*FOXP3*, *BATF*), with a recognised role in differentiation, maturation and functional stability, others, such as TNF receptor superfamily (TNFRSF) genes are less expected. Furthermore, TNFRSF genes are often among the top differentially expressed in the SF, both at population level and in many clusters. A family of 27 genes, they encode a heterogeneous group of cytokine receptors

with transmembrane domain and are found on a number of cells, both of adaptive and innate immunity, where they mediate both co-stimulatory and regulatory responses (Locksley et al., 2001). Their role in Treg functions has gained increasing attention recently. Activation of GITR (*TNFRSF18*), OX40 (*TNFRSF4*) and TNF-RII (*TNFRSF1B*), via NF-κB, was found to provide crucial survival and stability signals to effector Tregs, (Vasanthakumar et al., 2017). OX40 expression (gene *TNFRS4*) appeared to be crucial for accumulation of Treg cells in the tissue, and protection against T cell–transfer colitis (Griseri et al., 2010). *TNFRSF1B* expression was shown to maintain FOXP3 demethylation status in Tregs, hence preserving their suppressive function and preventing their conversion to IL-17A-producing cells (Tseng et al., 2019), an interesting observation considering it was particularly high in the the KLRB1+ Tregs cluster which showed clear Th17-like features in our dataset. These and other reports suggest that these markers could provide environmental adaptation and survival in a TNF-rich environment, such as the SF, while preserving, or even enhancing, their suppressive function. However, in a recent scRNAseq analysis of Tregs from murine non lymphoid tissues *Tnfrsf4* (OX40) and *Tnfrsf18* were among the upregulated genes in the colon and the skin of healthy mice (Miragaia et al., 2019), suggesting they might be also part of a non specific tissue module, expressed irrespective of local inflammation. Of note, in the same work, the authors, found genes such as *Lmna* and *Srgn* also upregulated. With the data available, it is difficult to distinguish tissue-derived genes in steady state from inflammation-driven. A future area of research might be interested in defining how tissue-derived signals, such as soluble inflammatory mediators and resident cells, induce the changes in the Treg transcriptome that favour tissue

adaptation and effector pathway expression. The observed strong upregulation of GITR in Tregs in the SF is a particularly interesting finding: biology of GITR is complex and its role on Tregs is only partially understood. Although both Tregs and Teffs can express GITR, the physiological function is probably cell type- and context-dependent. Ligation of GITR with an agonist antibody on Teffs increases effector functions and their resistance to Treg suppression. Agonist anti-GITR monoclonal antibodies are in fact being tested as treatments against solid tumours, potentially representing a new line of immunotherapies that enhance costimulatory functions versus the cancer cells (Zappasodi et al., 2019). Its function on Tregs is less clear: ligand-mediated activation of GITR has been reported to induce loss of suppression and instability (Kanamaru et al., 2004), but also enhance Treg maturation (Mahmud et al., 2014). The expression of the natural GITR ligand (GITRL) has been described on synovial macrophages in RA (Bae et al., 2007). It is possible that the expression of GITR on SF Tregs might be detrimental for their function in vivo, which could in part explain their inability to prevent synovitis during a SpA flare. Another model speculates a role of GITR in a mechanism called “contra-suppression” (Shevach and Stephens, 2006): the initial phases of the GITR-GITRL crosstalk would involve Teffs, leading to enhancement of their differentiation and activation. As the immune response progresses, GITR is downregulated on Teffs making them more susceptible to Treg-suppression. This could represent an important factor in the termination of an exaggerated inflammatory response, such as the synovial effusion, which can often be self-limiting. The timing of the signals that regulate the overexpression of GITR on SF Tregs, and whether different ligands are involved,

and, finally, whether blocking antibodies could represent a viable approach to downregulate Teff responses, are all interesting area of future research.

In 1.2.3, I discussed the concept of Treg plasticity, which is the ability of Tregs to adapt to the environment often acquiring transcription factors associated to other T helper lineages. Of note, ROR-γt was the sole T helper-related TF strongly characterising a Treg subset in our data, the KLRB1+ cluster. *TBX21 (T-bet)* and *GATA3* were not differentially expressed in any of the other Treg clusters. Although it is possible that a transcriptional drift of Tregs towards Th17 in AS and PsA, both conditions imprinted by strong "type 17" immunity and clinically validated to respond to IL-17A blockade. CD161+ Tregs have also been identified and characterised by us and other groups (Pesenacker et al., 2013; Povoleri et al., 2018), in the PB of healthy individuals and in the SF of JIA and RA (a condition where the role of Th17 biology is less clear). Furthermore, specialised ROR-γt+ Tregs might represent a subset with marked recirculatory ability, unlike *TBX21*- and *GATA3*-expressing Tregs, which might have more pronounced tissue-residency programmes (eg. in the gut or the skin) and be rarely find in the peripheral circulation. In KLRB1+ cells, a clear RORγt-dependent program, with upregulation of several Th17-associated genes, such as *CCR6*, *IL6R* and *IL1R*, was observed. The expression of these genes in Tregs could represent a functional advantage over Th17, depriving them of differentiating cues (IL-6 and IL-1β), or, in the case of CCR6, favour co-localisation with Th17, as hypothesised when Th17-like signature in Foxp3+ cells was first described in the mouse intestine (Chaudhry et al., 2009). According to this hypothesis, the production of inflammatory cytokines (eg. IL-17A) regulated by ROR-γt, could

then be interpreted as a by-product of the expression of a certain TF, rather than a sign of dysregulation.

On the other hand, proinflammatory cytokines, and IL-6 in particular, have also been reported to be sufficient causes of Tregs functional instability. The influence of IL-6 on the Th17/Treg balance is debated, and it might be context or subset dependent. IL-6 induces Th17 differentiation and, in parallel, alters the methylation of a non intronic upstream enhancer of *Foxp3*, limiting its transcription (Lal et al., 2009). This occurrence has been described in an in vivo model of RA (Komatsu et al., 2014), where IL-6 was able to render Tregs pathogenic. Thus, blocking IL-6R or Stat3 in Tregs may represent a viable strategy to improve the Treg stability, enhance their suppressive ability or prevent dysregulation. In Tregs isolated from PB of patients with giant cell arteritis treated with the anti-IL-6R tocilizumab, Tregs showed enhanced suppressive ability and decreased production of IL-17 upon stimulation compared to conventional treatments (Miyabe et al., 2017), although IL-6 blockade failed to demonstrate efficacy in SpA. At the same time, IL-6R signalling may be required for development or function of certain Treg subsets. A subpopulation of synovial Tregs with unstable Foxp3 protein expression was observed in the SF of JIA patients (Bending et al., 2015). Exposure in vitro to soluble mediators contained in the SF, including IL-6, increased expression of Foxp3 and enhanced regulatory properties. Furthermore, the *IL6R* locus is polymorphic: single nucleotide polymorphisms, causing altered signalling, have been described in AS (International Genetics of Ankylosing Spondylitis Consortium (IGAS) et al., 2013)., type 1 diabetes (Ferreira et al., 2013) and asthma (Ferreira et al., 2011). It is conceivable that in patients that carry the risk variant, elevated IL-6 levels, as often found in sites of inflammation, might be able to disable regulatory functions

in susceptible Tregs, as suggested in one study that phenotyped IL-6R+ Tregs (Ferreira et al., 2017). Based on our gene expression data, KLRB1+ Tregs are likely competent regulators, rather than an intermediate of differentiation toward Th17, or even Th17 cells transiently expressing Foxp3 upon activation. An interesting feature of the KLRB1+ cluster observed in our analysis is the strong downregulation of TIGIT, which matches the observation that IL-6R-expressing Tregs, with a distinct Th17-like module, have low levels of TIGIT (Ferreira et al., 2017). Furthermore, the KLRB1+ cluster has many similarities with a subset of Tregs identified through scRNA-seq in the healthy human colon (James et al., 2020), also characterised by the expression of *CCR6*, *LAG3*, *IL10*, *CTLA4*, very similar to the CD161+ Treg subset previously described in the PB, and especially SF, of patients with JIA (Pesenacker et al., 2013; Duurland et al., 2017). It is very likely, also in the light of their lack of expression of *IKZF2,* that KLRB1+ cells in the blood and joint are the equivalent of the RORγt^{+} Helios^{-} Tregs described in the mouse intestine, induced by commensal microbiota and key regulators of mucosal immune homeostasis, and, more recently, in the aforementioned human gut cell atlas (James et al., 2020). The translocation of gut-derived effector cells from to the sites of joint inflammation, the so-called gut-joint axis, has historically attracted great attention in SpA research. While CD8^{+} effector cells, expressing integrins and other markers of gut priming have been identified in the joints in AS patients (Qaiyum et al., 2019), the existence of similar migration patterns by regulatory cells can only be based on indirect observations, including the ones provided here. Tregs can indeed migrate into and out of the colon from peripheral lymphoid organs (Morton et al., 2014), but the trafficking of specific Treg subsets to distant inflammation sites to suppress specific Th-driven

pathology is an attractive, yet unproven, scenario. The recruitment of these cells to the sites of Th17 inflammation could be instrumental to exert specific regulatory functions, but the mechanisms of suppression have not being clarified, possibly including CTLA-4, IL-10, and based on the gene expression data shown, LAG-3.

A second intestinal subset with which the KLRB1+ cluster has strong similarities are type 1 regulatory cells, or Tr1. They are instrumental in the prevention of tissue inflammation, autoimmunity and graft-versus-host disease and have a unique effector profile that distinguishes them from other T helper subsets, included conventional Tregs, by their lack of expression of Foxp3. Characterized by the coexpression of CD49b (integrin $\alpha 2$) and LAG-3 (Gagliani et al., 2013), their suppressive activity is strongly dependent on IL-10 and LAG-3 itself. Intrigued by the selective expression of *LAG3* in two of the clusters identified, a feature shared by intestinal Tregs, the LAG-3 protein expression on Tregs and its possible mechanism of suppression will be evaluated the next chapter. I did not identify Tr1 in our dataset

$CD8^+$ Tregs in the PB and SF of SpA are an interesting, if unexpected, finding. Although described many years ago (Gershon and Kondo, 1970) and identified in autoimmune diseases, tumour immune infiltrates and chronic viral illnesses (Billerbeck and Thimme, 2008), little is known regarding their function in negative regulation (Yu et al., 2018), that relies, according to the various reports, on cell contact dependent mechanisms (CTLA-4), tolerisation of APCs, perforin-mediated cytotoxicity. One study, in which the authors describe this subset expanding after in vivo immunisation with bacillus Calmette-Guérin and its presence in the human mycobacterial granuloma, largely confirms the phenotype

I observed, including the expression of *CCL4* and *LAG3* and the conserved expression of *FOXP3* (Joosten et al., 2007). Although a direct effect of CCL4 on the downregulation of TCR signalling in Teffs was proposed, Tregs are known to produce the chemokine CCL4, to attract, and suppress, the Teffs that express its ligand, CCR5 (Patterson et al., 2016). Very recently, it was shown in EAE that regulatory antigen-specific $CD8^+$ cells could suppress self reactive $CD4^+$ and control the disease (Saligrama et al., 2019). Another chemokine, *CCL5* (also known as RANTES), highly expressed by this cell subset and among the highest upregulated gene in the SF, is also a ligand for CCR5, whose expression on effector $CD8^+$ was found upregulated in the SF compared to the circulation (Penkava et al., 2020). An intriguing consideration, originating from the differential gene expression analysis, is that CD8+ Treg localise halfway between regulatory T cells and cytotoxic CD8, possessing transcriptional and effector programmes of both lineages, although they fall closer to Tregs in the unsupervised clustering. The evaluation of this subset in AS and analysis of cell markers will be explored in 5.3.2.

Although performed only on one dataset for time constraints, one of the goals of this part of the work was to characterise clonally expanded Tregs at single cell level. The identification and characterisation of antigen-specific Tregs in humans has historically proven difficult because of technical limitations, the principal being the relative small numbers of Tregs compared to other $CD4^+$ subsets. The observed TCR repertoire of SF Treg cells was very diverse, with no overlap with PB Treg cells. The identification of one clone (**Figure 4.11**) provided some insights into gene regulation of antigen-experienced human Treg cells, information that can help understand tolerogenic antigen-specific

responses. Several questions remain unanswered: the relationship between antigen specificity and regulation of transcriptional profile, i.e. how the TCR signals shapes the transcriptional state, is for example still unclear. For instance in our dataset, the Treg cells expressing identical TCR α/β sequences had indeed with related gene programs, mostly localising inside one cluster, but with few clones presenting less related transcriptional identities. I could not see any clone represented simultaneously in Tregs and Teffs, but with the limited cell number sampled, we cannot exclude the existence of shared clonotypes.

The transcriptional profile of the clone, compared to the rest of the cells, showed overexpression of interesting genes: CCR8 was also reported being a marker for suppressive Tregs (Barsheshet et al., 2017), with a role in restraining inflammation in EAE. Also of interest is the expression of the two IL-1 receptors: in vitro experiments show that, upon TCR engagement, IL-1R1 is upregulated on activated Tregs together with the decoy receptor IL-1R2, which has a capacity to neutralize IL-1β, suggest a potential role of these markers in modifying inflammatory cytokines and controlling local inflammation (Mercer et al., 2010). Other genes, such as *MAGEH* and *LAYN,* strongly characterised intratumoral Tregs in a scRNA-seq experiment, together with *IL1R1, IL1R2, CCR8 (***Figure 4.11***).* This expression pattern correlated with worse survival in patients with colon and lung cancer, indicating that cells expressing those markers might be indeed antigen responsive, and competent suppressors (De Simone et al., 2016). In solid tumours, somatic hypermutation leads to the generation of new antigens and T cell clonal expansion. The occurrence of de novo in situ clonal expansion of antigen specific Tregs in the SF is something that only longitudinal studies could assess. Finally, *TNFRSF9*, encoding for a costimulatory molecule CD137

(also known as 4-1BB) is an intriguing finding in clonal Tregs. Its expression on protein level after exposure to antigens will be explored in 5.3.3, with our data supporting its potential utility as marker for antigen-specific Tregs.

In conclusion, in this chapter scRNAseq was applied to profile 18,011 cells (AS n=14,945, PsA n=3,066) to define the diversity of the transcriptional phenotypes of Tregs in the PB and SF of two SpA conditions. The data demonstrate considerable phenotypic heterogeneity, which reflects in functionally specialised suppressive programs. It is possible to hypothesize that during joint inflammation, Tregs integrate environmental signals to tailor their transcriptional program in a manner that is instrumental for effective regulation of specific populations. One of the limitations of this study is the lack of a disease control, for example SF from a different inflammatory arthritis, like RA, to verify which clusters are specific of SpA. Related to this, knee joint effusion is arguably not a highly specific disease manifestation in AS, whose peculiar clinical feature is inflammation of the enthesis and the spine, two anatomical structures that are considerably more difficult to sample but might be including unique immune features. Thirdly, Tregs in our dataset were not stimulated. Despite our sequencing had an adequate read depth covering a great number of genes, it is possible that, phenotypic dysregulation (eg. the presence of a pro-inflammatory programme) could only emerge after stimulation. In fact, several gene variants associated with immune-driven diseases occur in cell activation pathways that are fundamental for Treg maturation and activation, such as CD28 or IL-2 signalling, and these variants might have potential to alter quantitative gene expression (Bossini-Castillo et al., 2019).

Some of the noteworthy elements emerged from this analysis, such as the utility of the costimulatory immune checkpoint CD137 in Tregs as marker of antigen recognition, the expression of LAG-3 on Tregs and its proposed mechanism of action, and the characteristics of CD8+ Tregs, will be addressed in depth in the next chapter.

4.5 REFERENCES

Bae, E., Kim, W.-J., Kang, Y.-M., Suk, K., Koh, E.-M., Cha, H.-S., Ahn, K.-S., Huh, T.-L., and Lee, W.-H. (2007). Glucocorticoid-induced tumour necrosis factor receptor-related protein-mediated macrophage stimulation may induce cellular adhesion and cytokine expression in rheumatoid arthritis. Clin Exp Immunol *148*, 410–418.

Barsheshet, Y., Wildbaum, G., Levy, E., Vitenshtein, A., Akinseye, C., Griggs, J., Lira, S.A., and Karin, N. (2017). CCR8+FOXp3+ Treg cells as master drivers of immune regulation. Proc. Natl. Acad. Sci. U.S.A. *114*, 6086–6091.

Bending, D., Giannakopoulou, E., Lom, H., and Wedderburn, L.R. (2015). Synovial Regulatory T Cells Occupy a Discrete TCR Niche in Human Arthritis and Require Local Signals To Stabilize FOXP3 Protein Expression. J. Immunol. *195*, 5616–5624.

Billerbeck, E., and Thimme, R. (2008). CD8+ regulatory T cells in persistent human viral infections. Human Immunology *69*, 771–775.

Bossini-Castillo, L., Glinos, D.A., Kunowska, N., Golda, G., Lamikanra, A., Spitzer, M., Soskic, B., Cano-Gamez, E., Smyth, D.J., Cattermole, C., et al. (2019). Immune disease variants modulate gene expression in regulatory CD4+ T cells and inform drug targets. BioRxiv 654632.

Butler, A., Hoffman, P., Smibert, P., Papalexi, E., and Satija, R. (2018). Integrating single-cell transcriptomic data across different conditions, technologies, and species. Nat. Biotechnol. *36*, 411–420.

Chaudhry, A., Rudra, D., Treuting, P., Samstein, R.M., Liang, Y., Kas, A., and Rudensky, A.Y. (2009). CD4+ regulatory T cells control TH17 responses in a Stat3-dependent manner. Science *326*, 986–991.

De Simone, M., Arrigoni, A., Rossetti, G., Gruarin, P., Ranzani, V., Politano, C., Bonnal, R.J.P., Provasi, E., Sarnicola, M.L., Panzeri, I., et al. (2016). Transcriptional Landscape of Human Tissue Lymphocytes Unveils Uniqueness of Tumor-Infiltrating T Regulatory Cells. Immunity *45*, 1135–1147.

Duhen, T., Duhen, R., Lanzavecchia, A., Sallusto, F., and Campbell, D.J. (2012). Functionally distinct subsets of human FOXP3+ Treg cells that phenotypically mirror effector Th cells. Blood *119*, 4430–4440.

Duurland, C.L., Brown, C.C., O'Shaughnessy, R.F.L., and Wedderburn, L.R. (2017). CD161+ Tconv and CD161+ Treg Share a Transcriptional and Functional Phenotype despite Limited Overlap in TCRβ Repertoire. Front Immunol *8*.

Fabregat, A., Jupe, S., Matthews, L., Sidiropoulos, K., Gillespie, M., Garapati, P., Haw, R., Jassal, B., Korninger, F., May, B., et al. (2018). The Reactome Pathway Knowledgebase. Nucleic Acids Res. *46*, D649–D655.

Ferreira, M.A.R., Matheson, M.C., Duffy, D.L., Marks, G.B., Hui, J., Le Souëf, P., Danoy, P., Baltic, S., Nyholt, D.R., Jenkins, M., et al. (2011). Identification of IL6R and chromosome 11q13.5 as risk loci for asthma. Lancet *378*, 1006–1014.

Ferreira, R.C., Freitag, D.F., Cutler, A.J., Howson, J.M.M., Rainbow, D.B., Smyth, D.J., Kaptoge, S., Clarke, P., Boreham, C., Coulson, R.M., et al. (2013). Functional IL6R 358Ala Allele Impairs Classical IL-6 Receptor Signaling and Influences Risk of Diverse Inflammatory Diseases. PLOS Genetics *9*, e1003444.

Ferreira, R.C., Rainbow, D.B., Rubio García, A., Pekalski, M.L., Porter, L., Oliveira, J.J., Waldron-Lynch, F., Wicker, L.S., and Todd, J.A. (2017). Human IL-6RhiTIGIT− CD4+CD127lowCD25+ T cells display potent in vitro suppressive capacity and a distinct Th17 profile. Clinical Immunology *179*, 25–39.

Gagliani, N., Magnani, C.F., Huber, S., Gianolini, M.E., Pala, M., Licona-Limon, P., Guo, B., Herbert, D.R., Bulfone, A., Trentini, F., et al. (2013). Coexpression of CD49b and LAG-3 identifies human and mouse T regulatory type 1 cells. Nature Medicine *19*, 739–746.

Gershon, R.K., and Kondo, K. (1970). Cell interactions in the induction of tolerance: the role of thymic lymphocytes. Immunology *18*, 723–737.

Griseri, T., Asquith, M., Thompson, C., and Powrie, F. (2010). OX40 is required for regulatory T cell-mediated control of colitis. J. Exp. Med. *207*, 699–709.

Guo, X., Zhang, Y., Zheng, L., Zheng, C., Song, J., Zhang, Q., Kang, B., Liu, Z., Jin, L., Xing, R., et al. (2018). Global characterization of T cells in non-small-cell lung cancer by single-cell sequencing. Nature Medicine *24*, 978–985.

Halim, L., Romano, M., McGregor, R., Correa, I., Pavlidis, P., Grageda, N., Hoong, S.-J., Yuksel, M., Jassem, W., Hannen, R.F., et al. (2017). An Atlas of Human Regulatory T Helper-like Cells Reveals Features of Th2-like Tregs that Support a Tumorigenic Environment. Cell Reports *20*, 757–770.

Huber, S., Gagliani, N., Esplugues, E., O'Connor, W., Huber, F.J., Chaudhry, A., Kamanaka, M., Kobayashi, Y., Booth, C.J., Rudensky, A.Y., et al. (2011). Th17 cells express interleukin-10 receptor and are controlled by $Foxp3^-$ and Foxp3+ regulatory CD4+ T cells in an interleukin-10-dependent manner. Immunity *34*, 554–565.

International Genetics of Ankylosing Spondylitis Consortium (IGAS), Cortes, A., Hadler, J., Pointon, J.P., Robinson, P.C., Karaderi, T., Leo, P., Cremin, K., Pryce, K., Harris, J., et al. (2013). Identification of multiple risk variants for ankylosing spondylitis through high-density genotyping of immune-related loci. Nat. Genet. *45*, 730–738.

Ilicic, T., Kim, J.K., Kolodziejczyk, A.A., Bagger, F.O., McCarthy, D.J., Marioni, J.C., and Teichmann, S.A. (2016). Classification of low quality cells from single-cell RNA-seq data. Genome Biology *17*, 29.

James, K.R., Gomes, T., Elmentaite, R., Kumar, N., Gulliver, E.L., King, H.W., Stares, M.D., Bareham, B.R., Ferdinand, J.R., Petrova, V.N., et al. (2020). Distinct microbial and immune niches of the human colon. Nature Immunology *21*, 343–353.

Joller, N., Lozano, E., Burkett, P.R., Patel, B., Xiao, S., Zhu, C., Xia, J., Tan, T.G., Sefik, E., Yajnik, V., et al. (2014). Treg cells expressing the coinhibitory molecule TIGIT selectively inhibit proinflammatory Th1 and Th17 cell responses. Immunity *40*, 569–581.

Joosten, S.A., Meijgaarden, K.E. van, Savage, N.D.L., Boer, T. de, Triebel, F., Wal, A. van der, Heer, E. de, Klein, M.R., Geluk, A., and Ottenhoff, T.H.M. (2007). Identification of a human CD8+ regulatory T cell subset that mediates suppression through the chemokine CC chemokine ligand 4. PNAS *104*, 8029–8034.

Kanamaru, F., Youngnak, P., Hashiguchi, M., Nishioka, T., Takahashi, T., Sakaguchi, S., Ishikawa, I., and Azuma, M. (2004). Costimulation via Glucocorticoid-Induced TNF Receptor in Both Conventional and CD25+ Regulatory CD4+ T Cells. The Journal of Immunology *172*, 7306–7314.

Komatsu, N., Okamoto, K., Sawa, S., Nakashima, T., Oh-hora, M., Kodama, T., Tanaka, S., Bluestone, J.A., and Takayanagi, H. (2014). Pathogenic conversion of Foxp3+ T cells into TH17 cells in autoimmune arthritis. Nat. Med. *20*, 62–68.

Kurtulus, S., Sakuishi, K., Ngiow, S.-F., Joller, N., Tan, D.J., Teng, M.W.L., Smyth, M.J., Kuchroo, V.K., and Anderson, A.C. TIGIT predominantly regulates the immune response via regulatory T cells. J Clin Invest *125*, 4053–4062.

Lal, G., Zhang, N., van der Touw, W., Ding, Y., Ju, W., Bottinger, E.P., Reid, St.P., Levy, D.E., and Bromberg, J.S. (2009). Epigenetic Regulation of Foxp3 Expression in Regulatory T Cells by DNA Methylation. J Immunol *182*, 259–273.

Locksley, R.M., Killeen, N., and Lenardo, M.J. (2001). The TNF and TNF Receptor Superfamilies Integrating Mammalian Biology. Cell.

Mahmud, S.A., Manlove, L.S., Schmitz, H.M., Xing, Y., Wang, Y., Owen, D.L., Schenkel, J.M., Boomer, J.S., Green, J.M., Yagita, H., et al. (2014). Costimulation via the tumor-necrosis factor receptor superfamily couples TCR signal strength to the thymic differentiation of regulatory T cells. Nature Immunology *15*, 473–481.

Mercer, F., Kozhaya, L., and Unutmaz, D. (2010). Expression and function of TNF and IL-1 receptors on human regulatory T cells. PLoS ONE *5*, e8639.

Miragaia, R.J., Gomes, T., Chomka, A., Jardine, L., Riedel, A., Hegazy, A.N., Whibley, N., Tucci, A., Chen, X., Lindeman, I., et al. (2019). Single-Cell Transcriptomics of Regulatory T Cells Reveals Trajectories of Tissue Adaptation. Immunity *50*, 493-504.e7.

Miyabe, C., Miyabe, Y., Strle, K., Kim, N.D., Stone, J.H., Luster, A.D., and Unizony, S. (2017). An expanded population of pathogenic regulatory T cells in giant cell arteritis is abrogated by IL-6 blockade therapy. Annals of the Rheumatic Diseases *76*, 898–905.

Morton, A.M., Sefik, E., Upadhyay, R., Weissleder, R., Benoist, C., and Mathis, D. (2014). Endoscopic photoconversion reveals unexpectedly broad leukocyte trafficking to and from the gut. Proc. Natl. Acad. Sci. U.S.A. *111*, 6696–6701.

Panduro, M., Benoist, C., and Mathis, D. (2016). Tissue Tregs. Annu. Rev. Immunol. *34*, 609–633.

Patterson, S.J., Pesenacker, A.M., Wang, A.Y., Gillies, J., Mojibian, M., Morishita, K., Tan, R., Kieffer, T.J., Verchere, C.B., Panagiotopoulos, C., et al. T regulatory cell chemokine production mediates pathogenic T cell attraction and suppression. J Clin Invest *126*, 1039–1051.

Penkava, F., Velasco-Herrera, M.D.C., Young, M.D., Yager, N., Lara, A.L., Guzzo, C., Maroof, A., Mamanova, L., Cole, S., Efremova, M., et al. (2019). Single-cell sequencing reveals a clonal expansion of pro-inflammatory synovial CD8 T cells expressing tissue homing receptors in psoriatic arthritis. BioRxiv 704494.

Penkava, F., Velasco-Herrera, M.D.C., Young, M.D., Yager, N., Nwosu, L.N., Pratt, A.G., Lara, A.L., Guzzo, C., Maroof, A., Mamanova, L., et al. (2020). Single-cell sequencing reveals clonal expansions of pro-inflammatory synovial CD8 T cells expressing tissue-homing receptors in psoriatic arthritis. Nature Communications *11*, 4767.

Pesenacker, A.M., Bending, D., Ursu, S., Wu, Q., Nistala, K., and Wedderburn, L.R. (2013). CD161 defines the subset of FoxP3+ T cells capable of producing proinflammatory cytokines. Blood *121*, 2647–2658.

Povoleri, G.A.M., Nova-Lamperti, E., Scottà, C., Fanelli, G., Chen, Y.-C., Becker, P.D., Boardman, D., Costantini, B., Romano, M., Pavlidis, P., et al. (2018). Human retinoic acid–regulated CD161 + regulatory T cells support wound repair in intestinal mucosa. Nature Immunology 1.

Qaiyum, Z., Gracey, E., Yao, Y., and Inman, R.D. (2019). Integrin and transcriptomic profiles identify a distinctive synovial CD8+ T cell subpopulation in spondyloarthritis. Ann. Rheum. Dis. *78*, 1566–1575.

Richter, K., Agnellini, P., and Oxenius, A. (2010). On the role of the inhibitory receptor LAG-3 in acute and chronic LCMV infection. Int. Immunol. *22*, 13–23.

Saligrama, N., Zhao, F., Sikora, M.J., Serratelli, W.S., Fernandes, R.A., Louis, D.M., Yao, W., Ji, X., Idoyaga, J., Mahajan, V.B., et al. (2019). Opposing T cell responses in experimental autoimmune encephalomyelitis. Nature *572*, 481–487.

Schmidt, A., Oberle, N., and Krammer, P.H. (2012). Molecular mechanisms of treg-mediated T cell suppression. Front Immunol *3*, 51.

Shevach, E.M., and Stephens, G.L. (2006). The GITR–GITRL interaction: co-stimulation or contrasuppression of regulatory activity? Nature Reviews Immunology *6*, 613–618.

Stoeckius, M., Hafemeister, C., Stephenson, W., Houck-Loomis, B., Chattopadhyay, P.K., Swerdlow, H., Satija, R., and Smibert, P. (2017). Simultaneous epitope and transcriptome measurement in single cells. Nature Methods *14*, 865–868.

Stuart, T., Butler, A., Hoffman, P., Hafemeister, C., Papalexi, E., Mauck, W.M., Hao, Y., Stoeckius, M., Smibert, P., and Satija, R. (2019). Comprehensive Integration of Single-Cell Data. Cell *177*, 1888-1902.e21.

Sun, J., Li, L., Li, L., Ding, L., Liu, X., Chen, X., Zhang, J., Qi, X., Du, J., and Huang, Z. (2018). Metallothionein-1 suppresses rheumatoid arthritis pathogenesis by shifting the Th17/Treg balance. European Journal of Immunology *48*, 1550–1562.

Tseng, W.-Y., Huang, Y.-S., Clanchy, F., McNamee, K., Perocheau, D., Ogbechi, J., Luo, S.-F., Feldmann, M., McCann, F.E., and Williams, R.O. (2019). TNF receptor 2 signaling prevents DNA methylation at the Foxp3 promoter and prevents pathogenic conversion of regulatory T cells. PNAS *116*, 21666–21672.

Vasanthakumar, A., Liao, Y., Teh, P., Pascutti, M.F., Oja, A.E., Garnham, A.L., Gloury, R., Tempany, J.C., Sidwell, T., Cuadrado, E., et al. (2017). The TNF Receptor Superfamily-NF-κB Axis Is Critical to Maintain Effector Regulatory T Cells in Lymphoid and Non-lymphoid Tissues. Cell Reports *20*, 2906–2920.

Westhovens, R., Robles, M., Ximenes, A.C., Nayiager, S., Wollenhaupt, J., Durez, P., Gomez-Reino, J., Grassi, W., Haraoui, B., Shergy, W., et al. (2009). Clinical efficacy and safety of abatacept in methotrexate-naive patients with early rheumatoid arthritis and poor prognostic factors. Ann. Rheum. Dis. *68*, 1870–1877.

Woo, S.-R., Turnis, M.E., Goldberg, M.V., Bankoti, J., Selby, M., Nirschl, C.J., Bettini, M.L., Gravano, D., Vogel, P., Liu, C.L., et al. (2012). Immune inhibitory molecules LAG-3 and PD-1 synergistically regulate T cell function to promote tumoral immune escape. Cancer Res *72*, 917–927.

Yu, Y., Ma, X., Gong, R., Zhu, J., Wei, L., and Yao, J. (2018). Recent advances in CD8+ regulatory T cell research. Oncol Lett *15*, 8187–8194.

Zappasodi, R., Sirard, C., Li, Y., Budhu, S., Abu-Akeel, M., Liu, C., Yang, X., Zhong, H., Newman, W., Qi, J., et al. (2019). Rational design of anti-GITR-based combination immunotherapy. Nature Medicine *25*, 759–766.

Zemmour, D., Zilionis, R., Kiner, E., Klein, A.M., Mathis, D., and Benoist, C. (2018). Single-cell gene expression reveals a landscape of regulatory T cell phenotypes shaped by the TCR. Nat. Immunol. *19*, 291–301.

Zheng, G.X.Y., Terry, J.M., Belgrader, P., Ryvkin, P., Bent, Z.W., Wilson, R., Ziraldo, S.B., Wheeler, T.D., McDermott, G.P., Zhu, J., et al. (2017). Massively parallel digital transcriptional profiling of single cells. Nature Communications *8*, 14049.

5 Functional *in vitro* characterization of Treg subsets

5.1 INTRODUCTION

In this chapter I will present functional experiments that validate the phenotypic data presented in Chapter 4. In particular, the scRNA-seq analysis showed, in two of the Treg subsets identified in both datasets described, a distinct profile characterised by the expression of *LAG3*, virtually absent in the other Tregs subsets. LAG-3 (Lymphocyte activation gene-3, also known as CD223) is a surface molecule similar to CD4, with which it shares 20% homology at the amino acid level (Triebel et al., 1990). LAG-3 is expressed on the cell membranes of tumour infiltrating lymphocytes (Demeure et al., 2001), activated $CD4^+$ and $CD8^+$ T cells (Durham et al., 2014) as well as Tregs (Huang et al., 2004). Upon its binding with the HLA class II molecule, it relays an inhibitory signal to the lymphocyte to modulate, or inhibit, the immune response. The LAG-3 protein expression in activated T cells from SpA patients will be investigated, and a novel LAG-3-mediated mechanism of suppression of myeloid cells, with translational potential of reducing immune responses in SpA, will be proposed. Next, the identification of $CD8^+$ regulatory T cells emerging from the scRNA-seq analysis, a somewhat unexpected finding, will be confirmed in the PB

and SF of SpA, and the expression of selected Treg markers in this subset will be compared to “bona fide” CD4+ Tregs. Lastly, the expression of the protein encoded by *TNFRSF9*, CD137, or 4-1BB, one of the genes strongly upregulated by clonal Tregs in the SF, will be measured against antigen recognition.

5.2 AIM

In this chapter the aim is to confirm selected aspects of the Treg subsets (revealed by unsupervised analysis of scRNA-seq data presented in Chapter 4) in order to identify functional features, including activation markers and mechanisms of suppression, with therapeutic potential.

5.3 RESULTS

5.3.1 LAG-3, expressed by Tregs, regulates monocyte inflammatory phenotype and function via HLA class II

5.3.1.1 LAG-3 is expressed by a subset of Tregs upon activation, and its expression is lower in SpA patients’ T cells and Tregs

Two of the specialized clusters that emerged from my single cell analysis of Tregs, one characterized by Th17-like transcripts and the latter expressing CD8 and cytotoxic proteins, expressed the coinhibitory gene *LAG3*. Because both subsets were increased in the SF compared to the PB and since LAG-3 is a relatively unexplored regulatory effector molecule in Tregs, I characterized the

expression of the LAG-3 protein on $CD4^+$ cells, and Tregs in particular. The protein LAG-3 is expressed on activated $CD4^+$, including Tregs, and $CD8^+$ cells. At least half of the LAG-3 cellular content is stored intracellularly. Upon T-cell activation, it is translocated to the cell surface in association with the microtubule system (Woo et al., 2010). To detect LAG-3 on T cells with flow cytometry, different protocols for cell activation and staining were tested. To increase permeability and detection of the LAG-3 intracellular pool, and to allow physiological microtubular transport, LAG-3 staining was performed at 37°C, together with the surface antibody mix. Relying on the intracellular transport system for its detection, LAG-3 staining was not compatible with brefeldin, monensin or other protein transport inhibitors commonly used for flow cytometric detection of intracellular proteins. A polyclonal PE-conjugated anti-LAG-3 antibody (clone FAB2319P, R&D) (**Figure 5.1A**) was used: based on the expression of the *LAG3* transcript in our single cell data, detected in 6.7% of the T cells, a stimulation with 1μg/ml anti-CD3 and anti-CD28 was considered adequate. The LAG-3 protein was barely detectable on unstimulated cells. To phenotype LAG-3-expressing cells, 14 PBMC samples (HC = 6, AS = 8) were single batch stained with flow cytometry antibodies and analysed.

Because LAG-3 is expressed by different T cell subsets, I first assessed the proportion of Tregs cells within LAG-3-expressing $CD4^+$. Because in vitro activation strongly upregulates CD25 (making the classification of Tregs as $CD4^+$ CD25+ CD127low unreliable), Tregs were defined as $CD4^+$ $Foxp3^+$ (**Figure 5.1B**). Approximately 40% of LAG-3^+ T helper cells were Tregs. Within LAG-3^+ Tregs, the majority were $CD161^+$, confirming that LAG-3 has a preferential expression in that specific Treg subset (**Figure 5.1C**). Conversely, up to 20% of

$CD161^+$ $Foxp3^+$ cells expressed LAG-3 upon stimulation, versus less than 10% of $CD161^-$ Tregs (**Figure 5.1D**). A multidimensional reduction (t-SNE) plot representative of all the LAG-3^+ $CD3^+$ cells from one AS patient, generated using the same markers (**Figure 5.1E**), showed that a subset of LAG-3^+ cells expressed CD8, although LAG-3^+ cells were in majority $CD4^+$, of which approximately half are $CD161^+$.

The LAG-3 protein expression was then compared in AS and HC (**Figure 5.2A**). A reduction of LAG-3 in $CD4^+$ cells was seen in AS, which was secondary to a specific downregulation in Tregs. CTLA-4, used as effector molecule comparison, was similarly expressed in AS and HC in the same cell subsets, indicating a downregulated expression of LAG-3 in $CD4^+$, and in particular in Tregs, from AS subjects. To verify the expression of *LAG3* at mRNA level across T cell subpopulations in AS, the single cell dataset was interrogated again (**Figure 5.2B**). *LAG3* was expressed in a percentage of Tregs, $CD8^+$ and various $CD4^+$ subsets, and generally increased in the correspondent clusters in the SF.

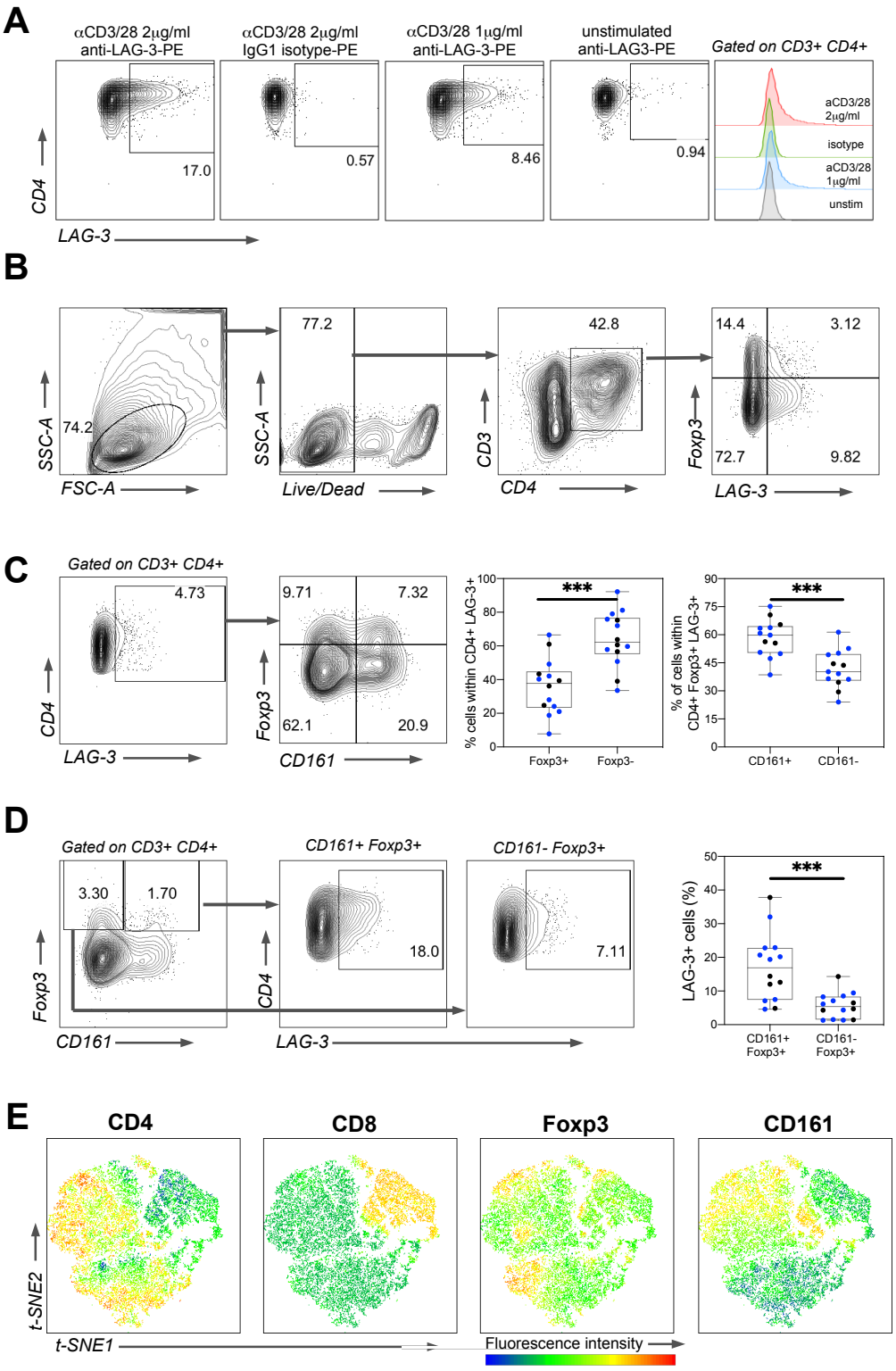

Figure 5.1. In peripheral blood, LAG-3 is expressed, upon unspecific TCR activation, by Tregs, including CD161+ Foxp3$^+$ cells, CD4$^+$ and CD8$^+$. (A) Selection of activation protocol for LAG-3 staining and isotype control. Plots gated on CD3$^+$ CD4$^+$. The stimulation with αCD3/28 1 μg/ml was deemed adequate. **(B)** Tregs in this assay were defined by the expression of Foxp3 (CD3$^+$ CD4$^+$ Foxp3$^+$). In this

example plot, approximately 25% of LAG-3$^+$ cells are Tregs. **(C)** LAG-3$^+$ T helper cells classified based on the expression of Foxp3 and CD161: approximately 40% of LAG3$^+$ T cells are Tregs (Foxp3$^+$), the majority of which are CD161$^+$ (HC (black dots) n=6, AS (blue dots) n=8). **(D)** LAG-3 expression in CD161$^+$ Tregs and CD161- Tregs. **(E)** t-SNE visualisation of 18,000 CD3$^+$ LAG-3$^+$ cells from one AS PBMC sample. Colors encode marker fluorescence.

5.3.1.2 LAG-3 regulates monocyte phenotype and function

Upon persistent antigenic stimulation, LAG-3 transmits a negative signal, through an unusual intracellular motif named "KIEELE", rendering the T cell inert and preventing immune over-activation. On Tregs, induction of exhaustion and acquired tolerance would not be evolutionary favourable. I then hypothesized a different, cell-type specific function of LAG-3 expression on Tregs. Because of the scarcity of LAG-3-expressing Tregs (without relying on in vitro expansion), the immune effects of a LAG-3 fusion protein, made by the recombinant human cytoplasmic side of LAG-3 combined with a human IgG1 Fc portion (LAG-3-Fc) (R&D), were tested. PBMCs from AS patients were incubated with LAG-3-Fc for two hours, before being stimulated with LPS. Cells were kept in culture for 18 hours, then harvested and stained with a flow cytometry panel focused on myeloid cells to specifically interrogate effects in HLA class II-expressing cells.

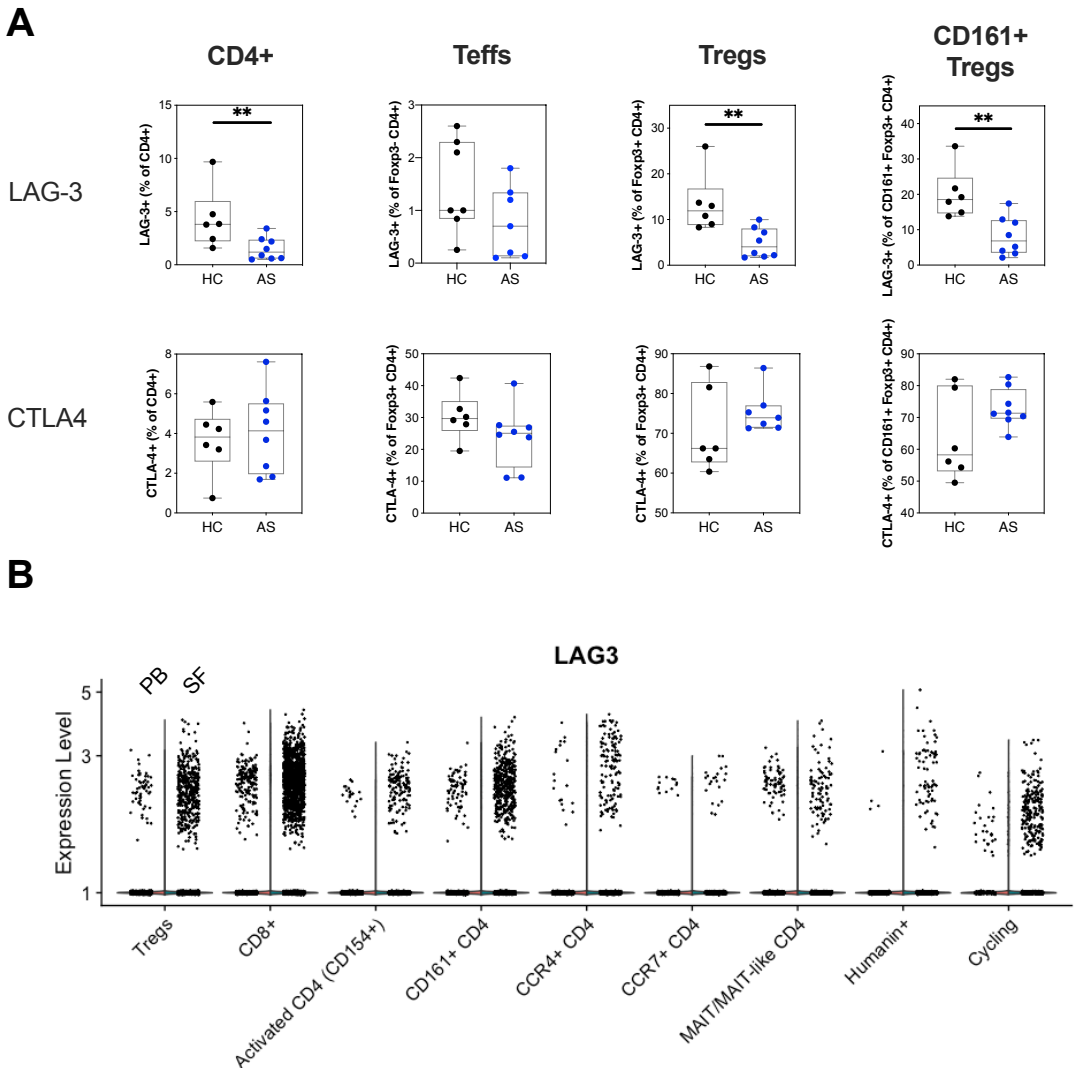

Figure 5.2. LAG-3 expression is reduced in AS Tregs in the peripheral blood. **(A)** Percentage of cells expressing LAG-3 and CTLA-4 within CD4+ cells, Tregs and CD161+ Tregs in the PB of HC (n=5-6) and AS (n=8) subjects. * p≤0.05, **≤ 0.01 (Mann-Whitney test). **(B)** *LAG3* mRNA expression across the T cell clusters identified by scRNA-seq analysis performed on the AS dataset (see 4.3.3.2 and **Figure 4.16**) (log-scale of normalised counts).

An initial change in size and granularity of monocytes was observed, with a downregulation of CD14 (**Figure 5.3A**). LAG-3-Fc reduced expression of CD16 and CX3CR1, markers conferring respectively differentiation and migration potential to circulating monocytes. The costimulatory markers CD80 and CD86 were not affected. In some experiments, the parallel use of the isotypic Fc portion

of LAG-3-Fc ruled out any significant effect of Fc binding on the monocytes (**Figure 5.3B**). An aliquot of cells was treated with brefeldin, added 4 hours after the LPS challenge to preserve intracellular cytokines. Preliminary intracellular staining of p40 (the cytokine subunit shared by IL-12 and IL-23) and TNF, both molecular targets of approved drugs in use in SpA, was performed on two samples. p40 in particular was clearly reduced by LAG-3-Fc (**Figure 5.3C**).

5.3.1.3 LAG3-Fc downregulates monocyte activation status and inflammatory response via HLA class II engagement

Given the observed effect on myeloid cells, I next determined whether LAG3 was directly repressing monocyte activation, or rather was dependent by co-regulation by autologous T cells. Monocytes were magnetically isolated (**Figure 5.4A**) and cultured with LAG-3-Fc. More controls were added, including a human Fc isotype control and an anti-HLA class II antibody (Tu39, directed against HLA-DR, -DP and -DQ) to verify if blocking the putative target of LAG-3-Fc, HLA class II, could revert the suppressive effect observed. The effect on CD40, a crucial costimulatory molecule for T cell activation and maturation, was also examined. LAG-3-Fc was able to directly regulate CD14, but not CD16. CD40 was also repressed (**Figure 5.4B**). The coexistence of the anti-HLA class II with LAG-3-Fc partially reverted the effect, indicating a competition for the same target. Here, CD80 and CD86 were downregulated by LAG-3, differently from what observed in the PBMC assay, where the presence of their natural ligand (CD28) on the T cell surface might have counteracted the LAG-3-mediated suppression.

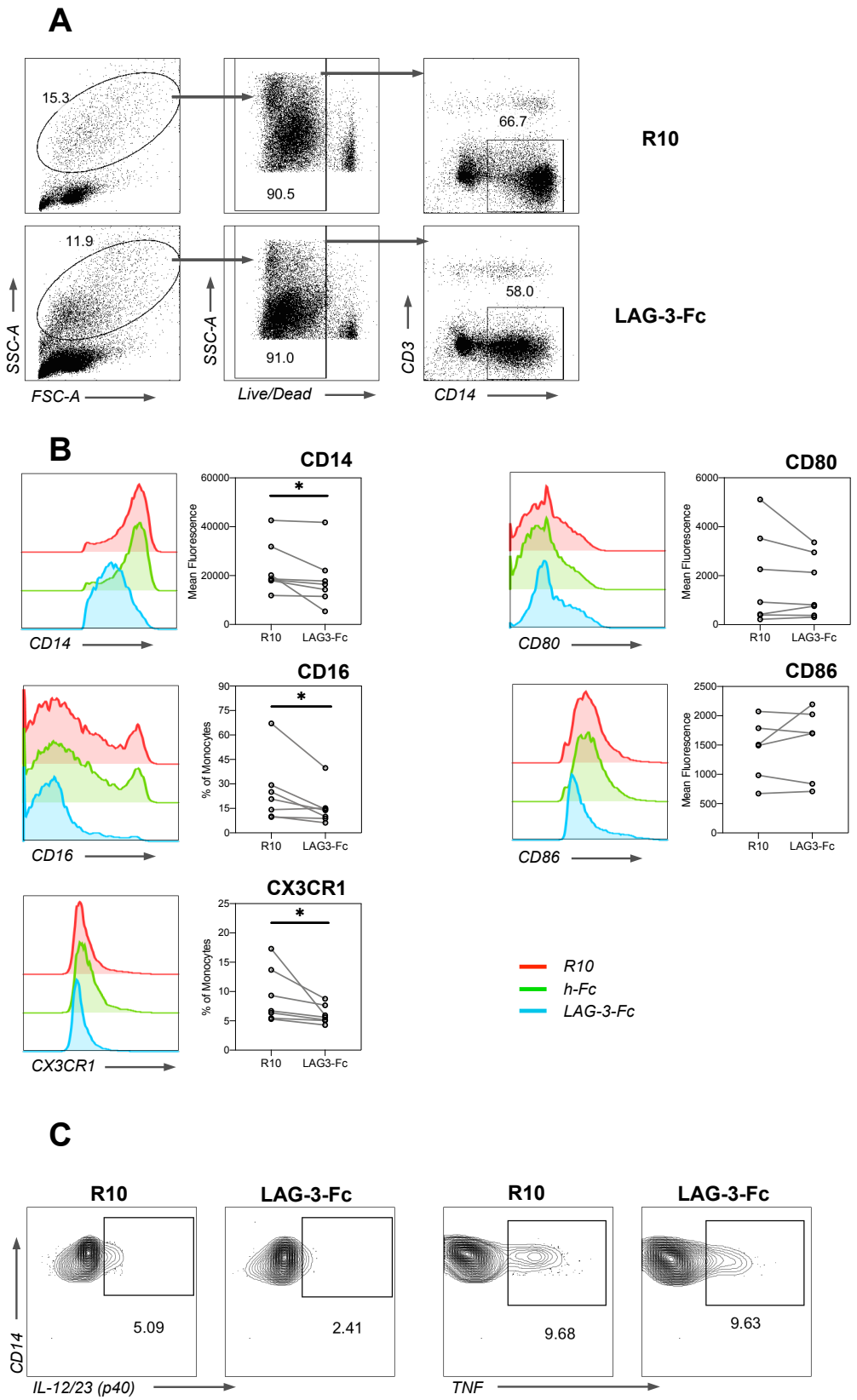

Figure 5.3. Soluble LAG-3 protein modifies monocyte phenotype downregulating selected activation and maturation markers. **(A)** Gating strategy to identify monocytes within PBMCs. **(B)** Selected surface marker

expression on monocytes (gated on CD3- CD14+) after overnight culture with LAG-3-Fc fusion protein. For markers with non bimodal distribution, geometric mean of fluorescence intensity was used. n=6 AS PBMC. For two replicates, hFc (human IgG1 Fc protein) was used as control. **(C)** Preliminary intracellular staining for IL-12/23 p40 and TNF, gated on monocytes. * $p \leq 0.05$, non parametric paired t-test.

Next, the production of inflammatory mediators by monocytes was tested: the intracellular content of the p40 subunit and TNF were strongly reduced by LAG-3-Fc, while blockade of MHC II reverted this effect in the case of TNF. No effect was seen with the Fc control or with anti-HLA class II antibody alone (**Figure 5.5**). Interestingly, IL-6 (measured in the supernatant) was not affected, while very low measured concentrations of IL-23 did not allow drawing reliable conclusions on its effect. In conclusion, LAG-3 was able to suppress both monocyte activation and the inflammatory response to LPS, suggesting a direct effect largely mediated by engagement of HLA class II. In particular, the downregulation of CD40, CD80 and CD86 (all providing a costimulatory signal to Teffs) indicates that LAG-3 might inhibit the ability by APCs to activate and expand Teffs.

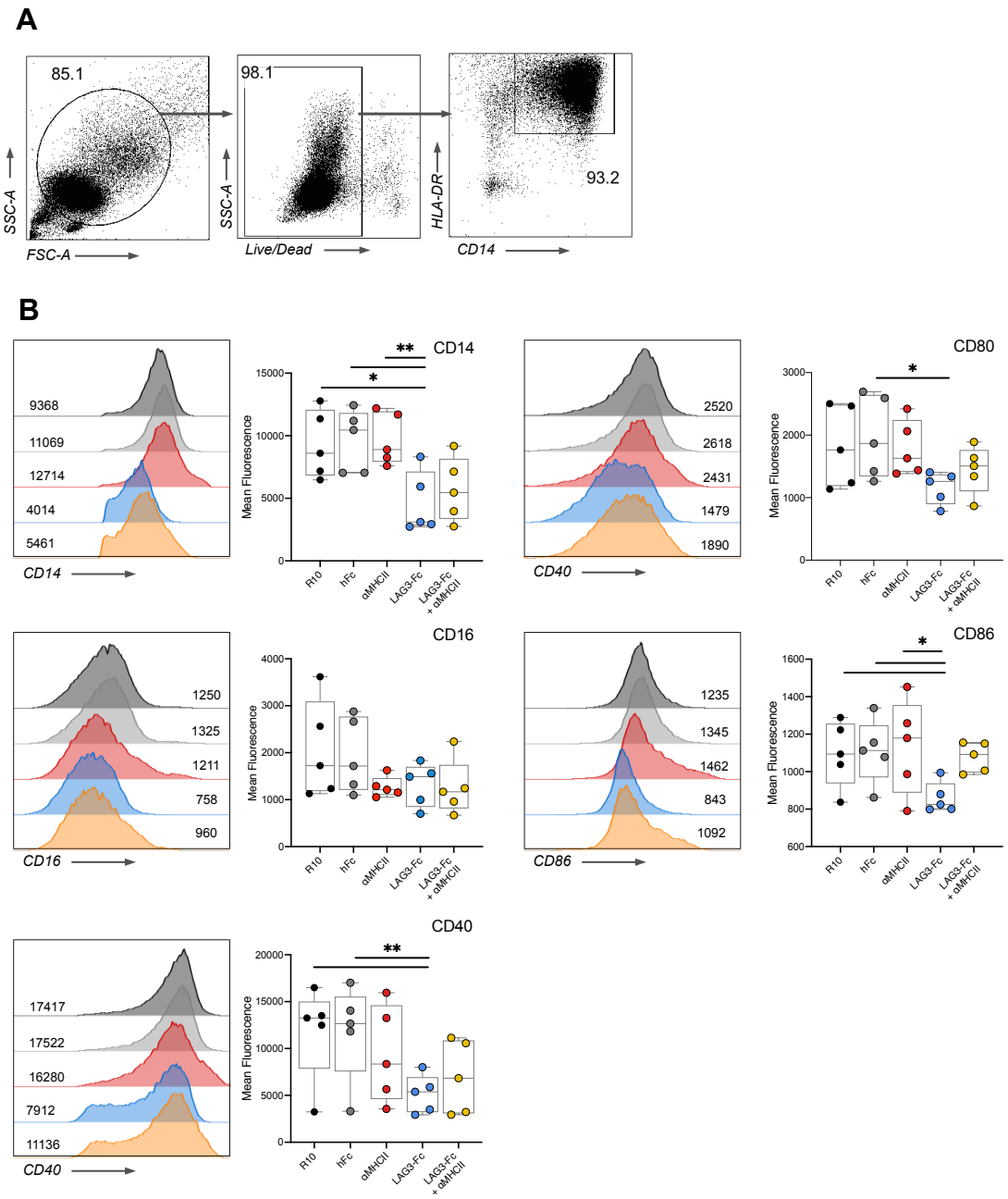

Figure 5.4. LAG-3 directly inhibits monocyte activation. (A) Monocytes were isolated by magnetic sorting and stimulated with LPS for 18 hours under the experimental conditions indicated. Monocytes defined as $CD14^{+}$ $HLA\text{-}DR^{+}$. **(B)** Activated monocytes stained for surface markers. For each marker, a representative stain from one individual (with geometric mean fluorescence intensity for each condition) is shown on the left and data points with minimum and maximum values and IQR on the right. Histogram color represents (left panel) matches dot plot in the right panel. n=5 AS samples.

5.3.1.4 *LAG3-mediated suppression is not observed on activated T cells but might be relevant in HLA class II-expressing cells*

Since $CD4^+$ and $CD8^+$ can express HLA class II antigens upon activation (Evans et al., 1978), the possibility that LAG3 could directly inhibit Teffs was explored. $CD4^+$ and $CD8^+$ were separately FACS sorted, and activated with anti-CD3 and -CD28 antibodies in the presence of LAG-3-Fc.

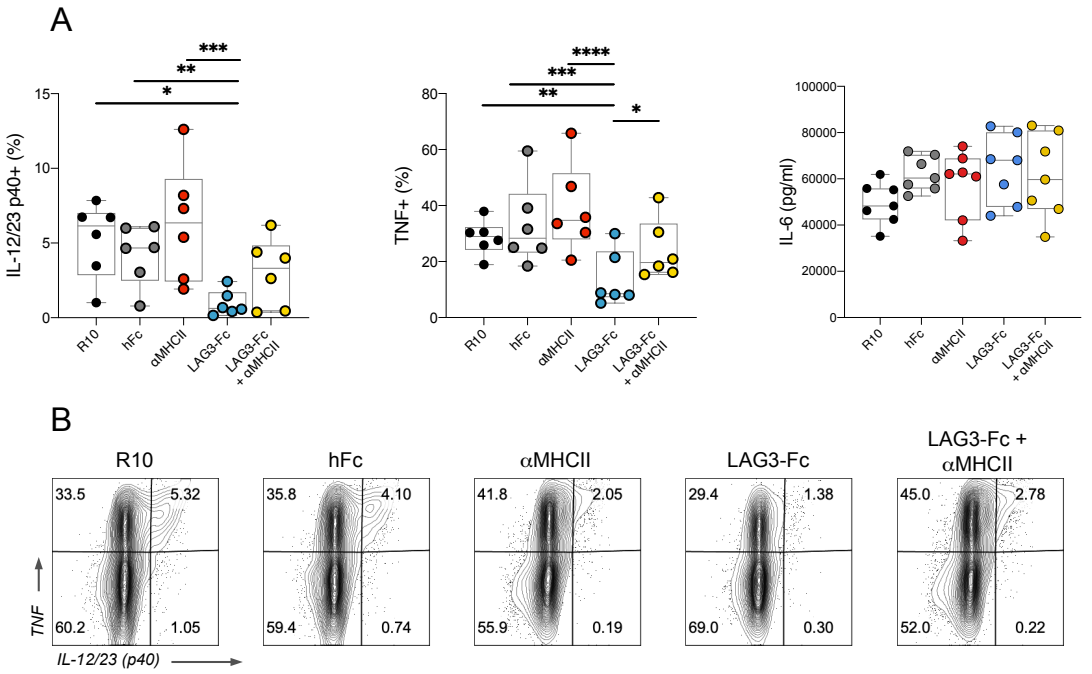

Figure 5.5. LAG-3 inhibits monocyte cytokine secretion of IL-12/23 and TNF. LAG-3 effect on TNF is partially reverted by HLA class II blockade. n=6-7 AS samples. * $p \leq 0.05$, **≤ 0.01, *** ≤ 0.001 (One-way ANOVA)

After three days, the cells were harvested and stained for IL-17A and IL-17F: no effect on the production of Th17 cytokines was seen (**Figure 5.6**), which might suggest that the LAG-3-induced downstream inhibitory signal is only seen in cells that express HLA class II constitutively, such as professional APCs (although the expression of HLA class II on T cells in the assay was not directly assessed). To survey which cells might represent a natural target of LAG-3-mediated suppression, the expression of the genes encoding for the HLA-DR chains and the HLA-associated invariant chain (*CD74)* were assessed in the AS single cell dataset (full data in 4.3.3.2), which included five subsets of myeloid origin from PB and SF (**Figure 5.7**). HLA-DR-associated genes were highly expressed in cells annotated as “HLA-DR+” and “intermediated monocytes”, representing different states of activation and differentiation towards macrophages, and on “pDCs” and “DCs”, suggesting that LAG-3 could potentially restrain other APC subsets. Furthermore, the expression of these genes was higher in the SF cells, indicating that the LAG-3 inhibitory mechanism could be particularly relevant on the professional APCs in the inflammatory sites rather than on circulating monocytes.

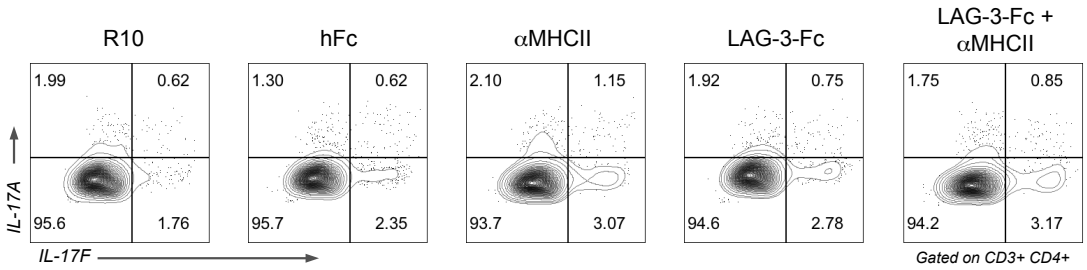

Figure 5.6 Soluble LAG-3 has no direct effect on Th17-type cytokine responses from activated CD4 and CD8 cells. $CD4^+$ and $CD8^+$ from n=2 AS patients were sorted, activated with anti-CD3/28 overnight, then the soluble mediators added. Cells were cultured for 72 hours, then treated with PMA, ionomycin and brefeldin for 4 hours before being stained for intracellular IL-17A and IL17-F. Example plots from one $CD4^+$ assay (gated on $CD3^+$ $CD4^+$).

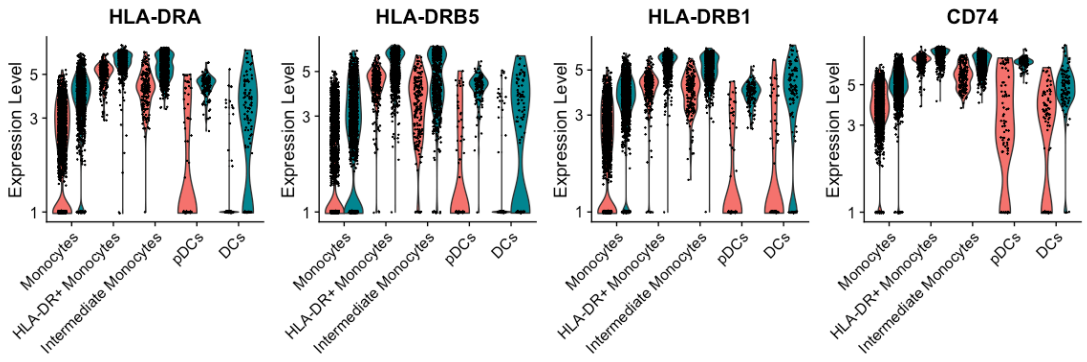

Figure 5.7. HLA class II genes are expressed across various myeloid subsets in AS, in particular in the SF. Expression of the genes encoding the HLA-DR alpha chain, the two most prevalent beta subunits, and the HLA-DR associated invariant chain CD74 in five clusters identified in the AS single cell dataset (see Figure 4.16). Expression (normalised counts, log-scaled) in PB cells (red) and SF (blue) are shown.

5.3.2 $CD8^+$ Tregs are present in the synovial fluid and are characterised by granzyme B and K expression

In the scRNAseq analysis, a subset of $CD8^+$ Tregs was identified by the unsupervised clustering analysis as transcriptionally close to $CD4^+$ Tregs (see **Figure 4.27** and **Figure 4.22**). The presence of this subset and some of its phenotypic characteristics were explored with flow cytometry in three further paired PB/SF samples (two PsA, one AS). Considering all $CD25^+$ $CD127^{low}$ cells within $CD3^+$ cells, distinct populations of CD4+ Tregs (representing approximately 99% of the cells) and $CD8^+$ Tregs are observed in the PB and SF (**Figure 5.8**). Differently from what shown by the scRNAseq, CD8+ Tregs were not enriched in the SF compared to the PB, constituting less than 1% of all $CD25^+$ $CD127^{low}$ T cells in both sites. Although the small number of cells did not allow detailed characterisation of this subset, granzyme B and K, two molecules that are virtually absent in $CD4^+$ Tregs, were characteristics of the subset. A small number of $CD8^+$ Tregs appeared to be negative for Foxp3 and CTLA-4, suggesting that the $CD25^+$ $CD127^{low}$ cells within the $CD8^+$ T cell subset might include a number of non Treg cells.

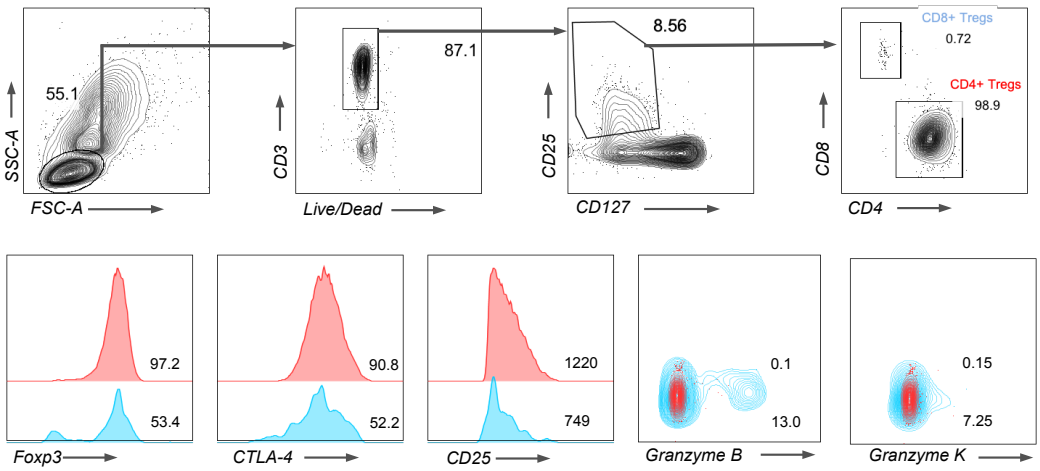

Figure 5.8. CD8$^+$ Tregs represent a small subset of regulatory cells found in the SF of SpA patients and are characterised by expression of granzyme B and K. Example staining of CD4 and CD8 expression in CD25$^+$ CD127^{low} cells obtained from SFMC from PsA. CD8$^+$ Tregs (blue), compared to CD4$^+$ Tregs (red), include a percentage of Foxp3$^-$ and CTLA-4$^-$ cells, and are characterised by production of granzyme proteins.

5.3.3 CD137 upregulation on SpA Tregs suggests Candida and Salmonella antigen driven Treg responses in SpA

To demonstrate the presence of antigen-specific Tregs in the PB of patients with AS, and to confirm the expression of CD137 in Tregs following antigen recognition, I modified the technique of (Bacher et al., 2016), based upon expression of CD137 and CD154 as markers of antigen recognition, respectively, in Tregs and in Teffs. Isolated PBMCs from six AS patients were incubated with protein mixtures of *Candida albicans* and *Salmonella*

typhimurium before being harvested for flow cytometry-based detection of CD137 and other markers. In this assay, the microbial-derived antigens are naturally processed and presented to the T cells by the APCs, which also provide costimulation. The predicted specific response to *C. albicans* and *S. typhimurium*, was compared to two alternative, non antigen-restricted activation mechanisms: LPS, that activates T cells upon soluble mediators release by innate cells following toll-like reception engagement, and SEB, a superantigen that crosslinks TCR with the HLA. Anti-CD3/28 antibodies were also used as positive control to provide unspecific, potent TCR activation. Tregs were defined by the presence of Foxp3, preferable in this assay to the conventional definition of $CD25^+$, whose expression is strongly altered by in vitro cell activation. The microbial antigen mixes did not increase the total Foxp3 population, compared to plain medium, differently from αCD3/28-mediated activation, that upregulated Foxp3 (**Figure 5.9A, B**). The frequency of $CD137^+$ cells was, in proportion, increased 2 to 10 times in Tregs compared to Teffs (**Figure 5.9C**). In other words, 90% of the CD137+ CD4+ cells were Foxp3+. The Treg response to *C. albican*s (0.23%–2.05% of CD4+ T cells, mean 1.28%) was remarkable, a result compatible with the dual nature of *C. albicans*, both a pathogen and a colonizing saprophyte of the skin and the gastrointestinal tract and hence able to drive tolerogenic responses. The data also show that regulatory antigen-specific responses are also seen towards pathogens, such as *S. typhimurium*. Variable antigenic concentrations and differences in protein processing make however direct comparisons across antigenic mixtures difficult. The small number of CD137+ cells identified by this assay did not allow further characterization of the cells, including expression of the other markers identified

by the RNA sequencing, such as the expression of CCR8, IL-1R1 and IL-1R2. However, CD137, encoded by *TNFRSF9,* was indeed elevated in Foxp3^{+} cells, supporting its utility to identify antigen-responsive Tregs. Our assay strongly suggests direct antigen-restricted activation, but cannot exclude concomitant bystander activation, although exposure to SEB and LPS, both challenges that do not rely on recognition of antigen-HLA class II complex, did not generate a differential expression of CD137 in Tregs and Teffs, indicating that CD137 expression might be a consequence of TCR engagement in Tregs.

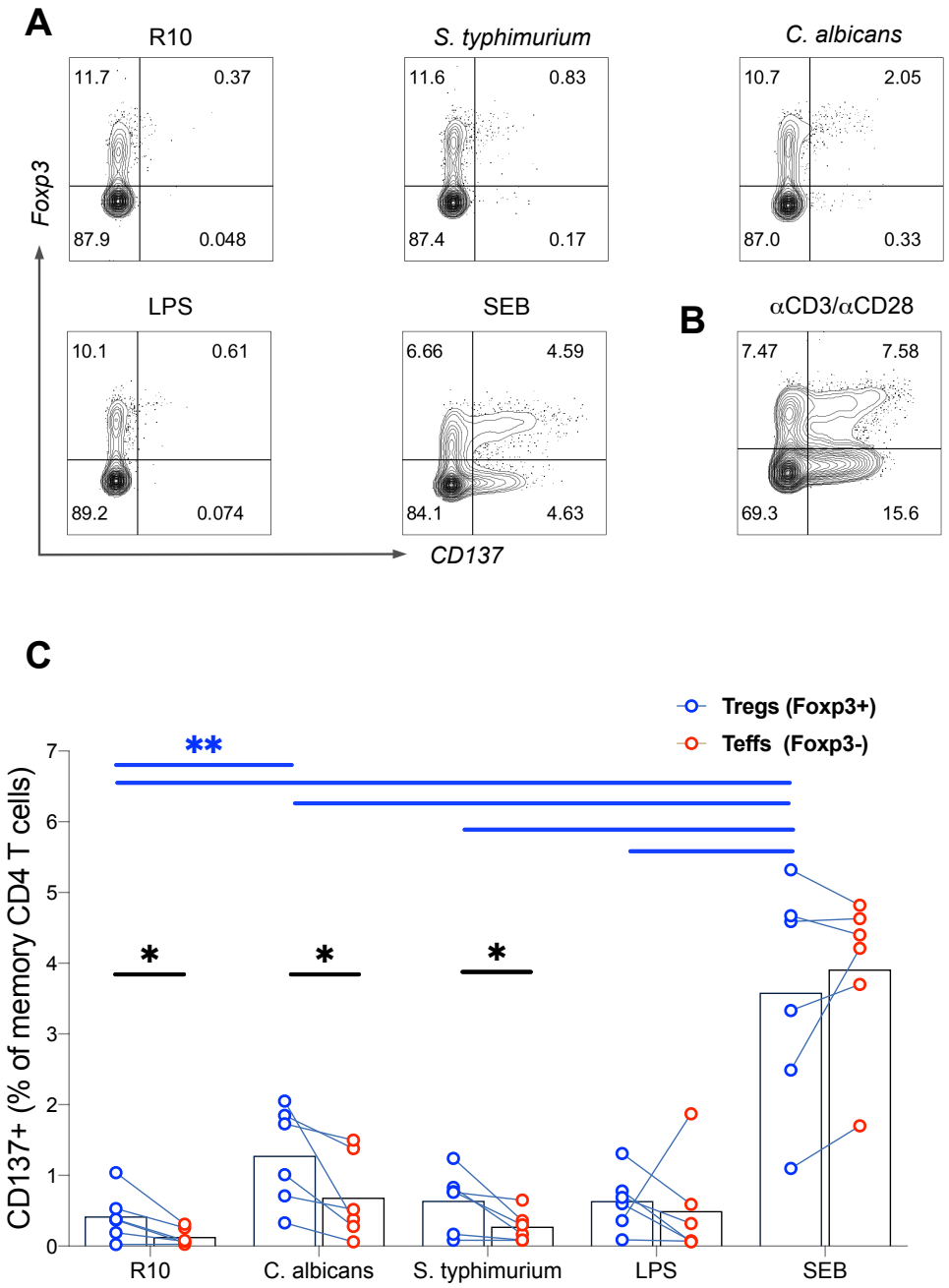

Figure 5.9. CD137 is expressed by Foxp3$^+$ memory CD4$^+$ T cells upon in vitro exposure to antigens. (A) Expression of Foxp3 and CD137 in memory CD4$^+$ after 18 hour culture with antigen mixes. PBMC were cultured in RPMI with, and stained with fluorescent antibodies surface and intracellular markers. **(B)** Activating antibodies for CD3 and CD28 used as a comparison for unspecific TCR activation. **(C)** CD137$^+$ expression in response to antigens is higher on memory Tregs (defined as CD4$^+$ CD45RA$^-$) than on memory Teffs. No difference was seen in response to stimuli (LPS and SEB) that do not rely on antigen presentation and recognition. *p≤0.05, **≤ 0.01 (Two-way ANOVA with Bonferroni correction; blue line: across condition comparison within cell-type; black line: across cell type comparison within condition).

5.4 DISCUSSION

A possible biological regulatory role for LAG-3 in modulating inflammatory responses, both cell-contact and humoral, is proposed here. LAG-3 is a ligand-activated marker, first discovered in 1990 in the form of a surface protein with structural and amino-acid sequence similarities with CD4 (Triebel et al., 1990). Characterized by a significant homology with CD4, it similarly binds MHC class II molecules, but with higher affinity. Initial knockout experiments, aimed at characterizing its function, did not show any significant effect on T cell activation (Miyazaki et al., 1996), but subsequent analyses demonstrated that mice developed autoimmune disease after T cell activation (Huang et al., 2004; Bettini et al., 2011), but not spontaneously. As explained, expression of LAG-3 on the T cell (often together with exhaustion markers), and its ligation sends a negative signal that restrains cell proliferation, in the attempt to prevent, or end, over-activation (a cartoon is shown in **Figure 5.10**). These observations have provided the rationale behind the development of immunotherapies targeting LAG-3, aimed at reverting regulatory responses in the tumour microenvironment and reinforcing immunity against cancerous cells. Anti-LAG-3 blocking antibodies are in fact showing promising results in particular in association with anti-CTLA4 (reviewed in (Andrews et al., 2019)). Involvement of LAG-3 on Teffs has been advocated in other conditions characterised by chronic antigen driven responses. LAG-3 was identified as critical in limiting the host response to HIV (Tian et al., 2015) and malaria (Butler et al., 2011), delaying their clearance.

The role of LAG-3 in Tregs is more difficult to pin down. One of the first studies (Huang et al., 2004) found that LAG-3 contributes to the suppressor activity toward Teffs, with conditional knockout cells exhibiting reduced functionality. One report (Liang et al., 2008) described how LAG-3-expressing Tregs binding to HLA class II on bone marrow derived DCs resulted in downregulation of CD86. This report first described a reverse signaling mechanism by LAG3$^+$ Tregs aimed at suppressing the APC function, which was replicated with soluble LAG-3 (pointing towards independence from T cell signaling). The authors further characterized the inhibitory signaling pathway following LAG-3 ligation on the APC, consisting in activation of the FcγR-associated immunoreceptor tyrosine-based activation motif (ITAM), followed by ERK phosphorylation, and SHP-1 recruitment (Liang et al., 2008). Only recently, the regulatory role of LAG-3 by Tregs was confirmed in an experimental inflammatory murine model. In the ILC3-driven experimental colitis model (Bauché et al., 2018), LAG-3$^+$ Tregs specifically targeted CX3CR1+ macrophages, decreasing their production of IL-23 and IL-1β and suppressing CD40 expression and NF-κB signalling, with amelioration of the disease. Notably, CX3CR1$^+$ macrophages, a specialised tissue-resident cell able to sample antigens in the lamina propria and present it directly to the T cells or transfer it to CD103+ DCs, are increased in many inflamed tissues in AS, including the intestine (Ciccia et al., 2018). The suggested relevance of LAG-3-mediated suppression in intestinal immunity is also indirectly confirmed by the characteristic expression of LAG-3 by Tr1 (Gagliani et al., 2013), a regulatory subset that has preferential localisation in the lamina propria. LAG-3 might then represent a specialised suppressive response originating in gut Tregs that are able to traffic

to other sites, perhaps in response to Th17-driven inflammation. (Kadowaki et al., 2016), describe antigen specific intraepithelial lymphocytes with characteristic *Lag3* expression in the gut and the CNS of in the course of EAE. New evidence of the presence of *Lag3*-expressing Tregs in the CNS was provided by conditional knock out of *Lag3* in Tregs, which led to loss of suppressive functions and worsening of EAE (Thaker et al., 2018). The majority of LAG-3-expressing Tregs are CD161^{+} Tregs, which, as discussed in Chapter 4, present features of intestinal origin. This description of LAG-3 as an enriched effector pathway in the SF is the first of this kind in a rheumatic condition. Furthermore, LAG-3 expression in murine and human T cells is often found in combination to IL-10, an occurrence described in Tr1 (Gagliani et al., 2013), and confirmed by the scRNA sequencing data. Both mechanisms of suppression are able to modulate innate cells in mucosal immunity (see (Shouval et al., 2014; Zigmond et al., 2014) for works on IL-10R signalling on colonic myeloid cells), suggesting co-expression of suppressive pathways towards the same biological functions. Finally, IL-27 promotes both LAG-3 expression and IL-10 production in murine and human T cells (Pot et al., 2009; Do et al., 2016), suggesting they both might be part of a coordinated suppressive programme, adapted to specific inflammatory environments. An unexpected observation, although made on a small cohort, is the reduced expression of LAG-3 in Tregs and CD161^{+} Tregs from AS patients. This suggests a disease-related impairment of a specific regulatory function. The clinical relevance of this observation is difficult to evaluate. Some experiments show that CD161^{+} Tregs are highly polymorphic, and, at least in vitro, able to adopt different suppressive mechanisms (Povoleri et al., 2018). In vivo, *Lag3*$^{-/-}$ Tregs in fact showed impaired regulatory function and the mice presented a more

severe course of autoimmune disease, but not spontaneous autoimmunity (Huang et al., 2004): LAG-3 could thus represent a key factor for Treg suppression only in certain inflammatory conditions, or a highly evolved function specialised to suppress specific immune targets, such as inflammatory myeloid cells, rather than a prerogative of Tregs. The association of LAG-3 with Tregs characterised by Th17-like features, as demonstrated by my data and by (Ferreira et al., 2017), induces to interpret LAG-3 may be a/the preferred effector of an anti-Th17 suppressive module. In Bauché et al., 2018, intestinal LAG-3$^+$ Tregs were indeed instrumental to control colitis driven by ILC3, a subset that is ROR-γt$^+$. Direct connection between LAG-3 and Th17 responses has yet to be proven, but it will likely represent a future research direction in the next years, in the larger aim of modulating natural occurring suppressive responses for different immune effector signatures.

Another overlooked aspect of Treg biology highlighted by these experiments is the direct modulation on immune cells different from Teffs. Monocytes have been characterised as a possible target of Treg action before. Monocytes cocultured with CD4+ CD25+ then stimulated with LPS showed limited upregulation of CD86 compared to control conditions (Taams et al., 2005). A follow up study by the same group found that Tregs induced alternative maturation of monocyte towards an M2 phenotype, resulting in reduced production of TNF and IL-6 (Tiemessen et al., 2007). These effects were in part secondary to soluble factors (IL-10, IL-4) as well as cell contact dependent mechanisms. Similar conclusions were reached by (Romano et al., 2018), who demonstrated that human monocytes exposed to Tregs had a reduced capacity to expand Teffs, including IL-17-producing T cells, as a consequence of

reduced costimulatory molecule CD86. In the light of the similar results I observed, it is possible that at least some of these observations were mediated by LAG-3. Similarly, our data show that a Treg-associated molecule is able induce phenotypic and functional changes in monocytes, which would then reflect on T effector responses, such as the downregulation of costimulatory markers (CD40, CD80, CD86) (a proposed model is shown in **Figure 5.11**). The ability of Tregs to modulate innate immune cells and the tissue microenvironment was described already many years ago (Gershon and Kondo, 1971) and termed “infectious tolerance”. Experimental SpA, mimicking a condition likely triggered by microbial cues and characterized by crosstalk between innate and adaptive immune cells, might represent a good model to further explore the translational potential of the LAG-3-mediated immunoregulation.

Several questions around the mechanism of LAG-3 suppression still persist. The autocrine negative signalling occurring after LAG-3 ligation on Teffs appears naturally in conditions of high antigenic stimulation. A recent paper confirmed that the T cell is downregulated only when LAG-3 recognizes stable complexes of peptide and MHC class II (Maruhashi et al., 2018). Whether the suppression of myeloid cells by Treg via LAG-3-MHC engagement would also need antigen expression on the HLA class II is difficult to predict. The monocyte regulation in the experiments shown was seen in the absence of exogenous antigens, but it cannot be excluded that monocytes were loaded with native antigens.

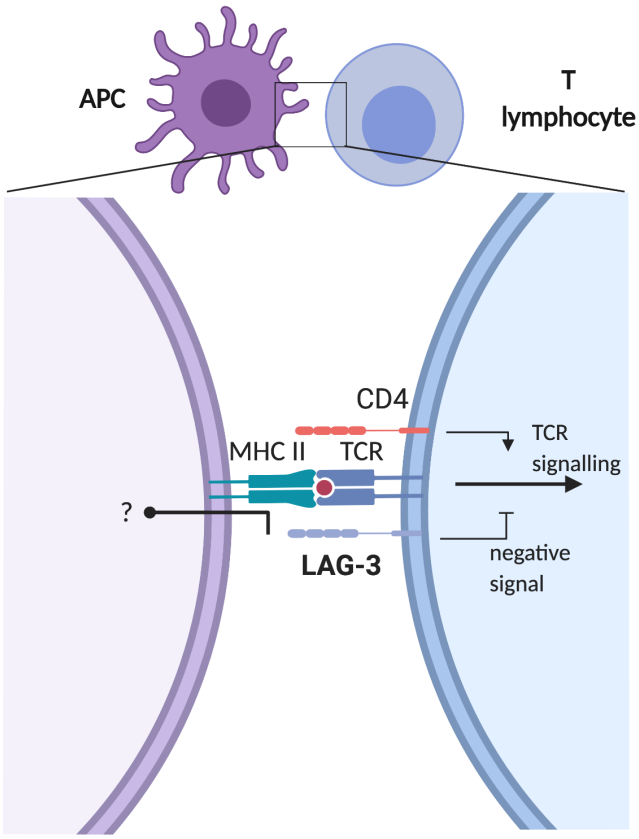

Figure 5.10. Scheme showing interactions between LAG3, HLA class II, TCR and CD4 in the T cell-APC immunological synapse.

Using LAG-3 to modulate myeloid inflammatory responses with potential indirect influence on Teffs cells has exciting translational potential immune driven diseases. Fusion proteins, composed of immunoglobulin Fc portions with biologically active molecules, such as abatacept and etanercept are already in use in rheumatic immune-driven conditions. Abatacept in particular, a fusion protein composed of a IgG1 Fc region and CTLA-4, mimics a natural inhibitory mechanism depriving the T cell of a costimulatory signal, resulting in modulation

of its effector response, similarly to what shown here in vitro. In the light of these considerations, LAG-3 should be considered an interesting regulatory pathway deserving translational consideration for immune driven conditions, including SpA.

I have shown that a subpopulation of $CD8^+$ Tregs is indeed present in the blood and SF of patients with SpA, as the sc RNA-seq analysis revealed. The phenotype, as shown by flow cytometry, confirms several RNAseq findings. The function of this rare, peculiar subset is still unknown. Tregs can express cytotoxic peptides: perforin and granzyme B expressing Tregs have potential to kill autologous APCs (Grossman et al., 2004), in particular granzyme-expressing Tregs reach up to 30% of the regulatory pool in the tumour environment, critically interfering with the immunosurveillance (Cao et al., 2007). Data from my AS single cell analysis showed that the cytotoxic module was mostly seen in $CD8^+$ Tregs rather than in any Treg subset, with the partial exception of KLRB1+ Tregs. (Zhang et al., 2009) identified these cells in the PB of AS for the first time, and described their potential to produce IL-4. The mechanism of recruitment and the relevance of this small subset in SpA remain enigmatic.

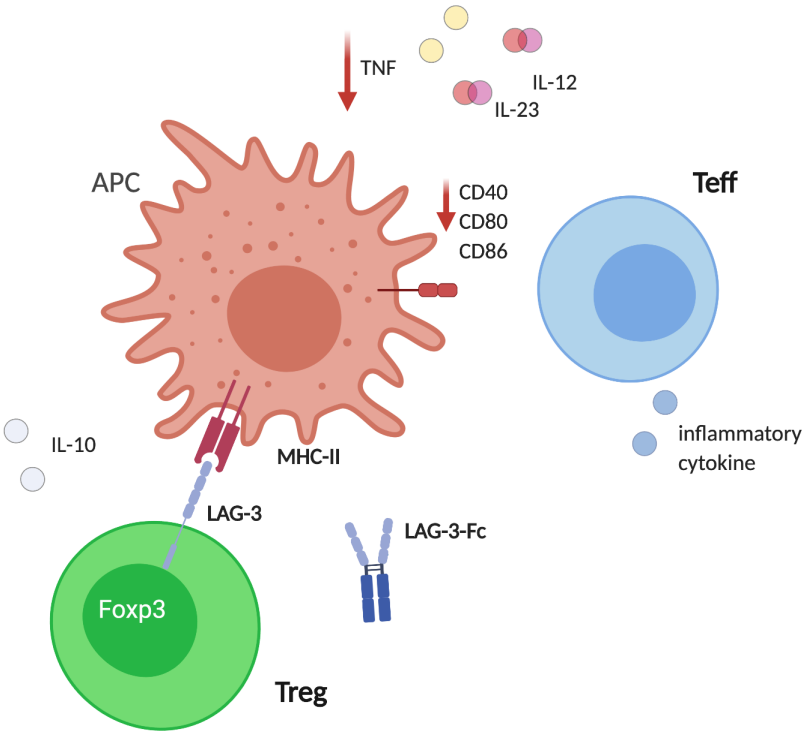

Figure 5.11. Proposed model of LAG-3-mediated suppression of APCs. LAG-3, expressed upon activation by Treg subsets, including CD161-expressing ROR-γt$^+$ Foxp3$^+$ and CD8$^+$, binds HLA II on the APC surface, triggering a direct immunoregulatory signal, that downregulates costimulatory molecules for T effectors, and the production of inflammatory cytokines.

In the last part of this chapter, an in vitro assay was used to analyze the expression of the costimulatory marker CD137 (4-1BB) on Foxp3+ cells after exposure to antigens. CD137 was characterized as a specific marker of TCR-induced activation of conventional CD4$^+$ and CD8$^+$ T cells (Watts, 2005). On Tregs, its expression has been used to describe alloantigen-reactive nTregs

(Schoenbrunn et al., 2012). The experimental data here collected confirm that CD137 is expressed by recently activated antigen-specific Tregs, as revealed by the gene expression profile of the clonally restricted Tregs identified in the SF (see 4.3.2.9), and support its use as a specific marker to detect antigen-experienced Tregs. This information could permit further functional characterization of antigen specific Tregs, or even allow clinical-scale enrichment of Tregs with desired TCR specificity to control autoimmune diseases. At the same time, using CD137 as a marker for antigen-specific Tregs could be employed in autoantigen screening platforms, for example through a proteomic library derived from tissue sites of organ inflammation, including the SF. Whether antigen contact, and consequently CD137 expression, confers particular properties on Tregs is still unclear. Previous in vitro observations have shown that CD137-expressing Tregs are efficient suppressors (Schoenbrunn et al., 2012), and could therefore represent a valuable subset for cell-based therapies. A recent study showed that *TNFRSF9* mRNA expression was decreased in subjects carrying disease risk alleles for inflammatory bowel diseases (Bossini-Castillo et al., 2019). Although it is not clear whether CD137 confers specific suppressive functions to Tregs, genetic variants might indirectly impair antigen specific Treg activation.

5.5 REFERENCES

Andrews, L.P., Yano, H., and Vignali, D.A.A. (2019). Inhibitory receptors and ligands beyond PD-1, PD-L1 and CTLA-4: breakthroughs or backups. Nature Immunology *20*, 1425–1434.

Bacher, P., Heinrich, F., Stervbo, U., Nienen, M., Vahldieck, M., Iwert, C., Vogt, K., Kollet, J., Babel, N., Sawitzki, B., et al. (2016). Regulatory T Cell Specificity Directs Tolerance versus Allergy against Aeroantigens in Humans. Cell *167*, 1067-1078.e16.

Bauché, D., Joyce-Shaikh, B., Jain, R., Grein, J., Ku, K.S., Blumenschein, W.M., Ganal-Vonarburg, S.C., Wilson, D.C., McClanahan, T.K., Malefyt, R. de W., et al. (2018). LAG3+ Regulatory T Cells Restrain Interleukin-23-Producing CX3CR1+ Gut-Resident Macrophages during Group 3 Innate Lymphoid Cell-Driven Colitis. Immunity *49*, 342-352.e5.

Bettini, M., Szymczak-Workman, A.L., Forbes, K., Castellaw, A.H., Selby, M., Pan, X., Drake, C.G., Korman, A.J., and Vignali, D.A.A. (2011). Cutting edge: accelerated autoimmune diabetes in the absence of LAG-3. J. Immunol. *187*, 3493–3498.

Bossini-Castillo, L., Glinos, D.A., Kunowska, N., Golda, G., Lamikanra, A., Spitzer, M., Soskic, B., Cano-Gamez, E., Smyth, D.J., Cattermole, C., et al. (2019). Immune disease variants modulate gene expression in regulatory CD4+ T cells and inform drug targets. BioRxiv 654632.

Butler, N.S., Moebius, J., Pewe, L.L., Traore, B., Doumbo, O.K., Tygrett, L.T., Waldschmidt, T.J., Crompton, P.D., and Harty, J.T. (2011). Therapeutic blockade of PD-L1 and LAG-3 rapidly clears established blood-stage Plasmodium infection. Nat. Immunol. *13*, 188–195.

Cao, X., Cai, S.F., Fehniger, T.A., Song, J., Collins, L.I., Piwnica-Worms, D.R., and Ley, T.J. (2007). Granzyme B and Perforin Are Important for Regulatory T Cell-Mediated Suppression of Tumor Clearance. Immunity *27*, 635–646.

Ciccia, F., Guggino, G., Zeng, M., Thomas, R., Ranganathan, V., Rahman, A., Alessandro, R., Rizzo, A., Saieva, L., Macaluso, F., et al. (2018). Proinflammatory CX3CR1+CD59+Tumor Necrosis Factor–Like Molecule 1A+Interleukin-23+ Monocytes Are Expanded in Patients With Ankylosing Spondylitis and Modulate Innate Lymphoid Cell 3 Immune Functions. Arthritis & Rheumatology *70*, 2003–2013.

Demeure, C.E., Wolfers, J., Martin-Garcia, N., Gaulard, P., and Triebel, F. (2001). T Lymphocytes infiltrating various tumour types express the MHC class II ligand lymphocyte activation gene-3 (LAG-3): role of LAG-3/MHC class II interactions in cell-cell contacts. Eur J Cancer *37*, 1709–1718.

Do, J. -s, Visperas, A., Sanogo, Y.O., Bechtel, J.J., Dvorina, N., Kim, S., Jang, E., Stohlman, S.A., Shen, B., Fairchild, R.L., et al. (2016). An IL-27/Lag3 axis enhances $Foxp3^+$ regulatory T cell–suppressive function and therapeutic efficacy. Mucosal Immunology *9*, 137–145.

Durham, N.M., Nirschl, C.J., Jackson, C.M., Elias, J., Kochel, C.M., Anders, R.A., and Drake, C.G. (2014). Lymphocyte Activation Gene 3 (LAG-3) Modulates the Ability of CD4 T-cells to Be Suppressed In Vivo. PLoS One *9*.

Evans, R.L., Faldetta, T.J., Humphreys, R.E., Pratt, D.M., Yunis, E.J., and Schlossman, S.F. (1978). Peripheral human T cells sensitized in mixed leukocyte culture synthesize and express Ia-like antigens. J. Exp. Med. *148*, 1440–1445.

Ferreira, R.C., Rainbow, D.B., Rubio García, A., Pekalski, M.L., Porter, L., Oliveira, J.J., Waldron-Lynch, F., Wicker, L.S., and Todd, J.A. (2017). Human IL-6RhiTIGIT− CD4+CD127lowCD25+ T cells display potent in vitro suppressive capacity and a distinct Th17 profile. Clinical Immunology *179*, 25–39.

Gagliani, N., Magnani, C.F., Huber, S., Gianolini, M.E., Pala, M., Licona-Limon, P., Guo, B., Herbert, D.R., Bulfone, A., Trentini, F., et al. (2013). Coexpression of CD49b and LAG-3 identifies human and mouse T regulatory type 1 cells. Nature Medicine *19*, 739–746.

Gershon, R.K., and Kondo, K. (1971). Infectious immunological tolerance. Immunology *21*, 903–914.

Grossman, W.J., Verbsky, J.W., Barchet, W., Colonna, M., Atkinson, J.P., and Ley, T.J. (2004). Human T Regulatory Cells Can Use the Perforin Pathway to Cause Autologous Target Cell Death. Immunity *21*, 589–601.

Huang, C.-T., Workman, C.J., Flies, D., Pan, X., Marson, A.L., Zhou, G., Hipkiss, E.L., Ravi, S., Kowalski, J., Levitsky, H.I., et al. (2004). Role of LAG-3 in regulatory T cells. Immunity *21*, 503–513.

Kadowaki, A., Miyake, S., Saga, R., Chiba, A., Mochizuki, H., and Yamamura, T. (2016). Gut environment-induced intraepithelial autoreactive CD4(+) T cells suppress central nervous system autoimmunity via LAG-3. Nat Commun *7*, 11639.

Liang, B., Workman, C., Lee, J., Chew, C., Dale, B.M., Colonna, L., Flores, M., Li, N., Schweighoffer, E., Greenberg, S., et al. (2008). Regulatory T Cells Inhibit Dendritic Cells by Lymphocyte Activation Gene-3 Engagement of MHC Class II. The Journal of Immunology *180*, 5916–5926.

Maruhashi, T., Okazaki, I., Sugiura, D., Takahashi, S., Maeda, T.K., Shimizu, K., and Okazaki, T. (2018). LAG-3 inhibits the activation of CD4 + T cells that recognize stable pMHCII through its conformation-dependent recognition of pMHCII. Nature Immunology 1.

Miyazaki, T., Dierich, A., Benoist, C., and Mathis, D. (1996). Independent modes of natural killing distinguished in mice lacking Lag3. Science *272*, 405–408.

Pot, C., Jin, H., Awasthi, A., Liu, S.M., Lai, C.-Y., Madan, R., Sharpe, A.H., Karp, C.L., Miaw, S.-C., Ho, I.-C., et al. (2009). Cutting edge: IL-27 induces the transcription factor c-Maf, cytokine IL-21, and the costimulatory receptor ICOS that coordinately act together to promote differentiation of IL-10-producing Tr1 cells. J. Immunol. *183*, 797–801.

Povoleri, G.A.M., Nova-Lamperti, E., Scottà, C., Fanelli, G., Chen, Y.-C., Becker, P.D., Boardman, D., Costantini, B., Romano, M., Pavlidis, P., et al. (2018). Human retinoic acid–regulated CD161 + regulatory T cells support wound repair in intestinal mucosa. Nature Immunology 1.

Romano, M., Fanelli, G., Tan, N., Nova-Lamperti, E., McGregor, R., Lechler, R.I., Lombardi, G., and Scottà, C. (2018). Expanded Regulatory T Cells Induce Alternatively Activated Monocytes With a Reduced Capacity to Expand T Helper-17 Cells. Front. Immunol. *9*.

Schoenbrunn, A., Frentsch, M., Kohler, S., Keye, J., Dooms, H., Moewes, B., Dong, J., Loddenkemper, C., Sieper, J., Wu, P., et al. (2012). A Converse 4-1BB and CD40 Ligand Expression Pattern Delineates Activated Regulatory T Cells (Treg) and Conventional T Cells Enabling Direct Isolation of Alloantigen-Reactive Natural Foxp3+ Treg. The Journal of Immunology *189*, 5985–5994.

Shouval, D.S., Biswas, A., Goettel, J.A., McCann, K., Conaway, E., Redhu, N.S., Mascanfroni, I.D., Al Adham, Z., Lavoie, S., Ibourk, M., et al. (2014). Interleukin-10 Receptor Signaling in Innate Immune Cells Regulates Mucosal Immune Tolerance and Anti-Inflammatory Macrophage Function. Immunity *40*, 706–719.

Taams, L.S., van Amelsfort, J.M.R., Tiemessen, M.M., Jacobs, K.M.G., de Jong, E.C., Akbar, A.N., Bijlsma, J.W.J., and Lafeber, F.P.J.G. (2005). Modulation of monocyte/macrophage function by human CD4+CD25+ regulatory T cells. Hum. Immunol. *66*, 222–230.

Thaker, Y.R., Andrews, L.P., Workman, C.J., Vignali, D.A.A., and Sharpe, A.H. (2018). Treg-specific LAG3 deletion reveals a key role for LAG3 in regulatory T cells to inhibit CNS autoimmunity. The Journal of Immunology *200*, 101.7-101.7.

Tian, X., Zhang, A., Qiu, C., Wang, W., Yang, Y., Qiu, C., Liu, A., Zhu, L., Yuan, S., Hu, H., et al. (2015). The upregulation of LAG-3 on T cells defines a subpopulation with functional exhaustion and correlates with disease progression in HIV-infected subjects. J. Immunol. *194*, 3873–3882.

Tiemessen, M.M., Jagger, A.L., Evans, H.G., van Herwijnen, M.J.C., John, S., and Taams, L.S. (2007). CD4+CD25+Foxp3+ regulatory T cells induce alternative activation of human monocytes/macrophages. Proc. Natl. Acad. Sci. U.S.A. *104*, 19446–19451.

Triebel, F., Jitsukawa, S., Baixeras, E., Roman-Roman, S., Genevee, C., Viegas-Pequignot, E., and Hercend, T. (1990). LAG-3, a novel lymphocyte activation gene closely related to CD4. J Exp Med *171*, 1393–1405.

Watts, T.H. (2005). TNF/TNFR family members in costimulation of T cell responses. Annu Rev Immunol *23*, 23–68.

Woo, S.-R., Li, N., Bruno, T.C., Forbes, K., Brown, S., Workman, C., Drake, C.G., and Vignali, D.A.A. (2010). Differential subcellular localization of the regulatory T-cell protein LAG-3 and the coreceptor CD4. Eur. J. Immunol. *40*, 1768–1777.

Zhang, L., Jarvis, L.B., Baek, H.-J., and Gaston, J.S.H. (2009). Regulatory IL4+CD8+ T cells in patients with ankylosing spondylitis and healthy controls. Ann. Rheum. Dis. *68*, 1345–1351.

Zigmond, E., Bernshtein, B., Friedlander, G., Walker, C.R., Yona, S., Kim, K.-W., Brenner, O., Krauthgamer, R., Varol, C., Müller, W., et al. (2014). Macrophage-Restricted Interleukin-10 Receptor Deficiency, but Not IL-10 Deficiency, Causes Severe Spontaneous Colitis. Immunity *40*, 720–733.

6 A Mitogen associated protein kinase (MAPK)- associated kinase 2 inhibitor regulates in vitro T cell inflammatory responses, including Th17, in Spondyloarthritis

6.1 INTRODUCTION

In Spondyloarthritis, the dysregulation of inflammatory cytokine expression is a hallmark of the disease. Selective inhibition of single inflammatory cytokines has been established as an effective treatment strategy in SpA, but is largely agnostic to the cells that produce these cytokines and the downstream mechanisms activated. Furthermore, the inhibition of a single cytokine (for example through a monoclonal antibodies directed against it) could in theory cause loss of efficacy or the appearance of undesirable immune driven manifestations.

An emerging therapeutic approach for immune driven disorders involves targeting the intracellular signaling pathways that lead to the production of inflammatory cytokines. Several molecules targeting the JAK/STAT pathway have been recently introduced into clinical use in RA, for which they proved at least as effective as TNF blockers, and hold great promise in SpA. Regulating

multiple inflammatory cytokines simultaneously could provide superior clinical efficacy compared with targeted blockade of individual factors.

The MAPK (Mitogen-activated protein kinase) family represents another key cellular response pathway to environmental or inflammatory extracellular stimuli, including those leading to endoplasmic reticulum stress (Darling and Cook, 2014). It consists of a series of phosphorylation intermediates that convey a signal to the nucleus that modifies the cell cycle, cellular motility, and, importantly, the biosynthesis of inflammatory cytokines (Arthur and Ley, 2013), The MAPK family member p38, because of its central role in mediating inflammatory responses, was identified as an attractive therapeutic target for inflammatory arthritis. The activation of p38, highly expressed in the rheumatoid synovium, initiates a signal that leads to increased production of TNF, IL-6, IL-1, and its inhibition proved effective in animal models of arthritis (Schett et al., 2008). Yet, in early phase human trials, p38 inhibitors yielded modest clinical efficacy, and were associated with toxicity and tachyphylaxis (loss of response observed in successive dosing, after an initial period of efficacy) (reviewed in Sweeney, 2009).

Research into possible alternative molecular targets within the same pathway identified the MAPK-associated protein kinase 2 (MAPKAPK, or MK2), a phosphorylation substrate of p38 heavily involved in regulating the inflammatory response (**Figure 6.1**). Targeting the pathway downstream was expected to prevent the feedback loops responsible for the “escape” seen in p38 inhibitors, and cause fewer side effects, while maintaining anti-inflammatory efficacy. Mice lacking MK2 show marked reduction in TNF production and are resistant to LPS-induced endotoxic shock (Kotlyarov et al., 1999)

MK2 regulates the production of inflammatory cytokines in the cell in a post-transcriptional manner. In the 3' untranslated region of mRNA, elements rich in adenine and uracil (AU-rich elements, or ARE) preserve the stability of the mRNA molecule and permit its translation into protein. Upon translocation into the nucleus, MK2 phosphorylates several ARE-binding proteins that prolong the mRNA bioavailability (Hitti et al., 2006; Ronkina et al., 2010). Consequently, blockade of MK2 causes instability and degradation of the mRNA molecule. This is thought to be one of the main post-transcriptional regulating mechanisms behind the production of inflammatory mediators such as TNF and IL-6, whereas the effect on T cell immunoregulatory functions is not known.

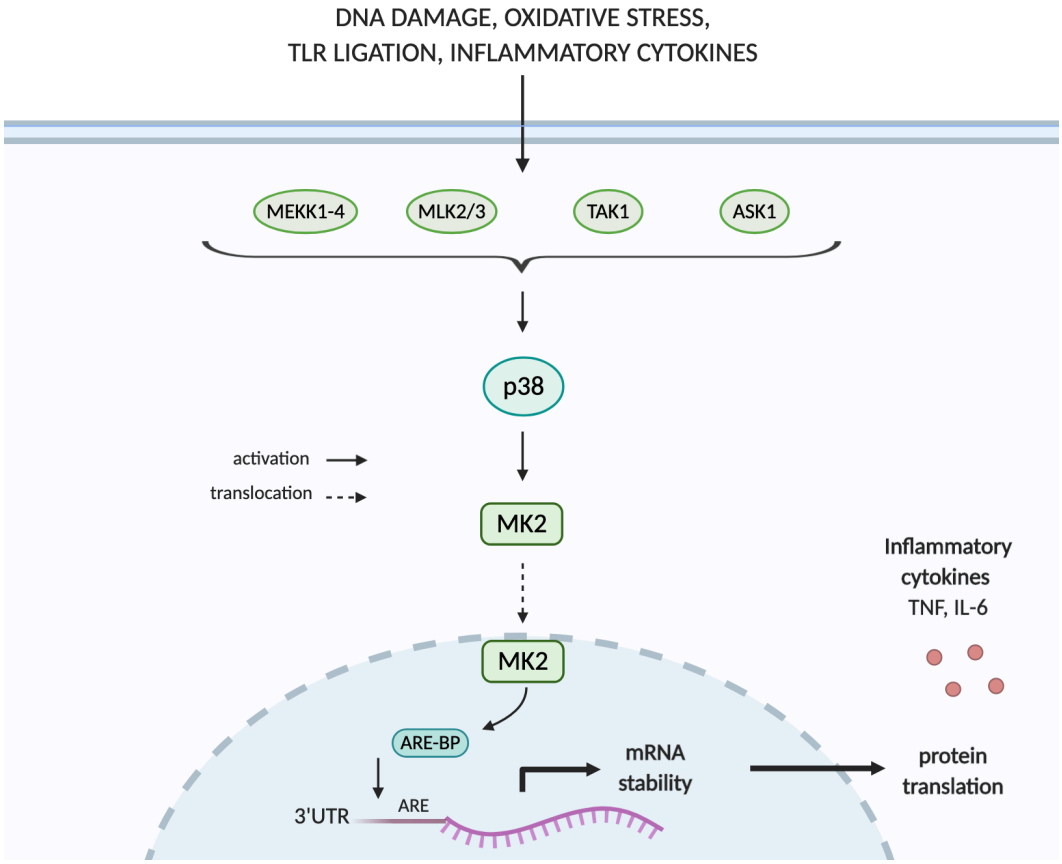

Figure 6.1. Cartoon showing signaling pathways activating MK2 and its function in cytokine biosynthesis. MEKK: mitogen-activated protein/ERK kinase kinase, TAK1: transforming growth factor-β activated kinase-1, ASK1: apoptosis signal-regulating kinase 1, ARE-BP: AU-rich binding protein, UTR: untranslated region

6.2 AIM

To evaluate the in vitro efficacy of a novel MK2 antagonist in suppressing inflammatory T cell responses in SpA, with particular interest in IL-17A and other IL-17-related cytokines.

6.3 RESULTS

6.3.1 MK2 inhibitor does not interfere with cell viability, and proliferation

A selective inhibitor for MK2 (CC786012, from now on referred to as MK2i) was provided by Celgene. The compound was dissolved in DMSO for in vitro experiments, and used in seriate dilutions in a series of cell-based assays. I found that MK2i did not cause in vitro T cell toxicity at doses <1 μM (**Figure 6.2A-B**). Importantly, considering the involvement of MK2 in the cell cycle regulation, cell proliferation was not affected (**Figure 6.2C**). Consequently, for the functional experiments, I used MK2i doses in the 0.1-1 μM range.

6.3.2 MK2 inhibits various T cell inflammatory cytokine responses

To test its in vitro action, I used T cells derived from patients with three forms of inflammatory arthritis (AS, PsA, RA). The patients' clinical characteristics are shown in **Table 6.1**. Magnetically isolated CD4+ T cells from peripheral blood were activated using anti-CD2/3/28 coated beads and low dose rhIL-2 (100 UI/ml) and maintained in culture for 6 days in the presence of

the inhibitor (MK2i) or DMSO-control, both added at day 0 and day 3. At day 6, the supernatant was collected for cytokine analysis with CBA. I measured IL-17A, IL-17F (Th17 signature cytokines), GM-CSF, IFN-γ (both described in specialized Th17 subsets) and IL-10, associated with non pathogenic Th17 responses (Aschenbrenner et al., 2018). MK2i reduced the TCR-induced production of IL-17A, IL-17F and IL-10 with doses as little as 0.1 μM. A significant reduction of IL-17F and GM-CSF was seen at higher doses, in the 0.5-1 μM range. The production of IFN-γ was only marginally affected (**Figure 6.3**).

In parallel, we performed flow cytometry for intracellular detection of IL-17A and Foxp3 after 6 days of culture in stimulating conditions (anti-CD2/3/28 coated beads and rhIL-2) (**Figure 6.4**). The Foxp3 expression and the proportion of Tregs ($CD25^+Foxp3^+$) were not altered by MK2i.

6.3.3 MK2 inhibition is effective on T cells obtained from both TNF blocker-treated and TNF blocker-naïve patients

MK2i was able to reduce inflammatory cytokines in T cells obtained from SpA patients both on TNFi and conventional treatments (**Figure 6.5**). Although the experiment was not designed to detect differences in the two groups, it appears that TNFi-treated patient samples show a similar, and for certain cytokines, clearer response to MK2i in vitro.

6.3.4 MK2 inhibitory mechanism of T cell responses persists in Th17 promoting conditions

Five SpA samples were cultured in Th17 promoting conditions, mimicking in vitro the upregulation of this immune axis observed in vivo in SpA. Despite the higher baseline levels of inflammatory cytokines produced when compared to the cells cultured in neutral conditions, MK2i was effective in limiting cytokine production (**Figure 6.6**).

	AS (n=16)	PsA (n=12)	RA (n=10)
Age (years), mean ± SD	46.4 ± 13.1	50.6 ± 12.9	61.7 ± 15.8
Male sex, number (%)	10 (62.5)	6 (50)	3 (27.3)
HLA-B27+, number (%)	10 (83.3) *	n/a	n/a
TREATMENT NSAIDs csDMARDS TNF-inhibitors Anti-IL-12/23	 10 2 # 6 -	 - 8 (2 #) 5 1	 - 8 (2 #) 4 -
DISEASE ACTIVITY SCORE, mean ± SD BASDAI DAS-28	 3.6 ± 2.7 ^ n/a	 - -	 n/a 2.6 ± 0.6 °
CRP, mean ± SD	13.5± 34.3	8.2 ± 8.1	5.3 ± 4.6

Table 6.1. Demographic and clinical characteristics of the patients. SD: standard deviation; NSAIDs: non steroidal anti inflammatory drugs; csDMARDS: conventional synthetic disease modifying anti-rheumatic drugs; BASDAI: Bath Ankylosing Spondylitis Disease Activity Index; DAS-28: disease activity score-28. * available in 12 patients; ^ available in 10 patients; ° available in 5 patients; # in combination with TNFi; n/a not applicable. Disease activity scores and treatment status at the time of sampling.

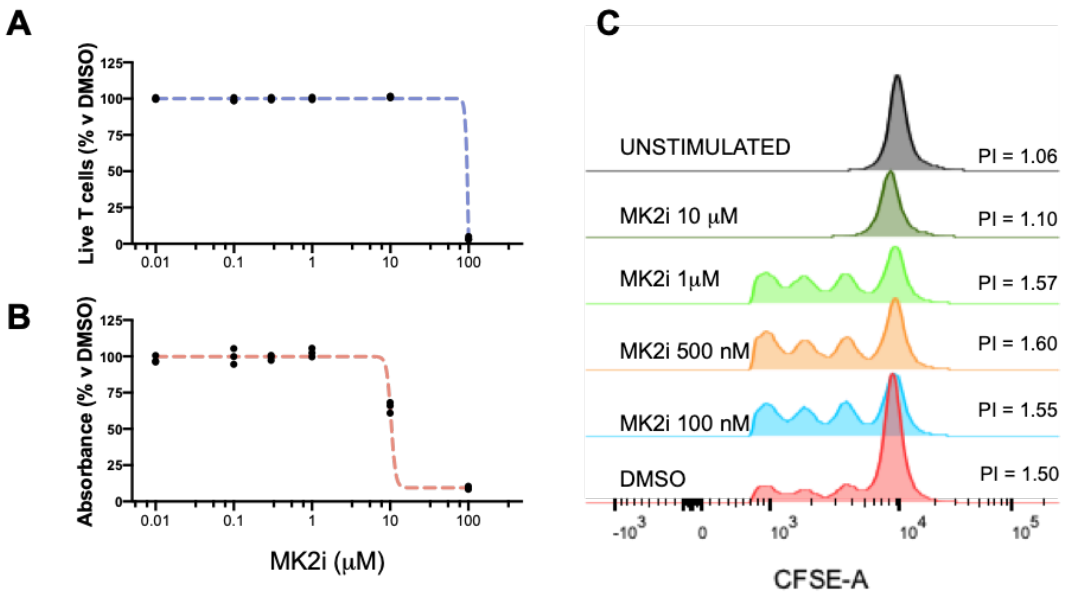

Figure 6.2. The small molecule inhibitor of MK2 CC786012 does not affect cell viability or proliferative ability at doses ≤ 1 μM. T cell viability in a 3 day PBMC culture in the presence of anti-CD3/28 antibodies, measured with a flow cytometric (A) and a colorimetric (B) method (n=3 AS samples). **(A)** Percentage of live cells, identified as $CD3^{+}CD4^{+}$ $eF780^{-}$ (viability fixable dye) and **(B)** PrestoBlue fluorescence compared to DMSO control. **(C)** T cell proliferation assay in a 3 day PBMC culture in the presence of anti-CD3/28 antibodies. Cells were stained with the Celltrace CFSE Proliferation dye at day 0. Fluorescence profile of CFSE shown. Proliferation modeling performed on FlowJo. PI: proliferation index.

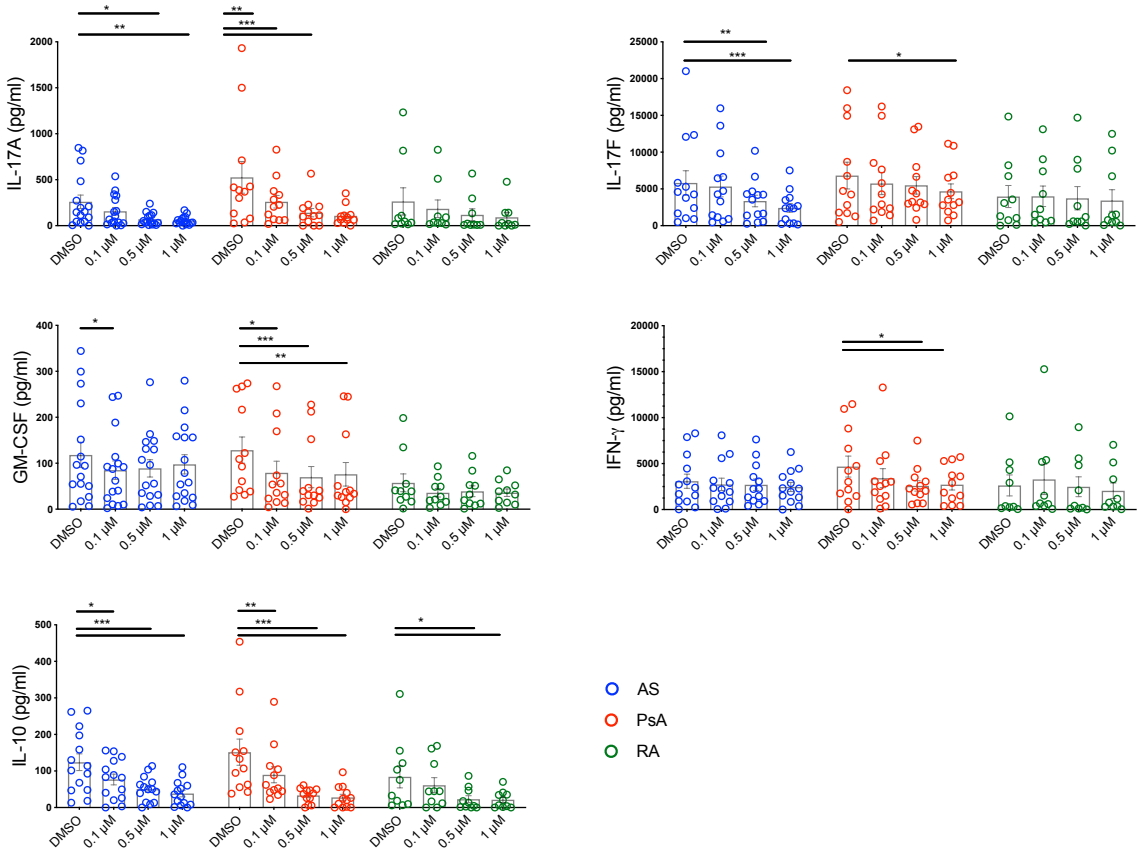

Figure 6.3. Selective inhibition of MK2 limits cytokine production by T cells from AS, PsA and RA patients. Concentrations of IL-17A, IL-17F, GM-CSF, IFN-γ and IL-10 measured in culture medium after 6 days activation/expansion of $CD4^+$ T cells cultured under neutral conditions (AS: n=14; PsA: n=12, RA: n=10). Mean + SEM. * $p \leq 0.05$, ** ≤ 0.01, *** ≤ 0.001 (Two way mixed design ANOVA).

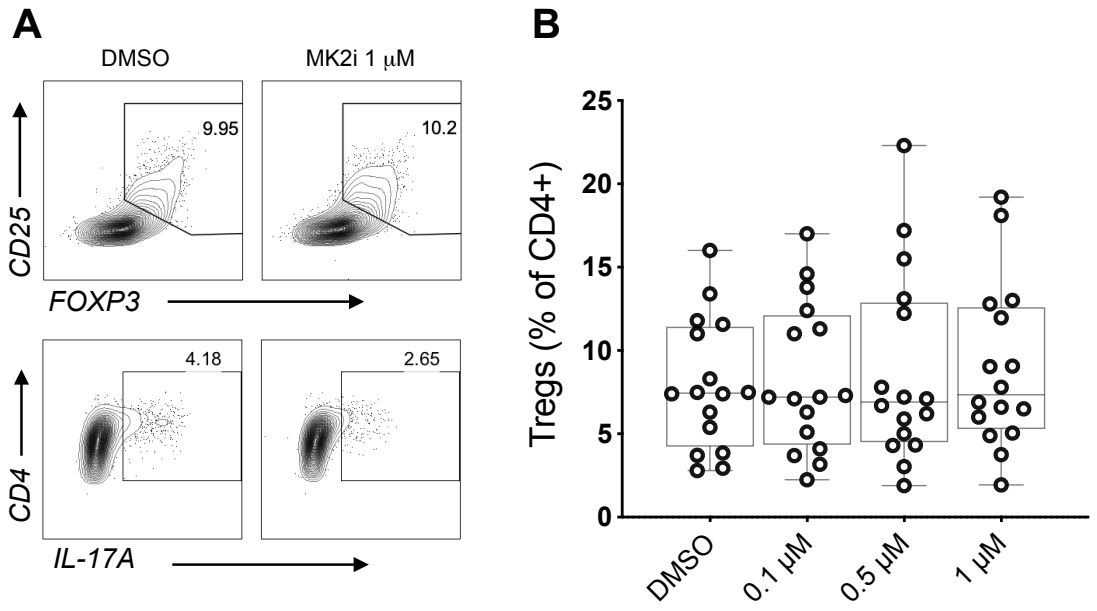

Figure 6.4. MK2 inhibition preserves Treg responses. **(A)** Representative flow cytometry plots from one AS patient sample showing staining of Tregs (top) and Th17 cells (bottom) (gated on $CD3^+$ $CD4^+$ live cells) in the presence or the vehicle or of MK2i (1 μM) after 6 days culture with anti-CD2/3/28 coated beads. **(B)** Percentage of Tregs with increasing doses of MK2i (n=16 AS patient samples). Box and whiskers represent respectively median and interquartile range, and minimum and maximum values.

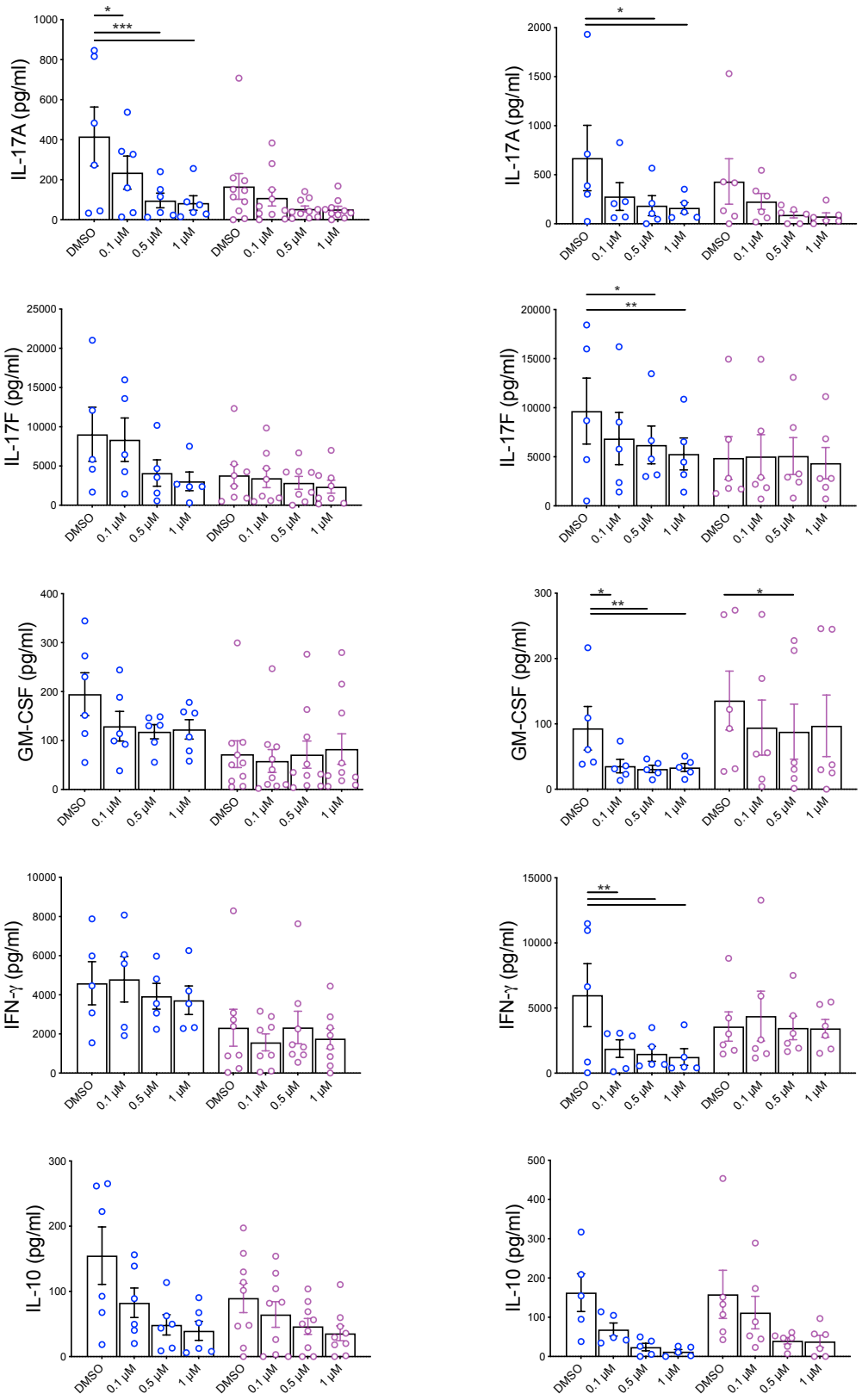
IL-17A (pg/ml)
IL-17A (pg/ml)
IL-17F (pg/ml)
IL-17F (pg/ml)
GM-CSF (pg/ml)
GM-CSF (pg/ml)
IFN-γ (pg/ml)
IFN-γ (pg/ml)
IL-10 (pg/ml)
IL-10 (pg/ml)
DMSO
0.1 µM
0.5 µM
1 µM
TNFi-treated
TNFi-naive

Figure 6.5 (previous page). Comparison of MK2 cytokine inhibition in T cell from TNFi-treated and TNFi-naïve SpA patients. **(Left)** AS patients (TNFi-treated n=6, TNFi-naive n=10). **(Right)** PsA patients (TNFi-treated n=5, TNFi-naïve n=6). Mean + SEM. * p ≤ 0.05, **≤ 0.01, *** ≤ 0.001 (Two way mixed design ANOVA).

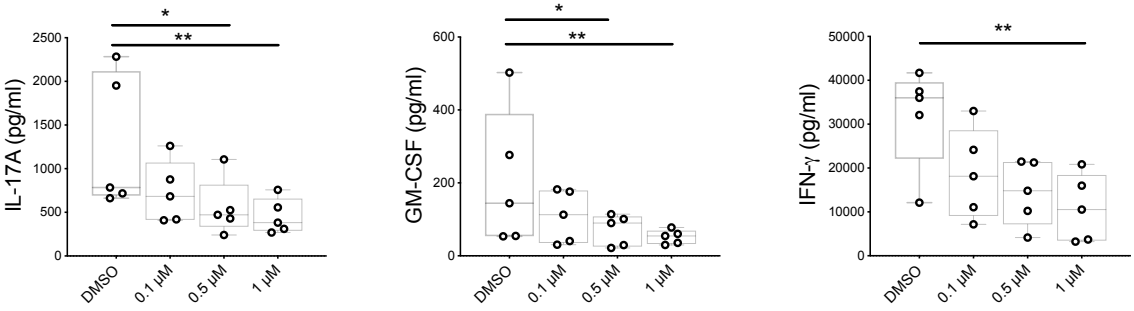

Figure 6.6. MK2 inhibition limits T cell inflammatory responses in cells cultured in Th17 promoting conditions. Concentrations of IL-17A, GM-CSF and IFN-γ produced by isolated PB CD4+ T cells cultured in the presence of IL-1β, IL-6, IL-23 for 6 days (n=5 SpA patients, AS n=3, PsA n=2). * p ≤ 0.05, **≤ 0.01 (One-way ANOVA).

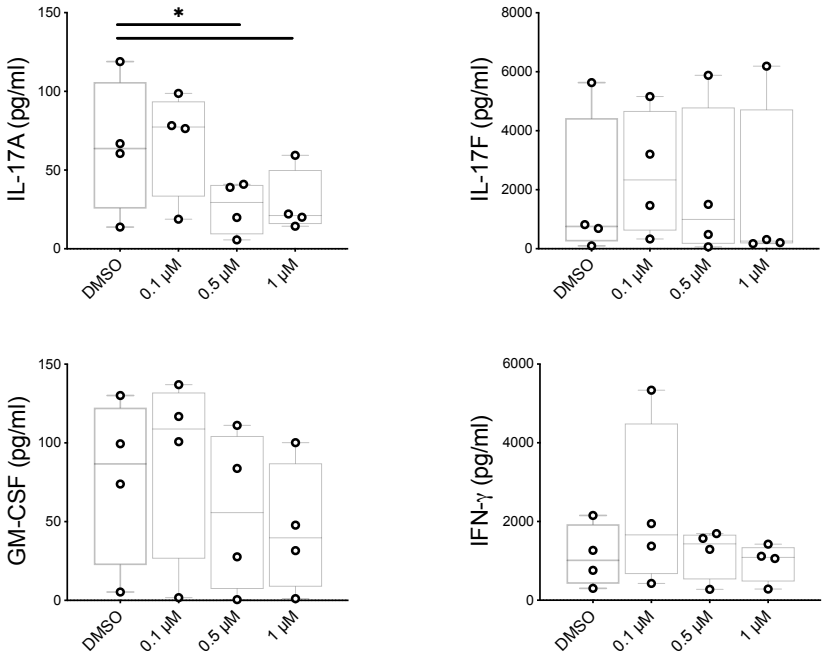

Figure 6.7. MK2 inhibition decreases IL-17A production in synovial fluid T cells. Concentrations of IL-17A, IL-17F, GM-CSF and IFN-g produced by $CD4^+$ T cells isolated from synovial fluid (n=4: RA = 3, AS = 1). * $p \leq 0.05$ (Two-way ANOVA).

6.3.5 MK2 reduces IL-17A production from synovial fluid derived T cells

$CD4^+$ cells isolated from cryopreserved synovial fluid mononuclear cells from three RA patients and one AS were cultured as described in 6.3.2. Although further conclusions are limited by the small sample examined, MK2i caused a significant reduction of IL-17A (**Figure 6.7**).

6.4 DISCUSSION

Our in vitro system using human cells derived from patients with inflammatory arthritis show that the inhibition of MK2 decreases TCR-induced production of IL-17A with doses as little as 100nM. Inhibition of IL-17F and GM-CSF was seen with doses in the 0.5-1 μM range.

I observed, for most cytokines, a clearer biological response to MK2i in cells obtained from TNFi-treated patients. The difference in response does not seem to be secondary to disease activity or inflammatory status, as BASDAI and CRP were not different between the two treatment groups (BASDAI for AS patients: TNFi-treated 3.5±2.3 vs TNFi-naïve 4.0±3.3 for AS patients, CRP for PsA patients: TNFi-treated 7.5±7.5 vs TNFi-naïve 5.9±7.8). The baseline levels of inflammatory cytokine produced in the assay were generally higher in the TNFi-treated patients, as shown previously (Bystrom et al., 2017; Hull et al., 2015).

Here I also show that the cytokine regulation by MK2 is also seen after T-cell receptor stimulation, not just TLR engagement, making it a potential target for

T cell-mediated immune responses. Although I have not demonstrated that the MK2 inhibitor tested interferes with the post transcriptional control of IL-17A mRNA similarly to what demonstrated for TNF, the assay selected, using isolated CD4+ cells, suggests that the molecule has a direct effect. Together with pro-inflammatory cytokines, IL-10 was also suppressed, indicating that targeting these pathways can affect immunoregulatory functions. The small effect observed on IFN-γ □□□□□□□□□□, suggests that pathways other than MAPK regulate its production after TCR activation.

Work performed by other members of our group on isolated monocytes, and by the collaborators on whole PBMCs, show that the same compound inhibits a series of other cytokines, including TNF, IL-6, MCP-1, IL-23. The combined inhibitory effect across different cell linages could be synergistic and interfere with the upregulation of multiple cytokines seen in SpA.

In conclusion, the tested MK2 inhibitor targets T cell inflammatory responses including Th17, while sparing regulatory T cells. These findings encourage further investigation and make MK2 a promising novel therapeutic target in the treatment of Spondyloarthritis.

6.5 REFERENCES

Arthur, J.S.C., and Ley, S.C. (2013). Mitogen-activated protein kinases in innate immunity. Nat. Rev. Immunol. *13*, 679–692.

Aschenbrenner, D., Foglierini, M., Jarrossay, D., Hu, D., Weiner, H.L., Kuchroo, V.K., Lanzavecchia, A., Notarbartolo, S., and Sallusto, F. (2018). An immunoregulatory and tissue-residency program modulated by c-MAF in human T H 17 cells. Nature Immunology *19*, 1126–1136.

Bystrom, J., Clanchy, F.I., Taher, T.E., Al-Bogami, M.M., Muhammad, H.A., Alzabin, S., Mangat, P., Jawad, A.S., Williams, R.O., and Mageed, R.A. (2017). Response to Treatment with TNFα Inhibitors in Rheumatoid Arthritis Is Associated with High Levels of GM-CSF and GM-CSF+ T Lymphocytes. Clin Rev Allergy Immunol *53*, 265–276.

Darling, N.J., and Cook, S.J. (2014). The role of MAPK signalling pathways in the response to endoplasmic reticulum stress. Biochim Biophys Acta *1843*, 2150–2163.

Hitti, E., Iakovleva, T., Brook, M., Deppenmeier, S., Gruber, A.D., Radzioch, D., Clark, A.R., Blackshear, P.J., Kotlyarov, A., and Gaestel, M. (2006). Mitogen-activated protein kinase-activated protein kinase 2 regulates tumor necrosis factor mRNA stability and translation mainly by altering tristetraprolin expression, stability, and binding to adenine/uridine-rich element. Mol. Cell. Biol. *26*, 2399–2407.

Hull, D.N., Williams, R.O., Pathan, E., Alzabin, S., Abraham, S., and Taylor, P.C. (2015). Anti-tumour necrosis factor treatment increases circulating T helper type 17 cells similarly in different types of inflammatory arthritis. Clin. Exp. Immunol. *181*, 401–406.

Kotlyarov, A., Neininger, A., Schubert, C., Eckert, R., Birchmeier, C., Volk, H.D., and Gaestel, M. (1999). MAPKAP kinase 2 is essential for LPS-induced TNF-alpha biosynthesis. Nat. Cell Biol. *1*, 94–97.

Ronkina, N., Menon, M.B., Schwermann, J., Tiedje, C., Hitti, E., Kotlyarov, A., and Gaestel, M. (2010). MAPKAP kinases MK2 and MK3 in inflammation: complex regulation of TNF biosynthesis via expression and phosphorylation of tristetraprolin. Biochem. Pharmacol. *80*, 1915–1920.

Schett, G., Zwerina, J., and Firestein, G. (2008). The p38 mitogen-activated protein kinase (MAPK) pathway in rheumatoid arthritis. Annals of the Rheumatic Diseases *67*, 909–916.

Sweeney, S.E. (2009). The as-yet unfulfilled promise of p38 MAPK inhibitors. Nat Rev Rheumatol *5*, 475–477.

7 Final discussion and future directions

The data presented in this thesis provide an overview of the mechanisms of T cell regulation in Spondyloarthritis, either mediated by specialised cell subsets (Chapter 3-5), or by molecular interventions that restrain T cell inflammatory responses (Chapter 6). T cells have a wide array of interrelated functions: as orchestrators of the immune response, they have a central role in driving inflammatory chronic conditions such as Spondyloarthritides. Enhancing their intrinsic mechanisms of regulation, or, alternatively, interfering with the inflammatory, pathogenic functions are two strategies that offer numerous therapeutic opportunities.

The effector arms of the T cell immunity, in particular Th17, are widely considered overactive in SpA, but the role in the disease pathogenesis of the regulatory counterpart, represented by Tregs, has never been clarified. The first part of the work (Chapter 3) aimed to characterize Tregs at the population level in the blood of patients with SpA, compared to healthy volunteers, and in the SF. I found that the percentage of Tregs in the PB of patients was unchanged compared to healthy volunteers blood, and was not significantly affected by treatments. In the SF, a common site of inflammation in the course of SpA, Tregs were higher in percentage, and presented a memory, activated

phenotype, in an effort to counteract the inflammatory responses. Based from a proposed classification of circulating Tregs based on their chemokine receptors, which provide trafficking potential, several subpopulations of Tregs, mirroring correspondent effector T cell subsets could be identified, but little differences were seen comparing patients and controls. Furthermore, selected markers (eg. CD27, CTLA-4, TIGIT), associated with regulatory features, were not altered in SpA Tregs compared to the healthy controls. The limited number of markers simultaneously available in a conventional flow cytometry analysis in the face of the vast functional heterogeneity of Tregs, and the importance of an unbiased classification irrespective of *a priori* expectations, led to the decision to perform scRNA-seq on Tregs from PB and SF in five patients with active disease.

Chapter 4 provided the first single cell atlas of Tregs in a human inflammatory arthritic condition. Reports highlighting the diversity of Treg cell populations and their functional specialization using high resolution instruments have surfaced only recently, focusing so far on murine cells (Miragaia et al., 2019), or on circulating Tregs obtained from healthy subjects (Zemmour et al., 2018). I analysed two different datasets obtained from paired PB and SF samples from three patients with PsA and two with AS. Although two different methods to localise and identify Tregs for downstream analysis were used (unsupervised clustering based on shared transcriptional similarities for the PsA dataset, and FACS sorting using expressed surface markers for AS), the similarity of the findings across the two datasets provided internal validation. Despite some functional diversity, Treg subpopulations presented shared transcriptional features, such as the similar expression a core set of genes (*CTLA4*, *IL2RA*, *BATF*) that represents the Treg identity and likely reflects the

dominant role of Foxp3 on the Treg transcriptome. A similar hierarchy emerged analysing the distribution of immunosuppressive genes: key functional immunoregulatory molecules were expressed by a large majority of Treg cells (eg. *CTLA4*, *TIGIT*), while others were selectively present in distinct cell populations (*IL10*, *LAG3*, *PDCD1*, *GZMB*). This suggests the existence of two tiers of suppressive markers, the first constitutionally present, the latter acquired in specific conditions, possibly conferring suppressive functions adapted to specific inflammatory environments. Genes encoding trafficking markers (including chemokine receptors and integrin subunits) were not segregated in different clusters (with the partial exception of *CCR6*, *CCR7* and *CCR4*, each primarily expressed in one cluster), indicating that these features do not strictly mirror transcriptional identities in Tregs, differently to that described for Teffs.

Studies on antigen-specific suppressor immunity so far have been hindered by the difficulty of obtaining antigen-specific Treg clones for detailed cellular and molecular analysis, in particular considering that Tregs only represent 3-10% of all $CD4^+$ cells in the PB. Linking exact TCR sequences to the gene expression profile for each cell revealed the presence of an enriched clonotype in the synovial fluid of one PsA patient, and its related transcriptional program. The TCR sequences library of the AS dataset had not been analysed at the time of submission of this thesis, but will add further information on the topic, carrying even higher chances to identify clonal restricted responses, considering the high number of Tregs composing in the AS dataset.

Furthermore, this work, the first to study Tregs at single cell level in a site of inflammation, identified genes upregulated in the SF. This included increased expression of TNF receptor superfamily genes and interferon response genes,

likely reflecting a conditioned response to the synovial microenvironment, but no tissue-specific clusters. To determine how molecular cues induce these distinctive changes in the gene expression in the SF, simultaneous systems-level analysis of chromatin architecture and gene expression, or lineage tracing experiments, will likely be needed.

My analysis of Treg cells in SpA provides a useful support to understand the transcriptional landscape of Tregs and specialized immune effector pathways. The same five distinct clusters were identified in both datasets, with two further functionally distinct subsets found in AS, where the higher number of cells sampled may have helped reveal rarer subtypes.

My findings also support, although indirectly, a strong argument for the presence of a gut-derived regulatory Treg cell subset in the joint during an arthritis flare. The recent description of a similar Treg subset in the human colon, identified with analogous scRNA-seq technique (James et al., 2020), and the description of their preferred mechanisms (IL-10 and LAG-3) in the intestinal mucosa (Bauché et al., 2018; Huber et al., 2011), and the similarity with the KLRB1+ ($CD161^{+}$) Tregs subpopulation described here, allow me to speculate that Tregs programmed to suppress specific immune response in different organs (eg. the intestinal mucosa) are able to travel to different inflammatory sites to suppress specific responses, suggesting a regulatory specialisation that has been demonstrated only in mice. The molecular mechanisms behind the preferential expression of effector regulatory pathway in the various tissues and against various cellular targets are still poorly understood.

One of these immunoregulatory mechanism, LAG-3, is the focus of chapter 5. When expressed by Tregs, its binding onto myeloid cells was

previously only shown in vitro with murine bone marrow derived DCs (Liang et al., 2008) or in an experimental colitis models to CX3CR1+ macrophages (Bauché et al., 2018). I am providing the first in vitro evidences that LAG-3 could downregulate patient-derived myeloid cells. Interestingly, LAG-3 expression was lower in T cells from AS patients, in particular in Tregs. The reasons behind this downregulation are not clear: it might be explained by a switch towards others mechanisms of suppression, or an effect of the microenvironment. Some of the inflammatory cytokines that are elevated in SpA patients (IL-1β, IL-6, IL-23) signal through Stat3, which competes with the IL-2/Stat5 pathway that is predicted to control the *LAG3* induction (Durham et al., 2014). At the same time, relative gene expression profiling suggests that *LAG3* is elevated in SF Tregs, where its function is likely to be more relevant. Unfortunately, at the time of analysis no samples were available to repeat the experiments with SF-derived myeloid cells, so no firm conclusions as to whether there is a deficit in vivo are possible. Nevertheless, LAG-3-mediated immune regulation could be an area of therapeutic intervention. Inhibitory immune checkpoints could represent a new area of therapeutic focus for immune driven conditions: enhancing suppressive mechanisms could be a novel effective strategy for this group of conditions in which molecular targets are limited to a limited number of inflammatory cytokines. Outstanding questions relative to LAG-3's therapeutic potential remain. On T effectors, in murine cells the LAG-3 inhibitory signal appears only when an antigen is presented in the context of the MHC class II (Maruhashi et al., 2018). In the experiments here shown, cells were not pulsed with antigens yet LAG-3-Fc suppressed the LPS-driven activation. A few explanations can be proposed: that no antigen recognition is necessary for delivering the inhibitory

effect here described; that monocytes in my experiments were loaded with natural antigens, or that different structural conformations of the LAG3-HLA class II complex mediate different functions. A blocking anti-HLA class II antibody reversed the inhibitory effects of LAG-3 only for some markers, possibly because some effector responses might escape the inhibitory signal proposed by (Liang et al., 2008). Furthermore, the experiments were performed with a considerable number of controls and a small number of biological replicates, reducing the statistical power. More in vitro experiments are necessary, and the structure of the binding needs to be elucidated.

This part of the work highlights the importance of understanding Treg molecular mechanisms of suppression to optimise cell-based therapies, or to identify novel targets for specific inflammatory settings. In particular, of great interest would be discovering which Treg mechanisms are the most effective for controlling Th17 responses, as often conventional in vitro cell-based suppression assays constitute a very partial reproduction of more complex cellular cross-talks.

In conclusion, in Chapter 3 to 6 I showed a series of experiments that, using phenotypic, transcriptional and functional approaches, contribute to define the Treg landscape in SpA. It is likely that future research studies in the field of immune driven diseases will combine these levels of investigation in single, multimodal experiments, for example combining protein expression, chromatin accessibility and transcriptomics, all analysed in an integrated manner (Stuart et al., 2019) with novel high resolution technologies. Furthermore, a functional understanding of the genetic variations directly associated with Treg function, or affecting quantitative expression of regulatory genes, is certainly warranted.

Lastly, in Chapter 6, a different immunoregulatory strategy was explored: I tested a small molecule inhibitor of a MAPK signalling pathway intermediate (MK2), demonstrating, in T cells, reduced production and release of a series of inflammatory cytokine, some of which known mediators of inflammation and damage in SpA. Targeting intracellular signalling pathways is a recent, effective therapeutic approach in inflammatory arthritides (O'Shea et al., 2013). The molecular target tested by my experiments (MK2), although well characterised, is novel. In my experiments, the MK2 inhibitor had a safe profile in vitro and demonstrated inhibition of Th17 immune responses. The data presented, in addition to published reports indicating that MK2 inhibition downregulates SpA-approved targets such as TNF, and the pro-Th17 cytokine IL-6 (Ronkina et al., 2010), and experiments in vivo performed by our collaborators, make this novel therapeutic strategy very promising for the treatment of SpA and support the progression of the MK2 inhibition experimentation to a preclinical phase.

7.1 REFERENCES

Bauché, D., Joyce-Shaikh, B., Jain, R., Grein, J., Ku, K.S., Blumenschein, W.M., Ganal-Vonarburg, S.C., Wilson, D.C., McClanahan, T.K., Malefyt, R. de W., et al. (2018). LAG3+ Regulatory T Cells Restrain Interleukin-23-Producing CX3CR1+ Gut-Resident Macrophages during Group 3 Innate Lymphoid Cell-Driven Colitis. Immunity *49*, 342-352.e5.

Durham, N.M., Nirschl, C.J., Jackson, C.M., Elias, J., Kochel, C.M., Anders, R.A., and Drake, C.G. (2014). Lymphocyte Activation Gene 3 (LAG-3) Modulates the Ability of CD4 T-cells to Be Suppressed In Vivo. PLoS One *9*.

Huber, S., Gagliani, N., Esplugues, E., O'Connor, W., Huber, F.J., Chaudhry, A., Kamanaka, M., Kobayashi, Y., Booth, C.J., Rudensky, A.Y., et al. (2011). Th17 cells express interleukin-10 receptor and are controlled by Foxp3$^-$ and Foxp3+ regulatory CD4+ T cells in an interleukin-10-dependent manner. Immunity *34*, 554–565.

James, K.R., Gomes, T., Elmentaite, R., Kumar, N., Gulliver, E.L., King, H.W., Stares, M.D., Bareham, B.R., Ferdinand, J.R., Petrova, V.N., et al. (2020). Distinct microbial and immune niches of the human colon. Nature Immunology *21*, 343–353.

Liang, B., Workman, C., Lee, J., Chew, C., Dale, B.M., Colonna, L., Flores, M., Li, N., Schweighoffer, E., Greenberg, S., et al. (2008). Regulatory T Cells Inhibit Dendritic Cells by Lymphocyte Activation Gene-3 Engagement of MHC Class II. The Journal of Immunology *180*, 5916–5926.

Maruhashi, T., Okazaki, I., Sugiura, D., Takahashi, S., Maeda, T.K., Shimizu, K., and Okazaki, T. (2018). LAG-3 inhibits the activation of CD4 + T cells that recognize stable pMHCII through its conformation-dependent recognition of pMHCII. Nature Immunology 1.

Miragaia, R.J., Gomes, T., Chomka, A., Jardine, L., Riedel, A., Hegazy, A.N., Whibley, N., Tucci, A., Chen, X., Lindeman, I., et al. (2019). Single-Cell Transcriptomics of Regulatory T Cells Reveals Trajectories of Tissue Adaptation. Immunity *50*, 493-504.e7.

O'Shea, J.J., Laurence, A., and McInnes, I.B. (2013). Back to the future: oral targeted therapy for RA and other autoimmune diseases. Nat Rev Rheumatol *9*, 173–182.

Ronkina, N., Menon, M.B., Schwermann, J., Tiedje, C., Hitti, E., Kotlyarov, A., and Gaestel, M. (2010). MAPKAP kinases MK2 and MK3 in inflammation: complex regulation of TNF biosynthesis via expression and phosphorylation of tristetraprolin. Biochem. Pharmacol. *80*, 1915–1920.

Stuart, T., Butler, A., Hoffman, P., Hafemeister, C., Papalexi, E., Mauck, W.M., Hao, Y., Stoeckius, M., Smibert, P., and Satija, R. (2019). Comprehensive Integration of Single-Cell Data. Cell *177*, 1888-1902.e21.

Zemmour, D., Zilionis, R., Kiner, E., Klein, A.M., Mathis, D., and Benoist, C. (2018). Single-cell gene expression reveals a landscape of regulatory T cell phenotypes shaped by the TCR. Nat. Immunol. *19*, 291–301.